

Technical Report Documentation Page

1. Report No. FHWA/TX-15/0-6651-2	2. Government Accession No.	3. Recipient's Catalog No.	
4. Title and Subtitle CONTINUOUS PRESTRESSED CONCRETE GIRDER BRIDGES VOLUME 2: ANALYSIS, TESTING, AND RECOMMENDATIONS		5. Report Date Published: December 2016	
		6. Performing Organization Code	
7. Author(s) Mary Beth D. Hueste, John B. Mander, Reza Baie, Anagha S. Parkar, Akshay Parchure, Jennifer Michelle Prouty, and Tristan Sarremejane		8. Performing Organization Report No. Report 0-6651-2	
9. Performing Organization Name and Address Texas A&M Transportation Institute College Station, Texas 77843-3135		10. Work Unit No. (TRAIS)	
		11. Contract or Grant No. Project 0-6651	
12. Sponsoring Agency Name and Address Texas Department of Transportation Research and Technology Implementation Office 125 E. 11th Street Austin, Texas 78701-2483		13. Type of Report and Period Covered Technical Report: October 2011–August 2014	
		14. Sponsoring Agency Code	
15. Supplementary Notes Project performed in cooperation with the Texas Department of Transportation and the Federal Highway Administration. Project Title: Continuous Prestressed Concrete Girder Bridges URL: http://tti.tamu.edu/documents/0-6651-2.pdf			
16. Abstract The Texas Department of Transportation designs typical highway bridge structures as simple span systems using standard precast, pretensioned girders. Spans are limited to about 150 ft due to weight and length restrictions on transporting the precast girder units from the prestressing plant to the bridge site. Such bridge construction, while economical from an initial cost point-of-view, may become somewhat limiting when longer spans are needed. This project focused on developing additional economical design alternatives for longer span bridges with main spans ranging from 150–300 ft, using continuous precast, prestressed concrete bridge structures with in-span splices. Phase 1 of this study focused on evaluating the current state-of-the-art and practice relevant to continuous precast concrete girder bridges and recommending suitable continuity connections for typical Texas bridge girders; the findings are documented in the Volume 1 project report. This report summarizes Phase 2 of the research including detailed design examples for shored and partially shored construction, results of a parametric design study, and results of an experimental program that tested a full-scale girder containing three splice connections. The parametric design study indicated that for bridges spanning from 150–300 ft, continuous precast, prestressed concrete girder bridges with in-span splices can provide an economical alternative to steel girder bridges and segmental concrete box girder construction. The tested splice connections performed well under service level loads. However, the lack of continuity of the pretensioning through the splice connection region had a significant impact on the behavior at higher loads approaching ultimate conditions. Improved connection behavior at ultimate conditions is expected through enhanced connection details. Recommendations for design of continuous spliced precast girders, along with several detailing suggestions are discussed in the report.			
17. Key Words Precast Prestressed Concrete, Spliced Girder Technology, Bridge Girders, Splice Connection		18. Distribution Statement No restrictions. This document is available to the public through NTIS: National Technical Information Service Alexandria, Virginia http://www.ntis.gov	
19. Security Classif.(of this report) Unclassified	20. Security Classif.(of this page) Unclassified	21. No. of Pages 270	22. Price

CONTINUOUS PRESTRESSED CONCRETE GIRDER BRIDGES VOLUME 2: ANALYSIS, TESTING, AND RECOMMENDATIONS

by

Mary Beth D. Hueste, Ph.D., P.E.
Research Engineer
Texas A&M Transportation Institute

Akshay Parchure
Graduate Research Assistant
Texas A&M Transportation Institute

John B. Mander, Ph.D.
Research Engineer
Texas A&M Transportation Institute

Jennifer Michelle Prouty
Graduate Research Assistant
Texas A&M Transportation Institute

Reza Baie
Graduate Research Assistant
Texas A&M Transportation Institute

Tristan Sarremejane
Graduate Research Assistant
Texas A&M Transportation Institute

Anagha S. Parkar
Graduate Research Assistant
Texas A&M Transportation Institute

Report 0-6651-2
Project 0-6651

Project Title: Continuous Prestressed Concrete Girder Bridges

Performed in cooperation with the
Texas Department of Transportation
and the
Federal Highway Administration

Published: December 2016

TEXAS A&M TRANSPORTATION INSTITUTE
College Station, Texas 77843-3135

DISCLAIMER

This research was performed in cooperation with the Texas Department of Transportation (TxDOT) and the Federal Highway Administration (FHWA). The contents of this report reflect the views of the authors, who are responsible for the facts and the accuracy of the data presented herein. The contents do not necessarily reflect the official view or policies of the FHWA or TxDOT. This report does not constitute a standard, specification, or regulation. It is not intended for construction, bidding, or permit purposes. The engineer in charge was Mary Beth D. Hueste, Ph.D., P.E. (TX 89660).

The United States Government and the State of Texas do not endorse products or manufacturers. Trade or manufactures' names appear herein solely because they are considered essential to the object of this report.

ACKNOWLEDGMENTS

This project was conducted at Texas A&M University (TAMU) and was supported by TxDOT and FHWA through the Texas A&M Transportation Institute (TTI) as part of Project 0-6651, “Continuous Prestressed Concrete Girder Bridges.” The authors are grateful to the individuals who were involved with this project and provided invaluable assistance, including Darrin Jensen (TxDOT Project Manager), Dacio Marin (TxDOT Project Director) and the TxDOT Project Monitoring Committee: Shane Cunningham, John Holt, Mike Hyzak, Kevin Pruski, Duncan Stewart, and Tom Stout.

The following individuals were instrumental in providing support to ensure the successful completion of the project, and their contributions are appreciated:

- The High Bay Structural and Materials Testing Laboratory at TAMU, including Peter Keating, Matthew Potter, and Ramiro Vanoye-Trevino, provided invaluable advice and assistance during the full-scale specimen construction, instrumentation, and testing.
- A number of students assisted with construction and testing of the full-scale girder specimen, including Jonathan Fowler, Ryan Posluszny, Michael Garrett, Casey Jones, Ricardo Santos, William Spencer, and Lucas Taborga.
- Maria Medrano provided overall administrative and business support for the project.
- Jorge Hinojosa with Bexar Concrete Works worked with the project team to manufacture the precast girder segments for the full-scale tests.

TABLE OF CONTENTS

		Page
List of Figures.....		xi
List of Tables		xiv
1	Introduction	1
1.1	Background	1
1.2	Significance	2
1.3	Objectives and Scope	3
1.4	Research Plan	3
1.4.1	Parametric Studies	4
1.4.2	Experimental Testing.....	4
1.4.3	Develop Continuity Details and Design Recommendations.....	4
1.4.4	Develop Continuity Design Examples.....	5
1.4.5	Report Preparation	5
1.5	Report Outline	5
2	State-of-the-Art and Practice Context.....	7
2.1	Scope of Chapter	7
2.2	Highlights from TxDOT Phase 1 Report	7
2.2.1	On-Pier Splicing.....	7
2.2.2	In-Span Splicing.....	8
2.2.3	Highlights of Discussions with Industry Stakeholders	10
2.3	NCHRP REPORT 517 Highlights	13
2.3.1	Summary	13
2.3.2	AASHTO Code Revisions	14
2.4	Discussion of AASHTO LRFD Specifications Related to Spliced Precast Concrete Girder Bridges.....	17
2.4.1	General Criteria.....	17
2.4.2	Prestressing	18
2.5	Recent Research	20
2.6	Field Implementation in Texas: Sylvan Avenue Bridge	21
3	Prototype Bridge Design	27
3.1	Introduction	27
3.2	Bridge Geometry and Girder Cross Section.....	27
3.3	Design Assumptions and Parameters	30
3.4	Dead Loads.....	31
3.5	Live Loads	32
3.5.1	Design Truck and Design Lane Load	32
3.5.2	Design Tandem and Design Lane Load.....	33
3.6	Allowable Stress Limits	36
3.7	Limit States.....	37
3.7.1	Service Limit State.....	37
3.7.2	Flexure Strength Limit State.....	38
3.7.3	Shear Limit State.....	39
3.8	Deflection	40
3.9	Design Philosophy.....	41

3.9.1	General	41
3.9.2	Handling, Transportation and Erection	42
3.9.3	Construction on Site	45
3.10	Prestressing Layout	46
3.11	Moments during Stages of Construction	54
3.12	Service Stress Analysis	57
3.13	Deflection Check	64
3.14	Flexural Strength Check	65
3.15	Shear Strength Check	66
3.16	Splice Design	69
3.16.1	Splice Details	69
3.16.2	Prestressing and Reinforcement Details for the Splice	70
3.16.3	Flexural Strength Check	71
3.16.4	Shear Design	72
4	Parametric Study	77
4.1	Introduction	77
4.2	Design Cases	77
4.3	Design Parameters	78
4.4	Section Properties	79
4.5	Girder Weights	82
4.6	Prestressing	83
4.7	Service Stress Analysis	88
4.8	Deflections	94
4.9	Ultimate Flexural Strength Requirements and Ductility	95
4.10	Shear Design	97
4.11	Summary and Remarks	98
5	Design, Construction, and Pre-Test Behavior of Specimen	101
5.1	Introduction	101
5.2	Specimen Abstraction	101
5.2.1	Prototype Bridge	101
5.2.2	Specimen Details	102
5.2.3	Modified Tx70 Girder	108
5.3	Specimen Design	110
5.3.1	Design Philosophy and Modifications	110
5.3.2	Girder Segment Design	111
5.3.3	Splice Connection Design	118
5.4	Specimen Preparation	121
5.4.1	Overview	121
5.4.2	Bearing Pad, Pedestal Design, and Pedestal Construction	121
5.4.3	Casting the Girder Specimen at the Precast Plant	123
5.4.4	Fabricating Wooden Connection Formwork	127
5.4.5	Building Falsework and Deck Formwork	127
5.4.6	Casting Splices in the Laboratory	127
5.4.7	Casting Reinforced Concrete Deck in the Laboratory	128
5.4.8	Fresh Concrete Properties	128

5.4.9	Installing Gages, Linear Variable Differential Transformers, String Pots, and Demountable Mechanical Points.....	133
5.4.10	Post-Tensioning	133
5.5	Instrumentation.....	136
5.5.1	Rebar Strain Gages	136
5.5.2	Surface Strain Gages.....	138
5.5.3	Embedded Concrete Gages.....	139
5.5.4	Linear Variable Differential Transformers	140
5.5.5	String Potentiometers.....	141
5.5.6	Demountable Mechanical Points	142
5.5.7	Summary of Instrumentation	142
5.6	Pre-testing Data Analysis	144
5.6.1	Introduction.....	144
5.6.2	Creep Effect	144
5.6.3	Support Removal Effect.....	146
5.6.4	Post-Tensioning Effect.....	146
5.6.5	Summary of Strain Profile after PT	147
5.7	Prediction of Specimen moment-curvature Response.....	151
6	Experimental Results and Observations	157
6.1	Overview	157
6.2	Experimental Setup and General Observations.....	157
6.2.1	Testing Approach.....	157
6.2.2	Test 1 – Splice 2 up to Service Loads.....	159
6.2.3	Test 2 – Splice 3 up to Service Loads.....	160
6.2.4	Test 3 – Splice 2 Post-Cracking Performance	160
6.2.5	Test 4 – Splice 3 Post-Cracking Performance	166
6.2.6	Test 5 – Splice 1.....	167
6.3	Detailed Behavior and Analysis	173
6.3.1	Force and Deformation Behavior and Analysis.....	173
6.3.2	Moment-Curvature.....	175
6.3.3	Longitudinal Bar Strains	177
6.3.4	Transverse Hoop Stirrups	177
6.3.5	Concrete Strains	178
6.3.6	Strain Profiles.....	182
6.3.7	Longitudinal Beam Deflection Profile.....	189
6.4	Discussion and Findings.....	191
7	Summary, Conclusions, and Recommendations	193
7.1	Summary	193
7.2	Conclusions	194
7.2.1	General.....	194
7.2.2	Design Cases and Parametric Study	194
7.2.3	Fabrication and Construction.....	196
7.2.4	Performance of the Superstructure and Splices	197
7.3	Recommendations for design and Implementation	199
7.3.1	Feasibility.....	199
7.3.2	Construction.....	200

7.3.3	Design	201
7.3.4	Cross-Section Selection	203
7.3.5	Splice Performance and Detailing	204
7.4	Recommendations for Future Research	206
References		207
APPENDIX A. Material Properties: Concrete, Mild Steel, and Prestressing Strand		A-1
A.1	Concrete.....	A-2
A.1.1	Mixture Proportions	A-2
A.1.2	Fresh Concrete Properties	A-3
A.1.3	Hardened Concrete Properties	A-6
A.2	Mild Steel	A-27
A.3	Prestressing Strand	A-30
APPENDIX B. Detailed Drawings of Continuous Precast Prestressed Concrete Bridge Girder Specimen.....		B-1

LIST OF FIGURES

	Page
Figure 2.1. Design Examples from NCHRP Report 517 (Castrodale and White 2004).....	16
Figure 2.2. Use of Spliced Girders for the Sylvan Avenue Bridge.....	23
Figure 2.3. Construction Process for Sylvan Avenue Bridge (Webber 2014).....	25
Figure 3.1 Elevation View of Three-Span Continuous Bridge.....	28
Figure 3.2. Transverse Bridge Section at Midspan.....	28
Figure 3.3. Prismatic Modified Tx70 Girder.	29
Figure 3.4. Design Truck and Design Lane Load.	32
Figure 3.5. Design Tandem and Design Lane Load.	33
Figure 3.6. Critical Load Placement of HL-93 Vehicular Live Load over Continuous Span for Maximum Shear Demand.....	36
Figure 3.7. Critical Load Placement of HL-93 Vehicular Live Load over Continuous Span for Maximum Deflection.	41
Figure 3.8. Support Arrangement during Transportation of Drop-in and End Segments.....	43
Figure 3.9. Stages of Construction.....	48
Figure 3.10. Prestressing Details for Continuous Prestressed Concrete Shored Construction.	49
Figure 3.11. Post-Tensioning Layout for Continuous Prestressed Concrete Modified Tx70 Girder Bridge Using Shored Construction.....	53
Figure 3.12. Section Locations for Girder Moments and Stress Checks.	54
Figure 3.13. Moments Acting on Non-Composite Girder.	55
Figure 3.14. Moments Acting on Composite Girder.	56
Figure 3.15. Stress Check at Section A-A for (a) Construction and (b) In-Service before and after Losses.	58
Figure 3.16. Stress Check at Section B-B for (a) Construction and (b) In-Service before and after Losses.	59
Figure 3.17. Stress Check at Section C-C for (a) Construction and (b) In-Service before and after Losses.	60
Figure 3.18. Stress Check at Section D-D for (a) Construction and (b) In-Service before and after Losses.	61
Figure 3.19. Stress Check at Section E-E for (a) Construction and (b) In-Service before and after Losses.	62
Figure 3.20. Transverse Shear Demand and Capacity.	67
Figure 3.21. Shear Reinforcement Details.	68
Figure 3.22. Interface Shear Demand and Capacity	69
Figure 3.23. Partially Prestressed Splice Connection Detail.	70
Figure 4.1. Texas Girders Considered.	80
Figure 4.2. Texas U54 Girder.	81
Figure 4.3. Pretensioning and Stage I PT Schematic Layout for Shored Construction.....	84
Figure 4.4. Schematic Pretensioning Layout for Partially Shored Construction.....	85
Figure 4.5. Prestressing Layout for Shored and Partially Shored Construction.	86
Figure 4.6. Section Locations for Girder Moments and Stress Checks.	88
Figure 5.1. Elevation of the Prototype Bridge Showing the Test Specimen.	101
Figure 5.2. Cross-section of the Prototype Bridge Showing the Test Specimen.....	102

Figure 5.3. Replication of Maximum Moment and Shear at Service in Test Specimen.....	104
Figure 5.4. Plan View of the Test Specimen in the High Bay Laboratory.	105
Figure 5.5. Elevation View of Test Specimen.	106
Figure 5.6. Typical Section Geometry of Modified Tx70 Girder with Widened Web (Adapted from TxDOT 2010).	109
Figure 5.7. Test Specimen Design Moments Acting on Non-composite Girder.	114
Figure 5.8. Test Specimen Design Moments Acting on Composite Girder.	115
Figure 5.9. Service Stress Analysis for Specimen.	116
Figure 5.10. Splice Detail Used for Test Specimen.	119
Figure 5.11. Details of Concrete Pedestals.	122
Figure 5.12. Bearing Pad Details.	123
Figure 5.13. Installing Reinforcement at the Precast Plant.	124
Figure 5.14. Casting Girder Segments and Samples at the Precast Plant.	125
Figure 5.15. Transporting Girder Segments to the High Bay Laboratory.	126
Figure 5.16. Final Girder Segment Placement and Alignment in the High Bay Laboratory.	126
Figure 5.17. Splice Reinforcement and Formwork.	128
Figure 5.18. Falsework and Deck Formwork.	129
Figure 5.19. Adding Materials to Concrete Mixture for Connections.	129
Figure 5.20. Placing Concrete for Splice Connections (Continued).	131
Figure 5.21. Construction of the Deck Slab.	132
Figure 5.22. Splice DEMEC and LVDT Layouts.	133
Figure 5.23. Tendon Post-tensioning and Grouting Process.	135
Figure 5.24. Rebar Strain Gages in the Specimen.	137
Figure 5.25. Surface Gages on the Specimen.	139
Figure 5.26. Embedded Concrete Gages in the Specimen.	140
Figure 5.27. LVDTs Mounted on the Web of Specimen.	141
Figure 5.28. String Potentiometers Mounted on the Specimen.	142
Figure 5.29. Pretensioning Losses.	145
Figure 5.30. Effect of Post-Tensioning over 19 Days.	145
Figure 5.31. Post-tensioning Effect on Three Splices prior to Grouting.	148
Figure 5.32. Longitudinal and Vertical Strain in Anchorage Zone.	149
Figure 5.33. Pre-test Strain Profile History for Splice 2 (<i>Top row shows the pure effect of each phenomena, and bottom row shows the accumulative strain profile</i>).	150
Figure 5.34. Relationships Used to Describe Material Stress versus Strain.	153
Figure 5.35. Moment-Curvature Comparison at Different Locations for Positive and Negative Moments.	155
Figure 6.1. Side Elevation of the Specimen and Labeling.	158
Figure 6.2. Specimen Setup and Visual Condition during Test 1.	162
Figure 6.3. Specimen Setup and Visual Condition during Test 2.	163
Figure 6.4. Test Setup and Visual Condition of Splice 2 during Test 3.	164
Figure 6.5. Visual Condition of Specimen during Test 3.	165
Figure 6.6. Specimen Setup and Visual Condition during Test 4.	169
Figure 6.7. Specimen Setup and Visual Condition during Test 5.	171
Figure 6.8. Crack Pattern.	172
Figure 6.9. Force Deformation Diagram for Positive and Negative Moments.	174
Figure 6.10. Moment-Curvature Diagrams for Splices and Interior Support.	176

Figure 6.11. Longitudinal Reinforcement Behavior.....	179
Figure 6.12. Transverse Bar Behavior.....	180
Figure 6.13. Concrete Gage Readings and Associated Moment-Curvature Diagrams.....	181
Figure 6.14. Bending and Total Strain Profile of Splice 2 during Test 1.....	183
Figure 6.15. Bending and Total Strain Profile of Splice 3 during Test 2 – Part 1.....	184
Figure 6.16. Bending and Total Strain Profile of Splice 2 during Test 2 – Part 2.....	185
Figure 6.17. Bending and Total Strain Profile of Splice 2 during Test 3.....	186
Figure 6.18. Bending and Total Strain of Splice 3 during Test 4.....	187
Figure 6.19. Bending and Total Strain Profile of Splice 1 during Test 5.....	188
Figure 6.20. Longitudinal Beam Deformation.....	190
Figure A.1. Adding Materials to Concrete Mixture.....	A-5
Figure A.2. Spliced Girder Concrete Compressive Strength Data.....	A-9
Figure A.3. Girder Concrete Compressive Strength Experimental Data.....	A-10
Figure A.4. Girder Concrete Average Compressive Strength Experimental Data.....	A-11
Figure A.5. Connection Concrete Compressive Strength Experimental Data.....	A-12
Figure A.6. Deck Concrete Compressive Strength Experimental Data.....	A-13
Figure A.7. Spliced Girder MOE Experimental Data.....	A-14
Figure A.8. Girder Concrete MOE Experimental Data.....	A-15
Figure A.9. Connection Concrete MOE Experimental Data.....	A-16
Figure A.10. Deck Concrete MOE Experimental Data.....	A-17
Figure A.11. Spliced Girder STS Experimental Data.....	A-18
Figure A.12. Girder Concrete STS Experimental Data.....	A-19
Figure A.13. Connection Concrete STS Data.....	A-20
Figure A.14. Deck Concrete STS Experimental Data.....	A-21
Figure A.15. Spliced Girder MOR Experimental Data.....	A-22
Figure A.16. Girder Concrete MOR Data.....	A-22
Figure A.17. Connection Concrete MOR Data.....	A-23
Figure A.18. Deck Concrete MOR Experimental Data.....	A-24
Figure A.19. Spliced Girder Shrinkage Data.....	A-25
Figure A.20. Loading of the Creep Frames.....	A-26
Figure A.21. Data from the Creep Frames.....	A-27
Figure A.22. Mild Steel Stress-Strain Test.....	A-28
Figure A.23. Stress-Strain Curve for Mild Steel.....	A-30
Figure A.24. Prestressing Strand Tensile Test.....	A-31

LIST OF TABLES

	Page
Table 2.1. Local Post-Tensioned Splicing (adapted from Hueste et al. 2012).	8
Table 2.2. General Continuity Post-Tensioned Prestress (adapted from Hueste et al. 2012, based on Ronald 2001).....	9
Table 3.1 Section Properties for Prismatic Modified Tx70 Girder (9 in. Web).	29
Table 3.2. Design Parameters.	30
Table 3.3. Dead Loads for Modified Tx70 Girder.....	32
Table 3.4. LRFD Live Load DFs for Concrete Deck on I-Girder.	34
Table 3.5. Summary of Allowable Stress Limits in Girder.	37
Table 3.6. Summary of Allowable Stress Limits in Deck.	37
Table 3.7. Segment Lengths and Girder Weights.	43
Table 3.8. Summary of Pretensioning Design.....	44
Table 3.9. Stage I Post-Tensioning Design.	45
Table 3.10. Stage II Post-Tensioning Design.	46
Table 3.11. Girder Moments at Various Sections (kip-ft).	54
Table 3.12. Girder Stresses at Various Sections (ksi).....	63
Table 3.13. Live Load Deflection for Three-span Modified Tx70 Bridge.....	65
Table 3.14. Ultimate Demand and Capacity.....	66
Table 3.15. Reinforcement Details for the Splices.	71
Table 3.16. Prestressing Details for the Splices.....	71
Table 3.17. Shear Design Details for Splices.	72
Table 3.18. Principal Tension Stress Calculation.	73
Table 4.1. Design Cases.....	78
Table 4.2. Design Parameters.	79
Table 4.3. Section Properties for Texas Girders.	82
Table 4.4. Segment Lengths and Weights – Span Configuration (190-240-190 ft).	83
Table 4.5. Segment Lengths and Weights – Span Configuration (150-200-150 ft).	83
Table 4.6. Pretensioning – Span Configuration (150-200-150 ft).	86
Table 4.7. Pretensioning – Span Configuration (190-240-190 ft).	86
Table 4.8. Stage I PT – Span Configuration (150-200-150 ft).	87
Table 4.9. Stage I PT – Span Configuration (190-240-190 ft).	87
Table 4.10. Stage II PT Span Configuration (150-200-150 ft).	87
Table 4.11. Stage II PT – Span Configuration (190-240-190 ft).....	87
Table 4.12. Stresses at Sections A-A – Span Configuration (190-240-190 ft).....	89
Table 4.13. Stresses at Sections A-A – Span Configuration (150-200-150 ft).....	90
Table 4.14. Stresses at Section E-E – Span Configuration (190-240-190 ft).	90
Table 4.15. Stresses at Section E-E – Span Configuration (150-200-150 ft).	91
Table 4.16. Stresses at Section B-B – Span Configuration (190-240-190 ft).....	91
Table 4.17. Stresses at Section B-B – Span Configuration (150-200-150 ft).....	92
Table 4.18. Stresses at Section D-D – Span Configuration (190-240-190 ft).	92
Table 4.19. Stresses at Section D-D – Span Configuration (150-200-150 ft).	93
Table 4.20. Stresses at Section C-C – Span Configuration (190-240-190 ft).....	93
Table 4.21. Stresses at Section C-C – Span Configuration (150-200-150 ft).....	94

Table 4.22. Live Load Deflections – Span Configuration (190-240-190 ft).....	94
Table 4.23. Live Load Deflections – Span Configuration (150-200-150 ft).....	95
Table 4.24. Moment Capacity and Demand at Ultimate – Span Configuration (190-240-190 ft).....	96
Table 4.25. Moment Capacity and Demand at Ultimate – Span Configuration (150-200-150 ft).....	96
Table 4.26. Compression Steel for Ductility – Span Configuration (190-240-190 ft).....	97
Table 4.27. Compression Steel for Ductility – Span Configuration (150-200-150 ft).....	97
Table 4.28. Shear Design Details – Span Configuration (190-240-190 ft).....	97
Table 4.29. Shear Design Details – Span Configuration (150-200-150 ft).....	98
Table 5.1. Weight of Girder Segments.....	103
Table 5.2. Section Properties for Modified Tx70 Girder with Widened Web.....	109
Table 5.3. Design Parameters for Specimen.....	110
Table 5.4. Prestressing Summary for the Specimen.....	112
Table 5.5. Shear Reinforcement Details for Specimen.....	117
Table 5.6. Principal Tension Stress Calculations for Specimen.....	118
Table 5.7. Reduced Nominal Moment Capacity for Splice Connections.....	120
Table 5.8. Splice Concrete Mixture Proportions.....	127
Table 5.9. Summary of Fresh Properties of Concrete.....	129
Table 5.10. Post-tensioning Calculation.....	134
Table 5.11. Summary of Rebar Strain Gages.....	138
Table 5.12. Instrumentation Summary.....	143
Table 5.13. Concrete Properties for Numerical Analysis.....	152
Table 5.14. Properties of Mild Steel.....	152
Table 6.1. Table of Events at Splice 2 for Test 1.....	159
Table 6.2. Table of Events for Test 2.....	160
Table 6.3. Table of Events at Splice 2 for Test 3.....	161
Table 6.4. Table of Events for Test 4.....	166
Table 6.5. Table of Events at Splice 1 for Test 5.....	170
Table A.1. Girder SCC Mixture Proportions Summary.....	A-2
Table A.2. Splice Concrete Mixture Proportions.....	A-3
Table A.3. Overview of Fresh Property Tests for Concrete.....	A-4
Table A.4. Summary of Girder Concrete Fresh Properties.....	A-4
Table A.5. Slump of Connection Concrete.....	A-6
Table A.6. Summary of Deck Concrete Fresh Properties.....	A-6
Table A.7. Overview of Hardened Property Tests for Concrete.....	A-7
Table A.8. Test Matrix for Spliced Girder Segment Concrete by Batch.....	A-8
Table A.9. Girder Concrete Average Measured Compressive Strength (ksi).....	A-11
Table A.10. Connection Concrete Average Measured Compressive Strength.....	A-13
Table A.11. Deck Concrete Average Measured Compressive Strength.....	A-14
Table A.12. Girder Concrete Average Measured MOE (ksi) by Batch.....	A-15
Table A.13. Connection Concrete Average Measured MOE.....	A-16
Table A.14. Deck Concrete Average Measured MOE (ksi) by Batch.....	A-17
Table A.15. Girder Concrete Average STS (ksi) by Batch.....	A-19
Table A.16. Connection Concrete Average Measured STS.....	A-20
Table A.17. Deck Concrete Average Measured STS (ksi) by Batch.....	A-21

Table A.18. Girder Concrete Average MOR (ksi) by Batch.	A-23
Table A.19. Connection Concrete Average Measured MOR.	A-23
Table A.20. Deck Concrete Average Measured MOR.	A-24
Table A.21. Force Applied to the Creep Frames	A-26
Table A.22. Mechanical Properties of #5 Bars.	A-29
Table A.23. Mechanical Properties of #6 Bars.	A-29
Table A.24. Mechanical Properties of Prestressing Strands.	A-31

1 INTRODUCTION

1.1 BACKGROUND

Significant traffic and congestion across urban areas, as well as longer waterway crossings, creates a demand for medium- to long-span bridges. The construction of these longer spans plays a critical role in the development of modern infrastructure due to safety, environmental, and economic concerns. Bridge planning, design, and construction techniques have evolved to satisfy several parameters including feasibility, ease of construction, safety, maintainability, and economy. For over 60 years, precast, prestressed concrete girders have been effectively used in different states across the nation because of their durability, low life-cycle cost, and modularity, among other advantages. These girders are typically used for full length, simply supported bridges. However, there has been a growing need in the transportation sector to build longer spans with readily available standard precast, prestressed concrete girder shapes.

Methods used to extend span ranges with incremental variations in materials and conventional design procedures typically result in relatively small increases in span range for precast, prestressed concrete girders. On the other hand, splicing technology facilitates construction of longer spans using standard length girder segments. A spliced girder system can provide a number of constructible design options by altering parameters such as span and segment lengths, depth of superstructure, and number and location of piers.

Most prestressed concrete slab-on-girder bridges are simply supported with precast, pretensioned girders and a cast-in-place (CIP) deck. Spans are limited to about 150 ft due to weight and length restrictions on transporting the precast girder units from the prestressing plant to the bridge site. Such bridge construction, while economical from an initial cost point-of-view, may become somewhat limiting when longer spans are needed. According to the available literature, a several methods have been used to extend the span range of concrete slab-on-girder bridges. These include the use of high performance materials and modified girder sections (Abdel-Karim and Tadros 1995). However, it is necessary to modify the layout and provide continuity connections between the spans to significantly increase the span length.

Spliced girder bridge construction can provide a less complex solution compared to segmental concrete bridge girder construction by reducing the number of girder segments. Spliced precast, prestressed concrete girders were found to be the preferred solutions of contractors, as

observed in performance-based bids of projects in several states (Castrodale and White 2004). For these longer spans, continuity between the girder segments has the advantage of eliminating bridge deck joints, which leads to reduced maintenance costs and improved durability.

The performance and cost-effectiveness of a spliced girder system depends on the design and construction details. This involves a combination of the different design enhancements instead of applying them individually. The main challenges for designers, contractors, and fabricators are: (1) how to best apply prestressing considering transportation, erection, and service loads, and (2) how to best splice girders together to provide continuity. Naturally, the three facets of design, fabrication, and construction are inextricably connected. So, the challenge becomes how to best extend bridge spans from about 150 ft to as much as 300 ft.

This report documents Phase 2 of a two-phase research study sponsored by the Texas Department of Transportation (TxDOT). The Phase 1 Research Report (Hueste et al. 2012) includes a review of the key techniques that have been used for spliced continuous precast concrete bridge girder systems; a discussion of a number of construction considerations; a summary of preliminary designs; a proposed general framework for categorizing connection splice types; a summary of input from precasters and contractors; and some potential connection details.

This Phase 2 Research Report reviews key findings from Phase 1 of this study; presents an overview of a prototype continuous bridge girder design; presents detailed spliced, continuous, precast concrete bridge girder designs for both a shored and a partially shored case; presents the experimental program and results for a full-scale girder with three spliced connections; summarizes the spliced girder designs included in the parametric study; and provides recommended continuity connections and details for in-span splices.

1.2 SIGNIFICANCE

Bridges are a critical element of the transportation system and provide a link over urban congestion, waterways, and valleys. The capacity of individual bridges controls the volume and the weight of the traffic carried by the transportation system, and is also expensive at the same time. Therefore, it becomes necessary to achieve a balance between handling future traffic volume and load, and the cost of a heavier and wider bridge structure.

Economic, aesthetic, and environmental demands often result in the need for a longer span range, fewer girder lines, and a minimum number of substructure units in the bridge system.

Designers, fabricators, and contractors, upon successful collaboration, can take advantage of applying continuous construction to the standard precast, pretensioned girders developed by different states. Continuity in precast, prestressed concrete girders provides another cost-effective, constructible, and high performance alternative that can be used for longer spans that are often constructed with custom steel plate girders, steel box girders, and post-tensioned segmental girders.

This research study identifies and investigates continuity details for spliced continuous, precast concrete girder bridges. The key outcome of the project is recommendations for standard design procedures for this type of bridge system for use in Texas for prospective longer span bridge projects. Current design guidelines for spliced precast concrete girders are evaluated in light of the research findings, and specific design recommendations are provided for this class of bridge structures.

1.3 OBJECTIVES AND SCOPE

The objectives of this project are to review, evaluate, and recommend details for the design of durable and constructible connections that achieve structural continuity between the specific precast, prestressed concrete girder sections that are used in Texas with a goal of longer span-to-depth ratios and greater economy as compared to simply span construction. Phase 2 of this study, described in this report, focuses on the use of inflection point and other in-span splices. Specifications and continuity details are recommended, and proposed details are evaluated through experimental testing.

1.4 RESEARCH PLAN

The outcome of this research study will support TxDOT's implementation of continuous precast, prestressed concrete bridge girders to achieve longer span-to-depth ratios than currently possible with simple spans. The purpose of the Phase 1 tasks was to gather, review, and document the relevant research literature, current state-of-the-practice, and input from key stakeholders. This information was compiled in the *Phase I Research Report* (Hueste et al. 2012) for use in refining the work plan for Phase 2.

The purpose of the Phase 2 tasks is to continue the analytical and design studies; conduct experimental testing of selected continuity details; develop recommended continuity details,

specifications, and examples; host a workshop for TxDOT bridge engineers; and complete and submit the final research reports. The following tasks were carried out in order to achieve the objectives of Phase 2 of the project.

1.4.1 Parametric Studies

Parametric analysis and design studies further evaluated the impact of continuity on typical Texas precast, prestressed concrete bridges. An overview of a typical continuous precast girder design for shored construction is provided, and the remaining designs are summarized. Information from Phase 1 of this project gave a basis for selecting appropriate parameters and the corresponding range of values for each parameter. Parameters varied include the girder section type and depth, construction method (shored versus partially shored), and span configuration. In addition to determining and comparing trends with respect to increasing span lengths and construction approach, the parametric study identifies critical design limit states for the selected geometries.

1.4.2 Experimental Testing

The experimental program focused on testing one full-scale girder test specimen containing three splice connections between precast girder segments to evaluate the structural performance and integrity of the selected connection details. The segments were cast at a precast plant, and the remaining construction was completed in the laboratory. The specimen was fully instrumented, and measurements were collected electronically during post-tensioning (PT) and load testing. The loading sequence included modeling of service load conditions, and then the force was increased until failure occurred or the actuator limit was reached. The appropriateness of current analytical models and design provisions in estimating the measured response of the test specimens were determined.

1.4.3 Develop Continuity Details and Design Recommendations

This project focused on developing splice connection details for achieving continuity using precast, pretensioned bridge girders. A specific splice connection detail was designed and tested at full scale. Specific American Association of State Highway and Transportation Officials (AASHTO) Load and Resistance Factor Design (LRFD) design limit states that must be satisfied for the overall continuous girder design and splice connection design are presented and discussed. Additional design recommendations based on the project findings are provided.

1.4.4 Develop Continuity Design Examples

Detailed spliced girder design examples, found in the appendices of this report, illustrate applications of the recommended continuity design guidelines for typical Texas bridges. The design examples include a shored Tx70 prismatic girder and a partially shored Tx70 haunched girder. Both cases have a 240 ft main span and 190 ft end spans.

1.4.5 Report Preparation

A complete Phase 2 Research Report and a Project Summary Report document the findings of this project. The above listed tasks and related findings are reported herein. This Phase 2 Research Report includes (1) a summary of items included in the Phase 1 Research Report including the motivation for focusing on specific continuity details in Phase 2 of the research, (2) results of a parametric study to evaluate various spliced girder designs including an assessment of continuity effects, (3) results of the full-scale experimental testing of spliced girder connections, (4) recommended continuity design guidelines, and (5) detailed continuity design examples.

1.5 REPORT OUTLINE

Following this introductory chapter, Chapter 2 summarizes Phase 1 key findings and provides additional background on the state-of-the-art and practice relevant to Phase 2 objectives of this project. Chapter 3 describes the prototype bridge, from which the experimental study specimen was extracted, and provides an overview of the design. Chapter 4 documents the parametric study to evaluate the potential for spliced, continuous girders using TxDOT standard precast concrete shapes for both shored and partially shored construction. Chapter 5 describes the abstraction of the specimen followed by an overview of the specimen design, construction, PT process, instrumentation, and measurements prior to load testing. Chapter 6 documents the results of the experimental program and observations for the three splice connections tested under different levels of shear and moment demands. Chapter 7 summarizes the overall project, findings, and recommendations including a detailed assessment of current design requirements and guidelines relevant to spliced precast girders. In addition, recommendations for design and implementation are provided based on the results of this research project. Appendix A includes measured material properties for the concrete, mild steel reinforcement, and prestressing strands used to construct the test specimen. Appendix B provides detailed drawings of the test specimen.

2 STATE-OF-THE-ART AND PRACTICE CONTEXT

2.1 SCOPE OF CHAPTER

In the Phase 1 Research Report (Hueste et al. 2012), a detailed literature review was presented in which relevant past research related to spliced girders was addressed. In this chapter, highlights of the literature review from TxDOT Report 0-6651-1 (Phase 1 Research Report) are presented. In addition, more detailed information from National Cooperative Highway Research Program (NCHRP) Report 517 (Castrodale and White 2004) is provided including specific findings and proposed revisions to the AASHTO LRFD Specifications. Finally, research updates are described and a very recent field implementation of a spliced continuous prestressed concrete girder bridge is presented in detail.

2.2 HIGHLIGHTS FROM TXDOT PHASE 1 REPORT

2.2.1 On-Pier Splicing

On-pier splicing of girders is primarily used to provide span-to-span continuity, enhancing live load carrying capacity. Precast-prestressed girder units generally do not exceed 160 ft. While this limitation is typically governed by the prestressed girder weight, often girder unit lengths are limited to 140 ft due to transportation roadway restrictions between the casting plant and bridge site. Past research dealing with on-pier splicing can be divided into two main categories: (1) designs including PT options, and (2) reinforced concrete options that do not require field PT operations.

Hueste et al. (2012) presented a thorough literature review on previous studies and application of splicing in continuous prestressed concrete girder bridges in TxDOT Report 0-6651-1. The following references were presented in the Phase 1 literature review: Kaar et al. (1960), Mattock and Kaar (1960), Bishop (1962), Abdel-Karim and Tadros (1995), Lounis et al. (1997), Mirmiran et al. (2001), Tadros and Sun (2003), Castrodale and White (2004), Miller et al. (2004), Sun (2004), Dimmerling et al. (2005), Newhouse et al. (2005), Tadros (2007), and Koch (2008).

While certain on-pier splicing methods may be quite economical and include straightforward fabrication and erection details, the major disadvantage limiting the span length to 160 ft remains. For longer spans, the designer inevitably needs to consider using in-span splicing, which is the major subject of this research.

2.2.2 In-Span Splicing

In-span splicing provides the possibility to significantly increase the span length by providing continuity, potentially doubling the interior span limit to approximately 300 ft. Different types of in-span splicing designs have been described in the Phase 1 Research Report. Those designs can be divided into two broad categories including: (1) locally post-tensioned spliced and (2) general post-tensioning of girder segments to provide continuity.

2.2.2.1 Locally Post-Tensioned Spliced

This method does not aim to provide overall load balancing prestress; rather, it aims to limit field operations that use PT. While this approach is perhaps the most straightforward from a construction standpoint, there is a general lack of continuity and of advantageous load balancing. Table 2.1 provides more detail regarding this method of splicing.

Table 2.1. Local Post-Tensioned Splicing (adapted from Hueste et al. 2012).

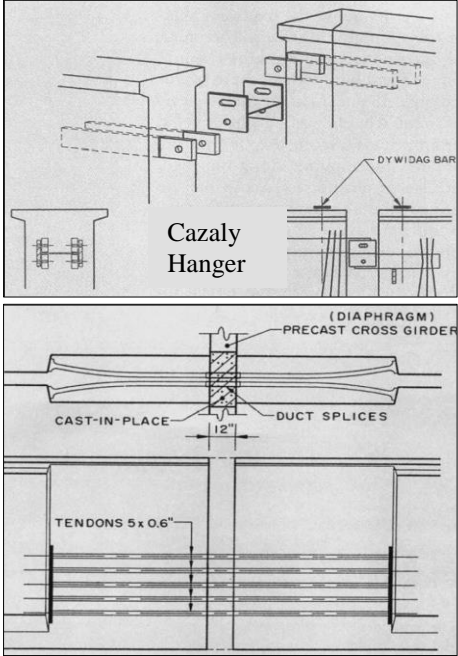
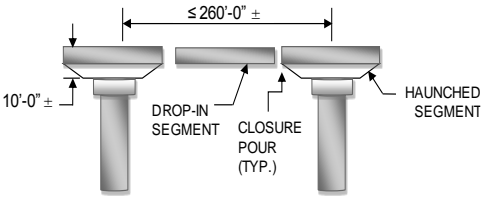
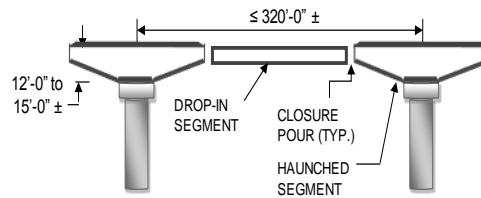
Splice Type	Advantages	Disadvantages
Prestressed for Simple Span and Partially Post-Tensioned for Continuity (Caroland et al. 1992)		
<p>Maximum Span length = 250 ft</p> 	<ul style="list-style-type: none"> ▪ Girder segments were made continuous by stressing partial (short) length post-tensioned strands between the adjacent ends of the girder segments. ▪ The partial length post-tensioned strands were found to fully withstand the service stresses and ultimate strength conditions. ▪ Economical solution compared to steel plate girder alternatives in span range of 130 ft to 250 ft. 	<ul style="list-style-type: none"> ▪ No continuity tendons were provided throughout the length of the bridge. Therefore, complete load balancing was not achieved. ▪ Special attention was required in construction of the partially post-tensioned splice connection. ▪ End blocks were needed in the girder segments to anchor the partial post-tensioned strands.

Table 2.2. General Continuity Post-Tensioned Prestress (adapted from Hueste et al. 2012, based on Ronald 2001).

Bridge Description	Advantages	Disadvantages
<p>Maximum Span Length = 260 ft</p>  <ul style="list-style-type: none"> ▪ Girder section is Florida bulb-tee with 78 in. depth ▪ Girder spacing = 11ft 6 in. ▪ Closure pour width =1 ft 6 in. ▪ Web thickness of bulb-tee = 9 in. ▪ Depth of Haunched segment = 10 ft ▪ Length of Haunched segment = 110 ft 	<ul style="list-style-type: none"> ▪ Stage 1 PT: Allowed girders to be made continuous. ▪ Stage 2 PT: Provided residual compression in the deck for serviceability and deflection control. ▪ Cost of PT was offset by use of few girder lines and greater spacing between girders. ▪ Span lengths were extended beyond the practical limits of standard precast shapes. ▪ No intermediate diaphragms were used. 	<ul style="list-style-type: none"> ▪ Cost of superstructure increased with longer spans. ▪ The deeper the haunch, the greater was the negative moment drawn toward interior piers. ▪ Long, slender bulb-tee girders deflected and twisted during handling and erection. ▪ Restriction in the length of the haunched segment based on the amount of prestress that can be provided in the top flange of the girder to resist cantilever bending before PT.
<p>Maximum Span Length = 320 ft</p>  <ul style="list-style-type: none"> ▪ Girder section is Florida bulb-tee with 78 in. depth ▪ Girder spacing = 9 ft 6 in. ▪ Closure pour width =1 ft 8.5 in. ▪ Web thickness of bulb-tee = 9 in. ▪ Depth of Haunched segment = 12 ft ▪ Length of Haunched segment = 115 ft ▪ For Girders and Closure pours: $f'_c = 8500$ psi ▪ For Deck: $f'_c = 6500$ psi ▪ Strands: 0.6 in. diameter, ASTM A416, Grade 270 low relaxation 	<ul style="list-style-type: none"> ▪ Fewer massive piers were used for longer spans. ▪ Wide web thickness of 9 in. to accommodate tendons with 16 strands. ▪ Shear key was provided in webs for interlocking. ▪ Blisters were used at closure points to overlap tendons. ▪ Minimum impact on surrounding environment and traffic during construction. 	<ul style="list-style-type: none"> ▪ Difficult to transport heavy haunched girder segments.

2.2.2.2 *General Post-Tensioning of Girder Segments to Provide Continuity*

As outlined in Table 2.2, post-tensioned prestress is applied over several girders to provide continuity. Generally, the tendons are placed in ducts that are stressed and later grouted. If the ducts are draped through the girder segments, load balancing of gravity effects may be applied. This negates deflections within each span, while the bridge deck section is subject to an almost constant state of axial compressive stress. By providing continuity load-balancing PT, span lengths may be substantially increased to some 300 ft. For more information, refer to Caroland et al. (1992), Janssen and Spaans (1994), Endicott (1996), Fitzgerald and Stelmack (1996), Ronald (2001), Tadros and Sun (2003), Castrodale and White (2004), Endicott (2005), and Nikzad et al. (2006). This previous body of work was considered in developing prototype designs for the present investigation.

2.2.3 **Highlights of Discussions with Industry Stakeholders**

The findings of the Phase 1 review of the literature and state-of-the-practice were presented in two focus group meetings consisting of (1) precasters that are responsible for casting the girder units and transporting them to the construction site, and (2) general bridge contractors that are concerned with the erection, splicing, and PT of the girder components, as well as the construction of the remainder of the bridge including the deck and substructure. In addition, members of the TxDOT project monitoring committee attended the meetings. The main findings from the focus group meetings are provided below. Additional input can be found in the Phase 1 Research Report (Hueste et al. 2012).

Findings from the precasters are:

- In general, all the precasting plants are well equipped to handle fabricating a variety of over-pier, end, and drop-in segments.
- Increasing the span length results in an increase in the weight of precast elements. Precautions should be taken so that the weight does not exceed 200 kips considering transportation limits.
- The desirable limits for I-girder segments is length around 140 ft, weight around 200 kips, and depth around 10 ft. For the U-girder shapes, researchers recommend limiting the segment length to 130 ft considering weight limits for transportation.

- The recommended maximum span length for a spliced girder bridge is around 260 ft, considering the stability issues of long-span drop-in segments and deep haunched over-pier segments.
- Use of a constant standard girder section depth for over-pier segments is preferred over the haunched girders to avoid issues related to high initial cost of fabrication, stability issues during transportation, and lifting weight issues onsite.
- There are no concerns with widening the webs to resolve the issue of maximum shear demand at the supports. The webs can be widened by increasing the space between the forms, which will result in widened top and bottom flanges of the girder section. It is a one-time cost to purchase a new soffit. Standardizing the precast elements will help reduce the overall cost.
- Fabricating end segments with thickened ends is not an issue. The length of an end block is typically 10–15 ft.
- Of the four different types of splice connections discussed (ranging from fully reinforced/non-prestressed to fully prestressed with PT), the precasters preferred partially prestressed spliced connection details.
- Some discussion was held about using longer precast panels over the supports with longitudinal prestressing. The precasters indicated that this should be no problem.

Findings from the contractors are:

- The proposed bridge system provides another alternative to steel girder bridges, especially in coastal areas where corrosion of steel bridges is an issue.
- Experienced contractors prefer to limit the span range for the continuous spliced girders to approximately \pm 250 ft to 270 ft.
- Unshored construction (no shoring towers) is preferred because it saves significant time during construction and reduces the construction costs. Often the required footprint is not available to place shore towers.
- Using fewer girders increases cost competitiveness of bridges.
- The contractor suggested that keeping the girder weights as low as possible and adopting repetitive girder details aid in better pricing by the precasters.

- Contractors prefer the constant web depth option for the haunched girders because it is easy to fabricate and has more stability.
- Contractors noted that the option of two separate girder segments spliced over the pier provides flexibility of splicing the girder segments within span on ground before lifting them into place on site. This is a preferred option because no temporary shoring is required onsite. However, issues related to the weight of the whole assembly and the size of the equipment in lifting and placing the spliced girder segments are anticipated.
- The main issue noted during erection of the girders is the lateral stability of the girder segments due to wind.
- The partially prestressed connection detail was the most preferred with respect to on-site construction due to its relative constructability.
- Contractors prefer having two design options for bid: one with a standard precast concrete girder shape and one with a steel plate girder.
- The quality control process is more complex for the proposed bridge system.
- Sequencing of the CIP concrete and PT operations are needed up front.
- Contractors look at both schedule and economy to determine the best option.

Additional findings from the designer/owner (TxDOT) are:

- TxDOT engineers noted that this bridge type would compete well with shorter span segmental bridges. They also indicated that they are not using steel girder bridges along the coast, and the proposed bridge type would not compete with just steel girder bridges.
- It would be useful to consider various design options using life-cycle cost analysis. TxDOT is just now starting to use life-cycle cost analysis. Traditionally, initial cost has been used to evaluate design options.
- TxDOT engineers preferred solutions where the fascia girder did not possess a widened end at the drop-in splice location. This sentiment was to preserve the clean lines of the side elevation of the bridge deck. However, this presents a significant challenge, with the resulting narrow web solution it is not possible to terminate and anchor the PT; the PT must run continuously through the splice. One option is retain the same profile as the girder only for the outside face of the fascia girder. The inside face of the fascia

girder, along with both faces of the interior girders, could be widened at the ends adjacent to the splices to accommodate the PT anchorage.

2.3 NCHRP REPORT 517 HIGHLIGHTS

2.3.1 Summary

Through the research investigation described in NCHRP Report 517 (Castrodale and White 2004), standard details and design examples for long-span continuous precast, prestressed concrete bridge girders were presented. From the results of the trial designs, changes and enhancements to the AASHTO code were also proposed. Castrodale and White (2004) also confirmed that precast, prestressed concrete bridge girders are rarely used for spans exceeding 160 ft due to material limitations, hauling size and weight limitations, and lack of design aids for the design of long span prestressed concrete girders. Castrodale and White (2004) identified around 250 proven, spliced, precast, prestressed concrete girder bridges built around the nation but the experience and information on these job specific projects was not available widely for use on similar proposed bridge projects.

This report provided the needed documentation on all the known technologies for extending the span lengths of the prestressed concrete girders to 300 ft. From the assessment of all these methodologies, this study concluded that the splicing of precast, prestressed concrete girders has the potential to significantly increase the span lengths without the need to change the section to more expensive segmental box girder alternatives.

Castrodale and White (2004) identified the use of splicing with multiple means and locations within the span, and provided a list of similarities and differences between spliced girder construction and the segmental bridge construction. NCHRP Report 517 summarized both material-related options and design enhancements for extending the span lengths. The material-related options included:

- High strength concrete.
- Specified density concrete.
- Increased strand size.
- Increased strand strength.
- Decks of composite materials.

The alternatives for design enhancements included:

- Modifying standard girder sections.
- Creating new standard girder sections.
- Modifying strand pattern or utilization.
- Enhancing structural systems.
- Enhancing analysis and design methods.

The multiple design examples presented in NCHRP Report 517 provide guidance for comparing the potential alternatives to extend span lengths. The three examples present how to design a single span spliced PCI BT-96 Girder, a two-span spliced U-Beam Girder, and a continuous three-span girder. The three examples have in-span splices. Figure 2.1 presents the three examples.

2.3.2 AASHTO Code Revisions

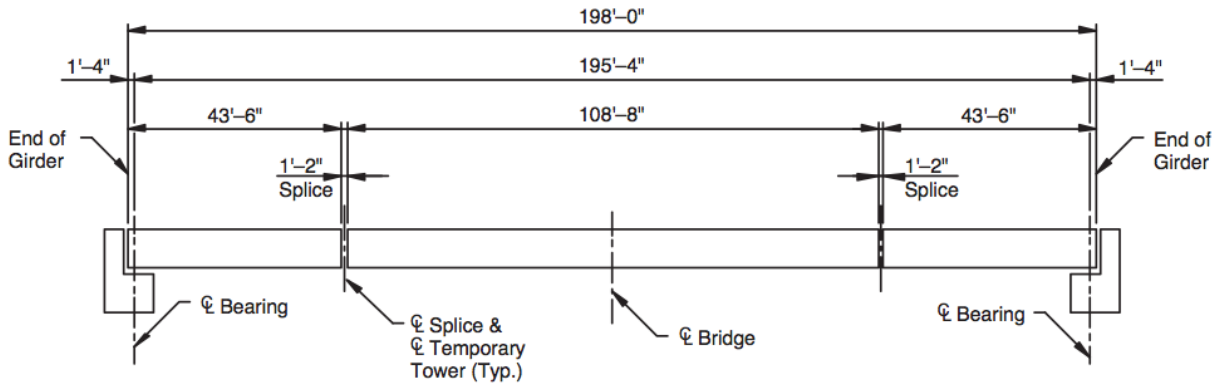
The proposed revisions to the AASHTO LRFD Specifications are found in Appendix E of the NCHRP Report 517 by Castrodale and White (2004). The proposed revisions were based on the second edition of the AASHTO LRFD Specifications and interim revisions from 1998 to 2003. Most of the proposed revisions were implemented in the 4th edition of the AASHTO LRFD Specifications (AASHTO 2007).

Among the changes are two definitions that were added to define “Segmental Construction” and “Spliced Precast Girder.” A new section was added to provide special considerations for spliced precast girders (AASHTO 2012, Article 5.14.1.3). Some of the main articles that were modified and added to the AASHTO LRFD Specifications are discussed as follows:

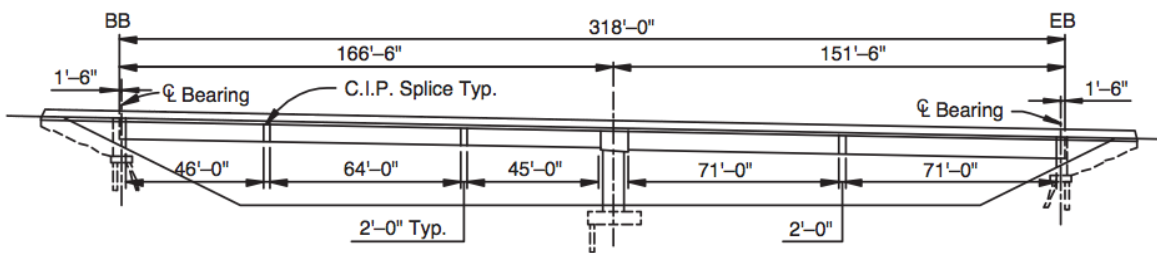
- As proposed by Castrodale and White (2004), the AASHTO LRFD Specifications (2012) include Article 5.14.1.3 dedicated to the design of spliced precast concrete girders and to clarify the differences between typical segmental bridges and spliced precast girder bridges. This article provides additional information for classifying spliced precast girder bridges from a design standpoint. Commentary Article C5.14.1.3.1 (AASHTO 2012) enumerates how spliced precast girder bridges are differentiated from segmental construction and identifies the design approach to be used. This article specifies the length

of individual segments, joints between the segments, number of girder lines, and cross section type as the main distinctions between segmental bridges and spliced concrete girder bridges.

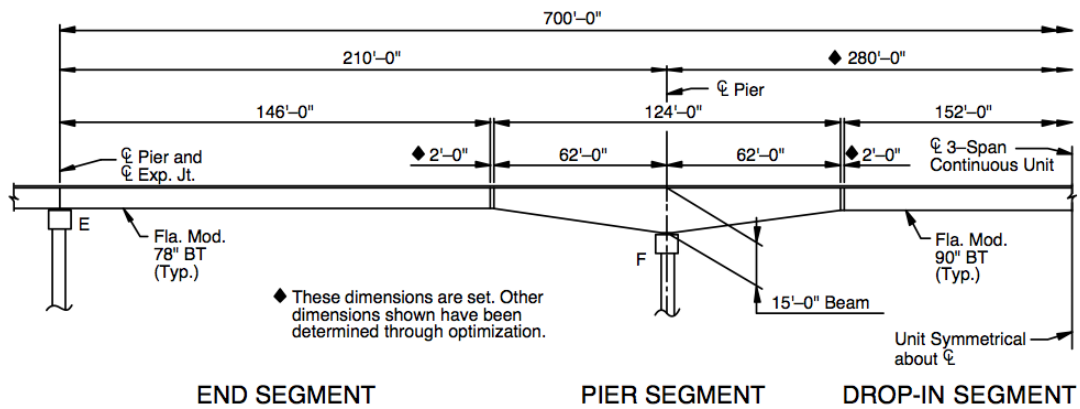
- Based on Article 5.2 (AASHTO 2012), a spliced precast concrete girder is defined as: “A type of superstructure in which precast concrete beam-type elements are joined longitudinally, typically using PT, to form the completed girder. The bridge cross-section is typically a conventional structure consisting of multiple precast girders.” AASHTO also indicates that spliced precast girder superstructures shall not be considered to be the same as segmental construction.
- Article 5.9.5.2.3 (AASHTO 2012) is applicable to spliced precast girders, where it is stated that the effect of each stage of PT should be considered for the elastic shortening losses in previously post-tensioned and pretensioned strands.
- Article 5.14.1.3.1 (AASHTO 2012) provides some guidance for calculation of prestress losses in spliced precast girder bridges. It also states that once the splices are poured, the structure may be treated as fully continuous at all limit states for loads applied after splicing.
- According to Article 5.14.1.3.2d AASHTO (2012), stress limits for temporary concrete stresses in joints for segmentally constructed bridges provided in Article 5.9.4.1 can be adopted for splices in spliced precast girder bridges.



(a) Simply supported bridge with two in-span splices.



(b) Two-span continuous bridge with one splice within each span.



(c) Three-span continuous bridge with two splices within the central span and one splice in each of the side spans. For long central spans, it is often necessary to use haunched girders over the piers in the negative moment regions.

Figure 2.1. Design Examples from NCHRP Report 517 (Castrodale and White 2004).

2.4 DISCUSSION OF AASHTO LRFD SPECIFICATIONS RELATED TO SPLICED PRECAST CONCRETE GIRDER BRIDGES

2.4.1 General Criteria

The relevant articles of the AASHTO LRFD Specifications (AASHTO 2012) that refer to general criteria relevant to spliced precast concrete girder bridges are presented and discussed in this section as follows:

- As opposed to simply supported girder bridges, continuity of spliced concrete girder bridges allows redistribution of force effects under inelastic behavior of the girder in negative moment based on Article 4.6.4.1 (AASHTO 2012). According to the same article, redistribution cannot be used if inelasticity is based on shear failure or uncontrolled buckling. Based on the experimental results, the considered Tx sections may have brittle behavior in the negative moment region. In order to take advantage of moment redistribution, more ductility can be provided by adding compression mild steel in the bottom flange or by increasing the dimensions of the bottom flange. Either approximate or refined methods can be used to take the effect of redistribution into consideration.
- Article 4.6.2.9.5 (AASHTO 2012) states that construction type and schedule, along with time-dependent prestress losses and secondary moment effects due to prestressing, shall be considered in segmental concrete bridges. Considering the importance of construction sequence and schedule in spliced girder bridges, this article should be generalized to spliced girder bridges, as well. Because the time-dependent losses in prestress primarily take place in the early ages of casting and stressing, construction schedule should be considered in stress analysis of the structure under construction loads. Article 5.14.1.3.1 does note the importance of the method of construction for spliced precast girders, including time of removal of any temporary supports.
- AASHTO (2012) Commentary Article C5.14.1.3.4 provides insight into different construction sequence possibilities and how they would affect the concrete strength and number of PT tendons required in the closure joint. It points out that deck replacement can be problematic if part of the PT is applied after casting the deck. Based on results of the experimental study, researchers concluded that the existence of compression in the deck due to PT can highly increase the durability of the structure, as minor cracks due to live

load will close after the loads are removed. Based on this observation, it is recommended that part of the PT is applied after the deck is cast and sufficient strength is achieved. In the cases that freeze/thaw cycles cause deck damage (mostly northern states), a sacrificial concrete layer with a waterproof layer on top of the deck is suggested to avoid the necessity of full deck replacement.

- Article 4.6.6 requires analysis of the structure under the effect of temperature gradient. Commentary Article C4.6.6 provides a detailed process for considering the effect of temperature gradient for axial expansion, flexural deformation, and internal stresses. Considering continuity of the structure, both primary and secondary effects of temperature gradient should be considered in stress analysis of the structure. The secondary thermal stresses for the interior spans of a continuous bridge may be quite significant and of a similar magnitude to the live load stresses (Priestley 1976).
- Article 4.7.4.3 (AASHTO 2012) specifies the requirement for seismic analysis of multispan bridges. Table 4.7.4.3.1-1 provides different methods of analysis based on different seismic zones and the relative importance of the bridge. Most in Texas are categorized as low seismic hazard (Zone 1), so seismic analysis is not required. For bridges constructed in West Texas, which are categorized as Seismic Zone 2, a proper method of seismic analysis should be adopted based on the specifications.

2.4.2 Prestressing

Relevant articles in the AASHTO LRFD Specifications (AASHTO 2012) regarding prestressing are discussed as follows:

- Articles 3.4.3.1 and 3.4.3.2 (AASHTO 2012) define the jacking force and anchorage zone design forces. Based on these articles, the anchorage zone shall be designed for 1.2 times the maximum jacking force.
- Article 5.4.6.2 (AASHTO 2012) specifies requirements for duct size. Minimum duct size is limited based on the nominal diameter of strands. It also requires the size of the duct to be less than 0.4 times the least gross concrete thickness. In a recent study by Williams et al. (2015), the ratio of 0.4 was not met, which led to a brittle shear failure initiated from the cracks in the web and eventually crushing concrete at the level of the PT ducts. Segal and Sanders (2014) conducted an experimental study on the effect of PT ducts on cracking

of narrow web sections during air pressure testing. Results suggested that use of duct tie reinforcement and increasing the space between the ducts decreases web cracking of such sections.

- Article 5.9.1 (AASHTO 2012) provides general design considerations for prestressing. These include Article 5.9.1.3 (AASHTO 2012), which requires a buckling check of thin webs. With increasing depth of the sections, which primarily comes from extending the web height, out-of-plane buckling of the web becomes more critical. In particular when the PT ducts run through thin webs, buckling of the webs needs to be investigated.
- Article 5.9.1.4 (AASHTO 2012) provides specifications for section properties of girders, before and after grouting. It requires that the section properties consider removing the area of ducts from the gross section prior to grouting. After grouting, either the gross or transformed girder section can be used for determining section properties. Reaching longer span lengths demands more steel for both prestressing and mild steel than for common structures. For this reason, it is suggested that the transformed section be used for a more accurate analysis of deflections.
- Commentary Article C5.9.1.6 (AASHTO 2012) defines the difference between center of gravity (c.g.) of the duct and that of the strands within the duct. Basically, the strands will press down to the bottom of the duct in negative moment regions (with convex layout) and will press up in positive moment regions (with concave layout). This will lead to a difference between the c.g. of the duct and strands, which is quantified in AASHTO Figure C5.9.1.6. Prestressing contractors can also provide charts for a specific duct diameter and number of strands. The deviation can be assumed to vary linearly from one peak to another.
- Article 5.10.4 (AASHTO 2012) focuses on tendon confinement. According to Article 5.10.4.3, in-plane force effects due to a change in the direction of tendons shall be considered. This article provides required local reinforcement to avoid any damage. In-plane forces should specifically be considered if the tendons come out of the deck (to maximize the drape). Any lateral deviation of duct that is considered to accommodate ducts in the anchorage zone shall be removed prior to transitioning the section from the thickened block to the standard section. The prestressing layout (including both pretensioning and post-tensioning) shall be positioned laterally symmetric throughout the entire length of the bridge, except for the thickened ends of anchorage zones. Otherwise provisions of Article

5.10.4.3.1b shall be considered to investigate the shear resistance of the concrete cover against pull-out by deviation forces.

- Article 5.11.4 defines the transfer length and development length for bonded pretensioning strands. As depicted in Figure C5.11.4.2-1, the effective prestress for service is available beyond the transfer length from the end of the strand, which is 60 strand diameters. On the other hand, the development length (l_d) shall be considered to achieve the stress in the prestressing steel at nominal resistance of the member.

2.5 RECENT RESEARCH

Alawneh (2013) suggested a spliced girder system as a replacement for traditionally curved bridges. In the proposed system, shorter straight segments were precast and spliced with an angle to simulate a horizontal curve with a 200 ft radius. Two specimens were constructed: one with I-girder segments and one adopting tub girder segments. Two splices were used to reach a test span of 600 ft. One of the splices matched the girder cross section, while the other splice was cast as a thickened section, adopting the thickness of the bottom flange for the thickness of the web. A single point load was applied at midspan. Flexural failure occurred in the midspan away from the splice zones.

Moore et al. (2014), in a recent companion study sponsored by TxDOT, compared the shear behavior of post-tensioned girders for steel ducts and plastic ducts. Through 11 tests with different duct materials and diameters and different web widths, the effect of duct material and duct diameter-to-web width ratio was investigated. They concluded that all the specimens failed due to localized crushing of the web concrete at the level of the PT ducts and duct material had little effect on the shear resistance of the web. On the other hand, the duct diameter-to-web width ratio played a significant role in the shear resistance of the web. The shear stress at ultimate changed from $0.2 f'_c$ for the lowest duct diameter-to-web width ratio of 0.33 to $0.16 f'_c$ for the ratio of 0.44.

Williams et al. (2015), as a follow up on the previous study, presented their study through Report 0-6652-2. In this research, they provided the results of a survey with the focus on duct material, shear interface detail, longitudinal reinforcement detailing, and length of splice. The report includes the results of an experimental program on shear behavior of in-span splices. Use of plastic ducts and a 9 in. web provided a critical shear section in the web that violated the

allowable limits of 0.4 in the AASHTO LRFD Specifications for the duct diameter-to-web width ratio. For this case, the ratio was 0.44, which was 10 percent higher than the AASHTO limit.

Two specimens were tested under the same loading setup. Concrete strength and prestressing levels were the same for both specimens. The major difference between the two specimens was the amount of longitudinal interface reinforcement at the splice connections. Specimen 1 included 14-#4 straight bars in the flanges passing through the splice region and 6-#3 straight bars passing through the web. In Specimen 2, 8-#6 straight bars passed through the bottom flange, 8-#5 bars were considered for the top flange, and the same 6-#3 bars were passed through the web. Specimen 2, with the higher amount of longitudinal reinforcement, showed about 5 percent more loading capacity and 20 percent more deflection before failure.

Based on the experimental data, Williams et al. (2015) proposed modifications to the AASHTO LRFD Specifications for the general shear design procedure. In the modifications, they included an additional strength reduction factor to account for the reduction in the shear resistance due to the presence of PT ducts.

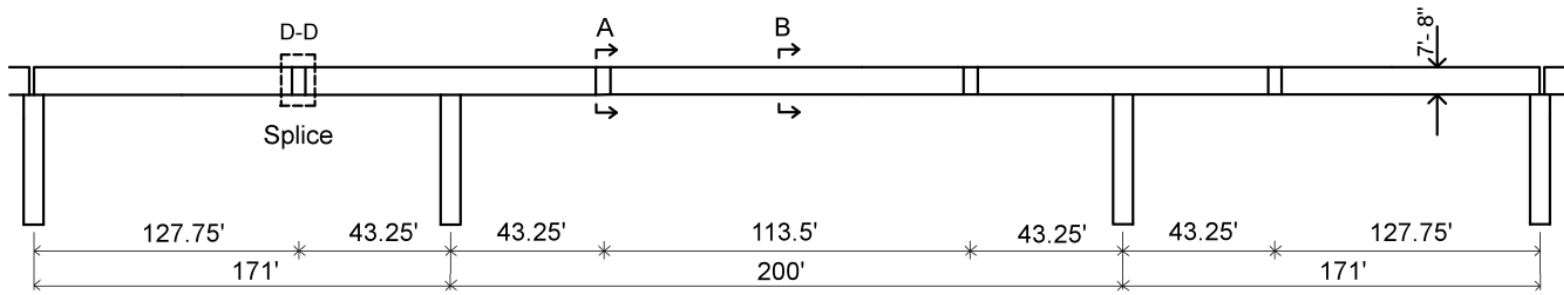
2.6 FIELD IMPLEMENTATION IN TEXAS: SYLVAN AVENUE BRIDGE

The recent design and construction of the Sylvan Avenue Bridge across the Trinity River near Dallas represents a current state-of-the-practice example of spliced girder construction in the state of Texas. This bridge has 23 spans and utilizes pretensioned simply supported girders, as well as continuous and post-tensioned girder construction with in-span splices. There are three post-tensioned portions among the 23 spans that are each composed of three continuous spans as shown in Figure 2.2. Most of the spans use a new Tx82 prestressed concrete section shape. However, in order to create the 250 ft span river crossing, it was necessary to use haunched girders as shown in Figure 2.2(b).

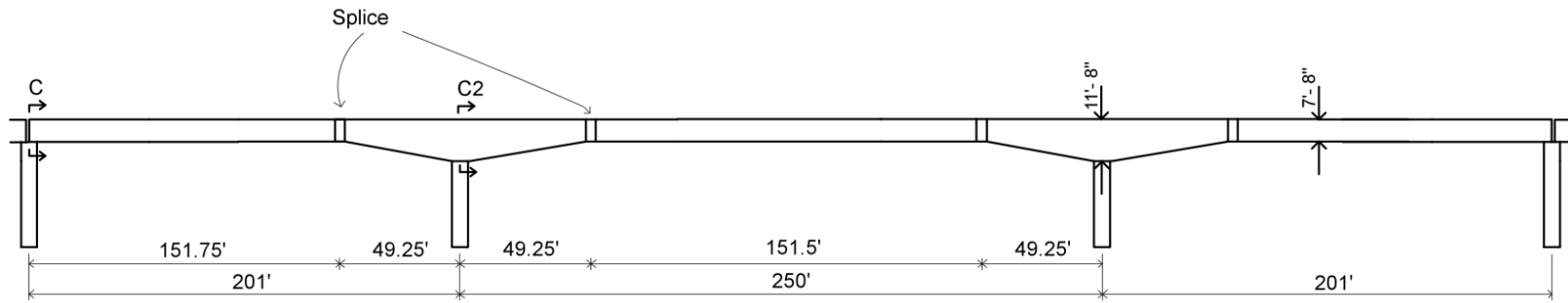
The haunch-modified girders were cast on soffits in order to create the centerline haunch. In contrast with TxDOT standard shapes where the girders customarily have a 7-in. wide web, the Tx82 modified girder has 10-in. wide web, primarily to accommodate the PT ducts. Figure 2.2 presents details of the cross-sections and splices.

Figure 2.3 shows some steps of the construction process in the photographic record. Figure 2.3(a) shows placement of the central drop-in girder in Span 11. In order to provide girder stability

during construction, it was necessary to provide a shore-tower beneath the splices within the back spans. This ensured that the cantilevered on-pier units were stable.

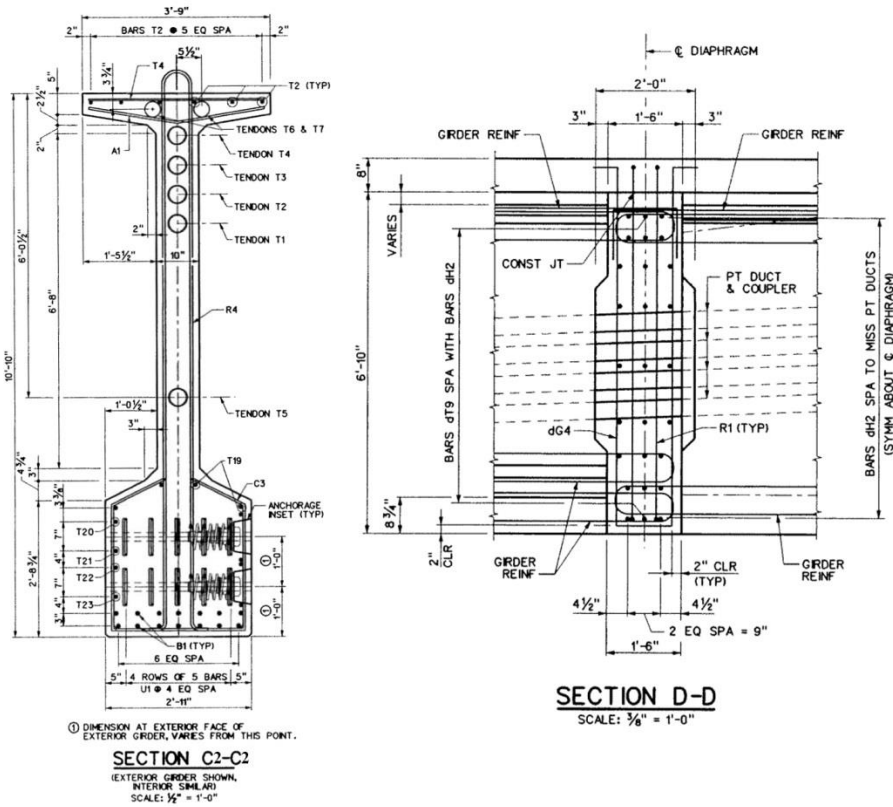
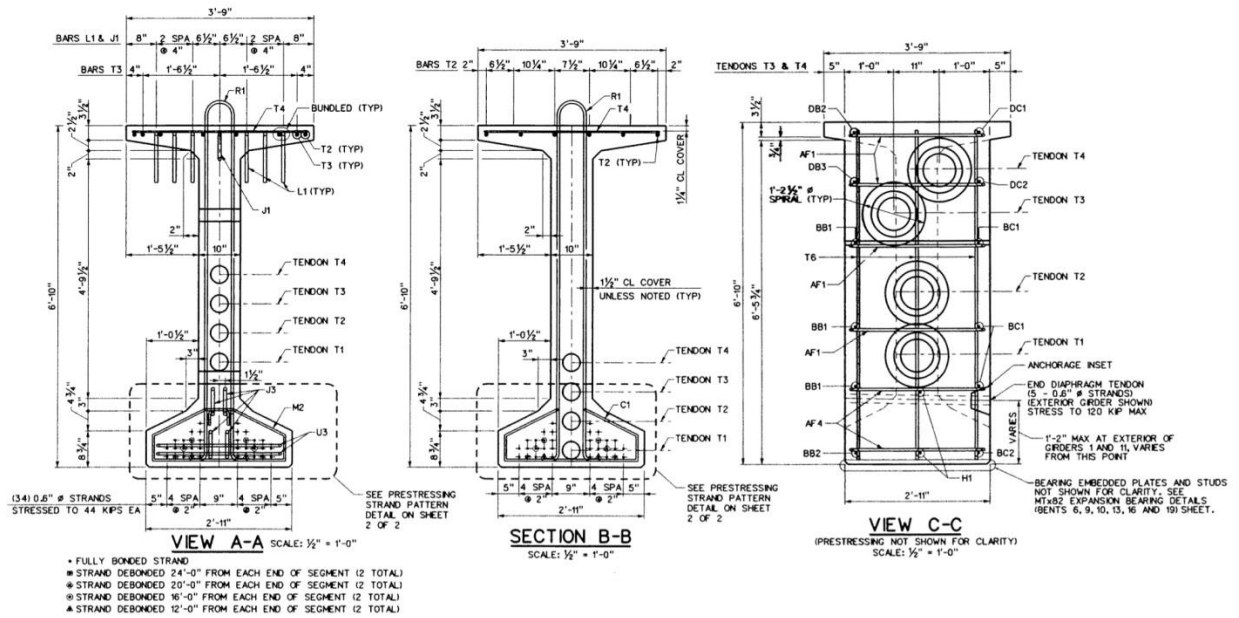


(a) Elevation for Spans 6 to 8 and 16 to 18.



(b) Elevation for Spans 10 to 12.

Figure 2.2. Use of Spliced Girders for the Sylvan Avenue Bridge.



(c) Section Views from Design Drawings (provided by TxDOT).

Figure 2.2 Use of Spliced Girders for the Sylvan Avenue Bridge (continued).



(a) Placing the Drop-in Segment within Span 11



(b) Shore Towers on Both Spans

Figure 2.3. Construction Process for Sylvan Avenue Bridge (Webber 2014).

3 PROTOTYPE BRIDGE DESIGN

3.1 INTRODUCTION

A full-scale girder test specimen with spliced connections was tested as part of the experimental program for this study. Various options were considered for the prototype bridge, from which the experimental study specimen was extracted. Numerous factors were considered to determine the final prototype bridge design, including feasibility of construction at a precast plant, transportation limitations and costs, laboratory crane capacity, and available actuator capacity for reaching ultimate strength of the specimen. Preliminary calculations based on the AASHTO LRFD Specifications (AASHTO 2012) suggested that a prismatic Tx70 continuous bridge girder designed for shored construction would be the best option. The Tx70 was selected as a minimum size that might typically be used in continuous bridge construction, while still allowing full-scale testing in the laboratory. The three spans of the prototype bridge was chosen to have a 190-240-190 ft configuration, with the end spans being 190 ft long and the middle span being 240 ft long. In this chapter, a review of the prototype bridge geometry and selected cross-section is presented. Then, a detailed design procedure along with the design assumptions is provided.

3.2 BRIDGE GEOMETRY AND GIRDER CROSS SECTION

The elevation view shown in Figure 3.1 represents the prototype three-span continuous prestressed concrete bridge. In consultation with a TxDOT panel of engineers, the following parameters were selected for the prototype design:

- A three-span configuration using 190-240-190 ft. The ratio of end span to center span length is 0.8.
- Based on transportation limitations, the length of the drop-in and end girder segments is 140 ft, while that of on-pier segment is 96 ft.
- Length of splice connections is 2 ft.
- Prismatic Tx70 girder sections modified such that a 9 in. web width is used to accommodate PT ducts, instead of the standard 7 in. web.

Figure 3.2 shows the bridge cross-section at midspan. The bridge has a total width of 46 ft and a total roadway width of 44 ft. The bridge superstructure consists of six modified Tx70 girders spaced 8 ft center-to-center, with a 3 ft overhang on each side, designed to act compositely with

an 8 in. thick CIP concrete deck. The deck includes 4-in. thick precast concrete stay-in-place precast concrete panels between girders that serve as formwork for the deck. The asphalt wearing surface thickness is 2 in. TxDOT standard T501 type rails are considered in the design. Three design lanes are considered for the purpose of design in accordance with the AASHTO LRFD Specifications (AASHTO 2012).

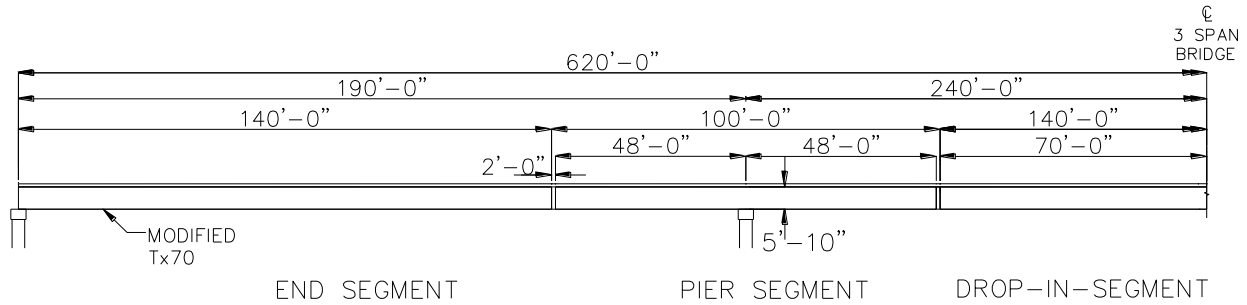


Figure 3.1 Elevation View of Three-Span Continuous Bridge.

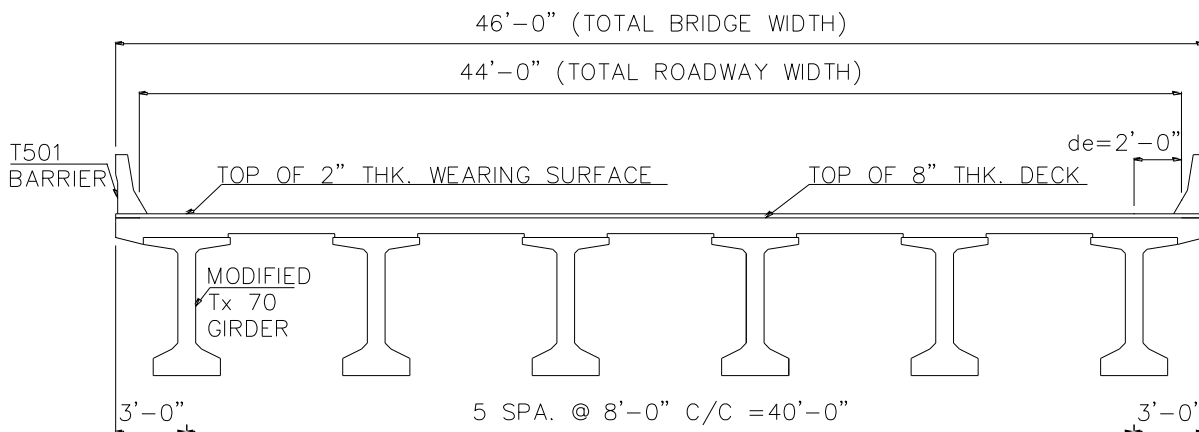


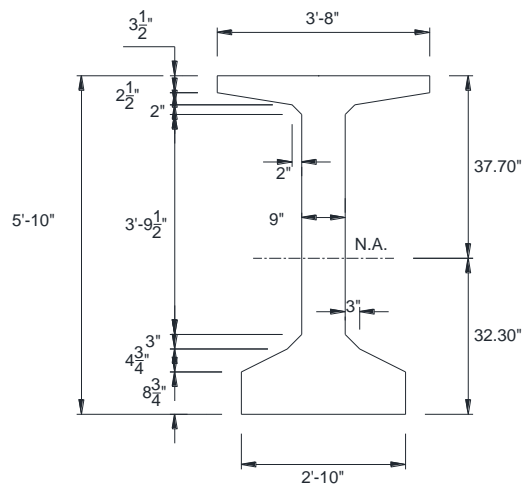
Figure 3.2. Transverse Bridge Section at Midspan.

A modified Tx70 girder has been considered for the design. The web width of the standard Tx70 girder has been increased to 9 in. to allow placement of PT ducts. The widened web width results in an increase in the width of the top flange to 44 in. and of the bottom flange to 34 in. The area of the 2 in. haunch is not considered in the calculation of the section properties and is only included in dead weight calculations.

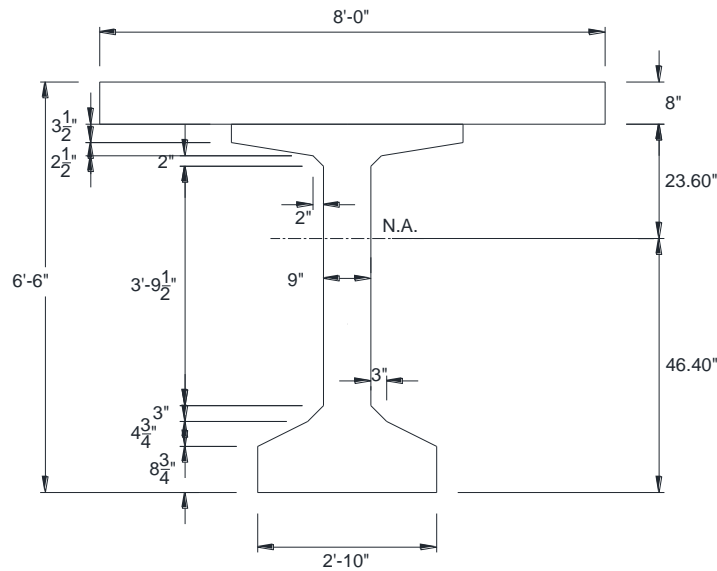
Table 3.1 provides the composite and non-composite uncracked elastic section properties for the modified Tx70 girder cross-section. Figure 3.1 shows the details of the non-composite and composite section for the prismatic modified Tx70 girder, respectively.

Table 3.1 Section Properties for Prismatic Modified Tx70 Girder (9 in. Web).

Girder Type	Depth of N.A. from Top of Girder, y_{top} (in.)	Depth of N.A. from Bottom of Girder, y_{bot} (in.)	Area, A (in. ²)	Moment of Inertia, I_x (in. ⁴)
Tx70 Modified	37.70	32.30	1106	687,081
Tx70 Modified Composite	23.60	46.40	1874	1,366,357



(a) Non-composite Section



(b) Composite Section

Figure 3.3. Prismatic Modified Tx70 Girder.

3.3 DESIGN ASSUMPTIONS AND PARAMETERS

Table 3.2 summarizes the design parameters selected for the prototype bridge. Material parameters such as concrete strength are based on standard practices that are followed by TxDOT throughout the state of Texas. A relative humidity of 65 percent is assumed based on the average value in Texas as specified in AASHTO LRFD Specifications (AASHTO 2012) Article 5.4.2.3. Additional parameters that describe the prestressing steel and mild steel are based on the AASHTO LRFD Specifications (AASHTO 2012).

Table 3.2. Design Parameters.

Parameter		Selected Value
Concrete Strength at Service for Deck Slab, f'_c		4 ksi
Precast Concrete Strength at Release, f'_{ci}		6.5 ksi
Precast Concrete Strength at Service, f'_c		8.5 ksi
Coefficient of Thermal Expansion of Concrete		$6 \times 10^{-6}/^\circ \text{F}$
Relative Humidity		65%
Mild Steel	Yield Strength, f_y	60 ksi
	Modulus of Elasticity, E_s	29,000 ksi
Prestressing Steel	Strand Diameter	0.6 in.
	Ultimate Tensile Strength, f_{pu}	270 ksi – Low Relaxation
	Yield Strength, f_{py}	$0.9 f_{pu}$
	Stress Limit at Transfer, f_{pi}	$f_{pi} \geq 0.75 f_{pu}$
	Stress Limit at Service, f_{pe}	$f_{pe} \geq 0.8 f_{py}$
	Modulus of Elasticity, E_p	28,500 ksi
	Coefficient of Friction, μ	0.25
	Wobble Coefficient	0.0002/ft
	Anchor set	0.375 in.

The following assumptions were made for the prototype bridge design, based on the project Phase 1 report (Hueste et al. 2012):

1. Stage I and Stage II PT tendons are stressed from both the ends to minimize friction losses and to provide symmetry of stresses in the girders.

2. The PT tendons used for the modified Tx70 girder are internal and bonded. The tendons are encased in a 4 in. diameter metal duct. A maximum of 19-0.6 in. diameter strands can be encased in a 4 in. diameter duct. All the PT tendons are located in a single vertical plane.
3. For the design under consideration, the entire deck is cast in a single operation.
4. A CIP reinforced concrete deck of 8 in. thickness is used. A 2-in. thick haunch is assumed between the girders and the deck to accommodate construction tolerances and variation in camber.
5. A 2-in. thick asphalt wearing surface is used but is not considered a part of structural composite section and is treated as additional superimposed dead load.
6. The weights of the deck forms, strongbacks, temporary diaphragms, and other temporary components are minor and neglected in the design.
7. Permanent intermediate diaphragms are not considered in the design. Temporary intermediate diaphragms can be provided at critical locations, such as splice connections and piers for lateral stability of the girder, until the deck slab attains composite action.
8. The composite section properties are based on the transformed effective width of the composite deck slab considering the specific modulus of elasticity for the girder and deck, respectively.
9. The sign convention for the design considers tension as positive and compression as negative.

3.4 DEAD LOADS

Dead loads for design are addressed in the AASHTO LRFD Specifications (AASHTO 2012) Article 3.5.1. Dead loads considered in the design include girder self-weight and weights of the haunch, slab, barrier, and wearing surface. For the haunch segment, self-weight varies linearly with increasing depth from a prismatic section at the splice to the centerline of pier. The load due to the deck is distributed to the individual girders based on the center-to-center spacing between girders. The loads due to the wearing surface and barrier loads act on the composite section and are distributed equally to all the girders. Table 3.3 gives the dead loads acting on each individual girder for the bridge considered.

Table 3.3. Dead Loads for Modified Tx70 Girder.

<i>Load Type</i>	<i>Value (kip/ft)</i>	<i>Applied to</i>
Self-weight prismatic	1.152	Girder Section
Self-weight haunch (for pier segment-hybrid case)	1.152–2.488	Girder Section
Deck weight	0.800	Girder Section
Haunch weight (between girder and deck)	0.079	Girder Section
Barrier weight	0.109	Composite Section
Wearing surface	0.187	Composite Section

3.5 LIVE LOADS

AASHTO LRFD Specifications (AASHTO 2012) Article 3.6 describes the HL-93 truck live load model. Three traffic lanes are considered for the design in accordance with the AASHTO LRFD Specifications (AASHTO 2012). The live load is to be taken as one of the following combinations, whichever yields maximum stresses at the section considered.

3.5.1 Design Truck and Design Lane Load

The HL-93 design truck consists of one front axle weighing 8 kips and two rear axles weighing 32 kips each, spaced 14-30 ft apart. A dynamic load allowance factor of 33 percent is considered for the design truck. The design lane load consists of 0.64 klf uniformly distributed in the longitudinal direction and is not subjected to a dynamic load allowance. Figure 3.4 shows the details for design truck and design lane load.

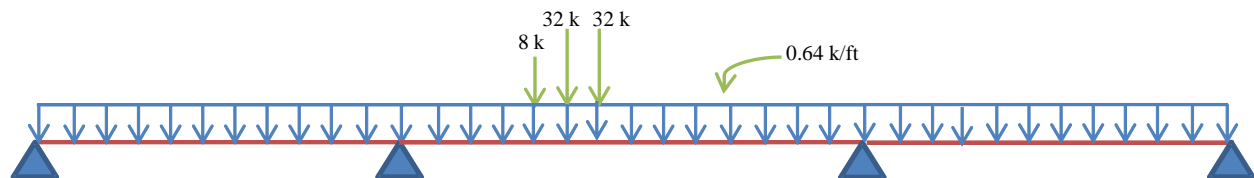


Figure 3.4. Design Truck and Design Lane Load.

3.5.2 Design Tandem and Design Lane Load

The design tandem load consists of a pair of 25 kip axles spaced 4 ft apart and is subjected to a dynamic load allowance. The design lane load consists of 0.64 klf uniformly distributed in the longitudinal direction and is not subjected to a dynamic load allowance. Figure 3.5 shows the details for design tandem and design lane load.

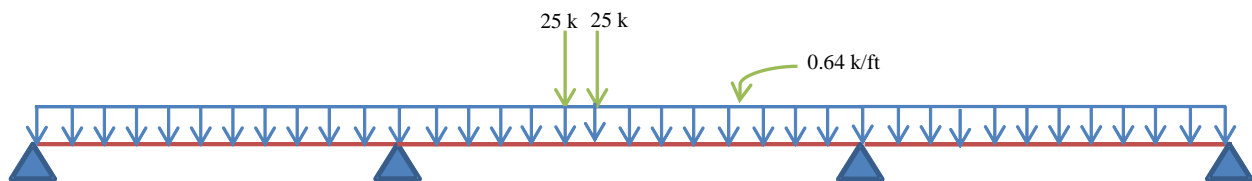


Figure 3.5. Design Tandem and Design Lane Load.

The live load moments and shear forces, including the dynamic load effects, are distributed to the individual girders using distribution factors (DFs). AASHTO LRFD Tables 4.6.2.2.2 and 4.6.2.2.3 specify the DFs for moment and shear for I-shaped girder sections. The use of these DFs is allowed for prestressed concrete girders having an I-shaped cross-section with a composite slab, if the conditions outlined below are satisfied. For bridge configurations not satisfying the limits below, refined analysis is required to estimate the moment and shear DFs. Table 3.4 gives the LRFD live load DFs for the case of a concrete deck on an I-girder.

Table 3.4. LRFD Live Load DFs for Concrete Deck on I-Girder.

<i>Category</i>	<i>DF Formulas</i>	<i>Range of Applicability</i>
Live Load Distribution per Lane for Moment in Interior Beam	One Design Lane Loaded: $0.06 + \left(\frac{S}{14}\right)^{0.4} \left(\frac{S}{L}\right)^{0.3} \left(\frac{K_g}{12.0Lt_s^3}\right)^{0.1}$ Two or More Design Lanes Loaded: $0.075 + \left(\frac{S}{9.5}\right)^{0.6} \left(\frac{S}{L}\right)^{0.2} \left(\frac{K_g}{12.0Lt_s^3}\right)^{0.1}$	$3.5 \leq S \leq 16.0$ $4.5 \leq t_s \leq 12.0$ $20 \leq L \leq 240$ $N_b \geq 4$ $10000 \leq K_g$ ≤ 7000000
Live Load Distribution per Lane for Moment in Interior Beam	One Design Lane Loaded: Lever Rule Two or More Design Lanes Loaded: $g = e g_{interior}$ $e = 0.77 + \frac{d_e}{9.1}$	$-1.0 \leq d_e \leq 5.5$
Live Load Distribution per Lane for Shear in Interior Beam	One Design Lane Loaded: $0.36 + \frac{S}{25}$ Two or More Design Lanes Loaded: $0.2 + \frac{S}{12} - \left(\frac{S}{35}\right)^{2.0}$	$3.5 \leq S \leq 16.0$ $4.5 \leq t_s \leq 12.0$ $20 \leq L \leq 240$ $N_b \geq 4$
Live Load Distribution per Lane for Shear in Interior Beam	One Design Lane Loaded: Lever Rule Two or More Design Lanes Loaded: $g = e g_{interior}$ $e = 0.6 + \frac{d_e}{10}$	$-1.0 \leq d_e \leq 5.5$

Note: The abovementioned terms in Table 3.4 are defined as follows:

$$K_g = n(I + Ae_g^2).$$

n = Modular ratio between the girder and slab concrete.

A = Area of the girder cross-section, in.²

e_g^2 = Distance between the centroid of the girder and the slab, in.

S = Beam Spacing, ft.

L = Span Length, ft.

N_b = Number of beams.

d_e = Distance from exterior web of exterior beam to the interior edge of curb or traffic barrier, in.

t_s = Thickness of slab, in.

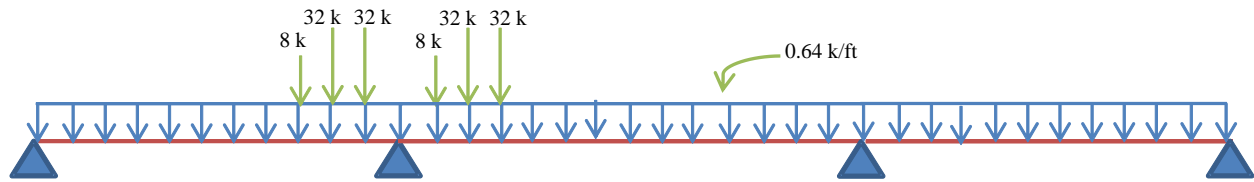
The following conditions must be met to use the DFs of Table 3.4:

- Width of slab is constant.
- Number of girders (N_b) is not less than four.
- Girders are parallel and of the same stiffness.
- The roadway part of the overhang, $d_e \leq 3.0$ ft.
- Curvature in plan is less than 4 degrees.
- Cross-section of the bridge girder is consistent with one of the cross-sections given in LRFD Table 4.6.2.2.1-1.
- $3.5 \leq S \leq 16.0$.
- $4.5 \leq t_s \leq 12.0$.
- $20 \leq L \leq 240$.
- $10,000 \leq K_g \leq 7,000,000$.

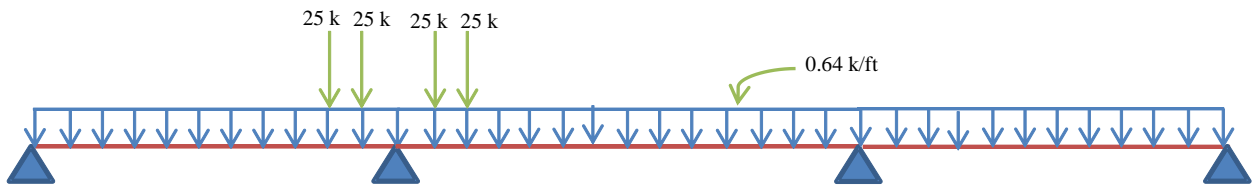
According to AASHTO LRFD Specifications (AASHTO 2012) Article 3.6.1.3.1, the maximum shear and negative moment under vehicular live load is calculated as the larger of:

- 90 percent of the effect of (Two Design Trucks + Design Lane Load).
- 100 percent of the effect of (Two Design Tandems + Design Lane Load).

The two design trucks or tandems are spaced a minimum of 50 ft between the lead axle of one truck/tandem and the rear axle of the other truck/tandem on either side of the interior support to produce the maximum negative moment demand and shear demand. The two design trucks/tandems must be placed in adjacent spans to produce maximum force effects. Figure 3.6 shows the details for design truck tandem and design lane load, and design tandem and design lane load.



(a) Design Truck and Design Lane Load



(b) Design Tandem and Design Lane Load

Figure 3.6. Critical Load Placement of HL-93 Vehicular Live Load over Continuous Span for Maximum Shear Demand.

3.6 ALLOWABLE STRESS LIMITS

The design of spliced girder bridges involves various stages. It is necessary to ensure that the girder stresses are within the allowable stress limits during all stages of construction. Table 3.5 and Table 3.6 summarize the allowable stress limits as given in the AASHTO LRFD Specifications (AASHTO 2012). The allowable stress limits have been computed for the girder for a specified concrete compressive strength at service (f'_c) of 8.5 ksi and a specified concrete compressive strength at transfer (f'_{ci}) of 6.5 ksi based on practical limits used by TxDOT. For the deck, a specified concrete compressive strength (f'_c) of 4 ksi is used. The reduction factor, ϕ_w , for the compressive stress limit at the final loading stage is taken equal to 1.0 when the web or flange slenderness ratio, calculated according to the AASHTO LRFD Specifications (AASHTO 2012) Article 5.7.4.7.1, is less than or equal to 15. When either the web or flange slenderness ratio is greater than 15, the provisions of the AASHTO LRFD Specifications (AASHTO 2012) Article 5.7.4.7.2 are used to calculate the value for the reduction factor ϕ_w (see AASHTO LRFD Article 5.9.4.2).

Table 3.5. Summary of Allowable Stress Limits in Girder.

<i>Stage of Loading</i>	<i>Type of Stress</i>	<i>Allowable Stress Limits</i>	
		<i>f' c or f' ci (ksi)</i>	<i>Limiting Value (ksi)</i>
Initial Loading Stage at Transfer	Compressive	$-0.60 f'_{ci}$	-3.90
	Tensile	$0.24\sqrt{f'_{ci}}$	0.612
Intermediate Loading Stage at Service	Compressive	$-0.45 f'_c$	-3.83
	Tensile	$0.19\sqrt{f'_c}$	0.554
Final Loading Stage at Service	Compressive: Case I	$-0.60\Phi_w f'_c$	-5.10
	Compressive: Case II	$-0.40 f'_c$	-3.40
	Tensile	$0.19\sqrt{f'_c}$	0.550

Note: Tension stresses are positive.

Table 3.6. Summary of Allowable Stress Limits in Deck.

<i>Stage of Loading</i>	<i>Type of Stress</i>	<i>Allowable Stress Limits</i>	
		<i>f' c (ksi)</i>	<i>Limiting Value</i>
Final Loading Stage	Compressive	$-0.60 f'_c$	-5.10
	Tensile	$0.19\sqrt{f'_c}$	0.554

Note: Tension stresses are positive.

3.7 LIMIT STATES

3.7.1 Service Limit State

For prestressed concrete members, the service load design typically governs; therefore, the design satisfying the service load criteria usually meets the flexural strength limit state. Service load stresses are checked during various stages of construction based on the limits given in Table 3.5 and Table 3.6. Tension in prestressed concrete members is checked considering the Service III limit state while compression is checked using the Service I limit state as specified in the AASHTO LRFD Specifications Article 3.4.1 (AASHTO 2012).

Service I – checks compressive stresses in prestressed concrete components:

$$Q = 1.00(DC + DW) + 1.00(LL + IM) \quad (\text{Equation 3.1})$$

where:

- Q = Total load effect.
- DC = Self-weight of girder and attachment (slab and barrier) load effect.
- DW = Wearing surface load effect.
- LL = Live load effect.
- IM = Dynamic load effect.

Service III – checks tensile stresses in prestressed concrete components:

$$Q = 1.00(DC + DW) + 0.80(LL + IM) \quad (\text{Equation 3.2})$$

3.7.2 Flexure Strength Limit State

The flexural strength limit state needs to be checked to ensure safety at ultimate load conditions. The flexural strength limit state design requires the reduced nominal moment capacity of the member to be greater than the factored ultimate design moment, expressed as follows:

$$\phi M_n \geq M_u \quad (\text{Equation 3.3})$$

where:

- M_u = Factored ultimate moment at a section, kip-ft.
- M_n = Nominal moment strength at a section, kip-ft.
- ϕ = Resistance factor.
= 1.0 for flexure and tension of prestressed concrete members.

The total ultimate design bending moment for the Strength I limit state, according to the AASHTO LRFD Specifications (AASHTO 2012) is as follows:

$$M_u = 1.25 (M_{DC}) + 1.5 (M_{DW}) + 1.75(M_{LL+IM}) \quad (\text{Equation 3.4})$$

where:

- M_{DC} = Bending moment due to all dead loads except wearing surface, kip-ft.
- M_{DW} = Bending moment due to wearing surface load, kip-ft.
- M_{LL+IM} = Bending moment due to live load and impact, kip-ft.

3.7.3 Shear Limit State

AASHTO LRFD Specifications Article 5.8 (AASHTO 2012) specifies the use of the Modified Compression Field Theory (MCFT) for transverse shear reinforcement. MCFT takes into account the combined effect of axial load, flexure, and prestressing when designing for shear. Shear in prestressed concrete members is checked through the Strength I limit state. The shear strength of concrete is based on parameters β and θ . The transverse reinforcement is based on demands of both transverse and interface shear. The interface shear design is based on shear friction theory where the total resistance is based on the cohesion and friction maintained by shear friction reinforcement crossing the interface shear plane.

The AASHTO LRFD Specifications (AASHTO 2012) require that transverse reinforcement is provided at sections with the following condition:

$$V_u > 0.5\phi(V_c + V_p) \quad \text{[AASHTO Eq. 5.8.2.4-1]}$$

where:

V_u = Factored shear force at the section, kips.

$$V_u = 1.25(DC) + 1.5(DW) + 1.75(LL + IM)$$

DC = Shear force at the section due to dead loads except wearing surface load, kips.

DW = Shear force at the section due to wearing surface load, kips.

$LL + IM$ = Shear force at the section due to live load including impact, kips.

V_c = Nominal shear strength provided by concrete, kips.

V_p = Component of prestressing force in the direction of shear force, kips.

ϕ = Strength reduction factor.

= 0.9 for shear in prestressed concrete members.

The nominal shear resistance at a section is the lesser of the following two values:

$$V_n = V_c + V_s + V_p \quad \text{[AASHTO Eq. 5.8.3.3-1]}$$

and

$$V_n = 0.25f'_c b_v d_v + V_p \quad \text{[AASHTO Eq. 5.8.3.3-2]}$$

Shear resistance provided by the concrete, V_c , is given as:

$$V_c = 0.0316\beta\sqrt{f'_c}b_vd_v \quad [\text{AASHTO Eq. 5.8.3.3-3}]$$

Shear resistance provided by the transverse steel reinforcement, V_s , is given as:

$$V_s = \frac{A_v f_y d_v (\cot \theta + \cot \alpha) \sin \alpha}{s} \quad [\text{AASHTO Eq. 5.8.3.3-4}]$$

where:

d_v = Effective shear depth, in.

b_v = Girder web width, in.

f'_c = Girder concrete strength at service, ksi.

V_p = Component of prestressing force in the direction of shear force, kips.

β = Factor indicating ability of diagonally cracked concrete to transfer tension.

θ = Angle of inclination of diagonal compressive stresses (slope of compression field), radians.

A_v = Area of shear reinforcement within a distance, s , in.²

s = Spacing of stirrups, in.

f_y = Yield strength of shear reinforcement, ksi.

α = Angle of inclination of diagonal transverse reinforcement to longitudinal axis, taken as 90 degrees for vertical stirrups.

3.8 DEFLECTION

As a final check for service conditions, the girders are checked for allowable deflection under live load and impact as specified in the AASHTO LRFD Specifications (AASHTO 2012) Article 2.5.2.6.2. The deflection limit state ensures that there are no undue vibrations in the bridge and also limits cracking in concrete members. In order to investigate maximum deflections for straight girder systems, all the design lanes are loaded and all the supporting components are assumed to deflect equally. The composite bending stiffness of an individual girder can be taken as the stiffness of the design cross-section, divided by the number of girders.

The limits for maximum deflection as specified in AASHTO LRFD Specifications (AASHTO 2012) Article 2.5.2.6.2 for concrete construction are based on the span length L as follows:

- Vehicular load, general = $L/800$.
- Vehicular and/or pedestrian loads = $L/1000$.

The live load is considered as specified in AASHTO LRFD Specifications (AASHTO 2012) Article 3.6.1.3.2, according to which, the deflection is calculated under the larger of the following:

- Design Truck Load alone.
- 25 percent of Design Truck Load and full Design Lane Load.

Figure 3.7 shows the critical load arrangement for vehicular live loads to produce maximum deflections in the continuous girders. Note that the axle loads shown are the full values, but should be reduced for the second load case provided above.

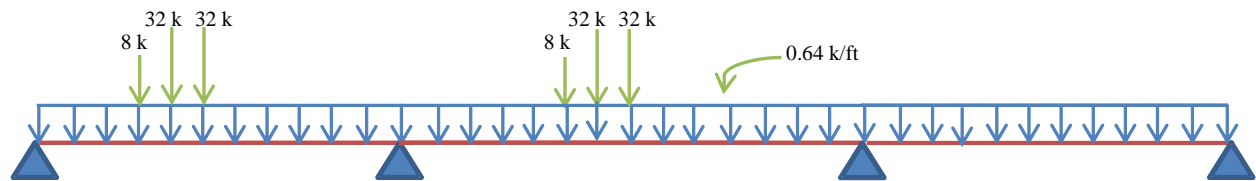


Figure 3.7. Critical Load Placement of HL-93 Vehicular Live Load over Continuous Span for Maximum Deflection.

3.9 DESIGN PHILOSOPHY

3.9.1 General

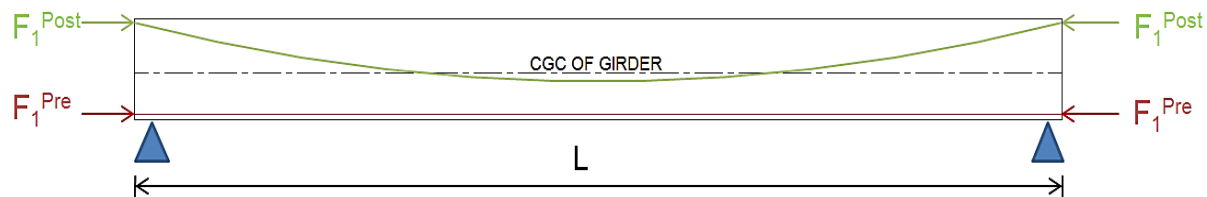
The principle of post-tensioning (PT) is to balance the dead load. After construction is complete, the net load on the prestressed members will consist primarily of the transient live load. Because the self-weight of the segments is significant, the post-tensioning is applied in two stages. Stage I post-tensioning (PT1) will balance the self-weight of the segments for transportation, erection, and the first stages of construction. PT1 tendons are placed in the individual segments. Stage II post-tensioning (PT2), on the other hand, is the continuity post-tensioning and is continuous along the entire length of the girder line to balance the deck weight and super-imposed dead loads. Pretensioning strands will also be provided within the individual girder segments to counteract the moments that are produced because of the eccentricity of the Stage I PT at the ends of the segments.

3.9.2 Handling, Transportation and Erection

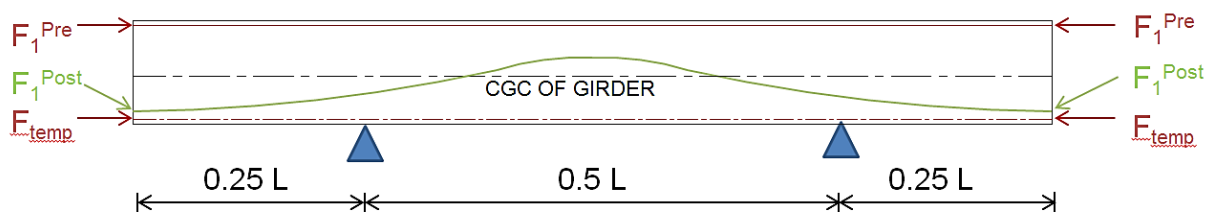
3.9.2.1 Overview

Pretensioning and Stage I PT are provided to balance the self-weight of the girders. One important issue during the hauling and erection is the location of the supports and lifting points. The lifting points and support locations should be determined according to the support locations for the segments during construction. For shored construction, the drop-in segments and end segments are supported at their ends, so end supports are used when they are transported from the precast plant to the construction site. The girder segments are pretensioned for self-weight during handling and transportation. Stage I PT is applied to balance the self-weight of the girders. Figure 3.8 (a) shows the support configuration during transportation of the drop-in and end segments.

On the other hand, the on-pier segment is supported at its midpoint, and will be seated on shore towers at its ends, so the post-tensioning profile will be selected to balance loads that produce negative moments. Hence, these segments are not designed to carry significant positive moments. To avoid any positive moments in the on-pier segments, they are transported by supporting it at the quarter span points from ends. The amount of prestress force required in the top flange of the on-pier segment is high because these segments cantilever over the piers and eventually support the ends of the drop-in and end segments. The on-pier girder segment is pretensioned for self-weight plus the girder reactions from the drop-in segment and end segment. Stage I PT is applied to balance the self-weight and the reaction from the drop-in and end segments. Also, until the stage when the pier segment supports the drop-in girder segment, the stresses in the bottom flange are high. This is offset by providing temporary Dywidag bars in the bottom flange. Figure 3.8 (b) shows the details of support configuration during transportation of the on-pier girder segment.



(a) Drop-in and End Segments



(b) On-Pier Segment

Figure 3.8. Support Arrangement during Transportation of Drop-in and End Segments.

The span lengths and weights of girder segments are taken into consideration during handling and transportation. In Texas, it is recommended that the maximum span length is limited to 160 ft, and the maximum weight is limited to 200 kips based on input from precasters and contractors (Hueste et al. 2012). Table 3.7 provides the span lengths and weights for the girder segments. The segment lengths and weights are within the recommended transportation limits.

Table 3.7. Segment Lengths and Girder Weights.

Girder Segments	Length (ft)	Weight (kips)
End Segment	140	161
Drop-in-Girder Segment	140	161
On-Pier Segment	96	111
Recommended Limit	160	200

3.9.2.2 Pretensioning

Table 3.8 presents the pretensioning design for the girder segments. For pretensioning the girder segments, 0.6 in. diameter Grade 270 low relaxation strands with an ultimate tensile strength (f_{pu})

of 270 ksi are considered. The initial stress in the pretensioning strands at transfer (f_{pi}) is taken as $0.75 f_{pu}$, which is 202.5 ksi. The force at transfer is calculated after taking the losses into account. Prestress losses of 20 percent are assumed in the pretensioned strands.

Table 3.8. Summary of Pretensioning Design.

Description	End Segment	On-Pier Segment	Drop-in Segment
	Bottom Flange	Top Flange	Bottom Flange
Strands (0.6 in. diameter)	32	26	24
Prestress Force at Transfer (kips)	1406	1142	1054
Prestress Force at Service (kips)	1125	913	843

3.9.2.3 Stage I Post-Tensioning

Table 3.9 presents the Stage I PT design for the girder segments. The Stage I PT is designed to balance the self-weight of the girder and is applied to each individual girder segment. An initial estimate of the amount of Stage I PT required can be obtained by the following relationship:

$$(F * \delta) = \frac{w * L^2}{8} \quad (\text{Equation 3.5})$$

where:

- F = Required PT force, kips.
- w = Girder weight per unit length, kips/ft.
- L = Span length, ft.
- δ = Eccentricity of tendons, ft.

For post-tensioning the girder, 0.6 in. diameter low relaxation strands with f_{pu} of 270 ksi are considered. The jacking force is assumed to be $0.70 f_{pu}$, which is 189 ksi. The force at transfer is calculated after taking the short-term losses into account. Prestress losses of 15 percent are assumed for the Stage I PT.

Table 3.9. Stage I Post-Tensioning Design.

Description	End Segment	On-pier Segment	Drop-in Segment
Tendons (19-0.6 in. diameter strands per duct)	19 (1 Duct)	38 (2 Ducts)	19 (1 Duct)
Prestress Force at Transfer (kips)	779	1558	779
Prestress Force at Service (kips)	662	1324	662

For the purpose of handling and transportation, four temporary unbonded Dywidag threadbars, having a 1.25 in. diameter and f_{pu} of 150 ksi, are provided in the bottom flange of the pier segments. Once the pier segment is erected on site, it will behave as a cantilever. The Dywidag bars are released and grouted to act as non-prestressed compression reinforcement.

3.9.3 Construction on Site

3.9.3.1 Construction Sequence

After the girders are transported to the job site, they are lifted and placed on piers and temporary shoring towers. Then Stage II PT is carried out to balance the weight of the deck and to provide compression in the deck. Figure 3.9 shows the details of various stages of construction. The step-by-step construction procedure is as follows:

1. Erect piers, temporary supports, and abutments. Place on-pier girder segments on the piers and secure the girders to the temporary shoring towers.
2. Attach strongbacks to the ends of the end segments at ground level. Erect the end girder segments on the abutments and shoring towers. Connect the strongbacks to the on-pier girder segments. The shoring towers should be capable of transferring the reaction from the end girder segments to the foundation.
3. Attach the strongbacks to the ends of the drop-in girder segment at ground level. Erect the drop-in-girder segment on the shoring towers. Connect the strongbacks to the on-pier girder segment. It is necessary to ensure that the end girder segments are installed prior to this step. This ensures that there is less rotation of the on-pier segment caused by the reaction of the drop-in-girder segment. Tie-downs can also be used to prevent the uplift at the end of the on-pier segment.
4. After all the segments have been placed, check the vertical alignment of the girder ends. Strongbacks help in maintaining the vertical alignment of the adjacent girders prior to

threading the PT strands through the ducts. Provide couplers between the ducts of adjacent girders at the splice locations. Then, thread the PT tendons through the ducts in the webs of the girders. Place additional reinforcement at splice locations between the girder segments and cast the splice concrete. Once the splice has cured and gained sufficient strength, remove the strongbacks.

5. Construct the formwork for the deck and place precast deck panels and deck reinforcement. Pour the concrete for the deck.
6. After the deck has cured and gained sufficient strength, stress the Stage II PT and then grout the tendons. Remove the temporary shoring towers.
7. Cast the barriers and wearing surface, and after a suitable time interval, when the CIP concrete components have attained their required design strength, the bridge can be opened to traffic.

3.9.3.2 Stage II Post-Tensioning

Table 3.10 shows the details for Stage II PT. Stage II PT was designed to act continuously to balance the deck and superimposed dead load and to be carried out on site after the girders are erected on the temporary supports and piers. Service stresses may control the amount of PT that is provided. For Stage II PT, 0.6 in. dia. low relaxation strands with f_{pu} of 270 ksi are considered. The jacking force in the PT tendons was assumed to be $0.70 f_{pu}$, which is 189 ksi. The force at transfer is calculated after taking the losses into account. Prestress losses of 15 percent were assumed for the Stage II PT.

Table 3.10. Stage II Post-Tensioning Design.

Description	Drop-in Segment	On-pier Segment	End Segment
Tendons (19-0.6 in. dia. Strands per duct)	57 (3 Ducts)	57 (3 Ducts)	57 (3 Ducts)
Prestress Force at Transfer (kips)	2337	2337	2337
Prestress Force at Service (kips)	1987	1987	1987

3.10 PRESTRESSING LAYOUT

Figure 3.10 shows an overview of the longitudinal prestressing profiles, along with cross-sections illustrating the pretensioning and post-tensioning layout segments at several key locations: $0.4L$

from the abutment support of end span (Section A-A), at the end span splice (Section B-B), at the face of the pier (Section C-C), at the interior span splice (Section D-D), and at the midspan of interior span (Section E-E). Figure 3.11 shows details of the PT layout for the three-span bridge.

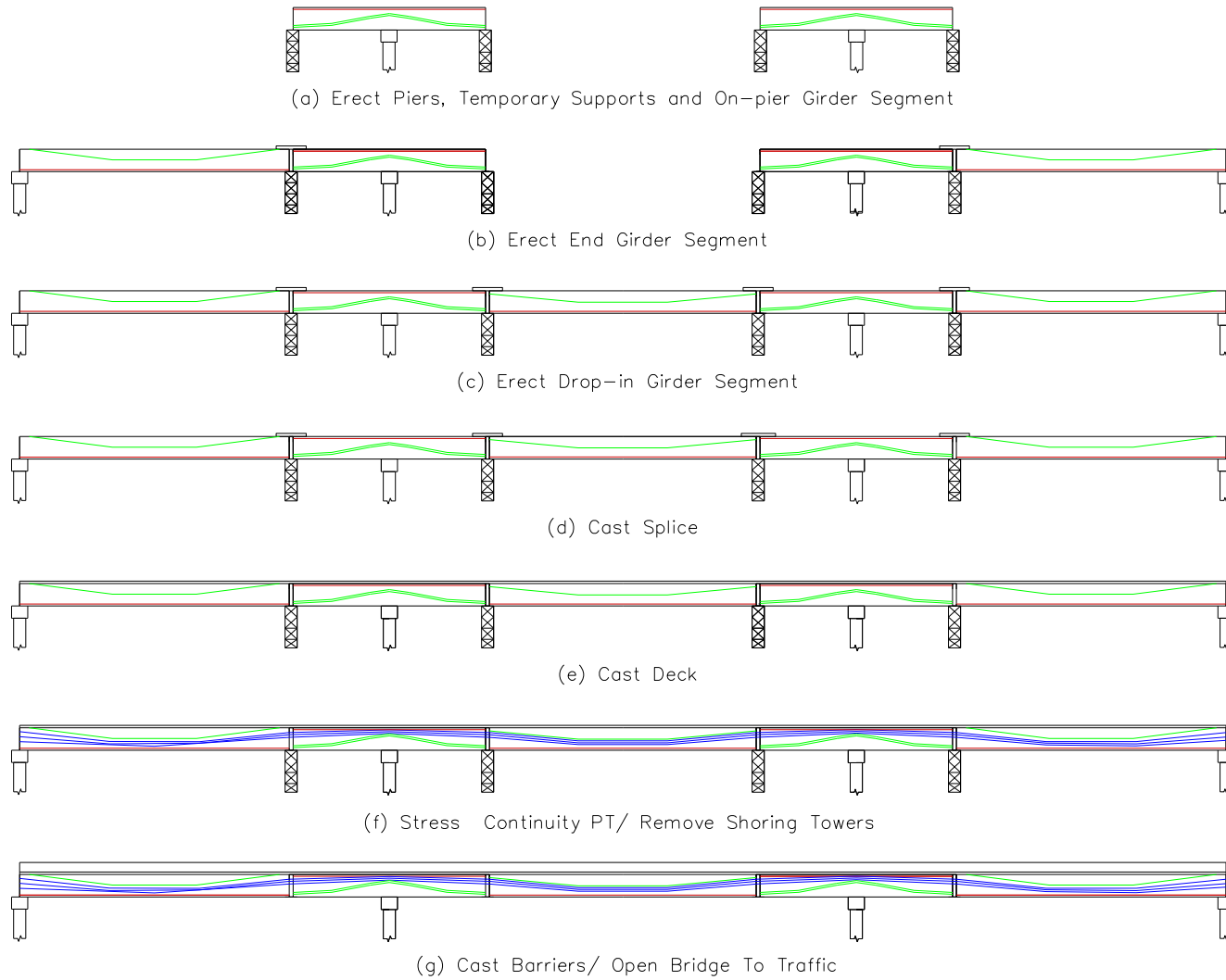
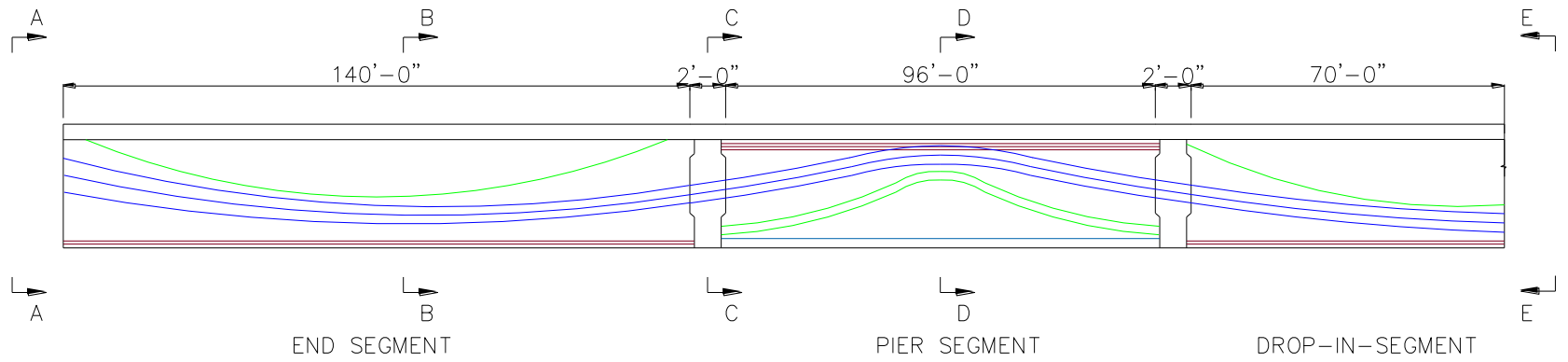
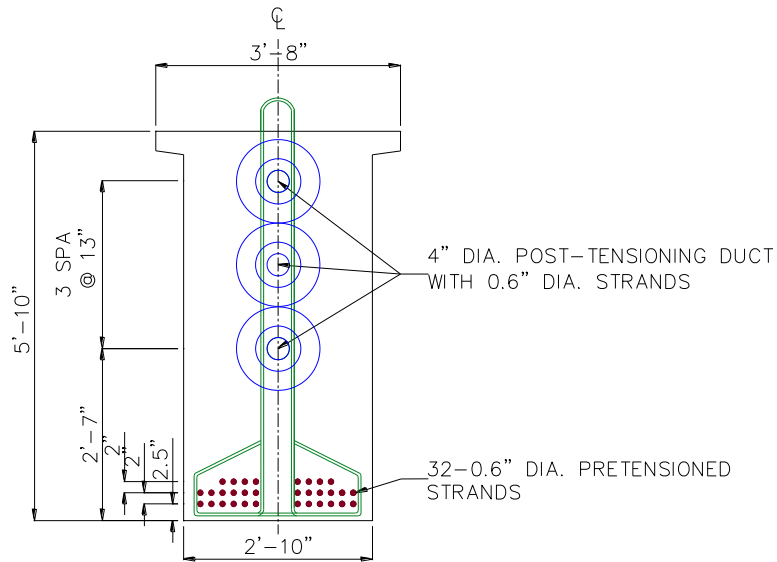


Figure 3.9. Stages of Construction.

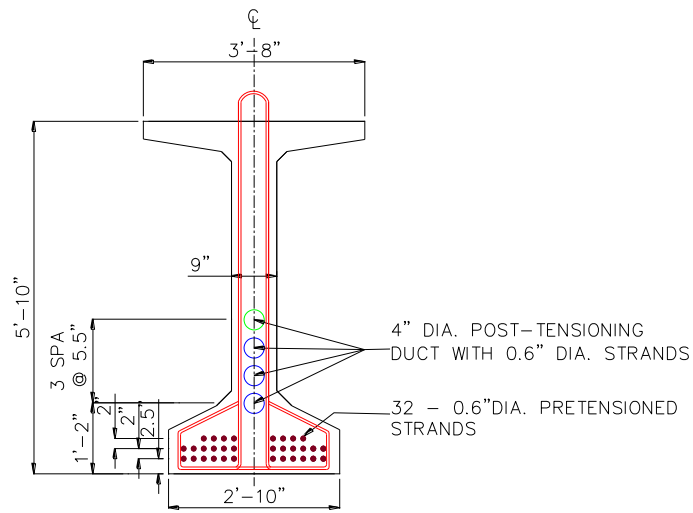


(a) Elevation View

Figure 3.10. Prestressing Details for Continuous Prestressed Concrete Shored Construction.

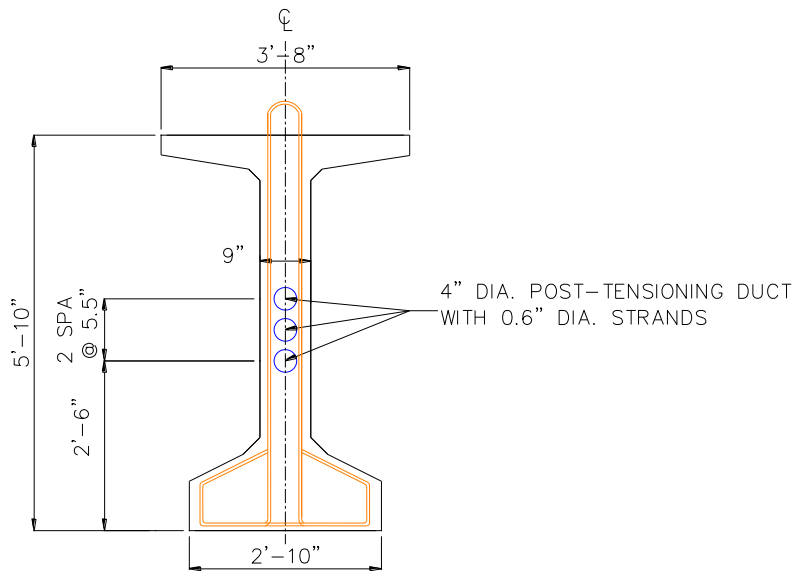


(b) Section A-A at Anchor End

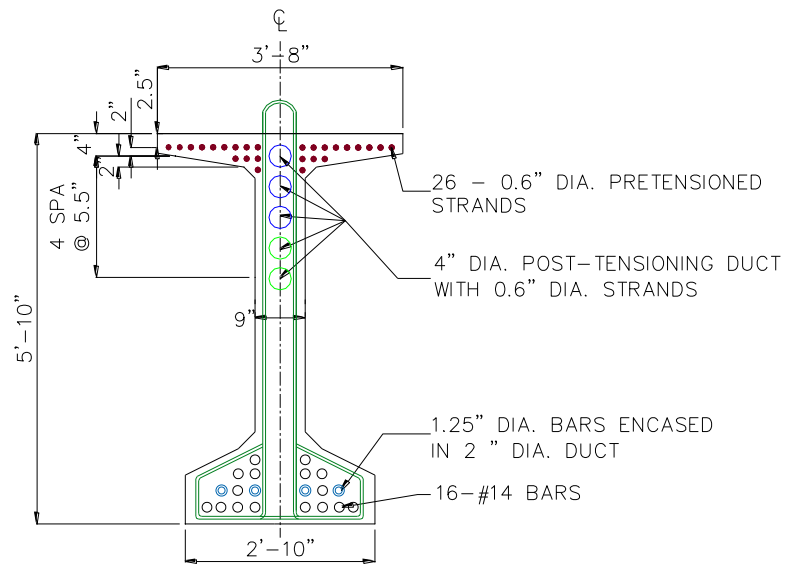


(c) Section B-B Near Midspan of End Span

Figure 3.10. Prestressing Details for Continuous Prestressed Concrete Shored Construction (cont.).

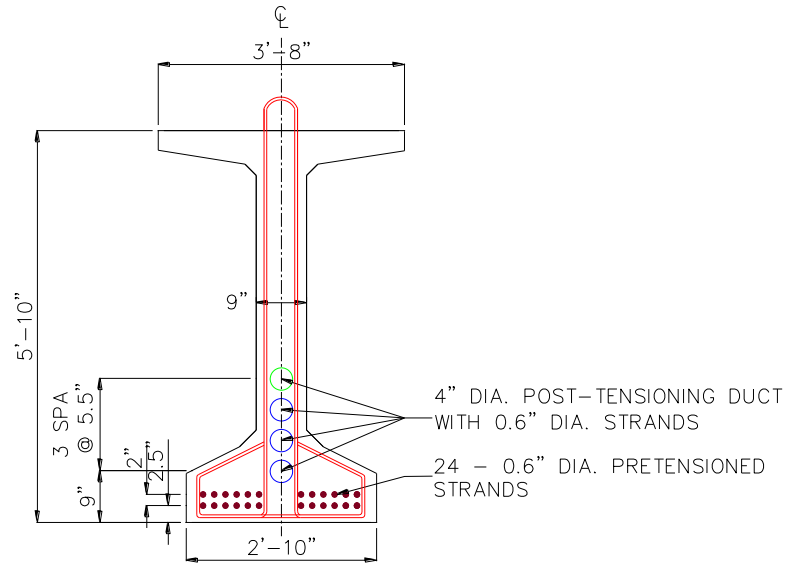


(d) Section C-C at Splice Connection in End Span



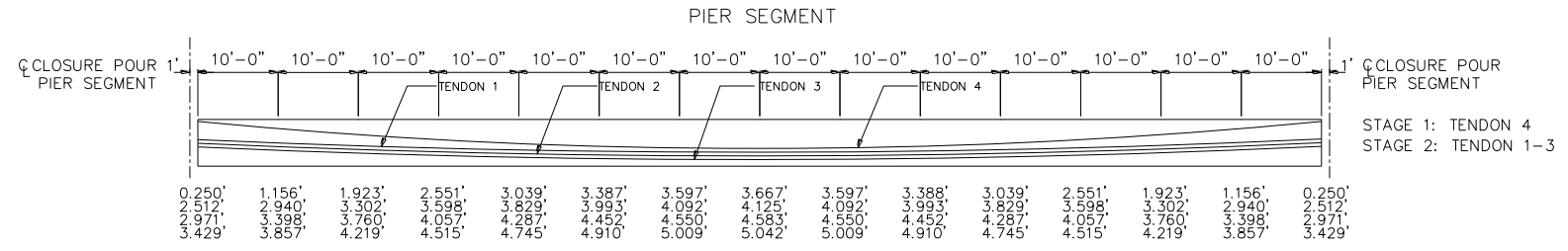
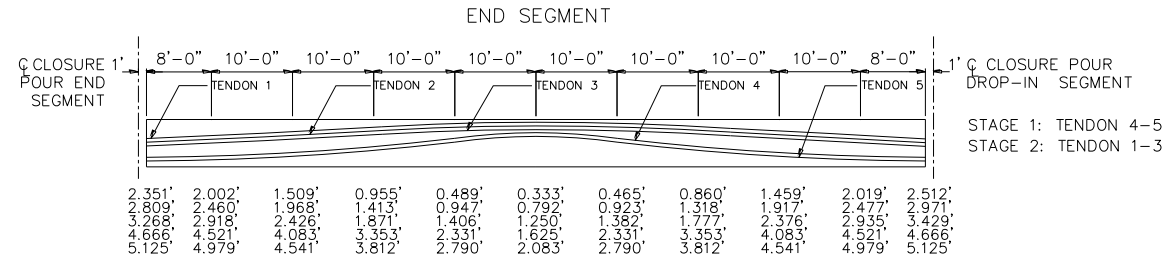
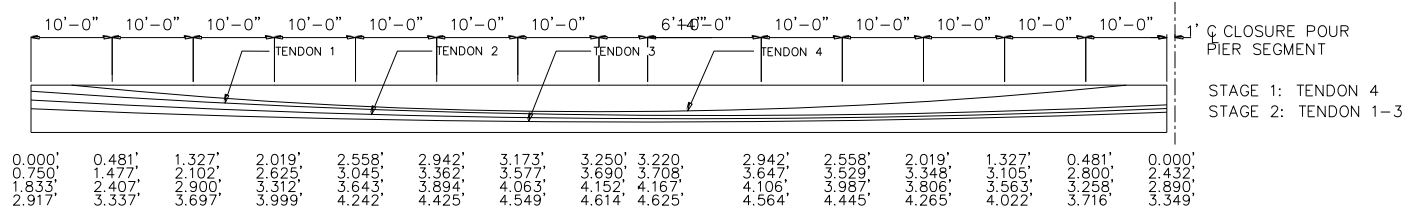
(e) Section D-D at Interior Pier

Figure 3.10. Prestressing Details for Continuous Prestressed Concrete Shored Construction (cont.).



(f) Section E-E Near Midspan of Drop-In Segment

Figure 3.10. Prestressing Details for Continuous Prestressed Concrete Shored Construction (cont.).



NOTES:
 1. DIMENSIONS TO \bar{C} OF TENDONS GIVEN FROM TOP OF GIRDER.
 FABRICATOR MUST ADJUST THE \bar{C} OF DUCT SO THAT \bar{C} OF TENDONS MATCHES THOSE SHOWN ON THIS SHEET.
 2. HORIZONTAL DIMENSIONS ARE MEASURED ALONG \bar{C} OF GIRDER.

Figure 3.11. Post-Tensioning Layout for Continuous Prestressed Concrete Modified Tx70 Girder Bridge Using Shored Construction.

3.11 MOMENTS DURING STAGES OF CONSTRUCTION

The moments during the various stages of construction considered are computed at selected locations along the structure. The moments are computed at $0.4L$ from the abutment support of end span (Section A-A), at the splice in end span (Section B-B), at the face of the pier (Section C-C), at the interior span splice (Section D-D), and at midspan of the interior span (Section E-E) as shown in the Figure 3.12. The moments due to girder self-weight, PCPs, and the wet CIP deck act on the non-composite girder section. The moments due to removal of shoring towers, superimposed dead load, and live load act on the composite girder section. The moments due to prestressing are computed before losses. Table 3.11 provides a summary of the moments at each of these locations. Figure 3.13 and Figure 3.14 show the moments due to the permanent loads acting on the non-composite girder section and the composite girder section, respectively.

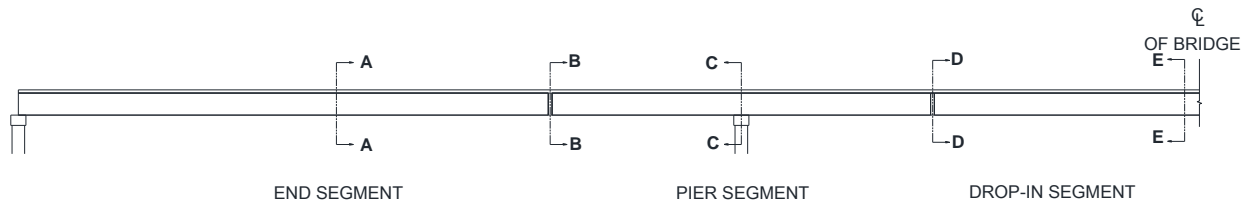
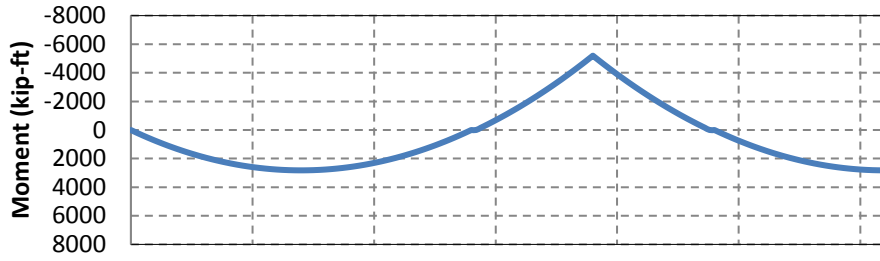


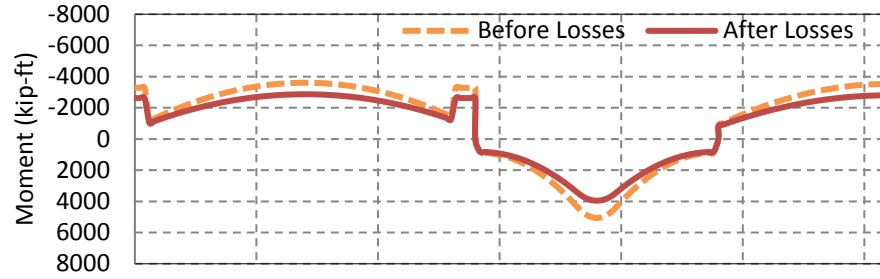
Figure 3.12. Section Locations for Girder Moments and Stress Checks.

Table 3.11. Girder Moments at Various Sections (kip-ft).

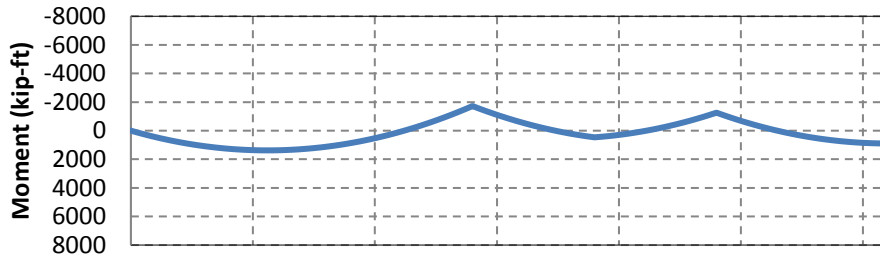
Loading	Section				
	A-A (End Segment)	B-B (Splice Exterior)	C-C (Pier)	D-D (Splice Interior)	E-E (Drop-in segment)
Girder Self-Weight	2822	-	-1383	-	2822
Pretensioning and Stage I PT	-3281	-	5185	-	-2896
Reaction from Drop-in Segment	-	-	-3871	-	-
Haunch and Deck	1293	-1719	-467	-1256	896
Stage II Post- tensioning	-4161	+195	5436	-327	-3344
Shoring Support Removal	942	1763	-4593	1306	1306
Superimposed Dead Load	725	11	-1391	15	739
Live Load	5736	3660	-5391	2371	6109



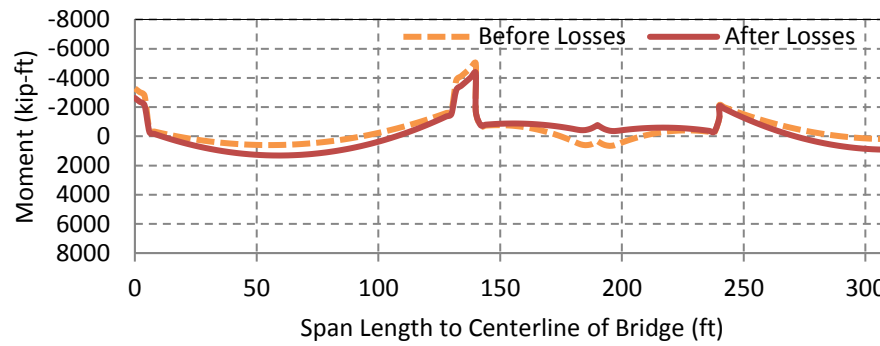
(a) Self-weight and Girder Reaction



(b) Pretensioning and Stage I Post-Tensioning

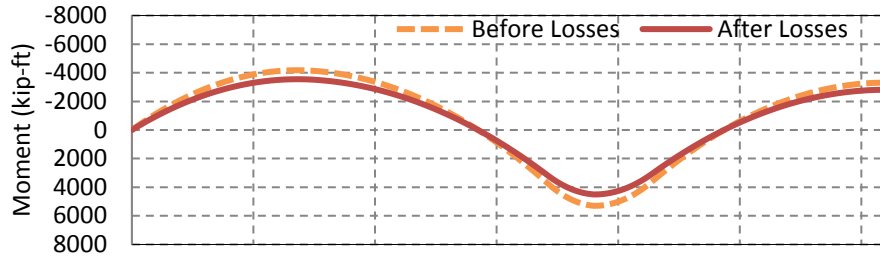


(c) PCP and Wet Deck Weight

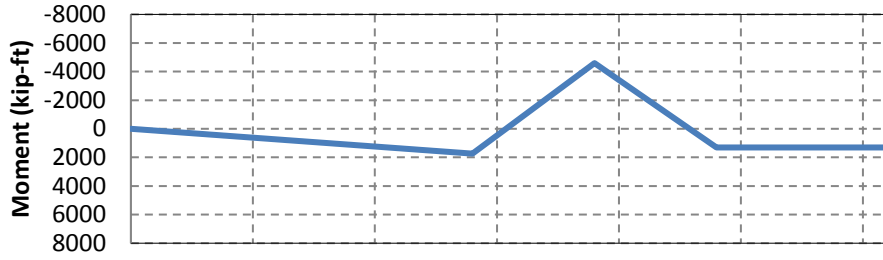


(d) Girder Moments with PCPs and Wet Deck

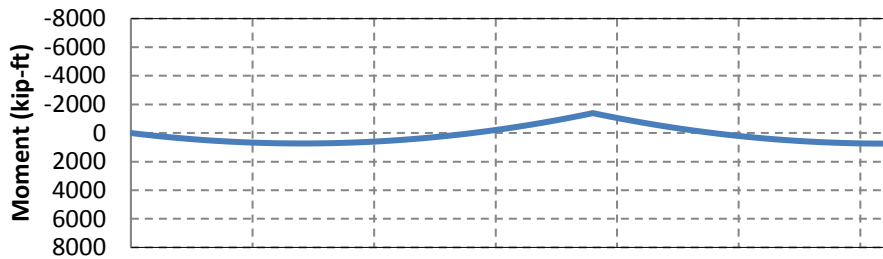
Figure 3.13. Moments Acting on Non-Composite Girder.



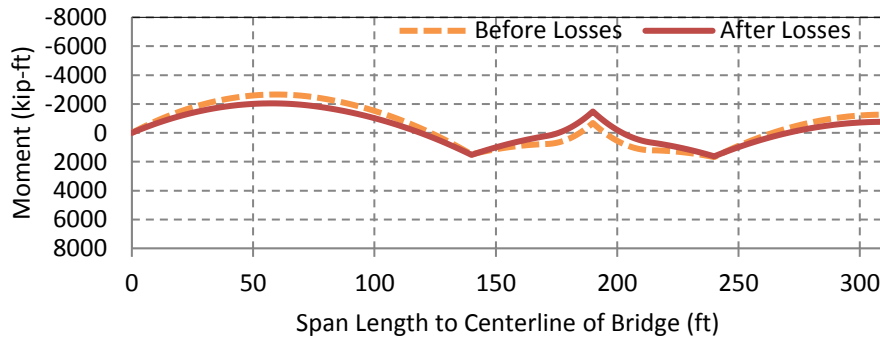
(a) Stage II Post-Tensioning



(b) Shoring Support Removal



(c) Superimposed Dead Load



(d) Total Composite Section Moments

Figure 3.14. Moments Acting on Composite Girder.

3.12 SERVICE STRESS ANALYSIS

Service stress analysis was carried out under the effects of dead loads, prestress, live loads, and temperature and thermal gradient. The stresses were checked at various steps of construction. The important construction steps for checking girder stresses are identified as follows:

- Step I: Girder segments supported on piers and temporary supports.
- Step II: Girders supporting weight of PCPs and wet CIP deck.
- Step III: Apply Stage II PT, remove shoring towers, and cast barriers.
- Step IV: Open bridge to service.

For the various stages of construction, stress checks are provided at the following points: (1) $0.4L$ of the end span, (2) at the splice in the end span, (3) at the face of pier, and (4) at the splice in the center span, and (5) at the midspan of center span. Compression in prestressed concrete girders is evaluated using the AASHTO Service I limit state while tension in prestressed concrete girders is evaluated using the AASHTO Service III limit state.

Figure 3.15 through Figure 3.19 present the stress blocks at Section A-A (at $0.40L$ in the end span), Section B-B (at the splice in the end span), Section C-C (at the face of the pier), Section D-D (at the splice in the center span), and Section E-E (at the midspan of the center span). Table 3.12 provides a summary of the stresses at the various sections.

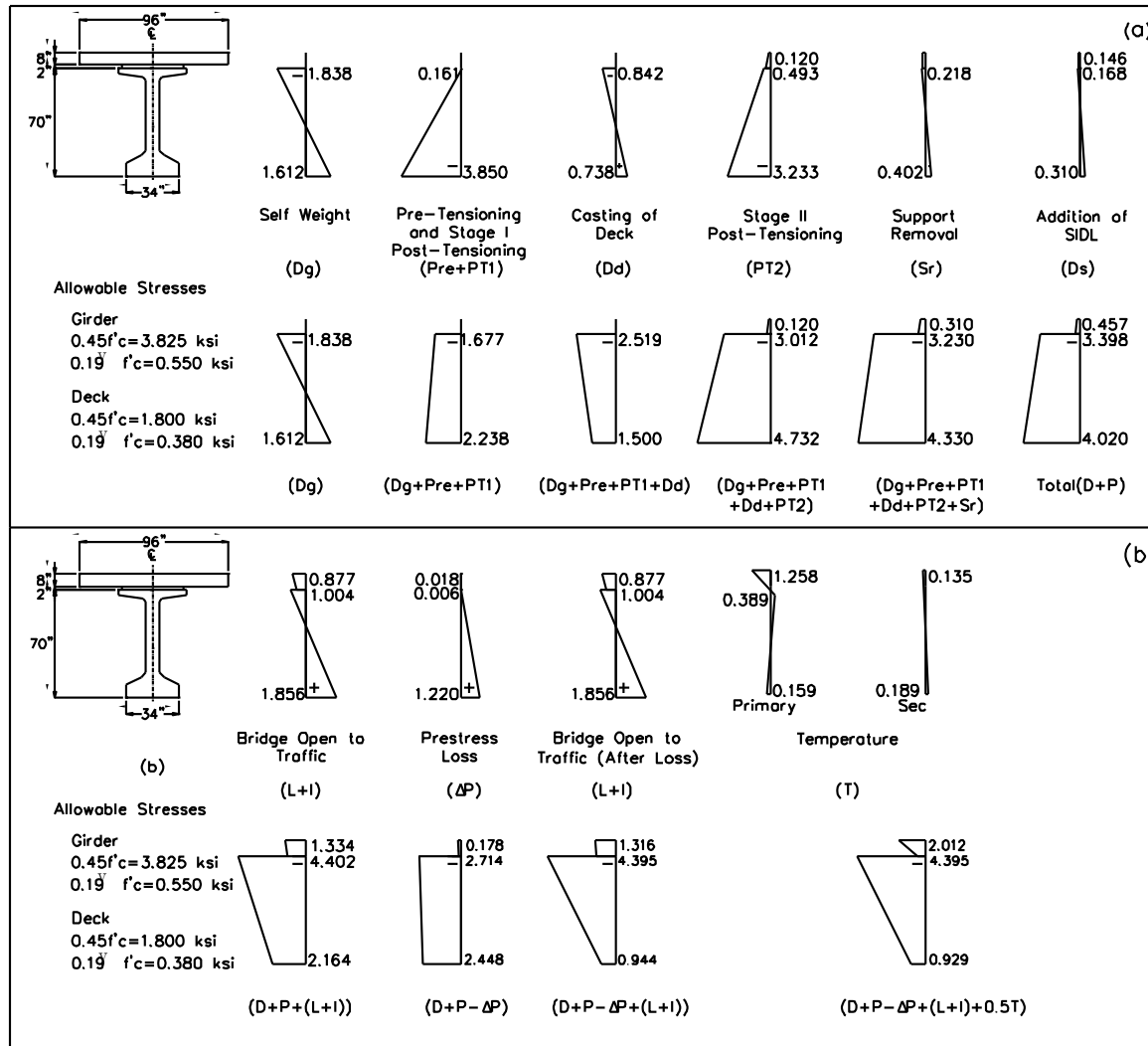


Figure 3.15. Stress Check at Section A-A for (a) Construction and (b) In-Service before and after Losses.

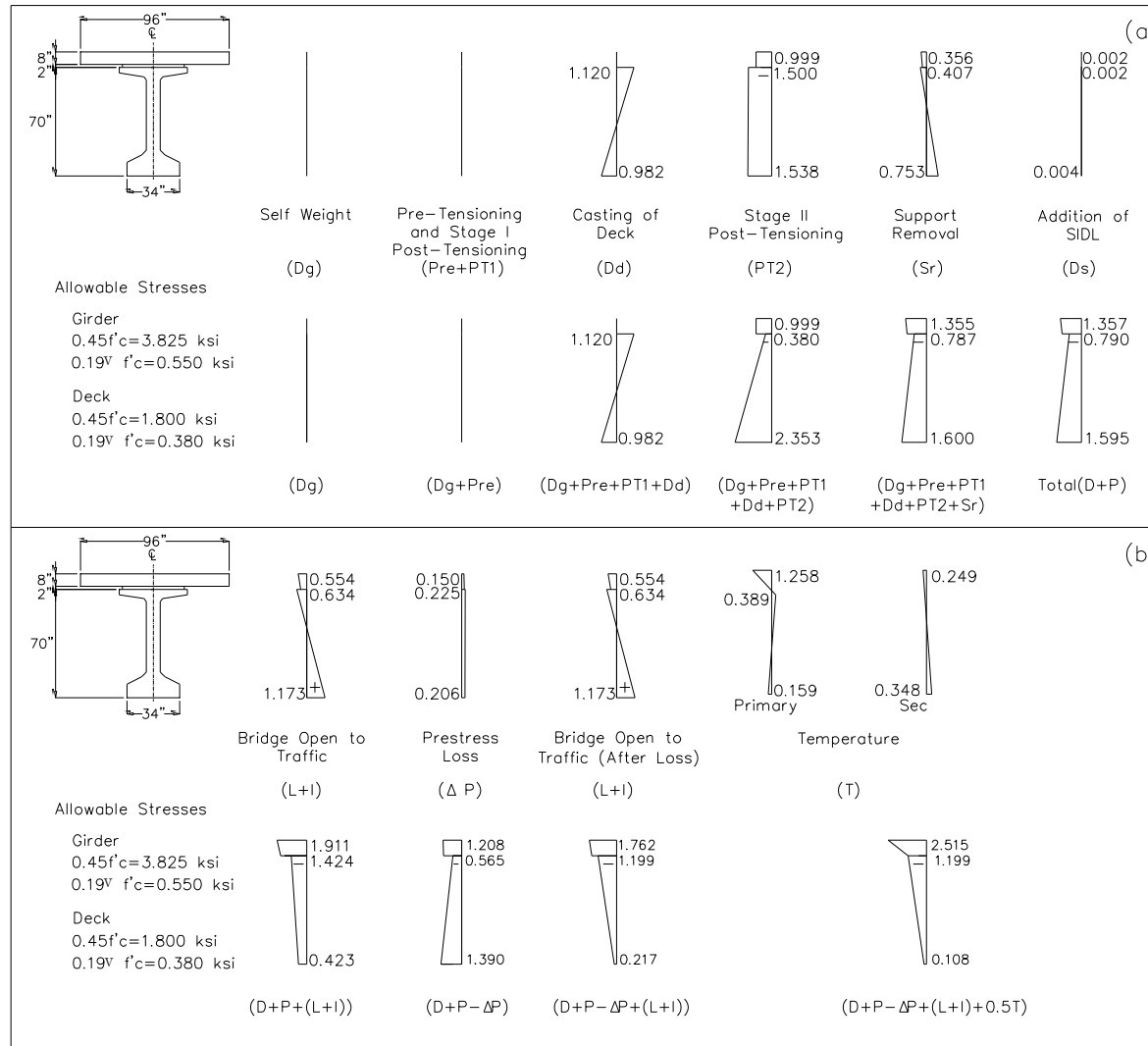


Figure 3.16. Stress Check at Section B-B for (a) Construction and (b) In-Service before and after Losses.

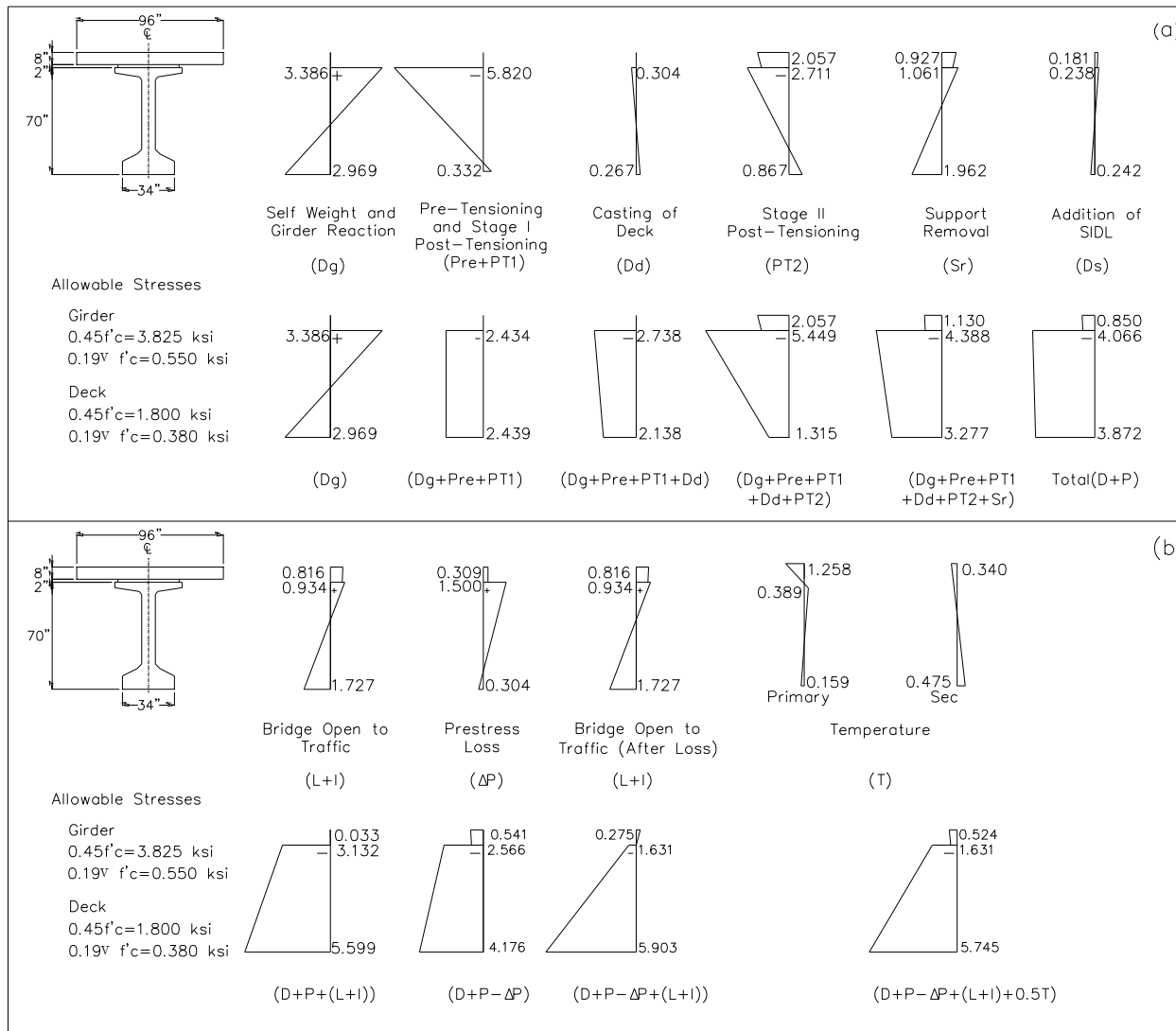


Figure 3.17. Stress Check at Section C-C for (a) Construction and (b) In-Service before and after Losses.

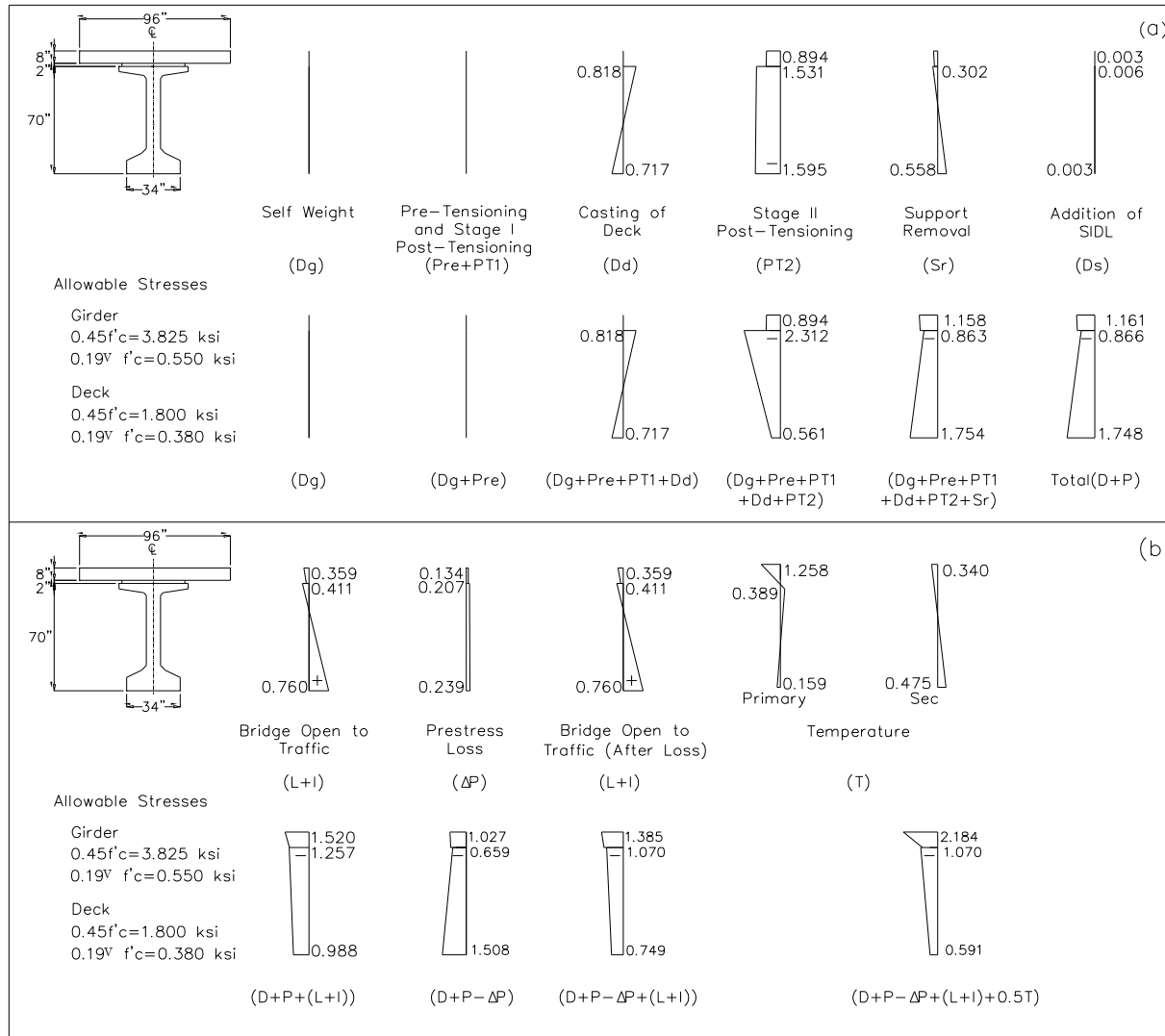


Figure 3.18. Stress Check at Section D-D for (a) Construction and (b) In-Service before and after Losses.

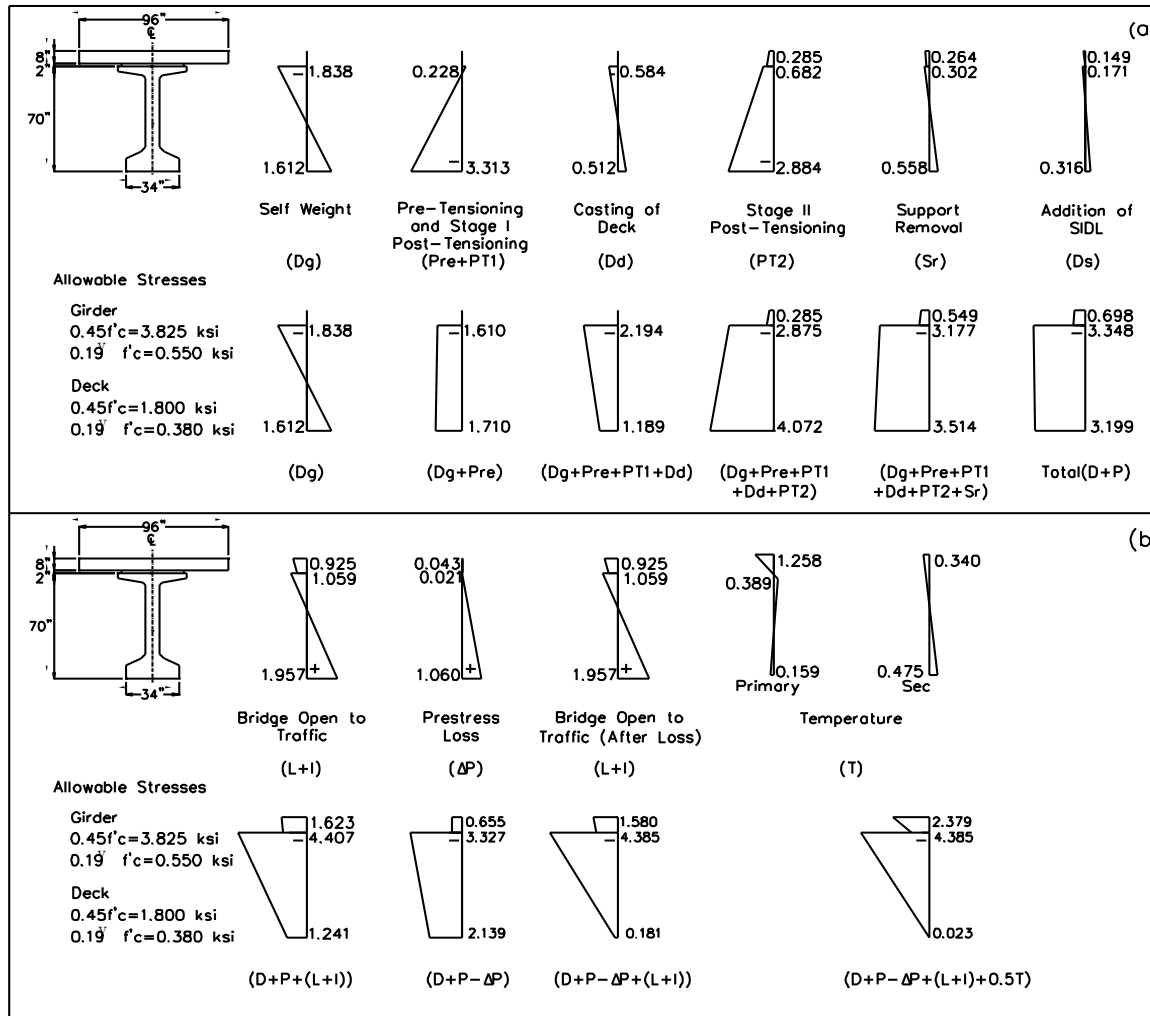


Figure 3.19. Stress Check at Section E-E for (a) Construction and (b) In-Service before and after Losses.

Table 3.12. Girder Stresses at Various Sections (ksi).

Loading	Component	Location	Section					Allowable Stress Limits	
			A-A (End Segment)	B-B (Splice Exterior)	C-C (Pier)	D-D (Splice Interior)	E-E (Drop-in segment)	Compression (Service I)	Tension (Service III)
Step I (Before Losses)	Girder	Top	-1.677	-	-2.434	-	-1.610	-3.825	+0.550
		Bottom	-2.238	-	-2.449	-	-1.700		
Step II (Before Losses)	Girder	Top	-2.519	+1.120	-2.738	+0.818	-2.194	-3.825	+0.550
		Bottom	-1.500	-0.982	-2.183	-0.717	-1.189		
Step III (After Losses)	Girder	Top	-3.391	-0.565	-2.566	-0.659	-3.327	-3.825	+0.550
		Bottom	-2.800	-1.390	-4.176	-1.508	-2.139		
	Deck	Top	-0.439	-1.208	-0.541	-1.027	-0.655	-2.400	+0.380
		Bottom	-0.531	-1.112	-0.608	-0.975	-0.694		
Step IV Service (After Losses)	Girder	Top	-4.395	-1.199	-1.631	-1.070	-4.385	-5.100	+0.550
		Bottom	-0.944	-0.217	-5.903	-0.481	-0.181		
	Deck	Top	-1.316	-1.762	+0.275	-1.385	-1.580	-2.400	+0.380
		Bottom	-1.194	-1.531	+0.009	-1.246	-1.393		

Both splice locations experience tensile stresses that exceed the allowable tensile stress limits at service conditions when the deck is poured (Step II). This stress exceedance is addressed by providing two #6 U bent mild steel reinforcement in the top flange. In addition, any cracks that may form will close when the Stage II PT operation is carried out.

The compressive stresses in the girder soffit at the interior support in the negative moment region were exceeded due to the large amount of PT tendons in the section. This stress exceedance may be addressed by increasing the specified concrete compressive strength to stay within the allowable compressive stress limit. Another option is to provide additional mild steel reinforcement in the compression zone. For this design, 16-#14 bars and four Dywidag bars were added in the bottom flange of the girder to improve the nominal capacity of the section as specified in the ultimate strength check. This additional mild steel reinforcement is also adequate to serve as compression reinforcement in the girder soffit at the interior support over the pier for the computed stress exceedance at service load conditions.

The deck in the pier region experiences tensile stresses due to negative bending under service conditions. However, these tensile stresses are within the allowable tensile stress limits.

3.13 DEFLECTION CHECK

The girder segments were checked for allowable deflection under live load and impact as specified in the AASHTO LRFD Specifications (AASHTO 2012) Article 2.5.2.6.2. Composite section properties were used to compute the deflections that occur under service loadings. According to the AASHTO LRFD Specifications (AASHTO 2012) Article 3.6.1.3.2, the deflection is calculated as the larger of:

- The design truck alone, or
- 25 percent of the design truck load and full design lane load.

The design truck load is multiplied by the dynamic load amplification factor to compute deflections. The limit for maximum live load deflection is specified as $L/800$ where L is the span length in inches (AASHTO 2012, Article 2.5.2.6.2). Table 3.13 gives the allowable and actual deflection values for the three-span bridge. The computed live load deflections are observed to be within the limits for both the exterior and interior spans.

Table 3.13. Live Load Deflection for Three-span Modified Tx70 Bridge.

Deflection	Exterior Span	Interior Span
Allowable (in.)	2.85	3.60
Actual (in.)	1.21	1.34

3.14 FLEXURAL STRENGTH CHECK

The flexural strength limit state must be checked to ensure safety at ultimate load conditions, and requires that the reduced nominal moment capacity of the member to be greater than the factored ultimate design moment, expressed as follows:

$$M_u \leq \phi M_n \quad (\text{Equation 3.6})$$

where:

M_u = Factored ultimate moment at a section, kip-ft.

M_n = Nominal moment strength at a section, kip-ft.

ϕ = Resistance factor.

= 1.0 for flexure and tension of prestressed concrete members.

The total factored moment at ultimate according to AASHTO LRFD Specification (AASHTO 2012) is given by:

$$M_u = 1.25 (M_{DC}) + 1.5 (M_{DW}) + 1.75 (M_{LL+IM}) \quad (\text{Equation 3.7})$$

where:

M_{DC} = Bending moment due to all dead loads, kip-ft.

M_{DW} = Bending moment due to wearing surface load, kip-ft.

M_{LL+IM} = Bending moment due to live load and impact, kip-ft.

The moment capacity and demand is checked at the following points: (1) $0.35L$ of the end span, (2) at the face of pier, and (3) at the midspan of the center span. The moment capacity at ultimate depends on the number of strands, diameter of strands, stress in the stands, design strength of concrete and the cross-section properties of the section. Table 3.14 gives the moment demand and capacity for the three-span bridge. The capacity is greater than demand at each section considered.

Table 3.14. Ultimate Demand and Capacity.

Capacity and Demand	End Span	Pier	Interior Span
Applied Demand, M_u (kip-ft)	14,940	20,680	15,330
Available Capacity, ϕM_n (kip-ft)	22,780	24,180	24,430

The negative moment capacity provided by the pretensioning strands and PT tendons at the interior support is supplemented by adding mild steel reinforcement. For this design, 16-#14 bars and four 1.25 in. diameter Dywidag bars are added in the bottom flange of the girder to provide the additional required capacity to meet the moment demand at the interior support over the pier. Note that the mild steel reinforcement provided in the bottom flange acts as compression steel.

3.15 SHEAR STRENGTH CHECK

Modified compression field theory (MCFT) was used for the transverse shear design as specified in the AASHTO LRFD Specifications (AASHTO 2012). MCFT takes into consideration the combined effect of axial load, flexure, and prestressing when determining the shear strength provided by the concrete section. Figure 3.20 shows the shear demand and shear design for the three-span prototype bridge from the abutment to the centerline of the symmetric structure. Figure 3.21 shows the details of the shear reinforcement. The stirrup layout is as follows:

- End girder segment:
 - #5 double-legged stirrups at a spacing of 4 in. are provided for a distance of 10 ft from the abutment end.
 - #5 double-legged stirrups at a spacing of 6 in. are provided from 10–20 ft from the abutment end.
 - #5 double-legged stirrups at a spacing of 12 in. are provided in the remaining portion of the end segment.
- Pier girder segment:
 - #5 double-legged stirrups at a spacing of 4 in. are provided for a distance of 29 ft from the centerline of pier toward the center span and 24 ft from the centerline of pier toward the end span in the ends of the pier segment.

- #5 double-legged stirrups at a spacing of 6 in. are provided in the remaining portions of the pier segment.
- Drop-in girder segment for center span:
 - #5 double-legged stirrups at a spacing of 6 in. are provided for a distance of 20 ft from each end of the drop-in segment.
 - #5 double-legged stirrups at a spacing of 12 in. are provided in the remaining portion of the drop-in segment.

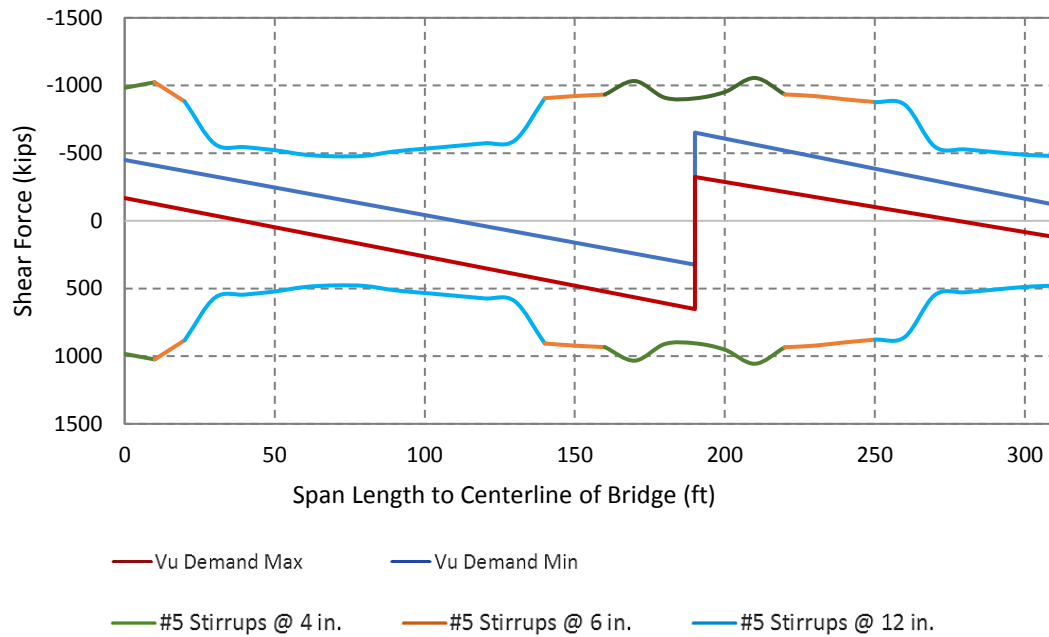
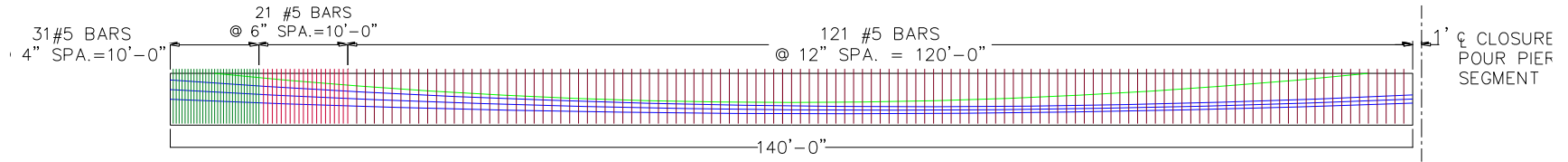
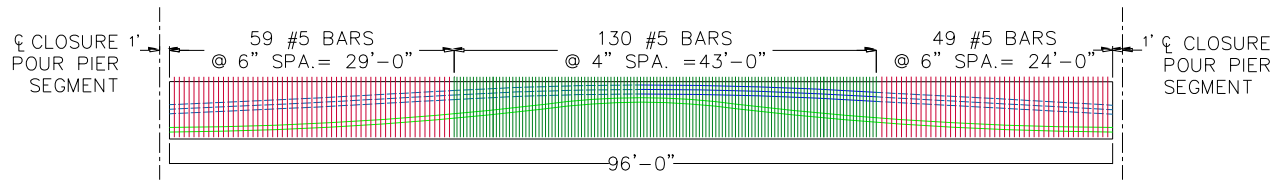


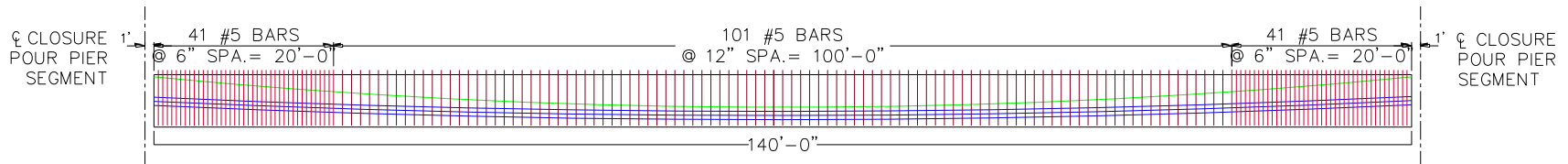
Figure 3.20. Transverse Shear Demand and Capacity.



(a) END SEGMENT



(b) ON-PIER SEGMENT



(c) DROP-IN SEGMENT

Figure 3.21. Shear Reinforcement Details.

The transverse bars were extended above the top flange to provide shear resistance for interface shear between the deck and the girder segments. The provided shear resistance at the interface plane was calculated based on Article 5.8.4.1-3 of the AASHTO LRFD Specifications (AASHTO 2012). The interface shear resistance is compared with the factored interface shear demand in Figure 3.22.

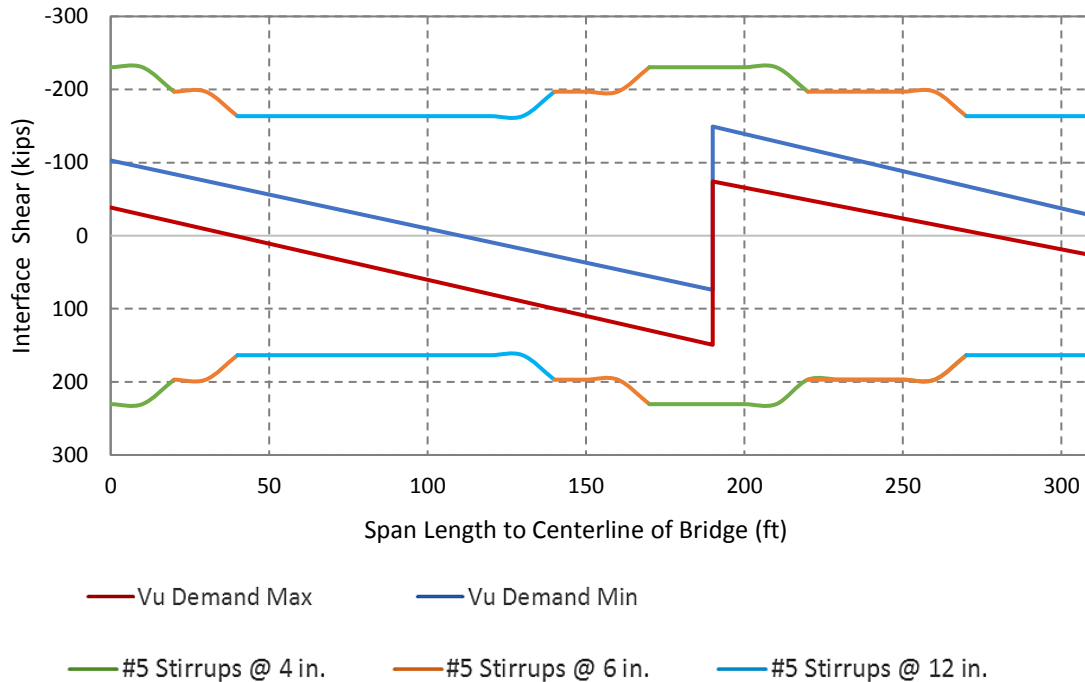


Figure 3.22. Interface Shear Demand and Capacity.

3.16 SPLICE DESIGN

3.16.1 Splice Details

Splices are located at the dead load point of contraflexure in the prototype bridge to minimize the load demands at the splice. The width of the splice connection should be kept as small as possible because there is no pretensioning in this region and a minimal amount of mild steel reinforcement is provided. However, the splice width should be large enough to splice the continuity PT tendon ducts and allow for proper vibration of the CIP concrete for the splice. The width of the splice connection detail is 24 in. (2 ft) based on discussions with TxDOT. Figure 3.23 shows the splice connection detail considered for the design.

A partially prestressed splice connection detail is used at all splice locations. Mild steel reinforcement is provided in addition to continuity PT through the splice connection. The mild steel reinforcement consists of 180° bent hooked bars anchored into the adjacent girder flanges and extending into the joint. The mild steel bent bars were designed for the maximum factored design loads. The combination of PT and mild steel is expected to provide better durability and performance. Vertical reinforcement is provided to strengthen the splice connection for shear. The integrity of the splice connection largely depends on the shear transfer mechanism at the interface of the precast girder and closure pour. This shear transfer mechanism is mainly provided by the compressive force provided by the continuous PT, the lapped 180° bent hooked bars in the connection, and a single shear key.

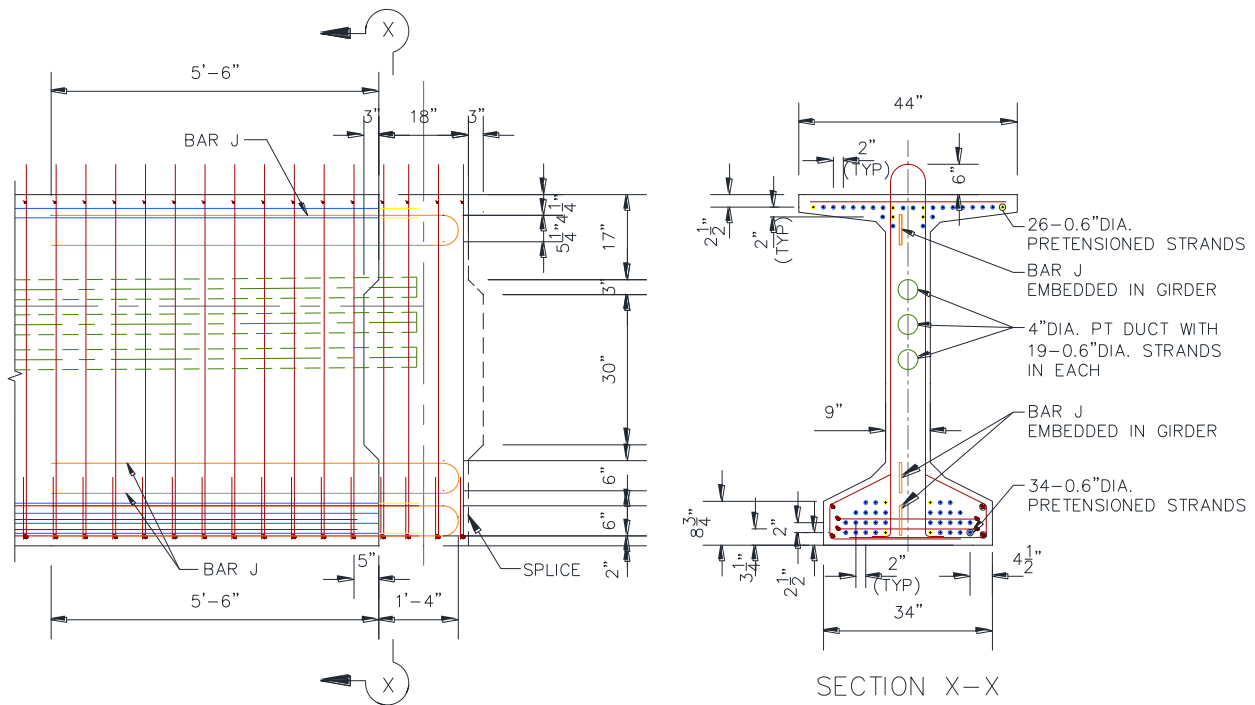


Figure 3.23. Partially Prestressed Splice Connection Detail.

3.16.2 Prestressing and Reinforcement Details for the Splice

Only the Stage II PT tendons are continuous through the splice connections. The pretensioned strands and the Stage I PT tendons terminate at the girder segment ends adjacent to the splice. Therefore, additional mild steel reinforcement was needed to achieve flexural strength at the

splices. For the proposed splice connection detail, additional capacity is provided by mild steel 180° bent bars with details as presented in Table 3.15 (see Figure 3.23). Table 3.16 presents the prestressing design summary for the splices.

Table 3.15. Reinforcement Details for the Splices.

Reinforcement Details		Splices
180° bent bars embedded in each girder segment at splice	Top flange of each girder segment	1 - #6
	Bottom flange of each girder segment	2 - #6

Table 3.16. Prestressing Details for the Splices.

Prestressing Details		Splices
Stage II PT	Tendons (0.6 in. dia.) (19 strands per duct)	57 (3 ducts)
	Force at Transfer	2337 kips

3.16.3 Flexural Strength Check

The flexural strength limit state of the splice connection was checked to ensure safety at the ultimate load conditions based on the AASHTO LRFD Specifications (AASHTO 2012). The total ultimate bending moment for the interior splice, corresponding to the in-span splice in the end span of the prototype bridge, is $M_u = 4874$ kip-ft. Only the Stage II PT tendons run continuously through the splice connection, while the pretensioning strands and the Stage I PT tendons terminate at the girder segment ends adjacent to the splice. To enhance the flexural capacity and for crack control, 180° mild steel bent bars are provided in the splice with details as follows (see Figure 3.23):

Top flange steel: 1 - #6 180° bent bar embedded

Bottom flange steel: 2 - #6 180° bent bars embedded

The reduced nominal capacity of the splice section, ϕM_n , is 7500 kip-ft. The flexural capacities provided by the PT strands and mild steel are 6700 kip-ft and 800 kip-ft, respectively.

3.16.4 Shear Design

3.16.4.1 Transverse Shear Design

MCFT is used for transverse shear design as specified in the AASHTO LRFD Specifications (AASHTO 2012). The total ultimate shear for the splice in the end span of the prototype bridge was $V_u = 420$ kips. Table 3.17 presents shear design details for the end-span splice.

Table 3.17. Shear Design Details for Splices.

Girder Segment	Shear Reinforcement	Nominal Capacity, V_n (kips)
End-Span Splice	4 - #5 Stirrups @ 6 in. spacing	900
Main Span Splice	4 - #5 Stirrups @ 6 in. spacing	900

Note: All shear reinforcement consists of double legged stirrups.

Due to the significant amount of shear reinforcement, TxDOT engineers recommended checking the principal tensile stress in the web of the Tx70 girder at the splice locations. AASHTO LRFD Specifications Article 5.8.5 (AASHTO 2012) requires checking the principal tension stress to verify the adequacy of the webs of segmental concrete bridges for longitudinal shear and torsion. This article states that the principal tensile stress resulting from long-term residual axial stress and maximum shear at the neutral axis of the critical web shall not exceed the tensile stress limit provided by AASHTO LRFD Specifications (AASHTO 2012) Table 5.9.4.2.2-1 ($0.11\sqrt{f'_c}$) for the Service III limit state at all stages during the life of the structure, excluding those during construction. When investigating principal stresses during construction, the tensile stress limits of Table 5.14.2.3.3-1 ($0.11\sqrt{f'_c}$) shall apply.

The principal stress was checked at the splice location in the end span and main span, as shown in Table 3.18. Shear and bending stresses in the concrete at the neutral axis of the web were calculated for the Service III limit state. The principal stress was calculated using classical beam theory and the principle of Mohr's Circle.

Table 3.18 shows the principal tension stress at the end span and main span splice locations with and without considering the vertical force component of draped longitudinal tendons V_p . AASHTO LRFD Specifications Article 5.8.5 (AASHTO 2012) specifies that V_p shall be

considered as a reduction in the shear force due to the applied loads. Also, from the load-balancing approach, the total dead load of the girder and deck slab is balanced by the prestressing and PT tendon profiles. Therefore, the principal tension stress values considering V_p are below the AASHTO LRFD Specifications (AASHTO 2012) specified allowable limit.

Table 3.18. Principal Tension Stress Calculation.

Location	Principal Tension Stress at Service (Not Considering V_p) (ksi)	Principal Tension Stress at Service (Considering V_p) (ksi)	Principal Tensile Stress Limit ($0.11\sqrt{f'_c}$) (ksi)
End Span Splice	0.242	0.066	0.321
Main Span Splice	0.249	0.068	0.321

3.16.4.2 Interface Shear Design for Girder-to-Splice Interface

The provisions for interface shear design as specified in the AASHTO LRFD Specifications (AASHTO 2012) Article 5.8.4 are followed for the design of the girder-to-splice interface. The required nominal interface shear strength at the interface plane is given as follows:

$$V_{nreqd} = \frac{V_u}{\phi} \quad (\text{Equation 3.8})$$

where:

- V_{nreqd} = Required nominal shear strength at the interface plane, kips.
- V_u = Factored shear force at the girder-to-splice interface, kips.
- ϕ = Resistance factor for shear in prestressed concrete members.
= 0.9 for normal weight concrete members (AASHTO LRFD Article 5.5.4.2).

The required nominal interface shear strength at the interface plane is $V_{nreqd} = 467$ kips. The interface shear resistance at the girder-to-splice interface is calculated per the AASHTO LRFD Specifications (AASHTO 2012) Article 5.8.4 based on shear friction theory. The nominal shear resistance of the interface plane is based on the cohesion factor, c , friction factor, μ , and the area of concrete engaged in interface shear transfer, A_{cv} . For this design, an intentionally roughened surface was considered. The values of corresponding design parameters for such condition are specified in the AASHTO LRFD Specifications (AASHTO 2012) Article 5.8.4 as cohesion factor

$c = 0.24$ ksi, friction factor $\mu = 1.0$, fraction of concrete strength available to resist interface shear $K_1 = 0.25$, and limiting interface shear resistance $K_2 = 1.5$ ksi. These values for the parameters were selected based on the *TxDOT Bridge Design Manual* (TxDOT 2013).

The nominal shear resistance of the interface plane is provided by the mild steel 180° bent bars, area of concrete engaged in interface shear transfer, and permanent net compressive force normal to the interface plane. The expression for nominal shear resistance of the interface plane is given as follows:

$$V_n = cA_{cv} + \mu[A_{vf}f_y + P_c] \quad (\text{Equation 3.9})$$

where:

- V_n = Nominal shear resistance of the interface plane, kips.
- c = Cohesion factor = 0.24 ksi.
- μ = Friction factor = 1.0.
- A_{cv} = Area of concrete engaged in interface shear transfer, in.²
- A_{vf} = Area of shear reinforcement crossing the shear plane within A_{cv} , in.²
- P_c = Permanent net compressive force normal to the shear plane = 1753 kips.
- f_y = Yield strength of shear reinforcement, ksi = 60 ksi.

In this case of the girder-to-splice interface:

$$A_{cv} = A_g - A_{duct} \quad (\text{Equation 3.10})$$

$$A_g = \text{Area of girder} = 1106 \text{ in.}^2$$

$$A_{duct} = \text{Area of PT ducts} = 3 (12.57) = 37.71 \text{ in.}^2$$

$$A_{cv} = 1106 - (3)(12.57) = 1068.30 \text{ in.}^2$$

The minimum interface shear reinforcement is determined as follows:

$$A_{vf} \geq \frac{0.05A_{cv}}{f_y} \quad (\text{Equation 3.11})$$

where:

$$A_{cv} = \text{Area of concrete engaged in interface shear transfer} = 1068.30 \text{ in.}^2$$

$$A_{vf} = \text{Area of shear reinforcement crossing the shear plane within } A_{cv}, \text{ in.}^2$$

$$f_y = \text{Yield strength of shear reinforcement} = 60.0 \text{ ksi.}$$

$$A_{vf} \geq \frac{0.05(1068.30)}{60} = 0.89 \text{ in.}^2$$

For the provided 3 - #6 mild steel 180° bent bars (double legged) at each girder-to-splice interface, the area of interface shear reinforcement is given as follows:

$$A_{vf} = (3)(2)(0.44) = 2.651 \text{ in.}^2 > 0.89 \text{ in.}^2$$

The nominal shear resistance, V_n , used in the design shall not be greater than the lesser of the following two expressions:

$$V_n \leq K_1 f'_c A_{cv} \quad (\text{Equation 3.12})$$

$$V_n \leq K_2 A_{cv} \quad (\text{Equation 3.13})$$

where:

f'_c = The 28-day compressive strength at service of the weaker concrete at the interface plane, ksi.

K_1 = Fraction of concrete strength available to resist interface shear = 0.25.

K_2 = Limiting interface shear resistance = 1.5 ksi.

$$V_n \leq (0.25)(8.5)(1068.30) \approx 2270 \text{ kips}$$

$$V_n \leq (1.5)(1068.30) \approx 1600 \text{ kips}$$

Therefore, the nominal shear resistance at the girder/splice interface is taken as 1600 kips, which is much larger than the required nominal interface shear strength of 467 kips at the interface plane.

The embedment length of the mild steel 180° bent bars into the girder flanges is determined based on the design recommendations for optimized continuity diaphragms (Koch and Roberts-Wollmann 2008). Their design recommendation for embedment length is based on the angle of inclination of the diagonal compressive stress or crack angle, θ , computed using the MCFT for transverse shear design. Using MCFT, as specified in AASHTO LRFD Specifications (AASHTO 2012) Article 5.8.3, a variable angle truss analogy is adopted in which the angle of the diagonal compressive stress, θ , is considered to be variable and is determined in an iterative manner. MCFT takes into account different factors such as strain condition of the section and shear stress in the concrete to predict the shear strength of the section. At the splice location, the angle of the diagonal compressive stress is $\theta = 29^\circ$. Therefore, the required embedment length of the provided #6 mild steel 180° bent bars at each girder-to-splice interface is 5 ft-6 in. (see Figure 3.23).

AASHTO LRFD Specifications (AASHTO 2012) Article 5.8.4.1 requires that shear friction reinforcement shall be anchored to develop the specified yield strength on both sides of

the shear plane by embedment, hooks, or welding. The splice connection detail is designed to develop the specified yield strength of the reinforcement on both sides of the interface shear plane. Therefore, the embedment length of the 180° bent bars was also checked to satisfy the development length requirements specified in AASHTO LRFD Specifications (AASHTO 2012) Article 5.11. The required development length for the #6 mild steel 180° bent bars at each girder-to-splice interface is 10 in. The provided 180° hook extends into the splice equal for a distance of 1 ft-4 in. The recommended embedment length of the bent bars into the girder segments is 5 ft-6 in., as determined above based on Koch and Roberts-Wollmann (2008). This length is larger than the standard AASHTO straight bar development length of 2 ft-2 in. for top bars. Therefore, the detailing of the connection #6 mild steel 180° bent bars on both sides of the shear plane provides full development of reinforcement.

4 PARAMETRIC STUDY

4.1 INTRODUCTION

The research team presented preliminary designs in the Phase 1 Research Report for this project (Hueste et al. 2012) as an initial evaluation intended to push the limits of span-to-depth ratios and design of continuous bridges using the current standard TxDOT girder sections. Based on the findings documented in the Phase 1 Research Report, TxDOT input was considered in finalizing the parameters for a parametric study focused on assessing a number of potential continuous bridge designs using standard TxDOT precast concrete bridge girder sections. Per TxDOT recommendations for long span construction, a three-span continuous spliced girder system was chosen for the parametric study. The main goal of this study was to evaluate the design parameters and factors that influence the design of continuous spliced girder bridges to satisfy the requirements for service stress limits, flexural strength, and shear strength. Shored and hybrid (partially shored) methods of construction were considered, adopting prismatic and haunched on-pier segments, respectively. Sequencing of the precast prestressed concrete girder fabrication, CIP concrete on site, and PT operations are important construction considerations that were taken into account in the parametric study.

4.2 DESIGN CASES

A parametric study was performed to further explore the design space for spliced girder bridges. For the parametric study, the Tx70, Tx82, and U54 girder cross-sections were considered. The Tx70 and Tx82 shapes were modified to have a wider web for the PT ducts. The limit state design requirements for service stresses, flexural strength, and transverse shear strength were evaluated. A comparative study was also carried out for the considered designs cases outlined in Table 4.1. The segment lengths are as follows:

- For a span configuration of 190-240-190 ft using Tx girders, the length of the drop-in and end girder segments is 140 ft, while the on-pier segment is 96 ft.
- For a span configuration of 150-200-150 ft using Tx girders, the length of the drop-in segment and end girder segments is 120 ft, while the on-pier segment is 76 ft.
- For a span configuration of 150-200-150 ft using a U54 girder, the length of the drop-in and the end girder segments is 100 ft, while the on-pier segment is 96 ft.

Table 4.1. Design Cases.

Design Case	Girder Type				Shored	Hybrid	Span Configuration (ft)
	Tx70 (9" web)	Tx82 (9" web)	Tx82 (10" web)	Texas U54	Prismatic	Haunched	
1	×				×		190-240-190
2		×			×		190-240-190
3			×		×		190-240-190
4	×					×	190-240-190
5	×				×		150-200-150
6		×			×		150-200-150
7				×	×		150-200-150
8	×					×	150-200-150

The following sections provide a summary of differences observed for the parallel designs conducted for the parametric study. Differentiating factors include section properties, girder weights, prestressing details, service stress analysis, transverse shear reinforcement, ultimate strength and ductility, deflections, and splice connection requirements.

4.3 DESIGN PARAMETERS

Table 4.2 summarizes the design parameters selected for the parametric study. Design parameters, such as concrete strength, are based on standard practices followed by TxDOT throughout the state of Texas. A relative humidity of 65 percent is assumed based on the average value in Texas, as specified in AASHTO LRFD Specifications Article 5.4.2.3 (AASHTO 2012). Additional parameters are consistent with TxDOT standard materials and parameters provided in the AASHTO LRFD Specifications (AASHTO 2012).

Table 4.2. Design Parameters.

Parameter		Selected Value
Concrete strength at service for deck slab, f'_c		4 ksi
Precast concrete strength at release, f'_{ci}		6.5 ksi
Precast concrete strength at service, f'_c		8.5 ksi
Coefficient of thermal expansion of concrete		$6 \times 10^{-6}/^{\circ}\text{F}$
Relative humidity		65%
Mild steel	Yield strength, f_y	60 ksi
	Modulus of elasticity, E_s	29,000 ksi
Prestressing steel	Strand diameter	0.6 in.
	Ultimate tensile strength, f_{pu}	270 ksi – low relaxation
	Yield strength, f_{py}	$0.9 f_{pu}$
	Stress limit at transfer, f_{pi}	$f_{pi} \geq 0.75 f_{pu}$
	Stress limit at service, f_{pe}	$f_{pe} \geq 0.8 f_{py}$
	Modulus of elasticity, E_p	28,500 ksi
	Coefficient of friction, μ	0.25
	Wobble coefficient	0.0002/ft
	Anchor set	0.375 in.

4.4 SECTION PROPERTIES

Table 4.3 summarizes the composite and non-composite section properties for the modified Tx70 (9 in. web), Tx70 haunched (9 in. web), Tx82 (9 in. web), Tx82 (10 in. web), and U54 girder sections. The area of the 2 in. haunch is not considered in the calculation of the section properties and is only included in dead weight calculations. Figure 4.1 and Figure 4.2 show the cross-section details. The modified Tx70 (9 in. web) uses an increased web thickness as compared to the standard 8 in. web to allow for PT ducts. For the Tx82 (9 in. web), the web height of the modified Tx70 girder is increased by 12 in. The girder is 82 in. deep with a top flange width of 44 in. and bottom flange width of 34 in. For the Tx82 (10 in. web) girder, the web of the Tx82 (9 in. web) is further widened by 1 in. This results in an increase in the width of the top flange and bottom flange. For the haunched Tx70 (9 in. web) girder, a constant web depth haunch is considered with an extended

bottom flange. The depth of the haunched girder varies from 70 in. at the ends to a maximum depth of 108 in. at the centerline of the pier.

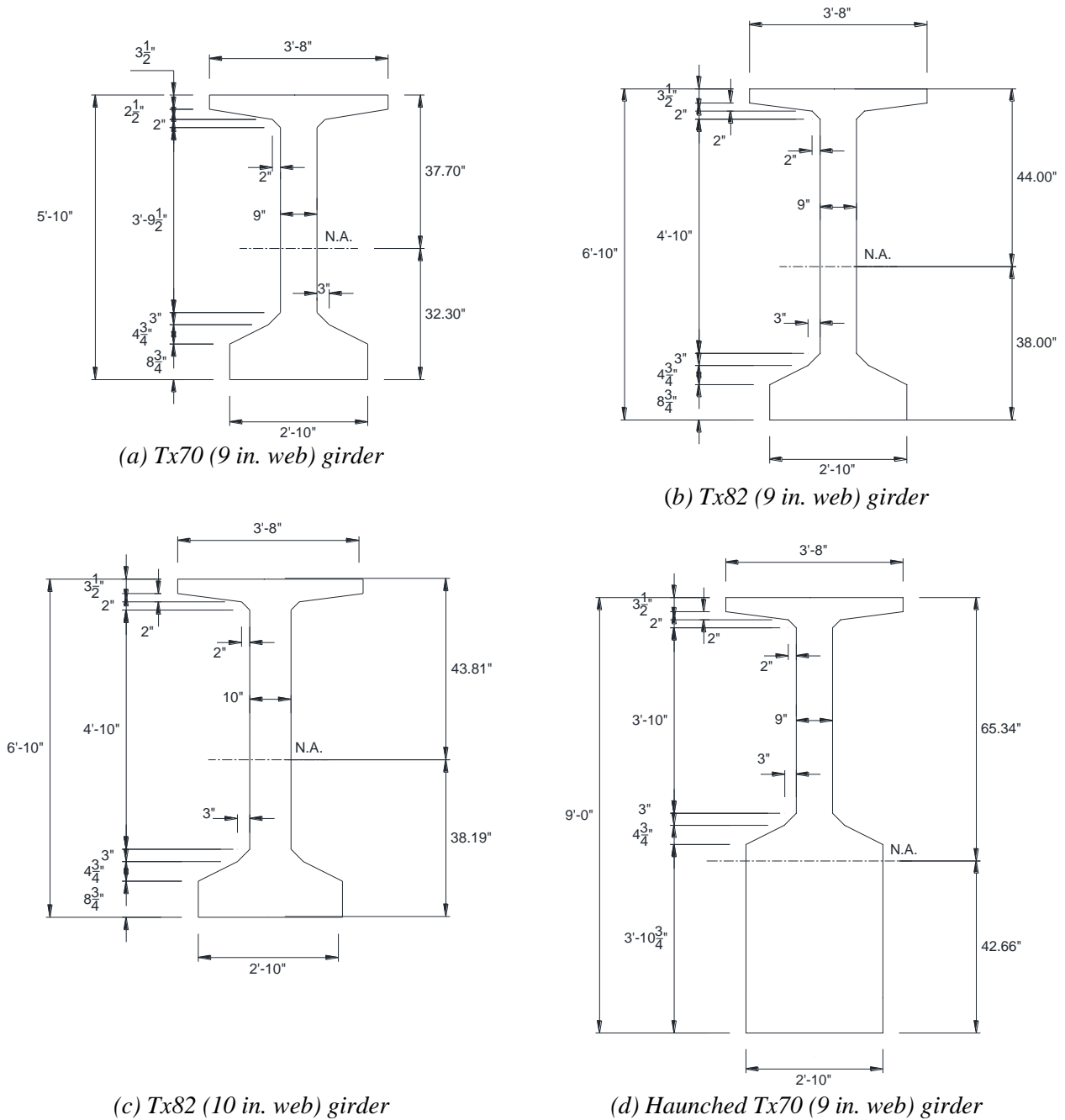


Figure 4.1. Texas Girders Considered.

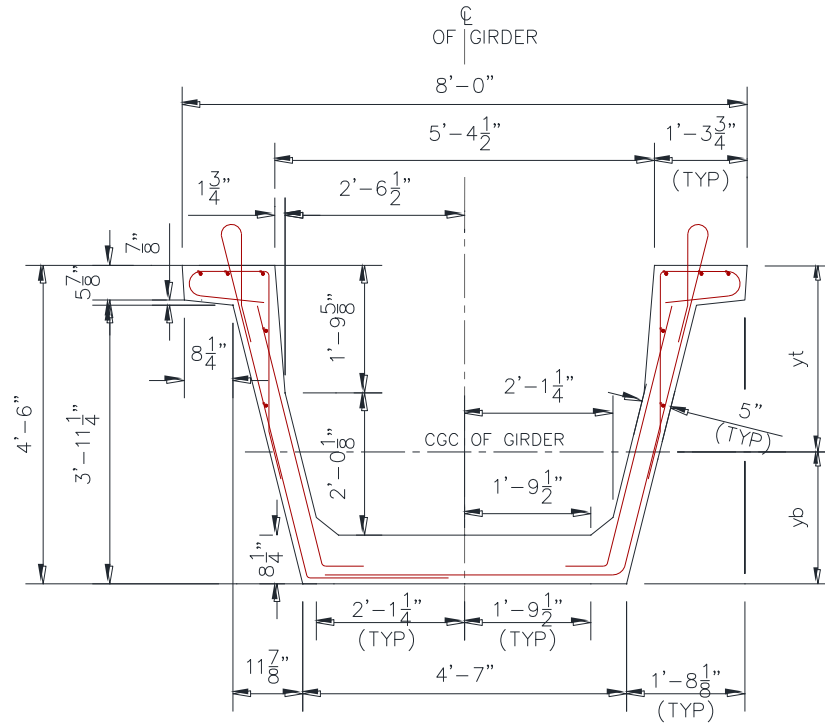


Figure 4.2. Texas U54 Girder.

Table 4.3. Section Properties for Texas Girders.

Girder Type	Description	Depth of N.A. from top of Girder, y_{top} (in.)	Depth of N.A. from bottom of Girder, y_{bot} (in.)	Area, A (in.²)	Moment of Inertia, I_x (in.⁴)
Tx70	9 in. web	37.70	32.30	1106	687,111
Tx70	Composite, 9 in. web	23.60	46.40	1607	1,287,145
Tx82	9 in. web	44.0	38.0	1214	1,088,079
Tx82	Composite, 9 in. web	28.87	53.13	1741	2,009,393
Tx82	10 in. web	43.81	38.19	1296	1,134,718
Tx82	Composite, 10 in. web	29.55	52.45	2064	2,066,899
Tx70	Haunched on-pier segment	65.34	42.66	2398	2,410,828
Tx70	Haunched Composite	52.49	55.51	2925	4,611,915
Texas U54	Standard	31.6	22.4	1120	403,020
Texas U54	Composite	18.1	35.9	1758	975,250

4.5 GIRDER WEIGHTS

Table 4.4 and Table 4.5 provide the segment lengths and weights for the girder segments considered for the parametric study. For the haunched segment, a constant web depth haunched girder is considered where the girder weight varies linearly from the girder end to the girder midspan. The weights of the girder segments are within the handling and transportation limitations.

Table 4.4. Segment Lengths and Weights – Span Configuration (190-240-190 ft).

Girder Segment	Length (ft)	Weight (kips/ft)	Total Weight (kips)
Tx70 (9 in. web) Prismatic	140	1.152	161
Tx82 (9 in. web) Prismatic	140	1.264	176
Tx82 (10 in. web) Prismatic	140	1.350	189
Tx70 (9 in. web) Prismatic	96	1.152	110
Tx82 (9 in. web) Prismatic	96	1.264	121
Tx82 (10 in. web) Prismatic	96	1.350	130
Tx70 (9 in. web) Haunched	96	1.152-2.488	182

Table 4.5. Segment Lengths and Weights – Span Configuration (150-200-150 ft).

Girder Segment	Length (ft)	Weight (kips/ft)	Total Weight (kips)
Tx70 (9 in. web) Prismatic	120	1.152	138
Tx82 (9 in. web) Prismatic	120	1.264	152
Tx70 (9 in. web) Prismatic	76	1.152	88
Tx82 (9 in. web) Prismatic	76	1.264	96
Tx70 (9 in. web) Haunched	76	1.152–2.488	146
Texas U54 Prismatic	100	1.167	117
Texas U54 Prismatic	96	1.167	112

4.6 PRESTRESSING

For shored construction, the Stage I PT and the pretensioning were designed to balance the self-weight of the individual girders for hauling, transportation, and erection. Ideally, only Stage I PT is required to fully balance the self-weight of the girder segments. However, in that case the PT ducts would have been running in the middle of the section, close to neutral axis. Therefore, no space would have been left for Stage II PT. As shown in Figure 4.3, by including pretensioning, the Stage I PT can be offset farther away from the neutral axis, which leaves that part of the section clear for the Stage II PT.

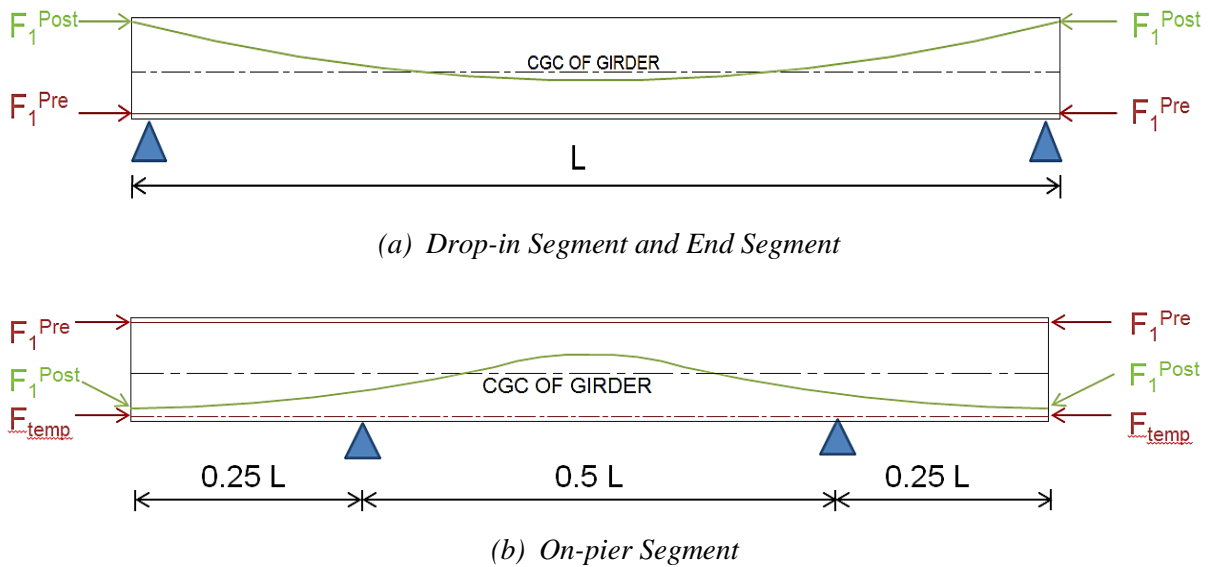


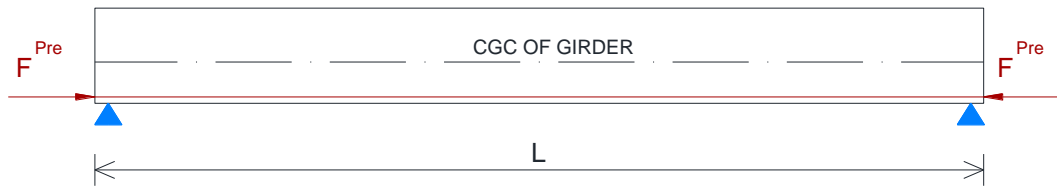
Figure 4.3. Pretensioning and Stage I PT Schematic Layout for Shored Construction.

For shored construction when both pretensioning and Stage I PT is considered, the layout of Stage I PT is design based on the available space considering the Stage II PT. When the drape and number of strands for Stage I PT is calculated, the number and position of pretensioning strands can be easily derived so that the overall prestressing layout (both Stage I PT and pretensioning) balances the self-weight of the girder segments.

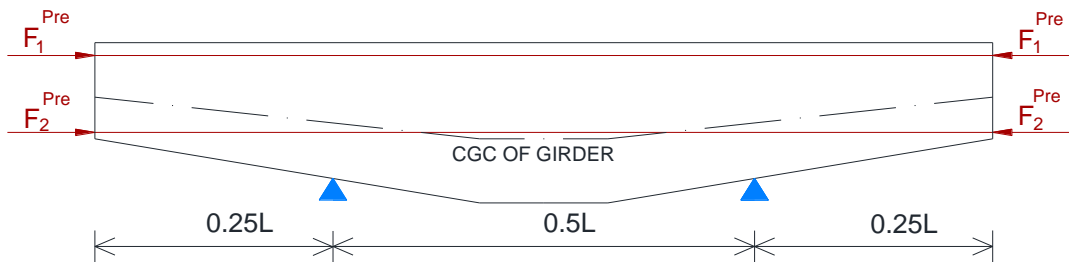
For partially shored construction on the other hand, the pretensioning alone is considered for the transportation and erection, as shown in Figure 4.4. For the drop-in segment and the end segment, the pretensioning is designed so that the stress in every section is within the allowable stress limits. The pretensioning of the on-pier segment is designed to carry the self-weight of the girder segment along with half of the drop-in segment weight. Table 4.6 and

Table 4.7 summarize the number of 0.6 in. diameter pretensioning strands provided for the girder segments.

Similar to the shored case, the Stage I PT for partially shored construction is also designed to balance the self-weight of the girder segments. However, unlike the shored case, the Stage I PT for partially shored construction is applied continuously after the splices are cast at the construction site. Table 4.8 and Table 4.9 provide details of the number of 0.6 in. diameter prestressing strands for the Stage I PT.



(a) Drop-in Segment and End Segment



(b) On-pier Segment

Figure 4.4. Schematic Prestressing Layout for Partially Shored Construction.

Stage II PT is provided to balance the deck weight and superimposed dead load and is provided continuously for both the shored and partially shored cases. Figure 4.5 presents schematics of the final prestressing layout for shored and partially shored construction. Because the Stage II PT balances the deck and superimposed dead load, the Stage II PT is the same for the Tx82 (9 in. web) and the Tx82 (10 in. web) designs. Increasing the depth results in a decrease in the number of PT strands required. Thus, the Stage II PT is less for the Tx82 girder as compared to the Tx70 girder. As the span length reduces, the amount of PT required is also reduced, as expected.

Table 4.10 and Table 4.11 provide details for the number of 0.6 in. strands used for the Stage II PT.

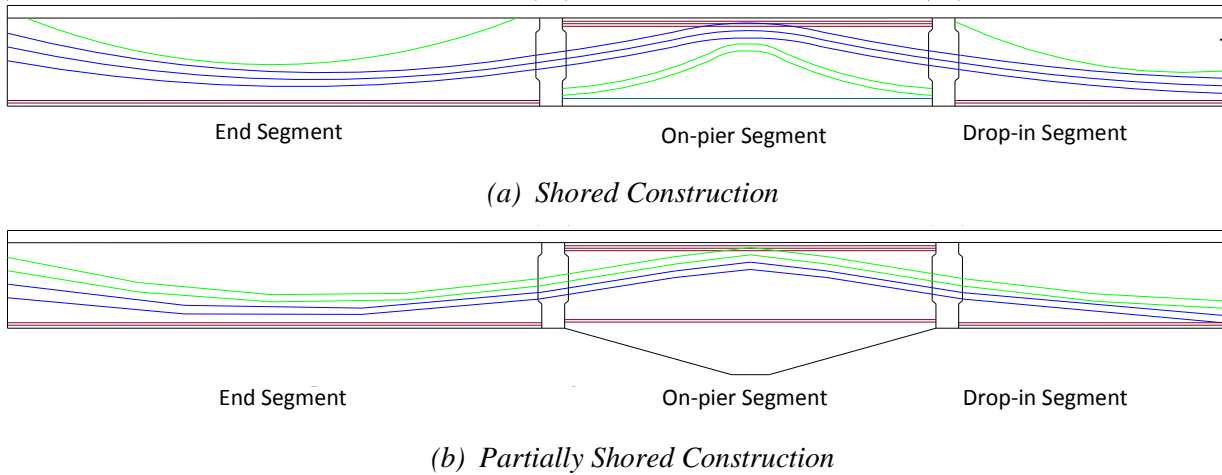


Figure 4.5. Prestressing Layout for Shored and Partially Shored Construction.

Table 4.6. Pretensioning – Span Configuration (150-200-150 ft).

Girder Section	End Segment	Drop-in Segment	On-Pier Segment
Tx70 (9 in. web) Shored	22	24	16
Tx82 (9 in. web) Shored	18	16	22
Texas U54 Shored	26	26	22
Tx70 (9 in. web) Partially Shored	22	24	22 top 20 bottom

Table 4.7. Pretensioning – Span Configuration (190-240-190 ft).

Girder Section	End Segment	Drop-in Segment	On-Pier Segment
Tx70 (9 in. web) Shored	32	24	26
Tx82 (9 in. web) Shored	22	20	26
Tx82 (10 in. web) Shored	26	24	26
Tx70 (9 in. web) Partially Shored	24	24	24 top 20 bottom

Table 4.8. Stage I PT – Span Configuration (150-200-150 ft).

Girder Section	No. of Strands		
	End Segment	Drop-in Segment	On-Pier Segment
Tx70 (9 in. web) Shored	14 (1 duct of 14)	14 (1 duct of 14)	32 (2 ducts of 16)
Tx82 (9 in. web) Shored	15 (1 duct of 15)	16 (1 duct of 16)	24 (2 ducts of 12)
Texas U54 Shored	20 (1 duct of 20)	20 (1 duct of 20)	36 (2 ducts of 18)
Tx70 (9 in. web) Partially Shored (continuous PT)	24 (2 ducts of 12)	24 (2 ducts of 12)	24 (2 ducts of 12)

Table 4.9. Stage I PT – Span Configuration (190-240-190 ft).

Girder Section	No. of Strands		
	End Segment	Drop-in Segment	On-Pier Segment
Tx70 (9 in. web) Shored	19 (1 duct of 19)	19 (1 duct of 19)	38 (2 duct of 19)
Tx82 (9 in. web) Shored	19 (1 duct of 19)	19 (1 duct of 19)	38 (2 duct of 19)
Tx82 (10 in. web) Shored	19 (1 duct of 19)	19 (1 duct of 19)	38 (2 duct of 19)
Tx70 (9 in. web) Partially Shored (continuous PT)	32 (2 duct of 16)	32 (2 duct of 16)	32 (2 duct of 16)

Table 4.10. Stage II PT Span Configuration (150-200-150 ft).

Girder Section	No. of Strands
Tx70 (9 in. web) Shored	30 (2 ducts of 15)
Tx82 (9 in. web) Shored	26 (2 ducts of 13)
Texas U54 Shored	48 (4 ducts of 12)
Tx70 (9 in. web) Partially Shored	22 (2 ducts of 11)

Table 4.11. Stage II PT – Span Configuration (190-240-190 ft).

Girder Section	No. Strands
Tx70 (9 in. web) Shored	57 (3 ducts of 19)
Tx82 (9 in. web) Shored	34 (2 ducts of 17)
Tx82 (10 in. web) Shored	34 (2 ducts of 17)
Tx70 (9 in. web) Partially Shored	30 (2 ducts of 15)

4.7 SERVICE STRESS ANALYSIS

The service stress analysis evaluated the flexural stresses for service level loads at several critical locations along the continuous girder, as shown in Figure 4.6.

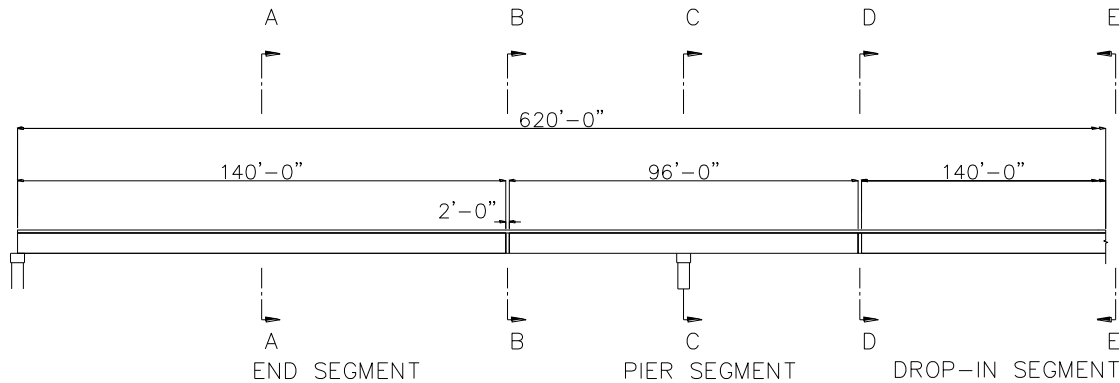


Figure 4.6. Section Locations for Girder Moments and Stress Checks.

Table 4.12 through Table 4.15 provide results for stresses at the midspan of the drop-in and end segments (Section A-A and Section E-E in Figure 4.6) during various stages of construction (described in Chapter 3) for the different design cases considered. The important construction steps for checking girder stresses are identified as follows:

- Step I: Set girder segments on piers and temporary supports.
- Step II: Girders support weight of PCPs and wet CIP deck.
- Step III: Apply Stage II PT, remove shoring towers, and cast barriers.
- Step IV: Open bridge to service.

As shown in Table 4.12 through Table 4.15, the stresses are within the allowable stress limits during all stages of construction for both the shored and partially shored cases. Table 4.16 through Table 4.19 provide results for stresses at the splice locations (Section B-B and Section D-D in Figure 4.6) during various stages of construction (described in Chapter 3) for the different cases considered for the parametric study. The bold values indicate exceedance of a limiting stress. For the shored construction case, the splice is cracked during the stage when the deck is poured. Note that a partially prestressed splice is used, and mild steel needs to be provided for serviceability and strength. The splice in the end span is more critical as compared to the splice in the interior span. Also, tensile stresses are observed at the bottom of the splice at service.

For the partially shored case, because the Stage I PT is carried through continuously, the splice is uncracked during construction and at service. Note that a CIP PT splice is used and mild steel reinforcement is provided for strength and ductility requirements. Table 4.20 and Table 4.21 provide results for stresses at the pier during various stages of construction (mentioned in Chapter 3) for the different cases considered for the parametric study. The bold values indicate exceedance of a limiting stress. For the shored case using Tx70 girders for a span configuration of 190-240-190 ft, the pier region of the beam experienced compressive stress levels that exceeded the allowable compressive stress at service conditions. This stress exceedance is addressed by providing supplemental mild steel reinforcement in the compression zone. For the shored case, the pier region of the beam also experienced tensile stresses.

For the partially shored case, the stresses are within limits during all the stages of construction and service. The pier region of the beam experienced tensile stresses but were within the allowable stress limits.

Table 4.12. Stresses at Sections A-A – Span Configuration (190-240-190 ft).

Loading	Component	Location	Tx70 (9 in. web) Shored	Tx82 (9 in. web) Shored	Tx82 (10 in. web) Shored	Tx70 (9 in. web) Partially Shored
Step I (Before Loss)	Girder	Top	-1.677	-1.089	-1.007	-1.189
		Bottom	-2.238	-1.740	-1.892	-0.747
Step II (Before Loss)	Girder	Top	-2.519	-1.752	-1.641	-2.145
		Bottom	-1.500	-1.167	-1.344	-1.997
Step III (After Loss)	Girder	Top	-3.391	-2.278	-2.187	-2.686
		Bottom	-2.800	-1.766	-1.832	-2.252
	Deck	Top	-0.439	-0.229	-0.213	-0.172
		Bottom	-0.531	-0.277	-0.259	-0.235
Service (After Loss)	Girder	Top	-4.395	-3.131	-3.014	-3.681
		Bottom	-0.944	-0.306	-0.417	-0.415
	Deck	Top	-1.316	-0.941	-0.903	-1.040
		Bottom	-1.194	-0.840	-0.805	-0.891

Table 4.13. Stresses at Sections A-A – Span Configuration (150-200-150 ft).

Loading	Component	Location	Tx70 (9 in. web) Shored	Tx82 (9 in. web) Shored	Texas U54 Shored	Tx70 (9 in. web) Partially Shored
Step I (Before Loss)	Girder	Top	-1.275	-0.883	-1.367	-0.540
		Bottom	-1.495	-1.396	-2.025	-1.167
Step II (Before Loss)	Girder	Top	-1.764	-1.232	-1.926	-1.271
		Bottom	-1.075	-1.095	-1.630	-2.197
Step III (After Loss)	Girder	Top	-2.198	-1.672	-2.659	-1.647
		Bottom	-1.369	-1.437	-2.237	-2.302
	Deck	Top	-0.286	-0.237	-0.451	-0.131
		Bottom	-0.378	-0.261	-0.543	-0.176
Service (After Loss)	Girder	Top	-2.963	-2.214	-3.530	-2.329
		Bottom	-0.195	-0.508	-0.506	-1.042
	Deck	Top	-1.048	-0.689	-1.378	-0.727
		Bottom	-0.926	-0.618	-1.256	-0.626

Table 4.14. Stresses at Section E-E – Span Configuration (190-240-190 ft).

Loading	Component	Location	Tx70 (9 in. web) Shored	Tx82 (9 in. web) Shored	Tx82 (10 in. web) Shored	Tx70 (9 in. web) Partially Shored
Step I (Before Loss)	Girder	Top	-1.610	-1.011	-0.934	-1.189
		Bottom	-1.700	-1.673	-1.829	-0.747
Step II (Before Loss)	Girder	Top	-2.194	-1.470	-1.373	-1.832
		Bottom	-1.189	-1.275	-1.449	-2.271
Step III (After Loss)	Girder	Top	-3.327	-2.195	-2.118	-2.335
		Bottom	-2.139	-1.567	-1.633	-2.602
	Deck	Top	-0.655	-0.388	-0.367	-0.134
		Bottom	-0.694	-0.403	-0.381	-0.206
Service (After Loss)	Girder	Top	-4.385	-3.095	-2.990	-3.310
		Bottom	-0.181	-0.028	-0.141	-0.800
	Deck	Top	-1.580	-1.139	-1.095	-0.986
		Bottom	-1.393	-0.997	-0.957	-0.850

Table 4.15. Stresses at Section E-E – Span Configuration (150-200-150 ft).

Loading	Component	Location	Tx70 (9 in. web) Shored	Tx82 (9 in. web) Shored	Texas U54 Shored	Tx70 (9 in. web) Partially Shored
Step I (Before Loss)	Girder	Top	-1.238	0.704	-1.422	-0.701
		Bottom	-1.673	-1.479	-1.987	-1.175
Step II (Before Loss)	Girder	Top	-1.702	-0.944	-1.902	-0.769
		Bottom	-1.276	-1.271	-1.647	-2.786
Step III (After Loss)	Girder	Top	-2.266	-1.407	-2.675	-1.171
		Bottom	-1.330	-1.655	-2.178	-2.954
	Deck	Top	-0.361	-0.194	-0.493	-0.028
		Bottom	-0.400	-0.227	-0.532	-0.098
Service (After Loss)	Girder	Top	-3.116	-2.041	-3.642	-1.850
		Bottom	-0.026	-0.568	-0.252	-1.698
	Deck	Top	-1.208	-0.723	-1.522	-0.622
		Bottom	-1.021	-0.645	-1.335	-0.547

Table 4.16. Stresses at Section B-B – Span Configuration (190-240-190 ft).

Loading	Component	Location	Tx70 (9 in. web) Shored	Tx82 (9 in. web) Shored	Tx82 (10 in. web) Shored	Tx70 (9 in. web) Partially Shored
Step I (Before Loss)	Girder	Top	-	-	-	-
		Bottom	-	-	-	-
Step II (Before Loss)	Girder	Top	+1.120	+0.882	+0.843	-1.253
		Bottom	-0.982	-0.762	-0.728	-0.989
Step III (After Loss)	Girder	Top	-0.565	-0.205	-0.197	-1.695
		Bottom	-1.390	-0.786	-0.737	-1.296
	Deck	Top	-1.208	-0.786	-0.753	-0.526
		Bottom	-1.112	-0.718	-0.686	-0.502
Service (After Loss)	Girder	Top	-1.199	-0.744	-0.719	-2.255
		Bottom	-0.217	+0.136	+0.156	-0.262
	Deck	Top	-1.762	-1.236	-1.189	-1.041
		Bottom	-1.531	-1.073	-1.031	-0.871

Table 4.17. Stresses at Section B-B – Span Configuration (150-200-150 ft).

Loading	Component	Location	Tx70 (9 in. web) Shored	Tx82 (9 in. web) Shored	Texas U54 Shored	Tx70 (9 in. web) Partially Shored
Step I (Before Loss)	Girder	Top	-	-	-	-
		Bottom	-	-	-	-
Step II (Before Loss)	Girder	Top	+0.536	+0.430	+0.798	-0.259
		Bottom	-0.460	-0.371	-0.565	-1.443
Step III (After Loss)	Girder	Top	-0.178	-0.323	-0.155	-0.502
		Bottom	-0.698	-0.523	-1.346	-1.900
	Deck	Top	-0.536	-0.536	-0.675	-0.216
		Bottom	-0.440	-0.497	-0.579	-0.240
Service (After Loss)	Girder	Top	-0.780	-0.771	-0.840	-0.909
		Bottom	+0.321	+0.246	-0.326	-1.149
	Deck	Top	-1.135	-0.910	-1.403	-0.570
		Bottom	-0.904	-0.793	-1.172	-0.508

Table 4.18. Stresses at Section D-D – Span Configuration (190-240-190 ft).

Loading	Component	Location	Tx70 (9 in. web) Shored	Tx82 (9 in. web) Shored	Tx82 (10 in. web) Shored	Tx70 (9 in. web) Partially Shored
Step I (Before Loss)	Girder	Top	-	-	-	-
		Bottom	-	-	-	-
Step II (Before Loss)	Girder	Top	+0.818	+0.645	+0.616	-1.282
		Bottom	-0.717	-0.557	-0.532	-0.964
Step III (After Loss)	Girder	Top	-0.659	-0.256	-0.243	-1.725
		Bottom	-1.508	-0.900	-0.850	-1.241
	Deck	Top	-1.027	-0.631	-0.602	-0.552
		Bottom	-0.975	-0.595	-0.567	-0.522
Service (After Loss)	Girder	Top	-1.070	-0.606	-0.582	-2.136
		Bottom	-0.481	-0.302	-0.271	-0.481
	Deck	Top	-1.385	-0.922	-0.884	-0.911
		Bottom	-1.246	-0.825	-0.790	-0.793

Table 4.19. Stresses at Section D-D – Span Configuration (150-200-150 ft).

Loading	Component	Location	Tx70 (9 in. web) Shored	Tx82 (9 in. web) Shored	Texas U54 Shored	Tx70 (9 in. web) Partially Shored
Step I (Before Loss)	Girder	Top	-	-	-	-
		Bottom	-	-	-	-
Step II (Before Loss)	Girder	Top	+0.485	+0.323	+0.605	-0.325
		Bottom	-0.415	-0.279	-0.428	-1.386
Step III (After Loss)	Girder	Top	-0.273	-0.460	-0.303	-0.549
		Bottom	-0.561	-0.380	-1.299	-1.863
	Deck	Top	-0.579	-0.560	-0.627	-0.202
		Bottom	-0.527	-0.515	-0.575	-0.237
Service (After Loss)	Girder	Top	-0.805	-0.857	-1.111	-0.858
		Bottom	+0.340	+0.301	-0.087	-1.292
	Deck	Top	-1.109	-0.892	-1.487	-0.482
		Bottom	-0.970	-0.778	-1.348	-0.441

Table 4.20. Stresses at Section C-C – Span Configuration (190-240-190 ft).

Loading	Component	Location	Tx70 (9 in. web) Shored	Tx82 (9 in. web) Shored	Tx82 (10 in. web) Shored	Tx70 (9 in. web) Partially Shored
Step I (Before Loss)	Girder	Top	-2.434	-2.919	-2.555	-0.701
		Bottom	-2.449	-1.626	-1.674	-0.874
Step II (Before Loss)	Girder	Top	-2.738	-3.158	-2.784	-1.314
		Bottom	-2.183	-1.419	-1.476	-1.323
Step III (After Loss)	Girder	Top	-2.566	-2.430	-2.014	-1.155
		Bottom	-4.176	-2.960	-3.030	-1.423
	Deck	Top	-0.541	-0.130	-0.117	-0.566
		Bottom	-0.608	-0.199	-0.184	-0.523
Service (After Loss)	Girder	Top	-1.631	-1.644	-1.244	-0.340
		Bottom	-5.903	-4.318	-4.346	-2.254
	Deck	Top	+0.275	+0.532	+0.525	+0.053
		Bottom	+0.009	+0.325	+0.324	+0.015

Table 4.21. Stresses at Section C-C – Span Configuration (150-200-150 ft).

Loading	Component	Location	Tx70 (9 in. web) Shored	Tx82 (9 in. web) Shored	Texas U54 Shored	Tx70 (9 in. web) Partially Shored
Step I (Before Loss)	Girder	Top	-2.652	-2.281	-3.010	-1.136
		Bottom	-1.112	-1.025	-1.595	-0.533
Step II (Before Loss)	Girder	Top	-2.562	-2.234	-3.123	-1.631
		Bottom	-1.188	-1.066	-1.515	-0.889
Step III (After Loss)	Girder	Top	-1.850	-1.622	-2.328	-1.364
		Bottom	-2.555	-2.350	-3.133	-1.011
	Deck	Top	-0.096	-0.068	-0.330	-0.372
		Bottom	-0.163	-0.127	-0.397	-0.346
Service (After Loss)	Girder	Top	-1.516	-1.080	-1.442	-0.823
		Bottom	-4.138	-3.280	-4.632	-1.561
	Deck	Top	+0.442	+0.384	+0.580	+0.038
		Bottom	+0.176	+0.230	+0.379	+0.010

4.8 DEFLECTIONS

Table 4.22 and Table 4.23 provide results for the live load deflections in the end span and center span for the cases considered for the study. According to the AASHTO LRFD Specifications (AASHTO 2012) Article 2.5.2.6.2, the limiting deflection is $L/800$, where L is the span length. This value for each span is provided in the last row of each table. The deflections are well within the limits for all of the design cases.

Table 4.22. Live Load Deflections – Span Configuration (190-240-190 ft).

Girder Section	End Span Deflection (in.)	Center Span Deflection (in.)
Tx70 (9 in. web) Shored	1.21	1.34
Tx82 (9 in. web) Shored	0.81	0.91
Tx82 (10 in. web) Shored	0.80	0.90
Tx70 (9 in. web) Partially Shored	1.15	1.06
Limit (in.)	2.85	3.60

Table 4.23. Live Load Deflections – Span Configuration (150-200-150 ft).

Girder Section	End Span Deflection (in.)	Center Span Deflection (in.)
Tx70 (9 in. web) Shored	0.90	1.22
Tx82 (9 in. web) Shored	0.60	0.82
Texas U54 Shored	1.20	2.40
Tx70 (9 in. web) Partially Shored	0.85	0.78
Limit (in.)	2.25	3.00

4.9 ULTIMATE FLEXURAL STRENGTH REQUIREMENTS AND DUCTILITY

Table 4.24 and Table 4.25 provide results for moment capacity and demand at ultimate loading conditions. The demand-to-capacity ratio (DCR) is also provided. Ductility over the pier governs the maximum span lengths. Ductility was considered by ensuring that the minimum tension strain in the flexural reinforcement ($\varepsilon_t = 0.005$) is achieved. This is required to use the maximum value for the reduction factor for the nominal flexural strength ($\phi=1.0$). For the shored case, mild steel reinforcement is added in the bottom flange of the on-pier girder segment, which acts as compression steel to improve ductility. In addition, the 1.25 in. diameter Dywidag bars, with a specified ultimate tensile strength of 150 ksi, that are provided during handling and transportation of girder segments are considered as a part of the compression steel during service. The amount of compression steel required decreases as the depth of the girder increases. Also, an increase in flange thickness results in a reduction in the required compression steel. However, an increase in web thickness has a minimum effect on the amount of mild steel required. The thicker bottom flange for the on-pier segment in the partially shored case helps provide higher moment capacity at ultimate. The amount of compression steel required reduces as the span lengths decrease. Table 4.26 and Table 4.27 provide results on the amount of mild steel added for ductility and crack control during construction stages (before the continuity PT is applied).

**Table 4.24. Moment Capacity and Demand at Ultimate – Span Configuration
(190-240-190 ft).**

Girder Section	Description	End Segment	On-Pier Segment	Drop-in Segment
Tx70 (9 in. web) Shored	Demand, M_u (kip-ft)	14,940	20,680	15,330
	Capacity, ϕM_n (kip-ft)	22,780	24,180	24,430
	DCR	0.66	0.86	0.63
Tx82 (9 in. web) Shored	Demand, M_u (kip-ft)	15,280	15,680	21,320
	Capacity, ϕM_n (kip-ft)	25,420	28,530	25,580
	DCR	0.61	0.55	0.83
Tx82 (10 in. web) Shored	Demand, M_u (kip-ft)	15,550	15,940	21,800
	Capacity, ϕM_n (kip-ft)	26,280	28,280	26,450
	DCR	0.59	0.56	0.82
Tx70 (9 in. web) Partially Shored	Demand, M_u (kip-ft)	14,340	25,430	13,430
	Capacity, ϕM_n (kip-ft)	24,590	39,360	26,000
	DCR	0.58	0.65	0.52

**Table 4.25. Moment Capacity and Demand at Ultimate – Span Configuration
(150-200-150 ft).**

Girder Section	Description	End Segment	On-Pier Segment	Drop-in Segment
Tx70 (9 in. web) Shored	Demand, M_u (kip-ft)	9550	14,700	11,440
	Capacity, ϕM_n (kip-ft)	14,400	19,840	15,880
	DCR	0.66	0.74	0.72
Tx82 (9 in. web) Shored	Demand, M_u (kip-ft)	9820	15,090	11,700
	Capacity, ϕM_n (kip-ft)	19,330	20,900	20,770
	DCR	0.51	0.72	0.56
Texas U54 Shored	Demand, M_u (kip-ft)	11,340	17,970	13,390
	Capacity, ϕM_n (kip-ft)	13,900	19,070	14,490
	DCR	0.82	0.94	0.92
Tx70 (9 in. web) Partially Shored	Demand, M_u (kip-ft)	9160	17,090	9560
	Capacity, ϕM_n (kip-ft)	18,810	32,900	21,410
	DCR	0.49	0.52	0.45

Table 4.26. Compression Steel for Ductility – Span Configuration (190-240-190 ft).

Girder Section	Compression Steel
Tx70 (9 in. web) Shored	16-#14 and 4 Dywidag
Tx82 (9 in. web) Shored	12-#14 and 4 Dywidag
Tx82 (10 in. web) Shored	10-#14 and 4 Dywidag
Tx70 (9 in. web) Partially Shored	-

Table 4.27. Compression Steel for Ductility – Span Configuration (150-200-150 ft).

Girder Section	Compression Steel
Tx70 (9 in. web) Shored	8-#14 and 4 Dywidag
Tx82 (9 in. web) Shored	2-#14 and 4 Dywidag
Texas U54 Shored	10-#14 and 4 Dywidag
Tx70 (9 in. web) Partially Shored (Hunched over Pier)	-

4.10 SHEAR DESIGN

Table 4.28 and Table 4.29 provide details for shear design. An increase in girder depth and web thickness results in increasing the shear capacity of the girders.

Table 4.28. Shear Design Details – Span Configuration (190-240-190 ft).

Girder Section	End Segment	On-Pier Segment	Drop-in Segment
Tx70 (9 in. web) Shored	#5@4 in. (0–10 ft)	#5@6 in. (0–29 ft)	#5@6 in. (0–20 ft)
	#5@6 in. (10–20 ft)	#5@4 in. (29–72 ft)	#5@12 in. (20–120 ft)
	#5@12 in. (20–140 ft)	#5@6 in. (72–96 ft)	#5@6 in. (120–140 ft)
Tx82 (9 in. web) Shored	#4@12 in. (0–140 ft)	#4@6 in. (0–38 ft)	#4@12 in. (0–140 ft)
		#4@4 in. (38–58 ft)	
		#4@6 in. (58–96 ft)	
Tx82 (10 in. web) Shored	#4@12 in. (0–140 ft)	#4@6 in. (0–38 ft)	#4@12 in. (0–140 ft)
		#4@4 in. (38–58 ft)	
		#4@6 in. (58–96 ft)	
Tx70 (9 in. web) Partially Shored	#4@6 in. (0–20 ft)	#4@6 in. (0–96 ft)	#4@6 in. (0–20 ft)
	#4@12 in. (20–140 ft)		#4@12 in. (20–120 ft)
			#4@6 in. (120–140 ft)

Note: All shear reinforcement consists of double legged stirrups.

Table 4.29. Shear Design Details – Span Configuration (150-200-150 ft).

Girder Section	End Segment	On-Pier Segment	Drop-in Segment
Tx70 (9 in. web) Shored	#4@12 in. (0–110 ft)	#4@6 in. (0–28 ft) #4@4 in. (28–48 ft) #4@6 in. (48–76 ft)	#4@12 in. (0–120 ft)
Tx82 (9 in. web) Shored	#4@12 in. (0–110 ft)	#4@6 in. (0–28 ft) #4@4 in. (28–48 ft) #4@6 in. (48–76 ft)	#4@12 in. (0–120 ft)
Texas U54 Shored	#4@12 in. each web (0–100 ft)	#4@6 in. each web (0–96 ft)	#4@12 in. each web (0–100 ft)
Tx70 (9 in. web) Partially Shored	#4@12 in. (0–110 ft)	#4@6 in. (0–76 ft)	#4@12 in. (0–120 ft)

Note: All shear reinforcement consists of double legged stirrups.

4.11 SUMMARY AND REMARKS

In-span splicing technique was applied for different span lengths and different standard shapes. Results show that achieving higher spans using the same cross section is feasible and economical. The LEAP CONSPLICE software (Bentley Systems 2013) was used to verify the results and provided a more detailed analysis of the long-term losses during the service life of the bridge. The software confirmed the hand calculation results. Based on the different case studies that were considered, the following observations were made.

- In-span splicing is an effective method for reaching longer span lengths, but requires special considerations with regard to construction sequence. Stresses should be checked at each stage of the construction.
- The moment capacity within the splice is considerably lower than for the adjacent girder segments. It is highly recommended to provide splices in low moment regions, namely points of contraflexure for the dead load. Therefore, it is suggested to use up to two splices in interior spans and one splice in the end spans.

- Assuming two splices per span and considering the length limit on individual girders, the maximum span length is limited to twice the maximum length for the individual girder segments.
- Providing the required PT to satisfy the allowable stress limits at different stages of construction and service can lead to a very large compression force in the bottom girder flange at the interior piers. To avoid compression failure and to enhance negative bending capacity and ductility, providing compression steel was required for the cases considered. Alternately, haunched sections can be provided over the piers.

5 DESIGN, CONSTRUCTION, AND PRE-TEST BEHAVIOR OF SPECIMEN

5.1 INTRODUCTION

The results of the parametric design and analysis study suggest that in-span splicing can be used to extend the span lengths of precast prestressed concrete girder bridges. But limited experimental data are available to evaluate the performance of in-span splices. This chapter provides details for an experimental program conducted to evaluate the performance of the in-span splice connections under varying levels of demand and different combinations of positive moment, negative moment, and shear. The prototype bridge and the abstraction of the specimen are described, followed by an overview of the specimen design, construction, post-tensioning process, and instrumentation plan.

5.2 SPECIMEN ABSTRACTION

5.2.1 Prototype Bridge

Chapter 3 describes the three-span prototype bridge. The bridge has a 190-240-190 ft span configuration, with the end spans being 190 ft long and the middle span being 240 ft long. Figure 5.1 shows the abstraction of the specimen from the prototype bridge. The splice corresponding to the splice in the end span of the prototype bridge was tested. The locations of the PT tendons at the corresponding splice location in the specimen were kept similar to those in the prototype bridge. Though shored construction was used for the prototype design, the proposed connection detail is also a representative of a partially shored construction technique where a temporary tower and/or strong-backs are provided at the in-span splice location and the on-pier girder segments need to be tied back for stability purposes.

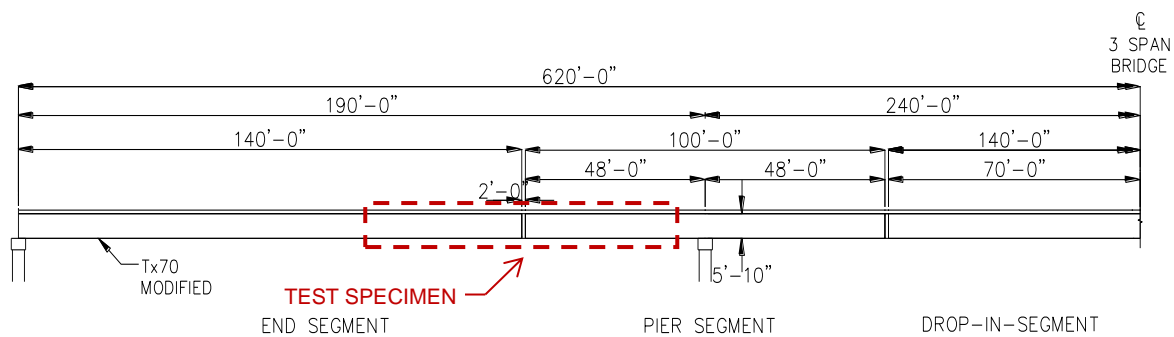


Figure 5.1. Elevation of the Prototype Bridge Showing the Test Specimen.

Figure 5.2 shows the cross-section of the bridge. The bridge has a total width of 46 ft and a total roadway width of 44 ft. The bridge superstructure consists of six modified Tx70 girders spaced 8 ft center-to-center, with a 3 ft overhang on each side, designed to act compositely with an 8 in. thick CIP concrete deck. The deck includes 4 in. thick precast concrete stay-in-place precast concrete panels between girders that serve as formwork for the deck. The asphalt wearing surface thickness is 2 in. A T501 traffic barrier was considered as presented in the standard drawings of the *TxDOT Bridge Design Manual (2013)*. Three design lanes were considered for the purpose of design in accordance with the AASHTO LRFD Specifications (AASHTO 2012). The specimen represents a typical interior girder as indicated in Figure 5.2.

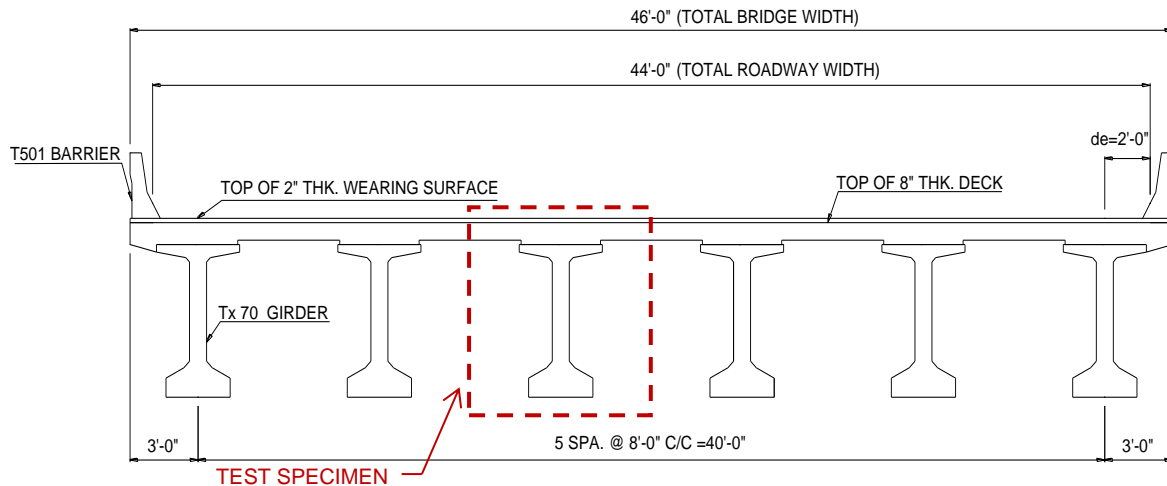


Figure 5.2. Cross-section of the Prototype Bridge Showing the Test Specimen.

Researchers conducted experimental testing to evaluate the performance of this specimen with a focus on the splice connection performance. The requirements for service limit state design, flexural strength limit state design, and shear strength limit state design were evaluated.

5.2.2 Specimen Details

The experimental program took place in the High Bay Structural and Materials Testing Laboratory (HBSMTL) at Texas A&M University. This facility has a 72-ft long strong floor and tie down locations are available on a 3-ft grid. Therefore, the length of the specimen was limited to 71 ft. Different options were considered by the research team to arrive at the final specimen presented

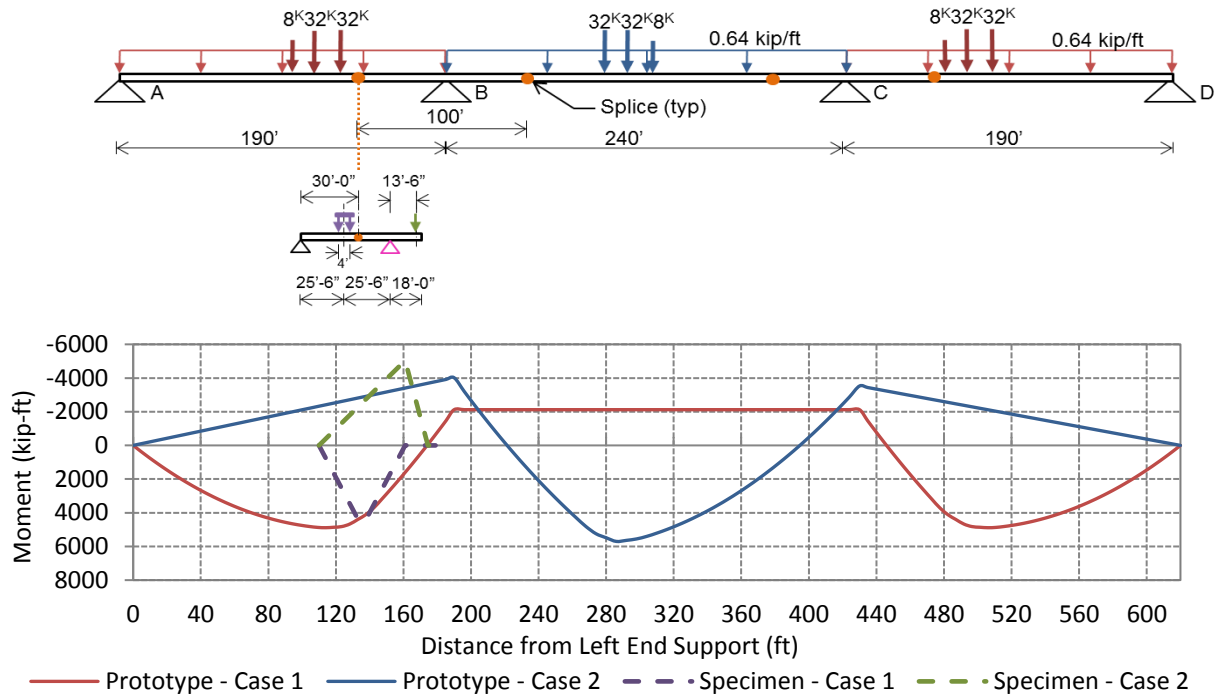
in this chapter. Specimen geometry and tests setups were designed to simulate the same demand on the main splice (middle splice, Splice 2). Figure 5.3 presents the comparison for demand moment and shear between the prototype bridge and the test specimen.

Figure 5.4 and Figure 5.5 show the elevation and plan views of the test-setup, respectively, providing the location of tie downs, pedestals, and splices. An interior splice was provided corresponding to the in-span splice within the end span of the prototype bridge, shown in Figure 5.1. However, due to the weight capacity limit of the crane in the HBSMTL, two additional splices were provided, connecting the girder segments to the thickened end blocks. Overall, the three splices divided the specimen into four segments. Appendix B provides detailed drawings for each girder segment within the specimen. Table 5.1 provides the weights of girder segments.

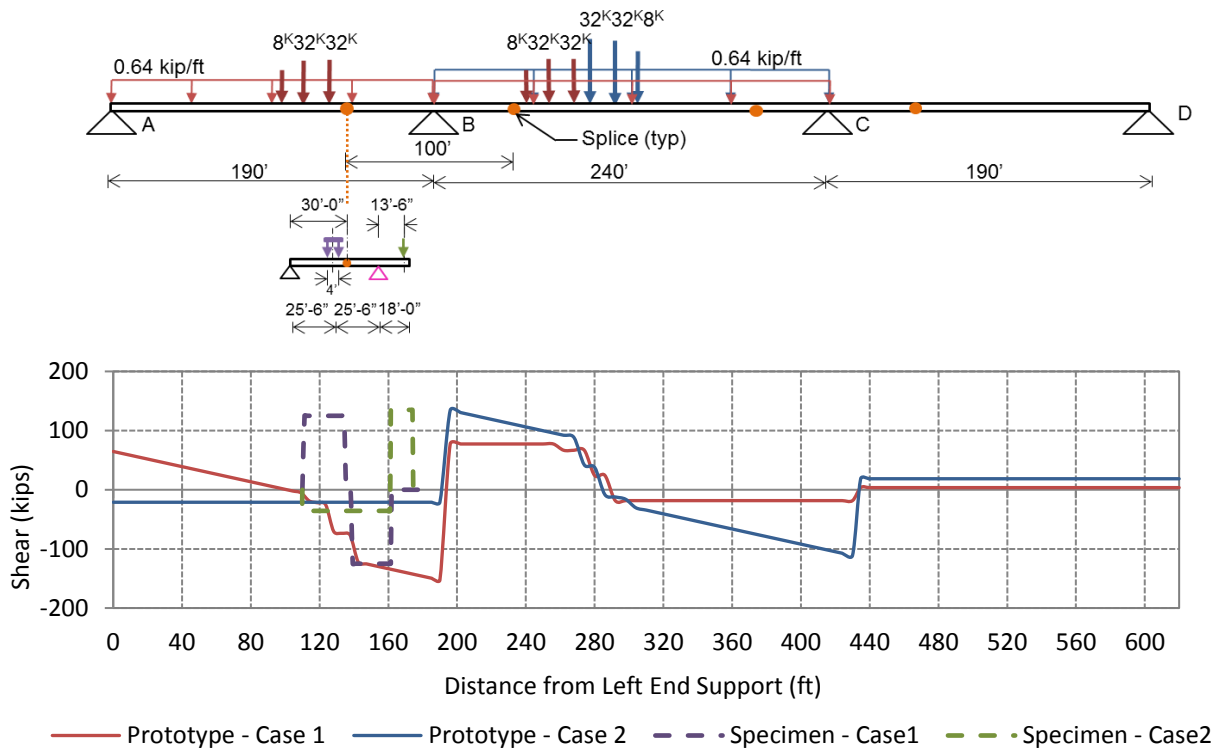
Table 5.1. Weight of Girder Segments.

Components		Length	Weight (kips)	Total Weight * (kips)
Thickened End Blocks 1 and 2	End Block Portion	9'-0"	23.9	28.4
	Tx70 Girder (Modified) Portion	2'-9"	4.5	
Segment 1	Tx70 Girder (Modified)	18'-0"	25.2	25.2
Segment 2	Tx70 Girder (Modified)	25'-0"	34.3	34.3

* Limiting lifting weight in the HBSMTL is 36 kips.



(a) Maximum Service Moment under Live Load with Impact from Prototype Bridge



(b) Maximum Service Shear under Live Load with Impact from Prototype Bridge

Figure 5.3. Replication of Maximum Moment and Shear at Service in Test Specimen.

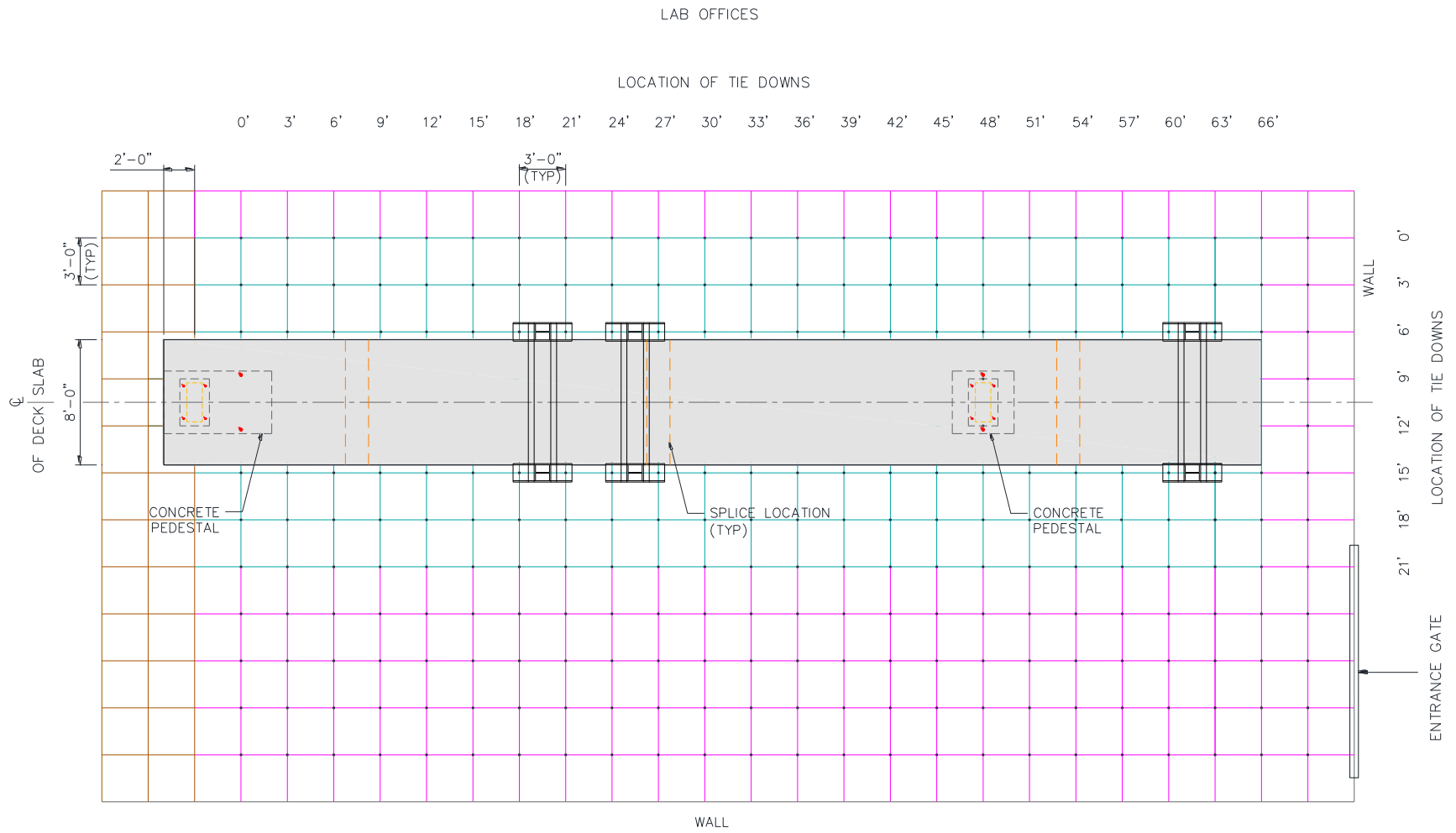


Figure 5.4. Plan View of the Test Specimen in the High Bay Laboratory.

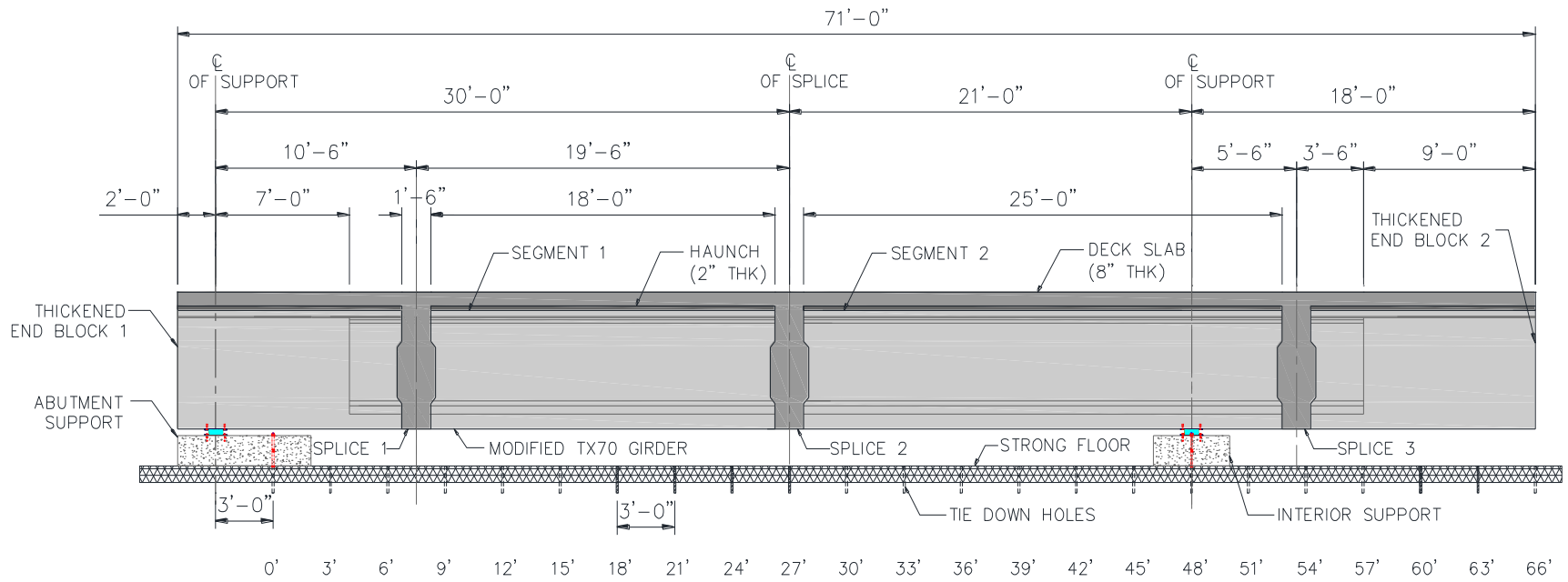


Figure 5.5. Elevation View of Test Specimen.

The research team tested all three splices in the specimen during five stages of testing. The first two test stages were non-destructive and were intended to evaluate the performance of the girder up to the service limit for positive and negative moment and shear. The next three tests focused on each splice and were intended to evaluate the post-cracking behavior of the girder up to ultimate strength. The finalized test specimen facilitated testing splice connections within the span (approximately at the dead load point of contraflexure), near the interior pier (high moment and high shear region), and near the abutment (low moment and high shear region) of the continuous bridge. Chapter 6 presents the test sequence and details for all stages of the experimental program.

The basic characteristics of the specimen are as follows:

- A modified Tx70 girder cross-section was used for the specimen to match the prototype bridge at full-scale. Modifications of the original section based on precaster requirements and preferences included: (1) widening the modified web width from 9 in. to 10 in., which also resulted in widening the top and bottom flange by 1 in.; (2) use of 3-5/8 in. diameter PT ducts rather than 4 in. diameter; and (3) increasing the top flange thickness to 5 in. minimum to accommodate the top pretensioning strands.
- An interior splice was provided corresponding to the in-span splice in the prototype bridge. Due to the weight capacity limit of the crane in the HBSMTL, two additional splices were provided connecting the girder segments to the thickened end blocks.
- Thickened end blocks were provided at both ends of the specimen to accommodate the necessary PT anchorage systems. The girder segments and end blocks were fabricated at a precast plant and transported to the laboratory.
- The concrete used for the prestressed concrete girder segments was specified as TxDOT Class H self-consolidating concrete with a required initial compressive strength at release f'_{ci} of 6.5 ksi and a required compressive strength at service f'_c of 8.5 ksi.
- The concrete used for the splice connections was selected after considering several alternative mixes and conducting trial batches. A conventional concrete mixture with 0.75 in. maximum size aggregate, river gravel coarse aggregate, a 9.5 in. slump, and a 28-day target f'_c of 8.5 ksi was used.

- A partially prestressed splice connection detail was used at all three splice locations. Mild steel reinforcement was provided in addition to continuity PT running through the connection. The mild steel reinforcement consisted of 180° bent hooked bars anchored into the adjacent girder flanges and extending into the joint. Additionally, two #6 transverse bars were placed inside each of the bent hooked bars to increase the effective bearing area.
- A reinforced concrete CIP deck slab, 92 in. wide and 8 in. thick, was cast in the laboratory. TxDOT Class S conventional concrete with a specified 28-day f'_c of 4 ksi was used for the deck slab. Deck reinforcement details for the specimen were provided in accordance with TxDOT construction practices. Typical clear cover provided was 2 in. and 1.25 in. for the top and bottom reinforcement, respectively.
- The continuity PT tendons were installed, stressed, and grouted in the laboratory by a post-tensioning contractor.

5.2.3 Modified Tx70 Girder

Figure 5.6 shows the details of the modified Tx70 girder cross-section used for the specimen. Table 5.2 presents the non-composite section properties of the modified Tx70 section. The standard Tx70 girder is 70 in. deep with top flange 42 in. wide, bottom flange 32 in. wide, and web thickness of 7 in. The web for the modified Tx70 girder segments was widened to 10 in. by spreading the standard girder side forms. An increased web width is required to accommodate the 19-strand PT ducts. The width of the top and bottom flanges was also increased by 3 in., making the top flange 45 in. wide and the bottom flange 35 in. wide. The top flange thickness was also increased to 5 in. minimum to accommodate the top pretensioning strands.

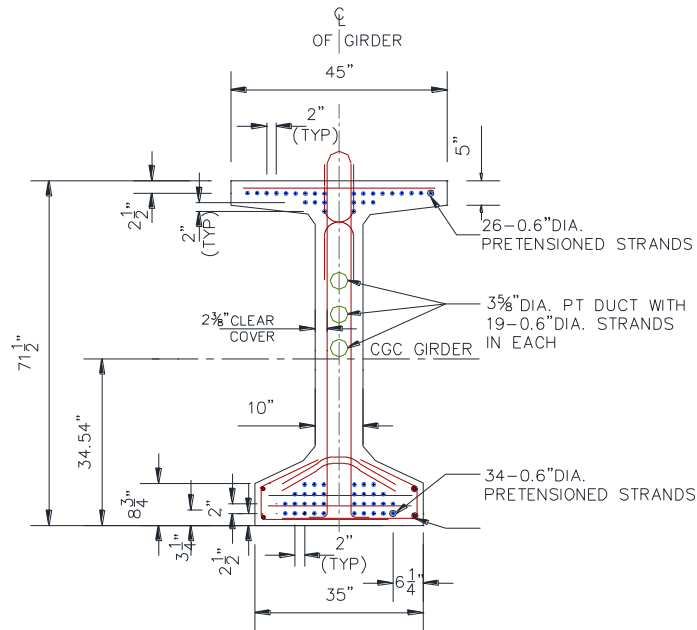


Figure 5.6. Typical Section Geometry of Modified Tx70 Girder with Widened Web (Adapted from TxDOT 2010).

Table 5.2. Section Properties for Modified Tx70 Girder with Widened Web.

Girder Type	Depth of N.A. from top, y_{top} (in.)	Depth of N.A. from bottom, y_{bot} (in.)	Area, A (in.²)	Moment of Inertia, I_x (in.⁴)	Weight (plf)
Modified Tx70	36.96	34.54	1243.5	805,053	1295
Composite Section	24.99	46.51	1980.0	1,424,995	2062

Table 5.3 presents the design parameters used for the specimen. These parameters are the same as those used for the modified Tx70 girder prototype bridge design. The design parameters are selected based on the current TxDOT state-of-practice and values commonly available from Texas precasters.

Table 5.3. Design Parameters for Specimen.

Parameter		Description/Selected Values
Specified Concrete Strength at Service for Deck Slab (CIP), f'_c		4 ksi
Specified Concrete Strength at Service (Precast), f'_c		8.5 ksi
Specified Concrete Strength at Release (Precast), f'_{ci}		6.5 ksi
Coefficient of Thermal Expansion of Concrete		$6 \times 10^{-6}/^{\circ}\text{F}$
Mild Steel (ASTM A615 Grade 604)	Yield Strength, f_y	60 ksi
	Modulus of Elasticity, E_s	29,000 ksi
Prestressing Steel	Strand Diameter	0.6 in.
	Ultimate Tensile Strength, f_{pu}	270 ksi (Low Relaxation)
	Yield Strength, f_{py}	$0.9 f_{pu}$
	Stress Limit at Transfer, f_{pi}	$f_{pi} \geq 0.75 f_{pu}$
	Stress Limit at Service, f_{pe}	$f_{pe} \geq 0.8 f_{py}$
	Modulus of Elasticity, E_p	28,500 ksi
	Wobble Coefficient, K	0.0002/ft
	Coefficient of Friction, μ	

5.3 SPECIMEN DESIGN

5.3.1 Design Philosophy and Modifications

Chapter 3 presents the design of the prototype bridge, which serves as the basis of the specimen design. This subsection describes how the experimental test specimen was designed to capture certain key features of the prototype. Due to the different span lengths, the PT drape of the duct is not so pronounced in the test specimen. However, the duct curvatures remain essentially the same because the load that is balanced (per unit length) is the same between the prototype bridge and the physical test specimen.

The specimen was designed to simulate the performance of the prototype bridge; however, minor changes were made of necessity as follows:

1. The prototype has four PT ducts, three for continuity and one to balance segment self-weight. The test specimen had only three ducts for continuity and overall load balancing; the fourth duct was replaced by concentric pretensioning (additional strands top and bottom).

2. The prototype bridge was designed for the modified Tx70 with a 9 in. web thickness. The web thickness was increased to 10 in. to match the precaster's available formwork. As a result, the width of the top and bottom flange also increased by 1 in.
3. To accommodate the pretensioning strands in the top flange, the thickness of the top flange was increased by 1.5 in. To maintain the total depth of the composite section, the thickness of the haunch between the slab and the girder was reduced from 2 in. to 0.5 in., maintaining the overall depth of 80 in. for the composite section.
4. The prototype bridge was designed for a deck slab width of 96 in. Due to lab constraints, the width of the specimen deck slab was slightly narrower (92 in.).
5. The shear transfer at the splice connections of the prototype bridge was checked based on intentionally roughening the surface of the girder faces at the splice connections to a 0.25 in. amplitude. The specimen, however, did not have intentionally roughened surfaces, which reduced the shear transfer capacity of the specimen compared to the prototype bridge design.
6. The thickened end blocks for the end segments in the prototype bridge were designed to be tapered off to the adjacent standard cross section. For the specimen, however, the end regions were squared off for ease of construction and due to constraints in the precast plant.

5.3.2 Girder Segment Design

Top and bottom pretensioning strands were designed based on the amount of steel provided in prototype bridge for pretensioning and Stage I PT. Stresses were checked to ensure they satisfied the limits for transportation and construction loads. Stage II PT was designed considering the same amount of steel (number of strands) as for the prototype bridge, but the drape was designed to balance the dead weight of the girder segments, splices, and deck slab. Table 5.4 presents the design summary for the specimen.

Table 5.4. Prestressing Summary for the Specimen.

Design Parameters		Description
Pretensioning	Strands (0.6 in. dia.)	26 strands
	Force at Transfer, F_{1i}	1143 kips
Stage I PT (Replaced by Pretensioning in the Specimen)	Strands (0.6 in. dia.)	34 strands
	Force at Transfer, F_{2ai}	1494 kips
Stage II PT	Tendons (0.6 in. dia.) (19 strands per duct)	57 strands (3 ducts)
	Force at Transfer, F_{2bi}	2337 kips

Figure 5.7 and Figure 5.8 show the prototype bridge moments at different loading and design stages, for the non-composite and composite girder sections, respectively. The load-balancing design moments at each design stage and service stresses were checked. In the load-balancing approach, the girder segments were designed such that the prestress moments in the girders were balanced at each stage throughout the loading history of the specimen construction. The different loading and design stages considered are as follows:

- Girder Section.
 - Self-weight + Pretensioning.
 - Self-weight + Pretensioning + Non-composite Deck Weight.
- Composite Girder and Deck Section.
 - Stage II PT + Superimposed Dead Load.
 - Stage II PT + Superimposed Dead Load + Removal of Temporary Shoring Towers.

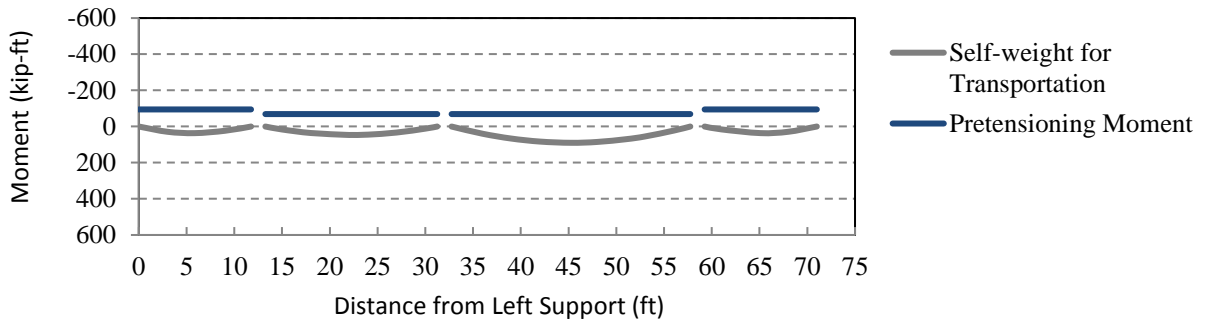
5.3.2.1 Flexure Considerations

Flexural stress analysis was carried out for the specimen girder segments under the total dead loads and prestressing force as well as construction loads during different stages of specimen construction. Figure 5.9 shows the stresses in the specimen at various steps of construction.

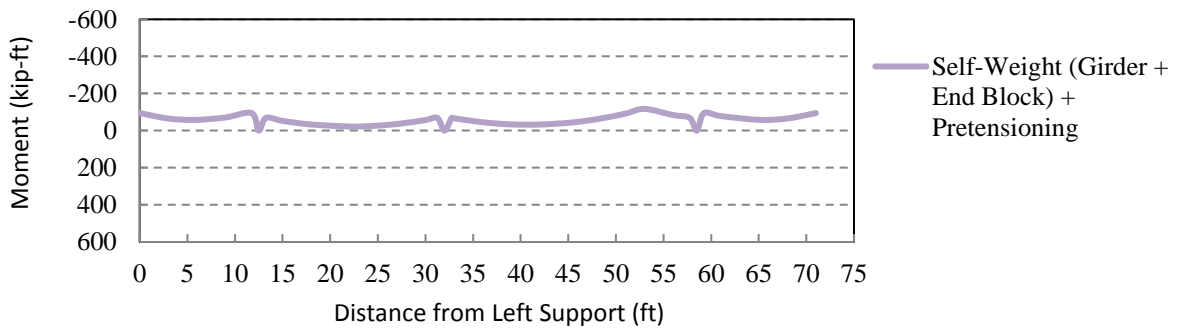
The specimen was also analyzed for actuator load beyond cracking up to ultimate conditions, or the maximum actuator load. Chapter 6 presents the results of the analysis, along with the experimental results.

Deck reinforcement details for the specimen were provided in accordance with current TxDOT construction practice for continuous bridge decks. The typical clear cover provided was 2 in. and 1.25 in. for top and bottom reinforcement, respectively. The reinforcement details are as follows:

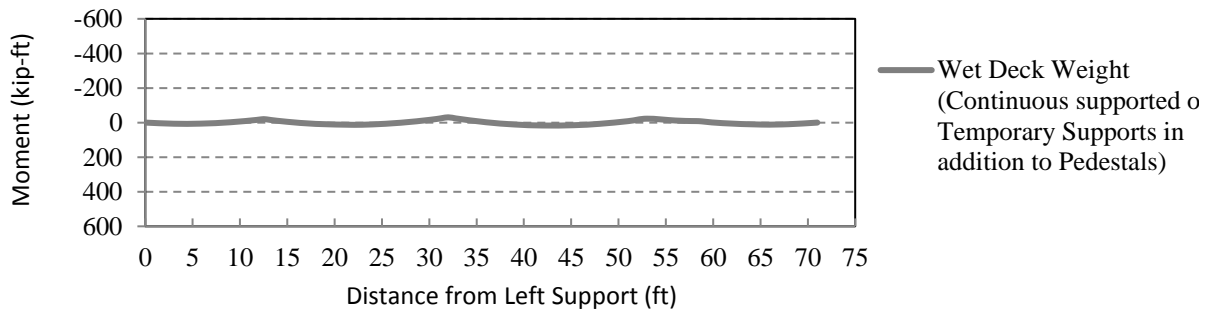
- Transverse steel: #5 bars at 6 in. spacing at top and bottom
- Longitudinal steel: #4 bars at 9 in. spacing at top
#5 bars at 9 in. spacing at bottom



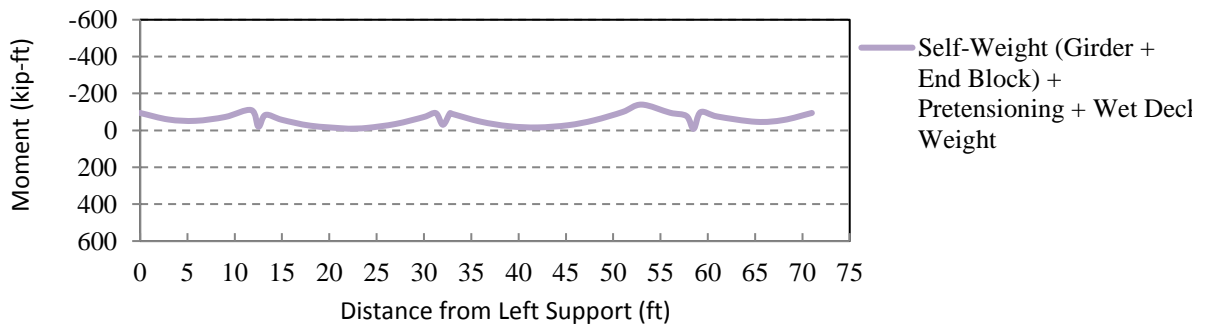
(a) Moments during Transportation



(b) Total Moments after Pretensioning



(c) Moment Due to Wet Deck Weight



(d) Total Moments after Adding Wet Deck Weight

Figure 5.7. Test Specimen Design Moments Acting on Non-composite Girder.

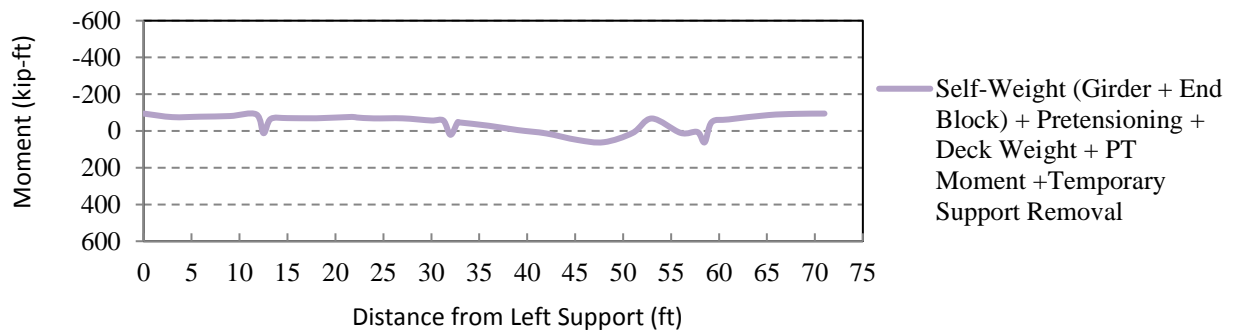
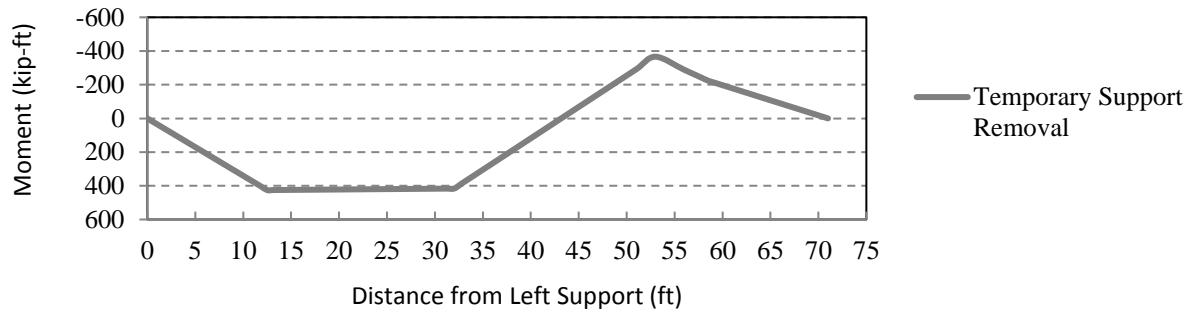
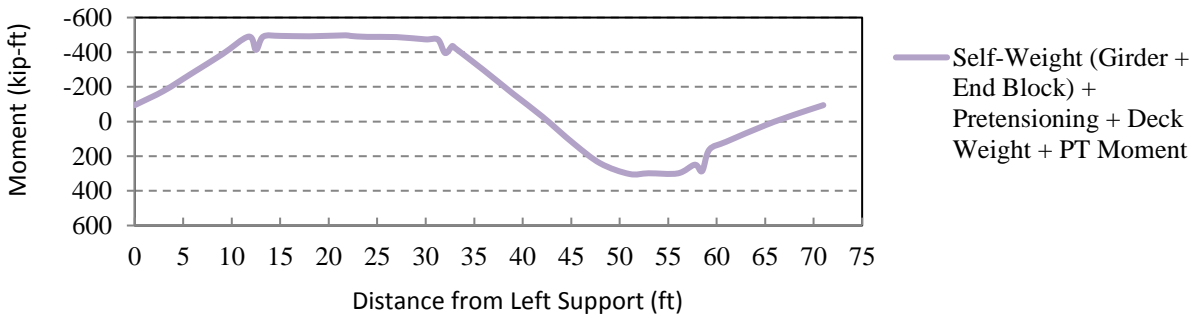
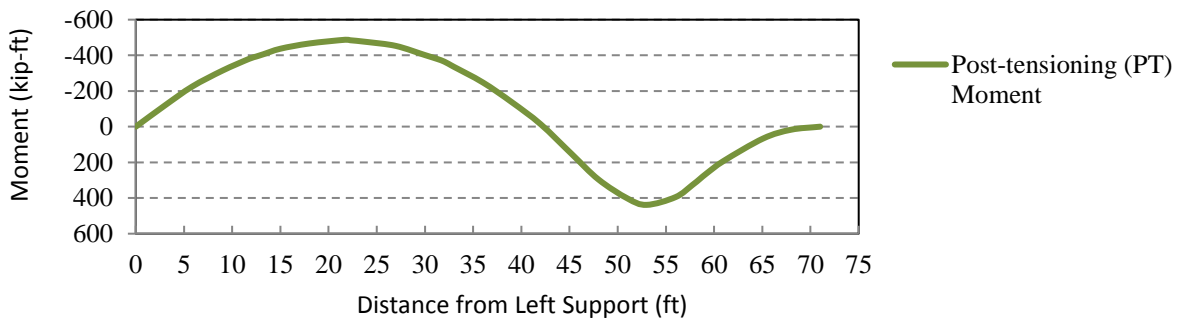
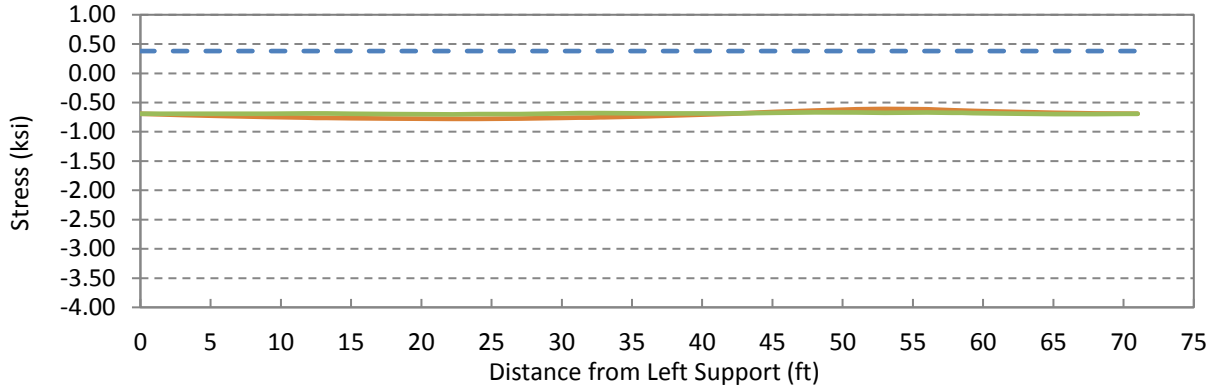
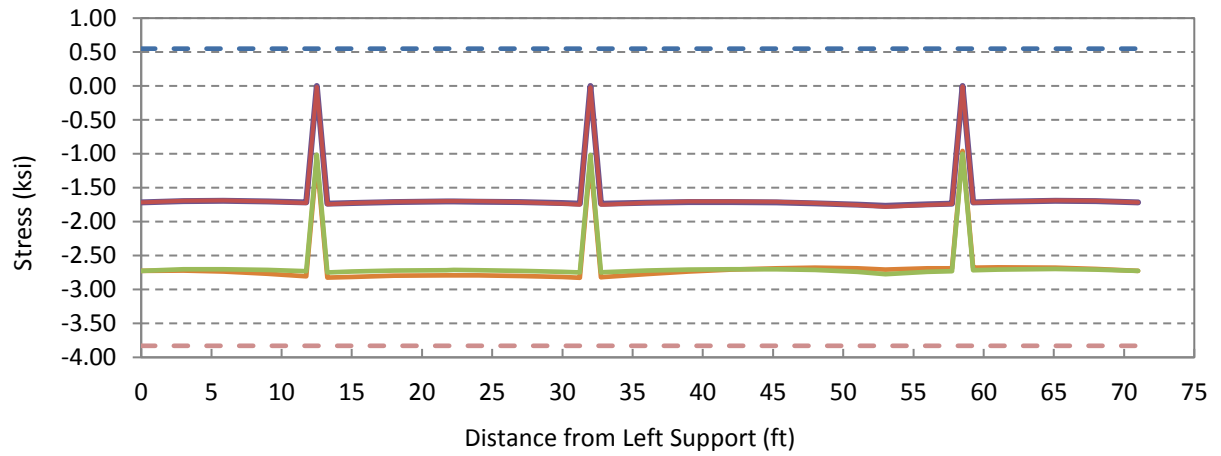


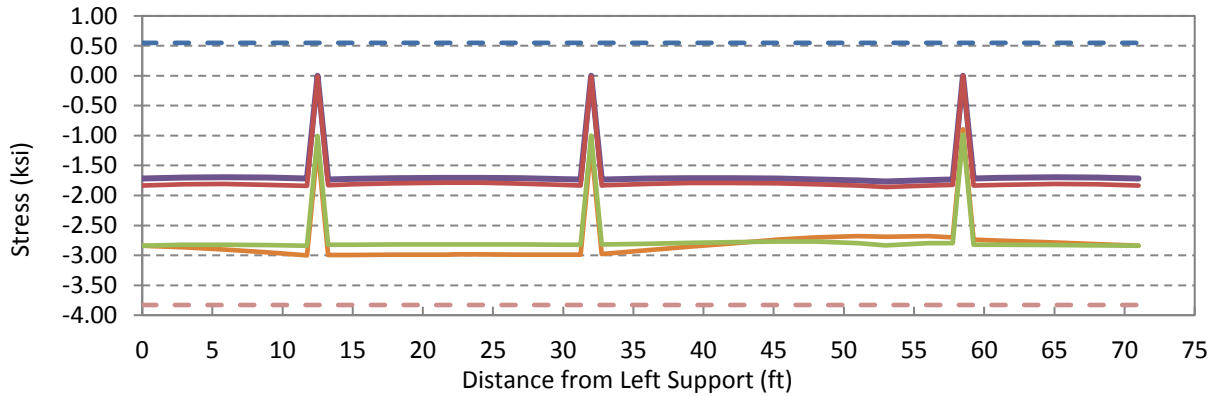
Figure 5.8. Test Specimen Design Moments Acting on Composite Girder.



(a) Stresses at Top of CIP Deck



(b) Stresses at Top of Girder



(c) Stresses at Bottom of Girder

- Allowable Tensile Stress - Girder
- Self-weight + Pretensioning
- Self-weight + Pretensioning + Wet Deck Weight
- Self-weight + Pretensioning + Deck Weight + Stage II PT
- Self-weight + Pretensioning + Deck Weight + Stage II PT + Temporary Support Removal
- Allowable Compressive Stress - Girder

Figure 5.9. Service Stress Analysis for Specimen.

5.3.2.2 Shear Considerations

Transverse Shear Design: MCFT was used for transverse shear design as specified in the AASHTO LRFD Specifications (2012). MCFT takes into consideration the combined effect of axial load, flexure, and prestressing when designing for shear. Table 5.5 presents the shear reinforcement details for the specimen, which are the same as those provided for the prototype bridge presented in Chapter 3. Chapter 3 provides additional details on the transverse shear design using MCFT.

Table 5.5. Shear Reinforcement Details for Specimen.

Location Description	Shear Reinforcement	Dimension from Segment End
Thickened End Block 1	#5@4 in.	0'-0" to 11'-6"
Splice 1 near End Support	#5@4 in.	0'-0" to 2'-0"
Segment 1	#5@4 in. #5@6 in.	0'-0" to 2'-8" 2'-8" to 17'-6"
Interior Splice 2	#5@6 in.	0'-0" to 2'-0"
Segment 2	#5@6 in. #5@4 in.	0'-0" to 8'-10" 8'-10" to 24'-6"
Splice 3 in Overhang	#5@4 in.	0'-0" to 2'-0"
Thickened End Block 2	#5@4 in.	0'-0" to 11'-6"

Note: All shear reinforcement consists of double legged stirrups.

Principal Tensile Stresses: AASHTO LRFD Article 5.8.5 (2012) requires that the principal tension stress be checked to verify the adequacy of the webs of segmental concrete bridges for shear and torsion. This article states that the principal tensile stress resulting from long-term residual axial stress and the maximum shear at the neutral axis of the critical web shall not exceed the tensile stress limit for the Service III limit state ($0.11\sqrt{f'_c}$) at all stages during the life of the structure, excluding those during construction. When investigating principal stresses during construction, the tensile stress limit in AASHTO LRFD Table 5.14.2.3.3-1 ($0.11\sqrt{f'_c}$) is used.

For the specimen, the principal stress was checked at the critical sections over the interior support and the three splice locations. Shear and bending stresses in the concrete at the neutral axis

of the web were calculated for the Service III limit state. The principal tension stress was calculated using classical beam theory and the principles of Mohr's Circle.

Table 5.6 shows the principal tension stress for service limit states at the selected locations with and without considering the effect of prestressing. The vertical component of the draped longitudinal tendons V_p will counteract the shear force in the section and reduces the shear demand carried by the concrete and transverse steel. For the case of load balancing, the effect of the vertical component of the PT cancels the dead load shear demand for the service limit state. AASHTO LRFD Article 5.8.5 (2012) specifies that V_p may be considered as a reduction in the shear force. The principle tension stress values considering V_p are below the AASHTO specified allowable limit. Note that the principal tension stress at service for Splice 3 is above the limit when V_p is not considered.

Table 5.6. Principal Tension Stress Calculations for Specimen.

Critical Location	Principal Tension Stress at Service (not Considering V_p) (ksi)	Principal Tension Stress at Service (Considering V_p) (ksi)	Principal Tensile Stress limit ($0.11\sqrt{f'_c}$) (ksi)
Interior Support	0.224	0.039	0.321
Splice 1 near End Support	0.126	0.015	0.321
Interior Splice 2	0.242	0.066	0.321
Splice 3 in Overhang	0.433	0.095	0.321

5.3.3 Splice Connection Design

Flexural Considerations: The interior splice (Splice 2) in the specimen represents the splice located in the end span of the prototype bridge. This splice location corresponds to the dead load point of contraflexure in the prototype bridge so as to minimize the load demands at the splice. The width of the splice connection should be kept as small as possible because there is no pretensioning in this region and a minimal amount of mild steel reinforcement is provided. However, the splice width should be large enough to splice the continuity PT tendon ducts and allow for proper vibration of concrete. The width of the splice connection detail was a maximum

of 24 in. per TxDOT recommendations. Figure 5.10 shows the splice connection detail used for the test specimen.

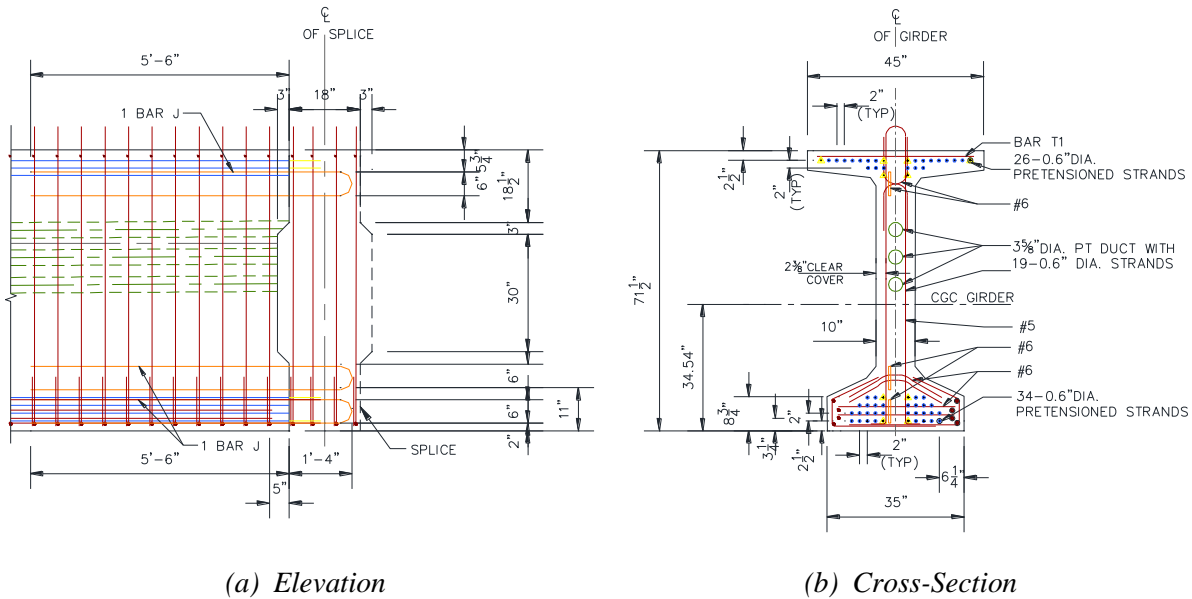


Figure 5.10. Splice Detail Used for Test Specimen.

Because it is not feasible to pretension the splice region, a minimalist partially prestressed concrete solution was designed where the continuity PT provides most (approximately 90 percent) of the flexural strength, with some supplementary capacity provided by several top and bottom mild steel U-bars that formed a non-contact splice within the splice region. The same connection detail was used at all three splice locations. The mild steel reinforcement consisted of #6 180° hooked bars anchored into the adjacent girder flanges and extending into the joint. This connection detail was considered appropriate for the prototype bridge because thickened ends of girders were not used at the splice connection.

The factored moment capacity of the splice was calculated based on the number, diameter, location, and stress in the tendons, along with the design strength of concrete and properties of the girder cross-section. Additional capacity was provided by the #6 mild steel 180° bent bars with details as follows (see J bars in Figure 5.10):

- Top flange steel: 1 - #6 180° bent bar.
- Bottom flange steel: 2 - #6 180° bent bars.

The embedment length of these bent bars was 5 ft 6 in. following the design recommendations of Koch and Roberts-Wollmann (2008). Their design recommendations for embedment length are based on the angle of inclination of the diagonal compressive stress computed using MCFT. In addition, two #6 transverse bars were tied inside each of the bent bars to increase the bearing capacity of the non-contact splice. The design capacity of the splice connection was calculated at three locations. Table 5.7 shows the ultimate moment capacity for the splice locations in the specimen. The mild steel contributes a minimal amount of flexural strength, ranging from approximately 4–8 percent of the total reduced nominal strength in bending.

Table 5.7. Reduced Nominal Moment Capacity for Splice Connections.

Description	Splice 1 Near End Support	Interior Splice 2	Splice 3 in Overhang
Continuity PT, ϕM_n (kip-ft)	7460	7400	10,310
Splice Reinforcement (180° bent bars), ϕM_n (kip-ft)	630	630	380
Total Capacity, ϕM_n (kip-ft)	8090	8030	10,690

Interface Shear Considerations: The integrity of the splice connection largely depends on the shear transfer mechanism at the interface of the precast girder and closure pour. This shear transfer mechanism was mainly provided by the shear key and the lapped 180° bent hooked bars in the connection. The interface shear resistance at the girder/splice interface was calculated as per AASHTO LRFD Article 5.8.4 based on shear friction theory. The nominal shear resistance of the interface plane is based on the cohesion factor, c , friction factor, μ , and the area of concrete engaged in interface shear transfer, A_{cv} . For the specimen, the case of normal-weight concrete placed against a clean concrete surface, free of laitance, without the roughened surface was used. The values of parameters specified in AASHTO LRFD Article 5.8.4 are cohesion factor $c = 0.075$ ksi, friction factor $\mu = 0.6$, fraction of concrete strength available to resist interface shear $K_1 = 0.2$, and limiting interface shear resistance $K_2 = 0.8$ ksi. Due to the relatively high concrete strength and high level of prestressing, the K_2 value is the critical parameter and limits the shear transfer capacity to 800 kips while shear demand for strength limit state is 448 kips in the prototype bridge.

5.4 SPECIMEN PREPARATION

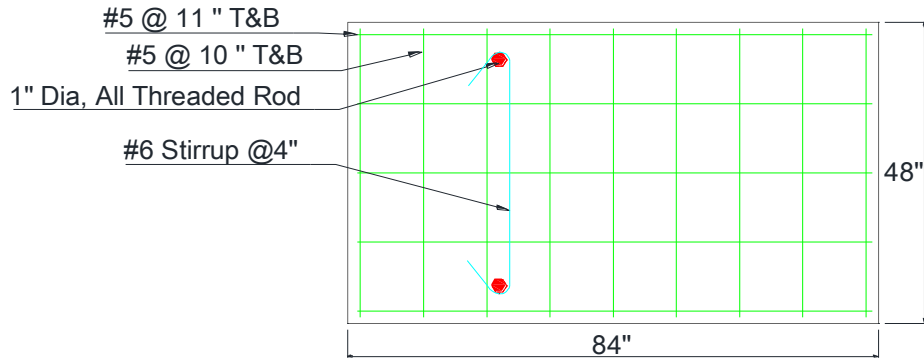
5.4.1 Overview

The PT ducts and anchorages introduced some new details in the girder fabrication. A precast plant having experience with a recent spliced girder project agreed to fabricate the segments. After fabricating the girder segments and transporting them to the HBSMTL, significant preparation was necessary prior to testing. A brief review of the construction process is presented below.

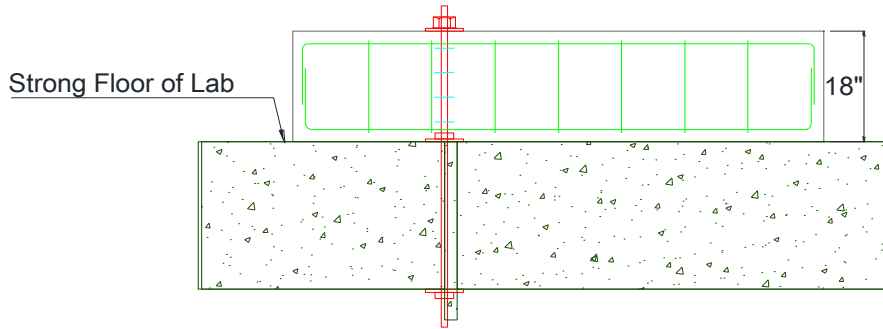
5.4.2 Bearing Pad, Pedestal Design, and Pedestal Construction

The specimen was supported on two concrete pedestals in the lab. The pedestals were tied down to the strong floor using threaded rods. The size of the pedestal was based on the 3 ft spacing between the tie downs in the strong floor. The height of the pedestals was selected to facilitate installation of string potentiometers below the girder and to accommodate the girder deflection during testing. Figure 5.11 presents detailed dimensions and details of the pedestals.

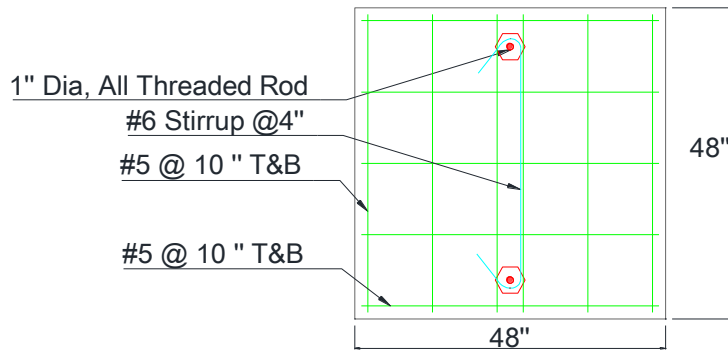
Laminated steel-reinforced elastomeric bearing pads were selected for the supports based on the reaction forces at the supports during testing. In addition, because these bearing pads are commonly used by TxDOT in practice, they are intended to simulate the condition at supports similar to the prototype bridge on site. Figure 5.12 presents the bearing pad dimensions.



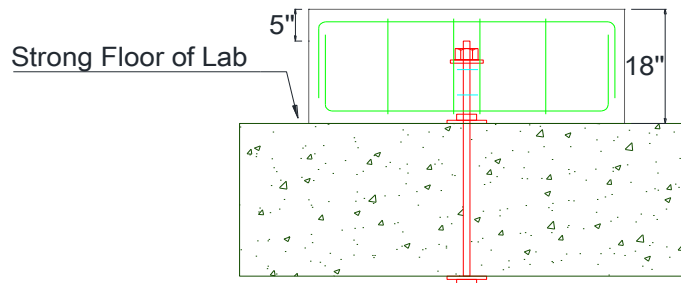
(a) 4x8 ft Pedestal, Plan View



(b) 4x8 ft Pedestal, Elevation View

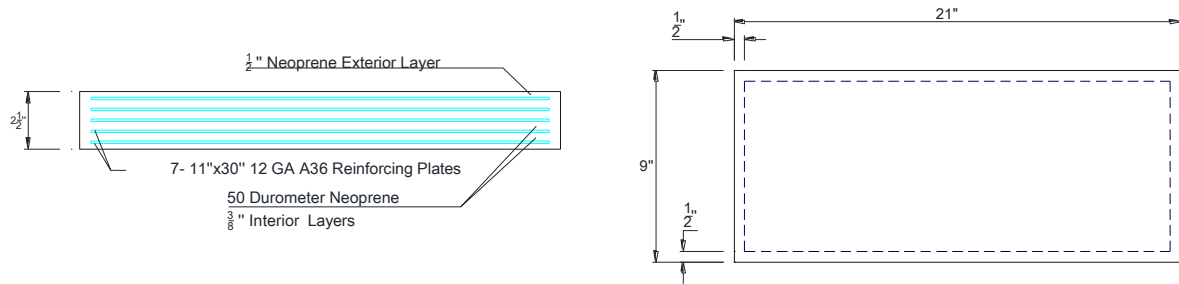


(c) 4x4 ft Pedestal, Plan View



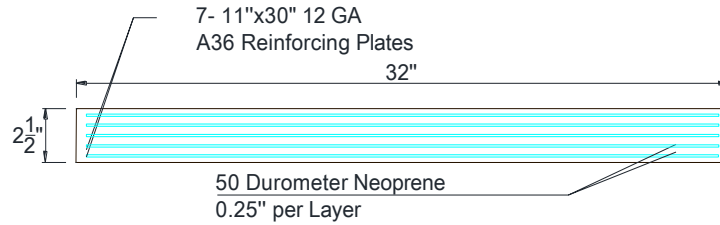
(d) 4x4 ft Pedestal, Elevation View

Figure 5.11. Details of Concrete Pedestals.

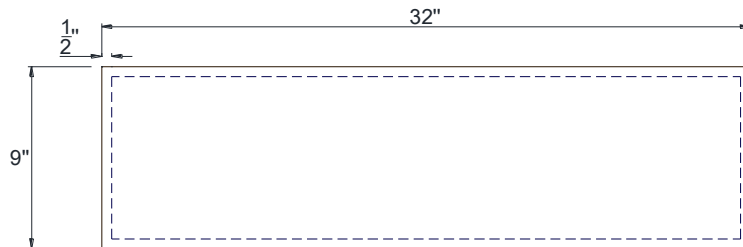


(e) 9x21 in. Bearing Pad, Elevation View

(b) 9x21 in. Bearing Pad, Plan View



(c) 9x32 in.² Bearing Pad, Elevation View



(d) 9x32 in. Bearing Pad, Plan View

Figure 5.12. Bearing Pad Details.

5.4.3 Casting the Girder Specimen at the Precast Plant

The four girder segments and end blocks for the specimen were fabricated at a precast plant. The gaged bars were prepared by the research group and placed in the girder according to the instrumentation plan. Gage wires were carefully tied to the closest vertical bars to protect them during the concrete placement. The wires were taken out of the formwork at the top of the segments. Figure 5.13 shows the placement and monitoring of the reinforcement. Casting of the specimen and concrete sample fabrication can be seen in Figure 5.14. A total of 156 cylinders, 13 MOR beams, and 12 shrinkage prism samples were taken from the different batches to monitor the mechanical properties of the concrete (see Appendix A).



(a) Installing Reinforcement



(b) Strain Gage



(c) Protecting Gage Wires



(d) Prestressing Strands



(e) Checking Gages

Figure 5.13. Installing Reinforcement at the Precast Plant.



(a) *Installing Formwork*



(b) *Casting Concrete Transported from Batch Plant*



(c) *Molds for Hardened Property Samples*



(d) *Preparing Samples*

Figure 5.14. Casting Girder Segments and Samples at the Precast Plant.

The girder segments were released two days after the pour. They were then hauled to the HBSMTL after they reached the required concrete strength at service f_{ci} of 6.5 ksi (see Figure 5.15). Figure 5.16 shows the final alignment of the girder segments in the HBSMTL with temporary supports in place to support each end of the girder segments.



(a) Girder Segments with Lifting Points



(b) Placing Girder Segments



(c) Verifying Segment Spacing and Placement

Figure 5.15. Transporting Girder Segments to the High Bay Laboratory.



(a) Top View - Girder Alignment



(b) Side View - Girder Alignment

Figure 5.16. Final Girder Segment Placement and Alignment in the High Bay Laboratory.

5.4.4 Fabricating Wooden Connection Formwork

Three pairs of wooden formwork for the splice connections were fabricated by the research group in the lab. The formwork was cut and screwed together to maintain the actual shape of the modified Tx70 cross section through the splices. Gage wires were sent through openings in the formwork with care to avoid gage losses. Figure 5.17 shows the splice reinforcement with gaging and the formwork attached on the back side.

5.4.5 Building Falsework and Deck Formwork

Wooden falsework was designed and constructed to provide support for the deck formwork and walkway, as presented in Figure 5.18. A railing was also provided alongside the walkway and at the end of the formwork for safety.

5.4.6 Casting Splices in the Laboratory

After the connection formwork was fabricated and properly lubricated, the high strength conventional concrete splices were cast in the laboratory. Different options were considered for mixture proportions for the concrete, and after 10 trial batches the final mixture proportions were selected. Table 5.8 summarizes the mixture proportion summary for the splice concrete. A concrete ready mix truck was hired and loaded with the appropriate amounts of 0.75 in. maximum size river gravel (coarse aggregate) and manufactured sand (fine aggregate) from a local batch plant. The gradation of the aggregates met TxDOT specifications. The remaining water, admixtures, and Type III cement were added to the concrete mix truck at the HBSMTL, as shown in Figure 5.19. The splices were cast in the laboratory as depicted in Figure 5.20.

Table 5.8. Splice Concrete Mixture Proportions.

Material		Type	Quantity
Cement (lb/yd ³)		III	700
Water (lb/yd ³)		-	200
w/c ratio		-	0.29
Aggregate (lb/yd ³)	Coarse (MNAS ¾ in.)	River Gravel	1935
	Fine	Mfd. Sand	1232
HRWRA/Superplasticizer (oz/yd ³)		PS 1466	91

5.4.7 Casting Reinforced Concrete Deck in the Laboratory

After the splice gained sufficient strength, the mild steel and concrete for the deck was placed, as shown in Figure 5.21. A TxDOT Class S concrete with specified 28-day strength of 4 ksi was used for the deck concrete. A smooth finish was provided after casting. The deck concrete cured for one week and then the formwork was removed.

5.4.8 Fresh Concrete Properties

Fresh properties of concrete were measured after the concrete was cast. Measured parameters included slump, unit weight, temperature, and relative humidity.

Table 5.9 summarizes the average fresh concrete properties for the girder segments, splice connections, and the deck concrete.



(a) Splice 1 (End)

(b) Splice 2 (Middle)

Figure 5.17. Splice Reinforcement and Formwork.



(a) South Side Formwork



(b) North Side Formwork

Figure 5.18. Falsework and Deck Formwork.



(a) Measuring Cement into Hopper



(b) Adding Cement to Truck



(c) Adding Admixture and Water to Truck

Figure 5.19. Adding Materials to Concrete Mixture for Connections.

Table 5.9. Summary of Fresh Properties of Concrete.

Component	Slump or Slump Flow (in.)	Unit Weight (kcf)	Air Content (%)	Concrete Temperature (°F)	Ambient Temperature (°F)	RH (%)
Girder Segment	24.8	0.145	8	96	107.4	24.4
Splice Connection	9.75	0.151	not measured	not measured	70 (typical)	48
Slab Deck	3.75	0.146	5.1	67.5	70 (typical)	40



(a) Casting Splices

Figure 5.20. Placing Concrete for Splice Connections.



(b) Casting Splices Complete

Figure 5.20. Placing Concrete for Splice Connections (Continued).



(a) Casting the Deck



(b) Finishing the Deck



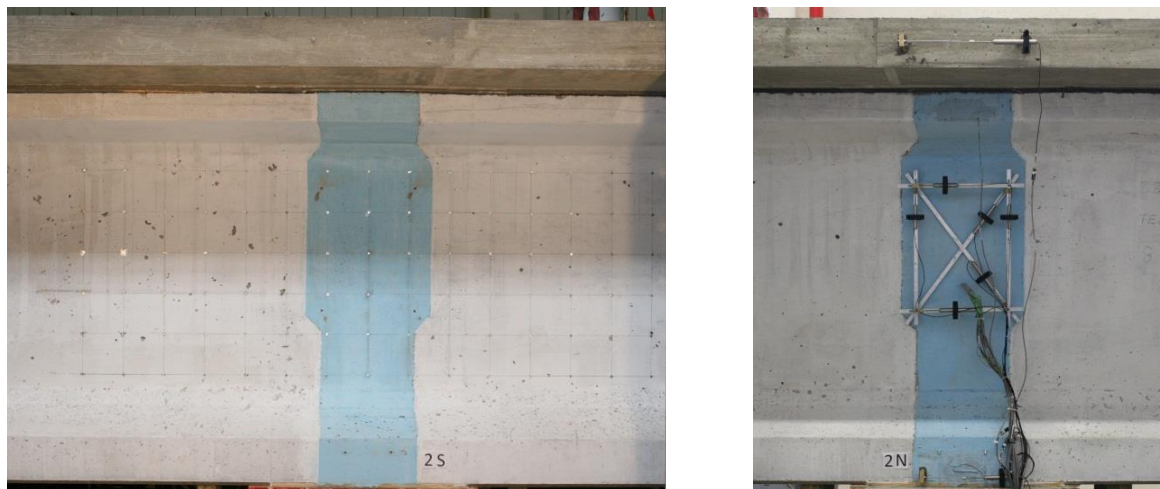
(c) Curing the Deck and Removing the Deck Formwork

Figure 5.21. Construction of the Deck Slab.

5.4.9 Installing Gages, Linear Variable Differential Transformers, String Pots, and Demountable Mechanical Points

Surface gages were attached on the top surface of the deck and to the sides of the top and bottom flanges of the precast girder according to the instrumentation plan described in Section 5.5. String potentiometers were placed 2 ft apart below the specimen to capture the deformation profile of the specimen.

A complete set of six linear variable differential transformers (LVDTs) was also mounted on the webs at each splice connection to map the deformed configuration of the splices and to measure the cracks. Demountable mechanical (DEMEC) points made from thin aluminum sheets were installed on the webs of the splice regions. DEMEC readings were carried out at specific load levels during each test to fully map the deformation of the web and formation of cracks. Figure 5.22 shows the DEMEC and LVDT configurations for Splice 2.



(a) DEMEC Points

(b) Splice LVDTs

Figure 5.22. Splice DEMEC and LVDT Layouts.

5.4.10 Post-Tensioning

After the concrete deck and splice concrete gained their design strength of 4 ksi and 8.5 ksi, respectively, the PT operation was carried out. A PT contractor cut and placed the strands, stressed the strands, and grouted the ducts. Strands were fed through the three ducts and were stressed from End Block 1, after being anchored at End Block 2.

A hydraulic self-reacting jack was used to stress the strands. A simple conversion factor was used to translate the desired force per tendon into the required pressure. The desired force was

also translated into strand elongation, which was double checked to ensure the target force per tendon was applied.

Table 5.10 provides a summary of the target values for the PT operation. The three PT tendons were stressed one at a time. The middle tendon was stressed first, and then the top and the bottom tendons were stressed, respectively. While calculating the target force, instantaneous and time-dependent losses were considered. The order of stressing each duct affects the instantaneous elastic shortening for each tendon. While calculating the stress for the first duct, the elastic shortening due to tensioning the second and third tendons was considered. In addition, the instantaneous loss due to anchorage set was considered. For the specific setup that was used for the specimen, the anchorage set was assumed to be 3/8 in.

Table 5.10. Post-tensioning Calculation.

Tendon Location (Sequence)	Target Applied Stress (ksi)	Target Applied Force (kips)	Elongation (in.)
Middle (First)	206	850	6-1/8
Top (Second)	203	836	6
Bottom (Third)	200	822	6

After the strands were stressed, the ducts were grouted. Two holes at the top of each end cap served to monitor the filling of the tendon. When grout flowed out of the top hole, the grouting was stopped, as the grout had fully filled the ducts.

Grout was fed through each duct from End Block 2, using an air compressor to provide sufficient pressure throughout the length of the duct and to avoid formation of voids in the ducts. A pre-bagged NA Grout was used, which is a high flow, non-aggregate, and non-shrink grout. Every 400 lb of grout cement were mixed with 15.5 gallons of water, based on common practice. A mud flow test was carried out to measure the flowability of the grout. A large range of 11 to 30 seconds is acceptable based on the Post-tensioning Institute Specifications (2001). The grout mix was observed to be highly flowable and had a flow time of 8.5 seconds, which was lower than the acceptable limit. However, according to EN 447 (European Committee for Standardization, 1996) any value lower than 25 seconds is acceptable.

Samples from each the three grout batches used for filling the PT ducts were taken for compressive strength testing. Standard 2 in. × 2 in. × 2 in. grout cube samples were made according to ASTM C109 (2013).



(a) Stressing Tendons



(b) Anchorage Plate and Anchor Wedges



(c) Measuring Pressure during Stressing



(d) Mixing Grout Mix and Water



(e) Grouting Ducts Using Air Pressure

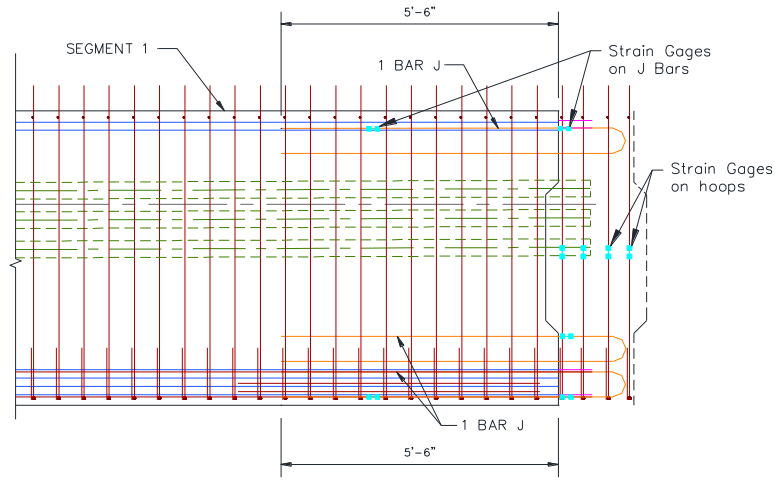
Figure 5.23. Tendon Post-tensioning and Grouting Process.

5.5 INSTRUMENTATION

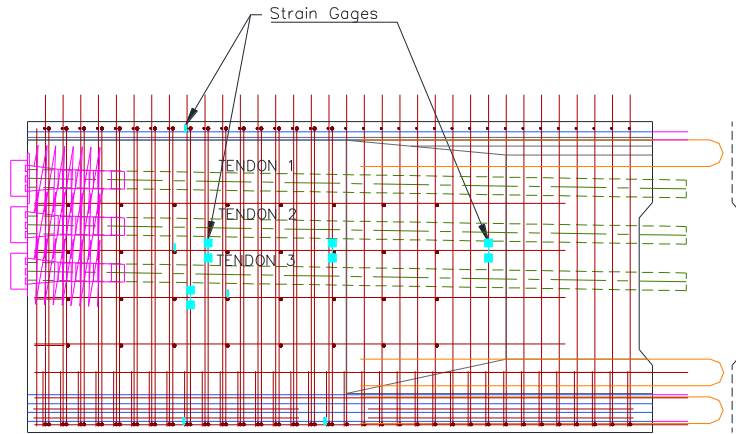
Different types of instruments were used to record data to investigate and understand the behavior of the specimen under the test loads described in the experimental program. The instrumentation included strain gages, embedded concrete gages, LVDTs, string potentiometers, and DEMEC points. The instruments were used to capture the deflections along the specimen length and the strain profiles at critical sections of the specimen. In addition, reinforcement was monitored to determine if yielding occurred.

5.5.1 Rebar Strain Gages

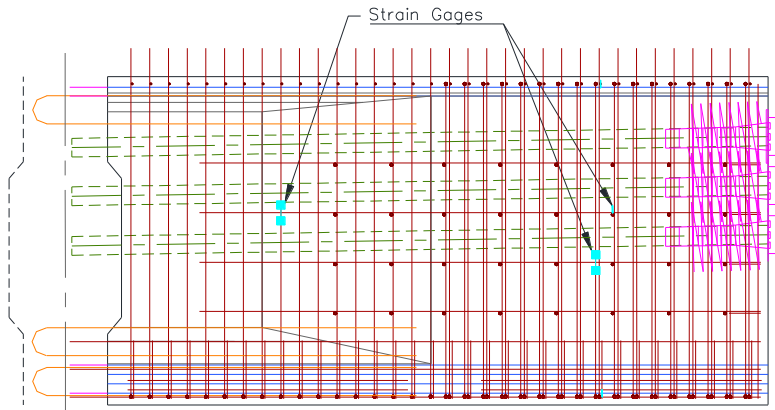
Figure 5.24 shows the locations of the rebar strain gages in the specimen. The strain gages were attached to reinforcement bars in the splice region and in the thickened end blocks. Table 5.11 summarizes rebar strain gage details according to the type of reinforcement bar. Because the research study was primarily focused on monitoring and assessing the performance of the proposed splice connection detail, most of the strain gages were attached in this area. The splice connection detail includes 180° bent hooked bars, and it was important to capture the stress, strain, and elongation in these bars. Two strain gages were attached on one leg of the 180° bent hooked bars at the top and bottom of each splice. Also, one strain gage was attached on one leg of each transverse shear reinforcement bar to measure shear demands. Ten strain gages were attached in the thickened end block to investigate the effect of post-tensioning and bursting forces during post-tensioning in this area.



(a) Strain Gage Locations in the Splice Region (typical)



(b) Strain Gage Locations in Thickened End Block 1



(c) Strain Gage Locations in Thickened End Block 2

Figure 5.24. Rebar Strain Gages in the Specimen.

Table 5.11. Summary of Rebar Strain Gages.

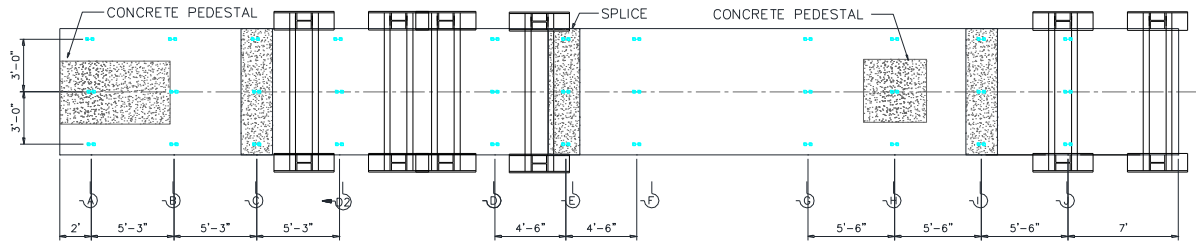
Description	No. of Gages per Splice	Total No. of Gages	Installation Notes
On 180° bent hooked bars in girder	4	12	Pre-installed on the reinforcement bars, which were placed at the precast plant before the girder segments were cast.
On 180° bent hooked bars in splice	6	18	Installed in laboratory before casting splices.
On transverse shear reinforcement bars in splice	4	12	Installed in laboratory before casting splices.
Total	14	42	

A commonly used general purpose strain gage (CEA-06-250UW-350) with a gage length of 0.25 in. was used for measuring rebar strain in select locations. To make a half-bridge or full-bridge configuration, strain gages are usually attached to the point of interest as a pair of two or in a set of four, respectively. The advantage of using a half-bridge or full-bridge configuration to measure strain is the ability to compensate for a secondary type of strain. For the specimen, the rebar at critical locations were primarily subject to axial strain. The temperature during the testing program in the laboratory was nearly constant, so no compensation for temperature induced strains was needed. In this case, the strain gages were attached to the rebar at the points of interest and a quarter-bridge configuration was used to read the strain.

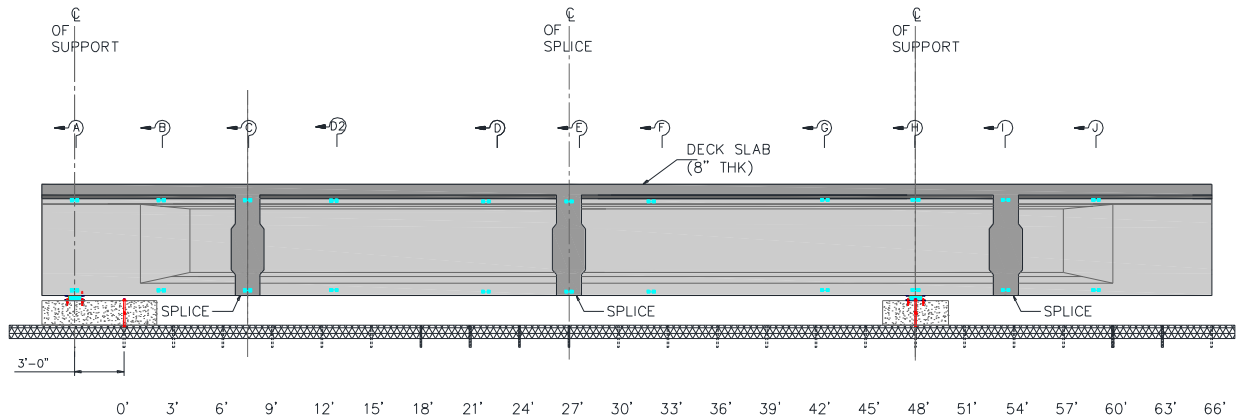
5.5.2 Surface Strain Gages

Surface strain gages (PL-60-11-3LT) were also used to capture the strain profile at important sections of the specimen during the loading and post-tensioning stages. Surface gages are similar to rebar gages, but because they are used on concrete, they are usually longer than those used for rebar (gage length = 2.36 in.). As shown in Figure 5.25, surface gages were attached on the top surface of the CIP concrete deck and on the side surfaces of the girder flanges. Three lines of strain gages were attached on top of the deck along the length of the specimen (see Figure 5.25[a]). Two lines of strain gages measured the strain and deformation on the deck near the edges, and the central line of gages measured the strain on top of the deck along the centerline of the girder. Two surface strain gages were attached on the side surfaces of the top and bottom flanges of the girder

at each critical location to capture the strain profile of those sections during post-tensioning and loading the specimen (see Figure 5.25[b]).



(a) Surface Strain Gage on Deck



(b) Surface Gages on Side of Girder Flanges

Figure 5.25. Surface Gages on the Specimen.

5.5.3 Embedded Concrete Gages

Embedded concrete gages were used to capture the strain and stress in the concrete, especially in the anchorage zones and the splice connections. The concrete gages around the PT ducts captured the effect of post-tensioning on the girder and the splice connection. Unlike the rebar strain gages, the embedded concrete gages were placed by attaching to the adjacent reinforcement using wires and then were embedded when the concrete was cast. These gages measured the axial strain in concrete. There are two different types of embedded concrete gages: one that only measures compressive strain and the other that measures both compressive and tensile strain in concrete. Within the specimen, the concrete was subjected to tensile stresses in some areas and cracked, therefore embedded concrete gages with the ability to measure both compression and tension were used.

In order to measure the strain profile in the splice section, three embedded concrete gages were placed in the splice region. Figure 5.26 shows the typical locations for the embedded concrete gages within the splice region and end blocks. These gages were used to observe the effect of post-tensioning at the splices and the anchorage zone. They were also used in the splice sections to capture the strain profile at different loading stages during laboratory testing.

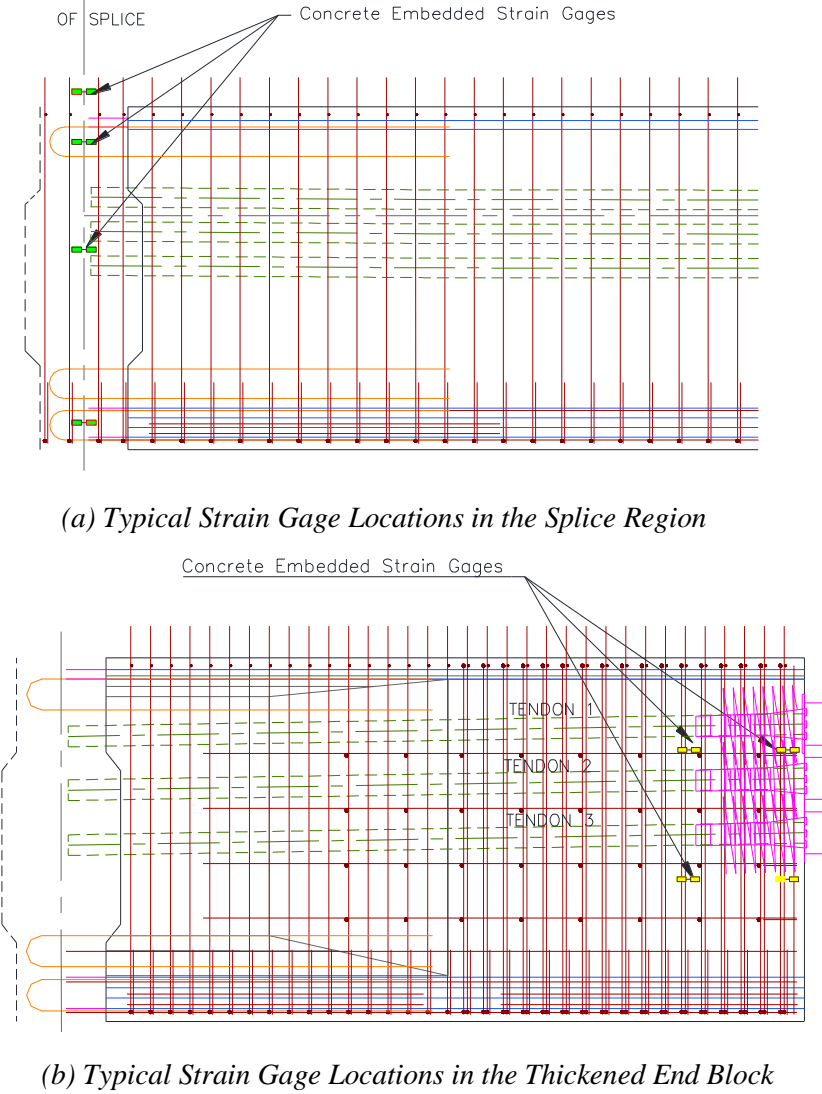
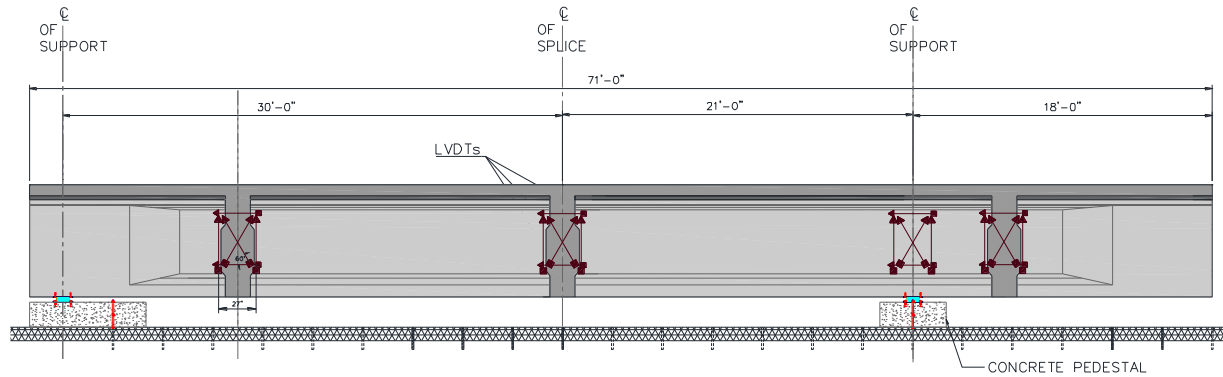


Figure 5.26. Embedded Concrete Gages in the Specimen.

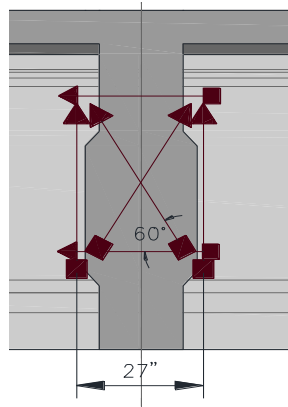
5.5.4 Linear Variable Differential Transformers

LVDTs are capable of measuring relative displacement between two specific points and are typically used to measure the average strain over a longer length. LVDTs were used to map the

splice deformation at different loading stages during testing. Figure 5.27(a) shows the location of mounted LVDTs on the specimen. Figure 5.27(b) shows the configuration detail of the mounted LVDTs.



(a) Locations of LVDTs



(b) Configuration of LVDTs

Figure 5.27. LVDTs Mounted on the Web of Specimen.

5.5.5 String Potentiometers

String potentiometers (string pots) are used to measure displacements and movements from a constant origin. String pots were placed under the girder at 2 ft increments to record the deformation profile of the girder during load testing. Figure 5.28 shows the layout of the string pots. The string pots were also used to capture the effect of post-tensioning, which introduced camber in the girder specimen.

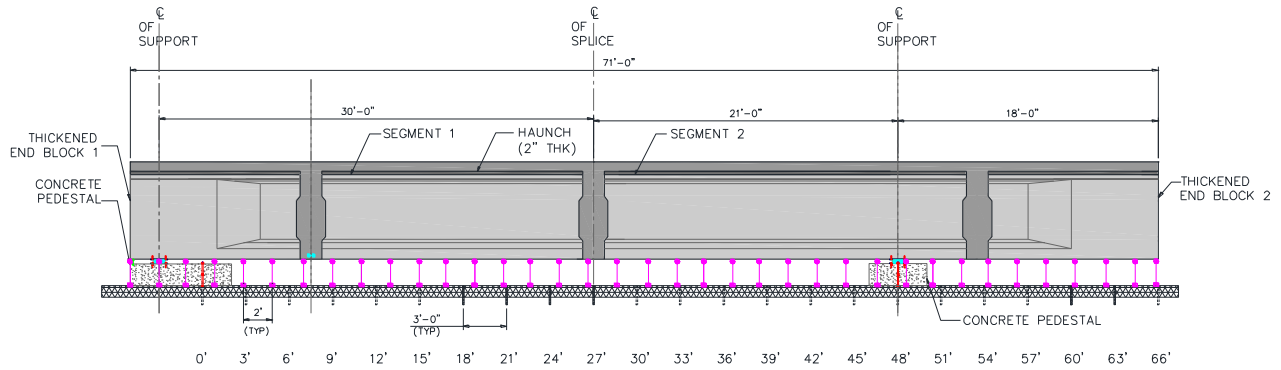


Figure 5.28. String Potentiometers Mounted on the Specimen.

5.5.6 Demountable Mechanical Points

DEMEC points were also used to map the deformation on the surface of the specimen. DEMEC points have several advantages including economy, reliability, and ease of installation. One disadvantage is that it is time consuming to measure and record all the distances between the DEMEC points and to map the deformed surface. Also, because there is no continuous data logging using the DEMECs, the experiment needs to be stopped at specific instances of interest in order to measure and record the useful data.

5.5.7 Summary of Instrumentation

Table 5.12 presents a summary of the number of gages used for the specimen.

Table 5.12. Instrumentation Summary.

Instrument Type	Location in the Specimen	Quantity	Measurement
Rebar Strain Gages	Splices	42	Strains in transverse reinforcement and 180° bent hooked bars in splices
Rebar Strain Gages	Thickened end blocks	10	Effect of PT forces on rebar in thickened end block
Concrete Strain Gages (Embedded)	Splice, thickened end blocks	20	Concrete strains in thickened end blocks and splice regions
Concrete Strain Gages (Surface)	Top and bottom flanges of girder segments and on top surface of deck	49	Strain in extreme fiber, moment-curvature relationship, load-displacement relationship
LVDTs	Splices, over interior support	24	Strains at splice regions and interior support
DEMEC Points	Splices, over interior support	280	Mapping the deformation in the splice region and at the interior support
String Pots	Movement of bottom girder face relative to strong floor along the length of the specimen	37	Deflection along the length of the specimen for moment-curvature relationship and load-displacement relationship
3-Wire Cable	Strain gages and string pots	10 (1000 ft each)	-
4-Wire Cable	LVDTs	2 (1000 ft each)	-

5.6 PRE-TESTING DATA ANALYSIS

5.6.1 Introduction

In order to fully understand the condition of the specimen prior to the testing phase, a study was carried out to consider the effect of prestressing, creep, and temporary support removal. Creep data were used to determine the effect of creep in the specimen due to post-tensioning. Data taken during post-tensioning the specimen were reviewed to determine the stress and strain at the splices. The reactions at the temporary supports were calculated, and the support removal effect was evaluated. For all cases, data from the concrete surface gages and embedded concrete gages were compared to the analytical predictions. This evaluation is summarized below. Additional details may be found in Sarremejane (2014).

5.6.2 Creep Effect

The testing started 22 days after the PT operation. Therefore, some portion of the PT losses occurred before the loading due to creep effects. Internal gages and surface gages recorded data to provide an insight on PT loss with time. Also different models were used to predict the effect of creep. Following the recommendations and equations from the AASHTO LRFD Specifications (2012), the prestress losses in the pretensioning were determined at the location of maximum positive moment. A one-day time step method was used to provide adequate accuracy. The state of stress was determined for each day including the losses from the previous iteration. Successive iterations were based on the updated values of the modified force from the previous step. Figure 5.29 presents the graph obtained, which clearly shows the phases of short- and long-term losses.

Figure 5.30 shows the readings for a number of gages in the three splices after the application of the post-tensioning. The data were recorded during the 19 days after post-tensioning and prior to the testing phase. After the PT was applied, the strains continued to increase over time exhibiting the long-term creep deformation process.

Around 13 days, the temporary supports were removed, modifying the state of stresses in the girder and the splices. Indeed, the full dead weight was applied to the structure, showing a sudden change in the strain readings, as depicted in Figure 5.30.

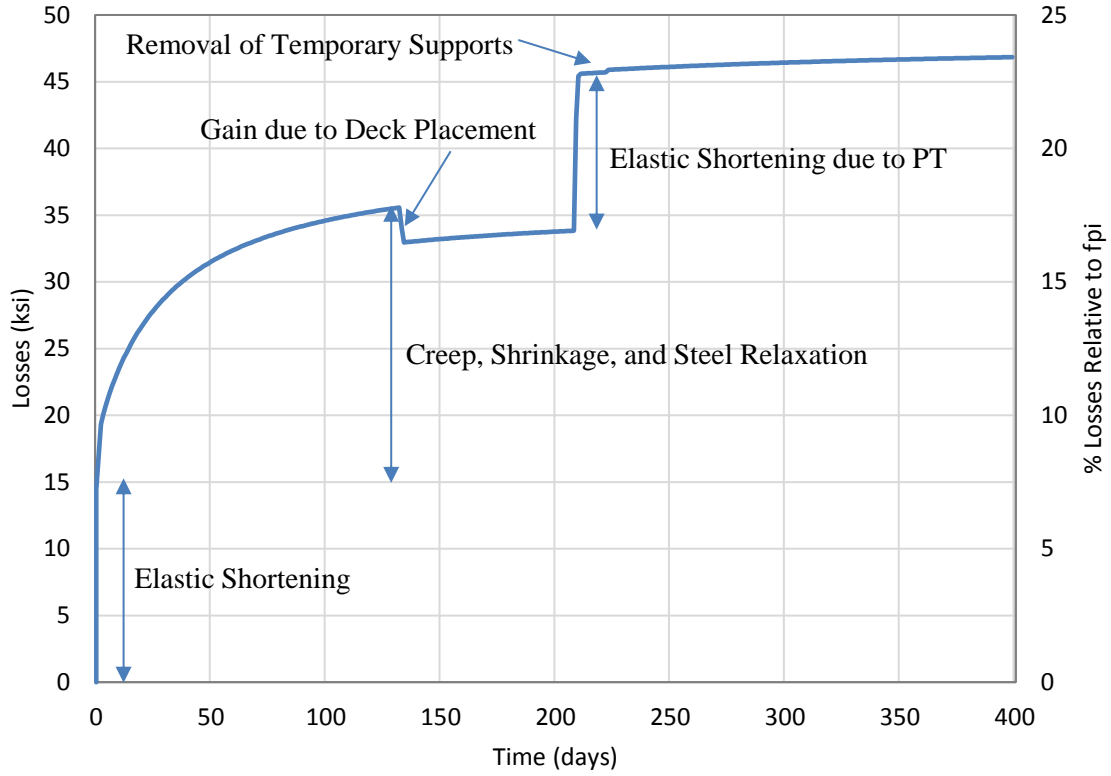


Figure 5.29. Pretensioning Losses.

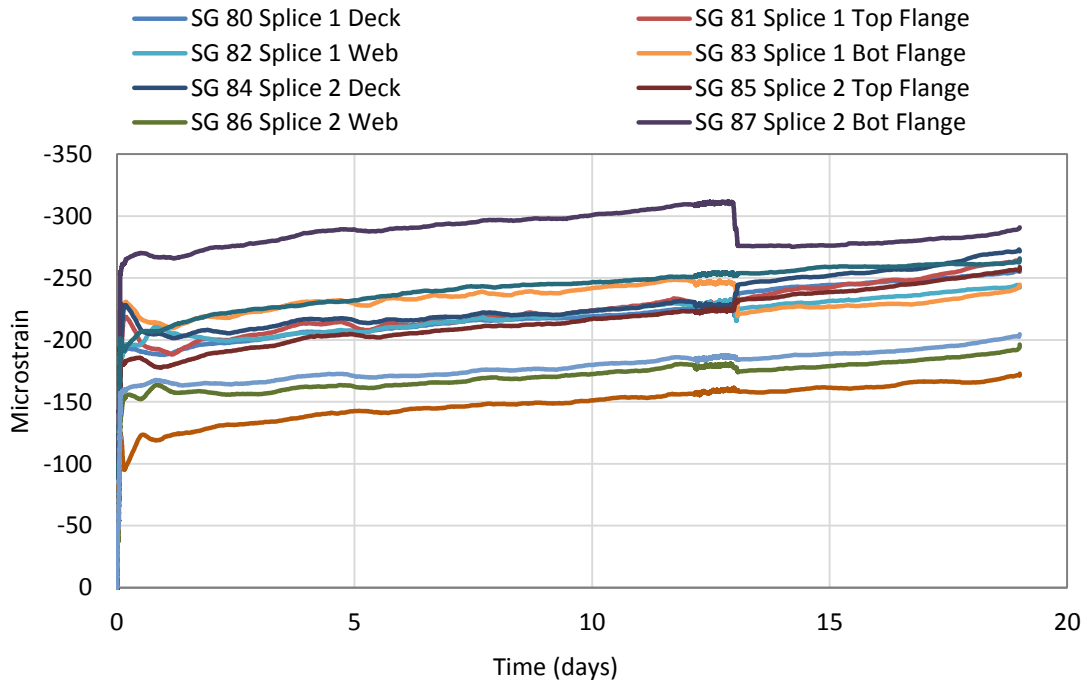


Figure 5.30. Effect of Post-Tensioning over 19 Days.

5.6.3 Support Removal Effect

Considering the shored method of construction, the splices in the girder specimen were located over temporary supports. The CIP deck was poured after the splices were cast and gained sufficient strength. The dead weight of the deck concrete increased the reactions at the temporary supports, and induced negative bending at the splice sections, similar to the prototype bridge but with a smaller magnitude given the shorter segment lengths for the specimen. The PT was designed to balance the dead weight of the structure, including girder and deck weight, but it failed to completely compensate for the deflection. As expected, the specimen did not completely lift off the temporary supports after post-tensioning. Hence, removal of the temporary supports below the splices resulted in a slight change in the strain profile.

5.6.4 Post-Tensioning Effect

5.6.4.1 Effect of Post-Tensioning on Splices

Figure 5.31 presents the post-tensioning effect at each of the three splices in the specimen. Graph A shows the compression effect of the PT as the strands are tensioned. The dashed purple line shows the predicted compression strain based on the target prestress force and the transformed area of the cross-section, without consideration of the PT eccentricity.

Graph B represents the effect of the eccentricity (e) of the PT ducts from the center of the gravity of the transformed section (c_{gc}). The three ducts in the specimen were stressed one at a time. Because the middle duct had less lateral eccentricity at the anchorage zones, it was stressed first. Due to the equal distance maintained between the three ducts, the middle duct coincided with the theoretical center of the gravity of the PT steel (PT c_{gs}) at every section. Therefore, the effect of post-tensioning the first duct is positive curvature for Splice 1 and Splice 2, and negative curvature for Splice 3.

The top duct was stressed second, bringing the steel centroid for the two stressed ducts, above the c_{gc} of the composite section, such that negative curvature at all three splices is expected. Finally stressing the bottom duct brought the steel centroid for the three stressed ducts to the intended location and produced positive curvature at the splices.

Graph C shows the final strain profile at the three splices after post-tensioning, including both the compressive effect of the PT and the effect of the eccentricity. Splices 1 and 2 are stressed to almost the same level with more compression in the bottom flange to balance the effect of dead

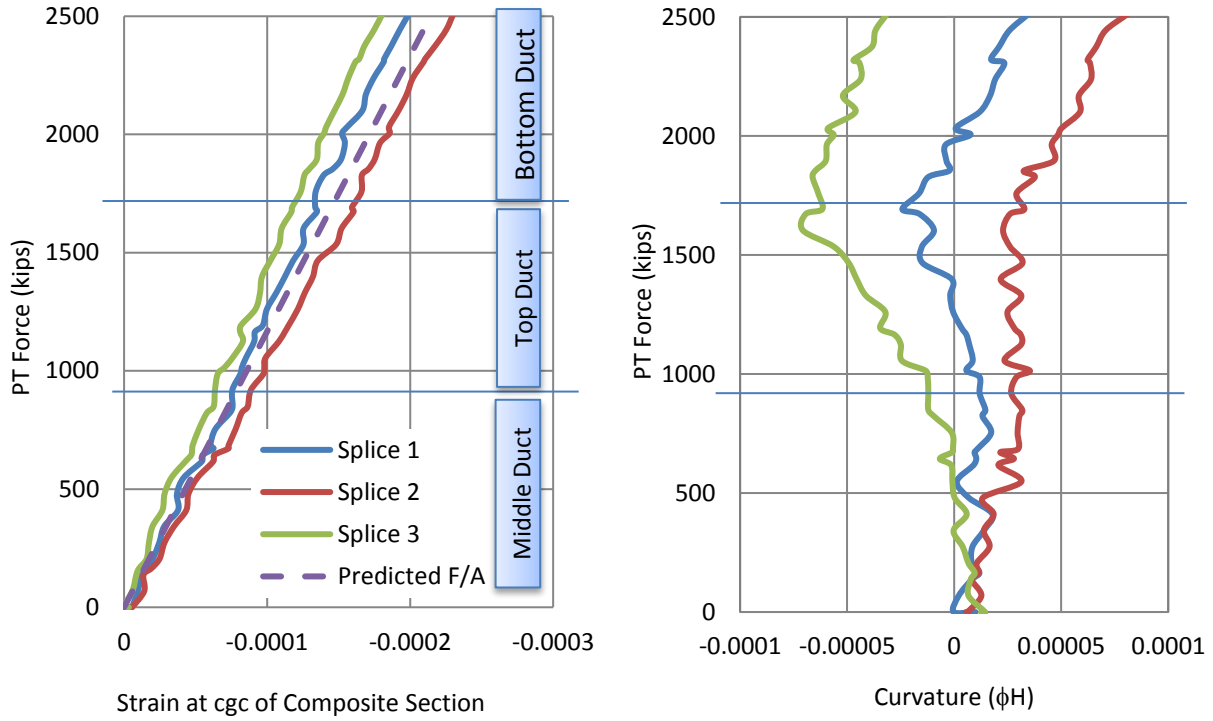
load after removing the temporary supports. For Splice 3, the overhang already lifted from its temporary support. Therefore, the PT balanced the dead weight, and a uniform state of compressive stress was produced in Splice 3.

5.6.4.2 Effect of Post-Tensioning on Anchorage Zones

A thorough analysis and design was carried out for the anchorage zones. Strut and tie modeling was used to analyze the bursting forces from the PT and the load transfer mechanism. Based on that analysis and also by considering the PTI guidelines (PTI 2001) for the anchorage zone design, mild steel was designed. To evaluate the strains and demands on the selected reinforcement in the anchorage zones, embedded concrete gages and rebar gages were installed in the end blocks to provide response data during testing. Figure 5.32 presents the strains in the anchorage zone during stressing of the PT tendons and summarizes the strain in each thickened end, for the vertical and longitudinal gages. Very small vertical strains occur in the anchorage zone due to stressing the PT tendons. Also, the recorded data suggest that gages at the anchorage end experienced higher strains in the longitudinal direction. Longitudinal strains in the jacking end were comparable to the average strain over the area of the thickened end (0.00013 strain), while longitudinal strains in anchorage end were five times higher than the average strain.

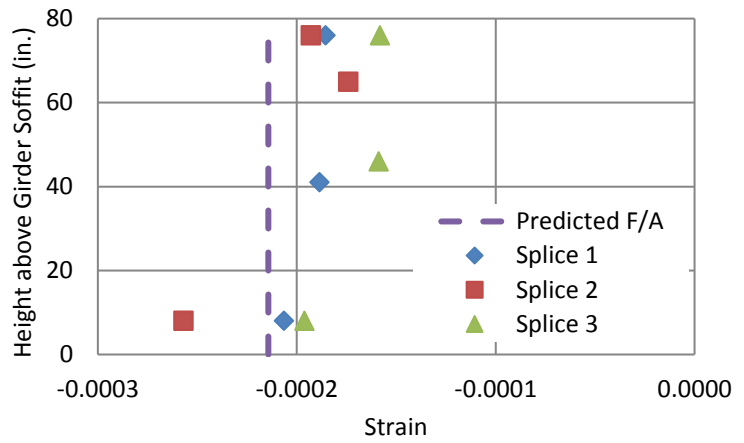
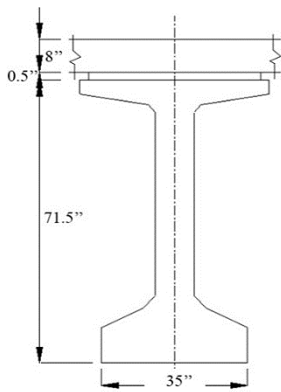
5.6.5 Summary of Strain Profile after PT

Figure 5.33 presents the history of the strain profile in the main splice (Splice 2) prior to the testing phase. The effect of each phenomenon is presented in the first row of Figure 5.33, and the accumulative effect considering the post-tensioning effect is reflected in the bottom row. The strain measurements from the embedded concrete gages match the prediction better than those from the surface gages. It can be noticed that the final strain is almost constant over the depth of the section, which suggests that the balanced design for the post-tensioning was successful.



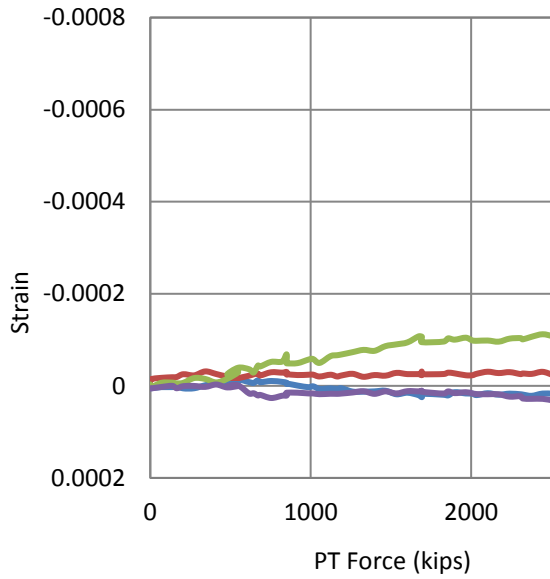
(a) Effect of Post-tensioning on Splices

(b) Dimensionless Curvature of Splices during Post-tensioning.

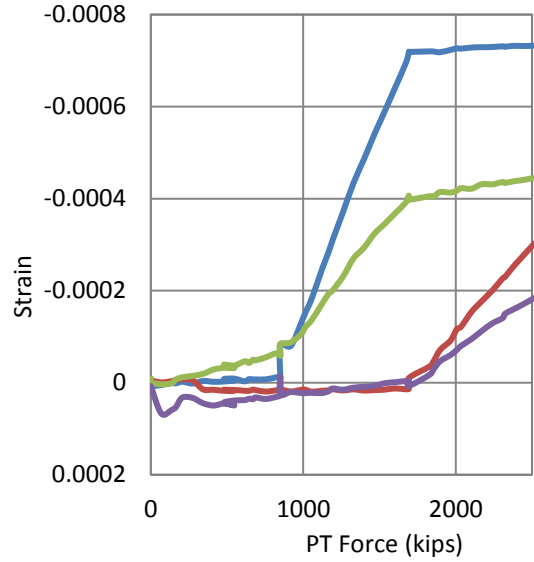


(c) Stress and Strain Profiles after Post-tensioning

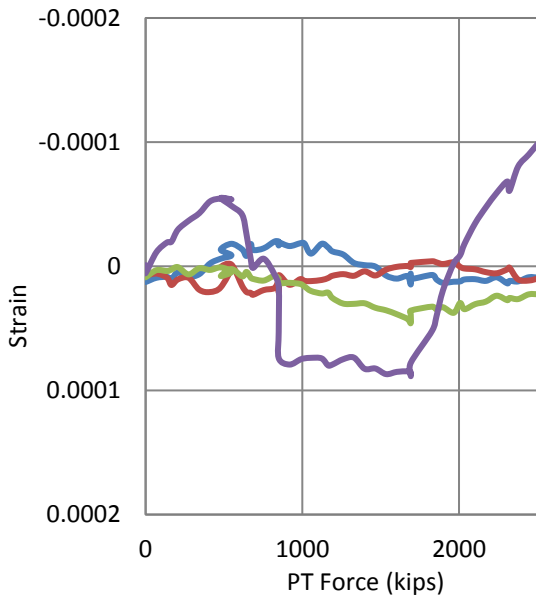
Figure 5.31. Post-tensioning Effect on Three Splices prior to Grouting.



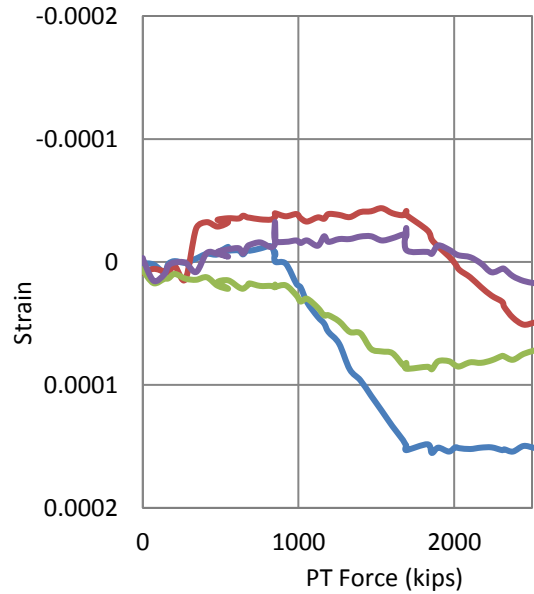
(a) Jacking End Block - Longitudinal Gages



(b) Anchorage End Block - Longitudinal Gages



(c) Jacking End Block - Vertical Gages



(d) Anchorage End Block - Vertical Gages

— At Anchorage Plate, Y=56 in. — At Anchorage Plate, Y=35 in. — At 21 ft, Y=55 in. — At 21 ft, Y=35 in.

Figure 5.32. Longitudinal and Vertical Strain in Anchorage Zone.

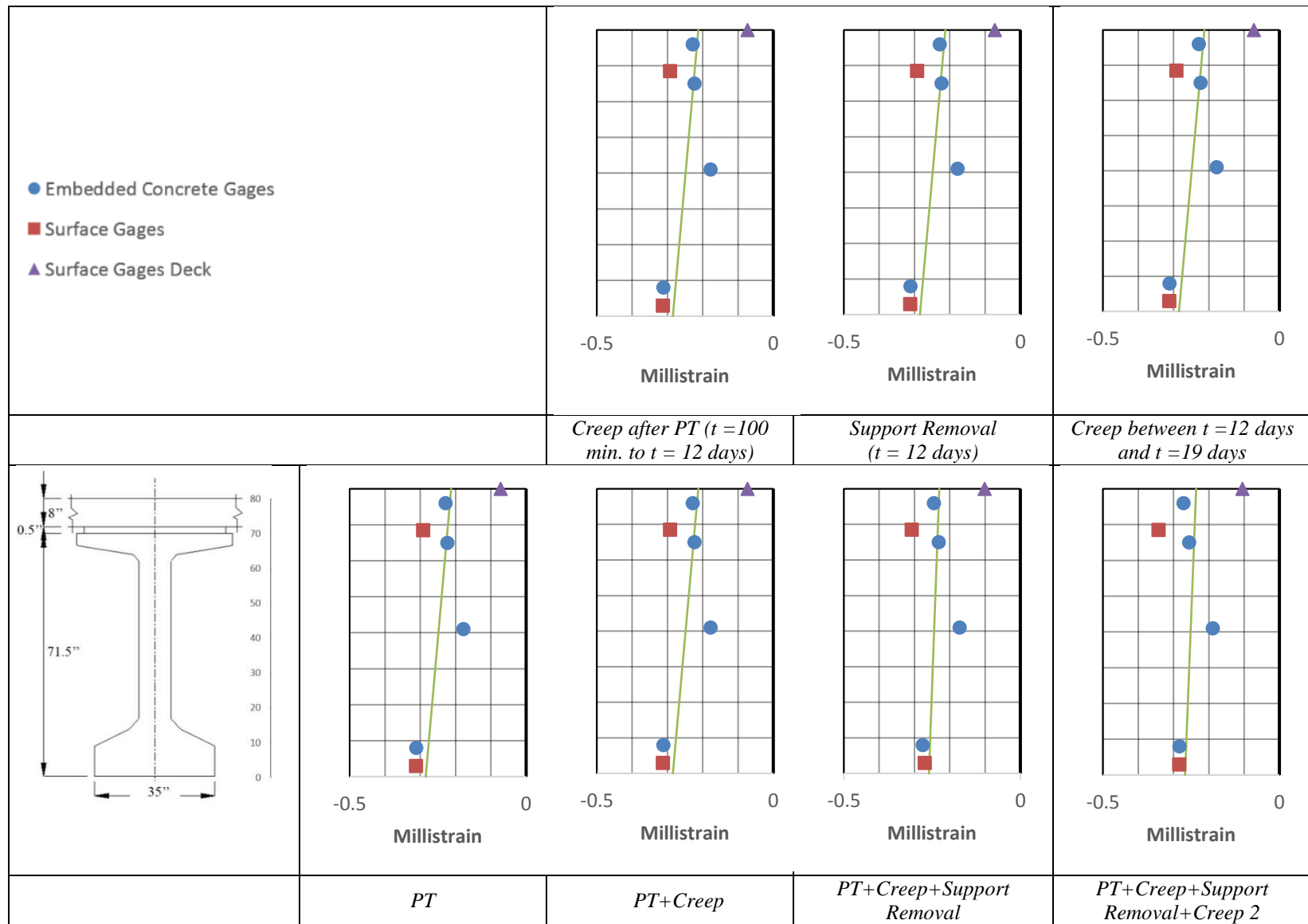


Figure 5.33. Pre-test Strain Profile History for Splice 2 (Top row shows the pure effect of each phenomena, and bottom row shows the accumulative strain profile).

5.7 PREDICTION OF SPECIMEN MOMENT-CURVATURE RESPONSE

A moment curvature analysis was conducted using a fiber element approach to capture the overall effect of the different contributions of pretensioning, post-tensioning, mild steel, girder concrete, and deck concrete. The method is based on dividing the section into horizontal fibers (layers parallel to the neutral axis for bending). For a given curvature, the analysis procedure finds the strain at the reference axis to produce force equilibrium in the section. Full non-linear stress-strain relations for concrete were adopted. In this study, the stress-strain relations for ordinary and high strength concrete developed by Karthik and Mander (2010) were used. The proposed model by Urmson and Mander (2011) was adopted to determine the behavior of the mild steel based on conducted stress-strain test results. The power equation proposed by Menegotto and Pinto (1973) was used to describe the stress-strain relationship for the prestressing strands. A modulus of elasticity of 28,500 ksi and an ultimate strength of 272 ksi was used in the model, based on the tension test results.

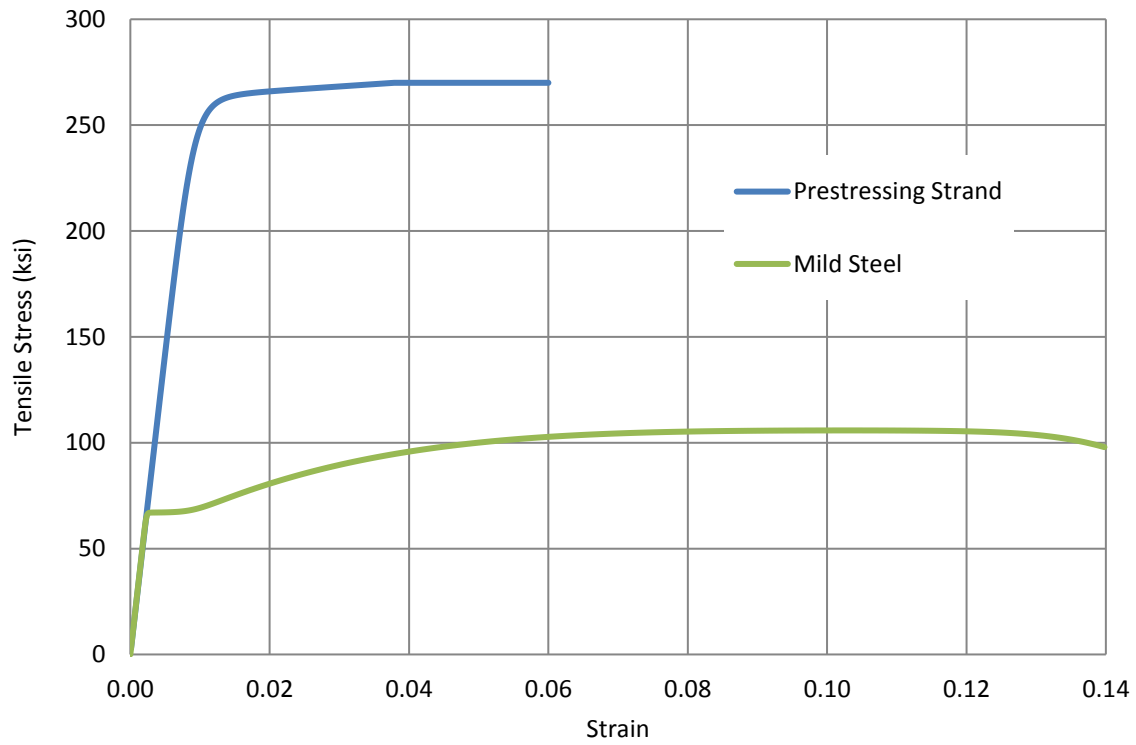
Moment-curvature is a function of material properties. To assure an appropriate estimate, the actual material properties related to the day of testing were used. Figure 5.34 shows the stress-strain behavior of the material, based on the actual test data and the abovementioned models. Table 5.13 and Table 5.14 summarize the material properties that were used for numerical modeling of the concrete and mild steel, respectively. Parameters used in Table 5.14 are defined as: f_y = yield stress, f_{su} = ultimate tensile stress, E_s = Young's modulus, E_{sh} = modulus at the onset of strain hardening, ε_{sh} = strain at the onset of strain-hardening, and ε_{su} = strain at ultimate tensile stress. Appendix A provides additional test data for characterizing the material properties for the girder specimen.

Table 5.13. Concrete Properties for Numerical Analysis.

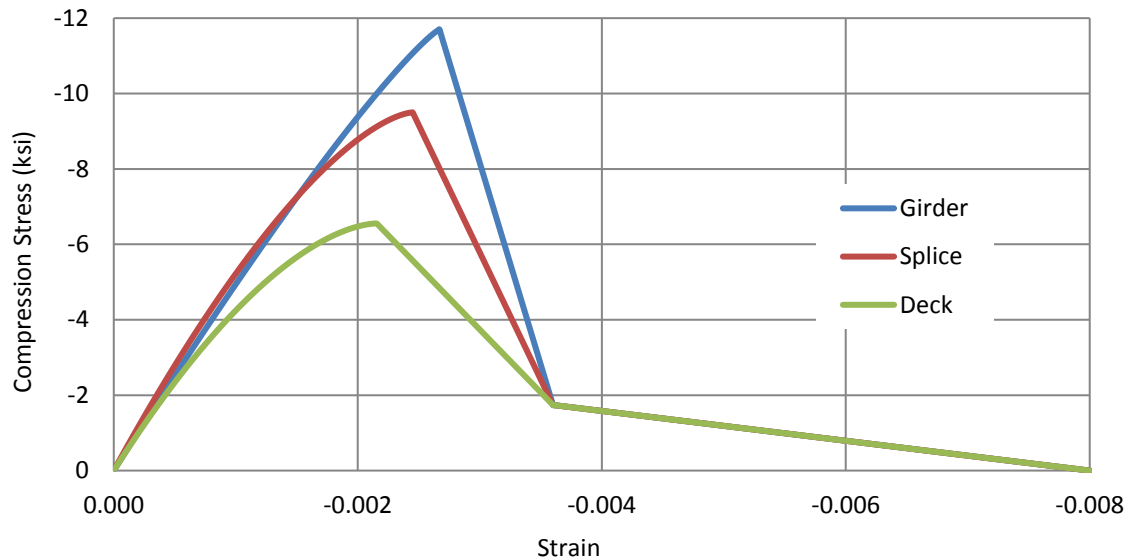
Part	Age of Concrete (days)	Parameter	At 28 Days (ksi)	At Age of Testing (ksi)
Girder Segments	222	f'_c	9.860	11.730
		f_r	1.084	1.170
		E_c	4742	5126
Splices	103	f'_c	8.790	9.500
		f_r	1.112	1.112
		E_c	5896	5895
Deck	95	f'_c	5.360	6.555
		f_r	0.685	0.500
		E_c	5089	5089

Table 5.14. Properties of Mild Steel.

f_y (ksi)	f_{su} (ksi)	E_s (ksi)	E_{sh} (ksi)	ϵ_{sh} (in./in.)	ϵ_{su} (in./in.)
67	106	29000	1440	0.0089	0.12



(a) Relationship Used for Mild Steel and Prestressing Strand Based on Urmson and Mander (2011) and Menegotto and Pinto (1973), respectively.



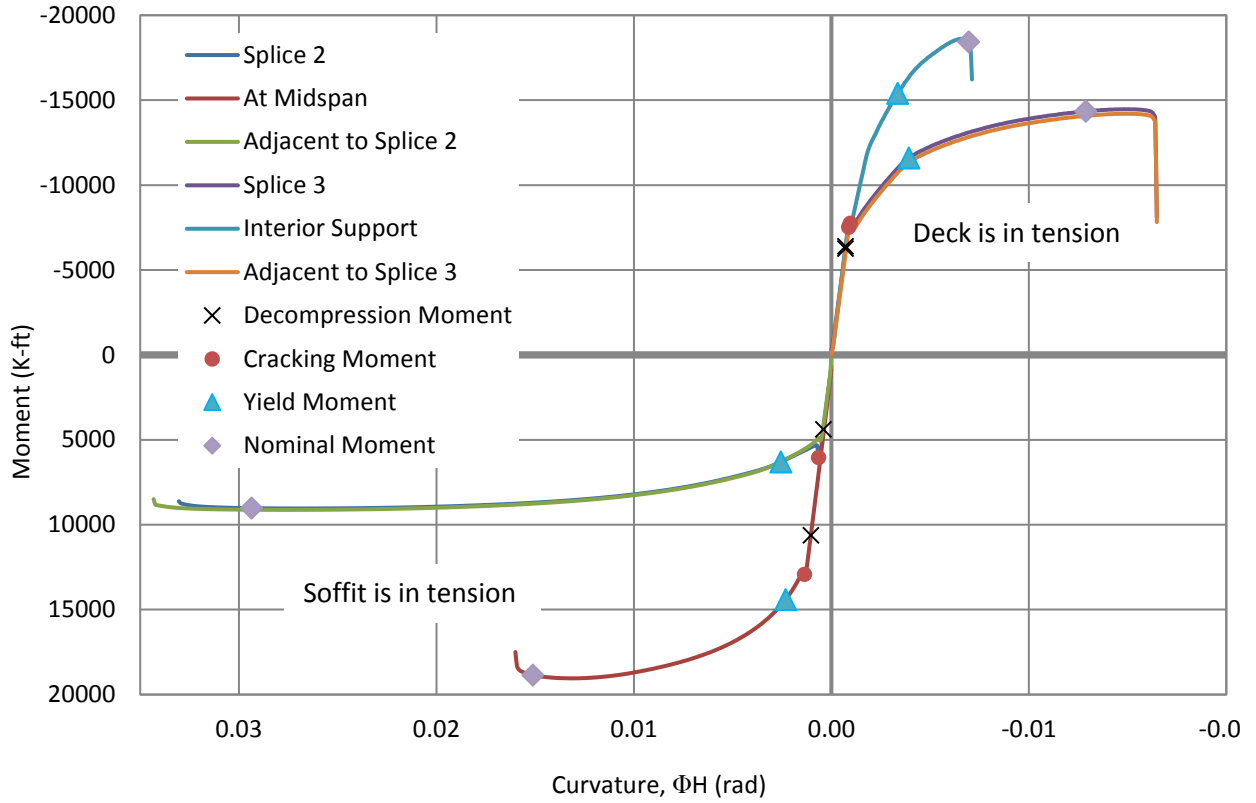
(b) Girder, Splice, and Deck Concrete Based on Model by Karthik and Mander (2010)

Figure 5.34. Relationships Used to Describe Material Stress versus Strain.

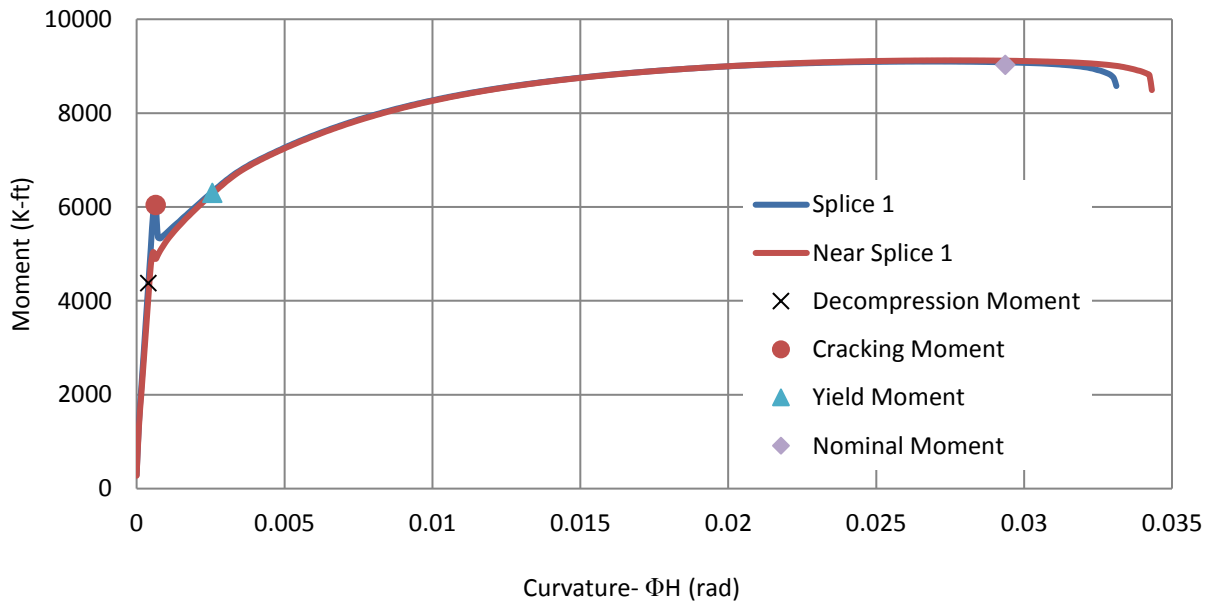
Figure 5.35 presents the moment-curvature analysis results. The analysis was conducted for the three splices and for the section over the interior support for both negative and positive moments. Decompression moment, cracking moment, yielding moment (in strands and in mild steel), and ultimate moment are marked, according to their definition, described below:

- Decompression Moment: For a prestressed section, decompression moment is defined as moment at which the bottom fiber (for positive moment) or top fiber (for negative moment) reaches zero strain.
- Cracking Moment: Defined for a concrete section, a moment at which the bottom fiber (for positive moment) or the top fiber (for negative moment) reaches the cracking stress for the concrete, f_r .
- Yielding moment: Defined for a reinforced concrete section, or a prestressed concrete section, the moment at which the bottom layer of steel (for positive moment) or the top layer of steel (for negative moment) reaches yield strain.
- Nominal Moment: For a concrete section, nominal moment is defined as moment at which the top fiber (for positive moment) or the bottom fiber (for negative moment) reaches a total compression strain of 0.003.

As shown in Figure 5.35, the section has a linear behavior until the moment reaches the cracking moment. As cracking initiates, some strain energy is released, which reduces the moment diagram slightly, but with increasing strain in the tension steel, the moment increases, until the tension steel yields (yield moment). After reaching the yield moment, the moment increases at a lower rate due to strain hardening, while the curvature increases rapidly. As the neutral axis rises in the section nearer to the extreme compression fiber, the stress and strain in the compression block increases. The section reaches its nominal moment capacity when the maximum total compression strain reaches 0.003, and shortly after that point, it fails and the capacity drops.



(a) Moment-Curvature: Interior Support, Splice 2 and 3, and Adjacent Girder



(b) Moment-Curvature: Splice 1 and Adjacent Girder

Figure 5.35. Moment-Curvature Comparison at Different Locations for Positive and Negative Moments.

6 EXPERIMENTAL RESULTS AND OBSERVATIONS

6.1 OVERVIEW

Experimental tests were conducted on each of the three splices within the girder specimen to investigate the performance of the splice connections under different combinations of flexure and shear at service and then up to ultimate strength conditions. The three splices were in part located to facilitate the specimen construction in the laboratory, but also to cover a range of possibilities that may exist in bridge design due to variable site configurations as follows:

- Splice 1: Near abutment region, representing moderate moment and high shear.
- Splice 2: The main splice for this research, located at the notational dead load inflection point for a continuous beam, where the positive moments under live plus impact loads (LL + I) remain quite high and the shear is moderate as well.
- Splice 3: Located near the interior support where the total negative moments are high (leading to tensile strains in the deck) coupled with high shear.

The experimental investigation was undertaken in the HBSMTL at Texas A&M University. This facility has a 72 ft long strong floor. Tie down holes are available on a 3 ft grid spacing, so the length of the specimen was limited to 71 ft. Two hydraulic actuators, each with a capacity of 600 kips, were used to load the specimen. The performance of the splices was investigated under service-level loads up to ultimate strength demands or the maximum actuator force, whichever controlled. This section compares the experimentally observed behavior with moment-curvature and force-deformation modeled performance.

6.2 EXPERIMENTAL SETUP AND GENERAL OBSERVATIONS

6.2.1 Testing Approach

The main purpose of the experimental program was performance evaluation of the proposed splice details for different combinations of shear and moment, such as moderate shear and high positive moment, high shear and high negative moment, and high shear and moderate positive moment. Different options were considered for specimen design and test setup. The final chosen setup was primarily based on weight lifting limitations for the girder segments. In this setup, the specimen was composed of three splices, two interior segments and two end blocks, each connected by a

CIP splice, and a CIP deck over the full length of the specimen. Figure 6.1 shows the labels for the different parts of the specimen, which can be summarized as:

- Splices are numbered from left to right as Splice 1, Splice 2, and Splice 3.
- Girder Segments are numbered from left to right as End Block 1, Segment 1, Segment 2, and End Block 2.
- Supports are labeled from left to right as Abutment Support and Interior Support.

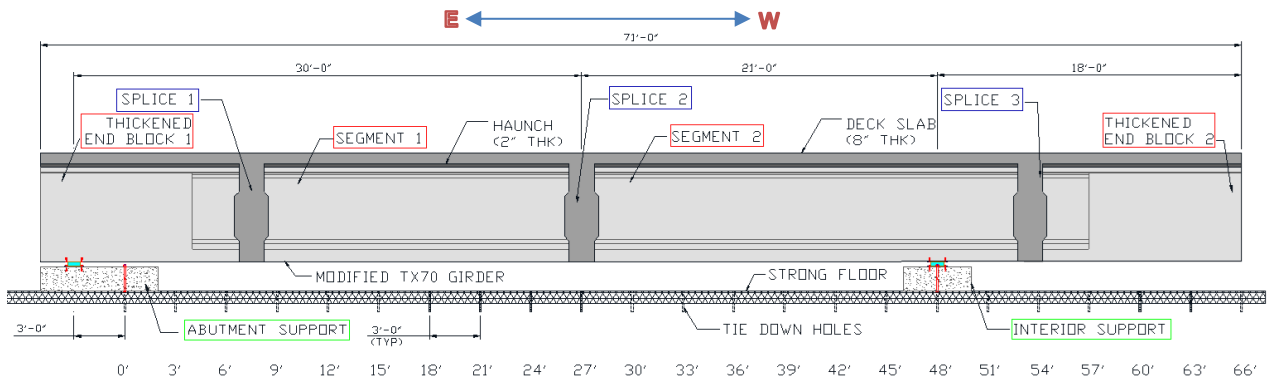


Figure 6.1. Side Elevation of the Specimen and Labeling.

Five stages of testing were adopted for the experimental investigation. Because service conditions are of high importance to the operational and owning agency, TxDOT, the first two tests investigated the service limits for positive and negative moments and their associated shear demands within the splices, as well as general service behavior throughout the specimen. The other three tests were focused on the performance at each splice, from the onset of the cracking moment through to the ultimate strength.

Data analysis was carried out on the data recorded by the data acquisition system. To remove excessive signal noise, some moving average smoothing was necessary along with appropriate zero corrections. The experimental results were then compared with predictive numerical models.

The following subsections describe the experimental setups for the different test phases, experimental observations, and data analysis outcome for each test:

- Test 1 assesses the performance of Splice 2 for shear and positive moment at service limits.
- Test 2 covers Splice 3 for shear and negative moment at service limits.
- Test 3 assesses the post-crack performance of Splice 2.
- Test 4 investigates Splice 3 under negative moment and shear up to ultimate.
- Test 5 assesses the service limits to yielding moment at Splice 1.

6.2.2 Test 1 – Splice 2 up to Service Loads

Figure 6.2 presents the actuator positions and an overall view of the experimental setup for Test 1. As shown in Figure 6.2(a), two actuators were placed adjacent to Splice 2 to create high shear and high positive bending moment leading to deck compression and high tensile strains at the soffit within the splice region. To simulate a 4 ft tandem axle spacing in accordance with design axle loads used in AASHTO LRFD Specifications (AASHTO 2012), a spreader beam was used to decrease the 6 ft distance of the actuators to 4 ft, as depicted in Figure 6.2(b).

Loads were applied incrementally in load control at the rate of 1 kip/s for each of the two actuators, as summarized in Table 6.1. At each of the target loads in Table 6.1 the specimen was thoroughly checked for new cracks and to determine whether pre-existing cracks propagated or widened.

Table 6.1. Table of Events at Splice 2 for Test 1.

Case	Parameter	Target Value	Actuator Load, P (kips)
1a	At Service for Shear	125 kips	$P = 125$
1b	At Decompression Moment	3650 kip-ft	$P = 174$
1c	At Service for Positive Moment	3990 kip-ft	$P = 190$

Figure 6.2(c) presents a photograph in the vicinity of Splice 2 at maximum service load for Test 1, where $P=190$ kips. No cracks were observed at any stage during Test 1, indicating the design objective of no cracking under service load conditions was fulfilled.

Prior to unloading from $P=190$ kips, DEMEC readings were also taken. Little could be gleaned from these measurements as displacement changes were within the noise limits of the DEMEC gages.

6.2.3 Test 2 – Splice 3 up to Service Loads

Figure 6.3 presents the actuator and overall experimental setup for investigating negative service moment performance of Splices 2 and 3. A single actuator force was applied near the cantilever end of the specimen as shown in Figure 6.3(a). To ensure uplift at the abutment support was avoided, a second actuator was provided close to that support. The two actuators were hydraulically connected in series to ensure the same load was applied at both locations. Spreader beams were used to divide the applied loads as shown in Figure 6.3(b).

Loads were applied at the rate of 1 kip/s with pauses for inspection at the limits indicated in Table 6.2. The main aim for Test 2 was to impose likely service loads that led to negative moments for Splice 2 and Splice 3. Figure 6.3 presents several photographs during Test 2.

Table 6.2. Table of Events for Test 2.

Case	Parameter	Test Location	Target Value	Actuator Load, P (kips)
2a	At Service for Shear	Splice 3 (N)	125 kips	$P = 125$
2b.1	Decompression Limit	Support	-4231 kip-ft	$P = 255$
2b.2	At Service for Moment	Splice 3 (N)	-2872 kip-ft	$P = 280$
2c	At Service for Shear	Splice 2 (M)	125 kips	$P = 305$
2d.1	At Service for Moment	Splice 2 (M)	-2872 kip-ft	$P = 365$
2d.2	At Cracking Moment	Support	-6900 kip-ft	$P = 370$

No service load cracks were observed up to and including $P=365$ kips, the load that induced the maximum design negative moment at Splice 2. At $P=370$ kips, a single crack with a width of 0.004 in. was observed in the deck slab above the support. Loading was continued to $P=400$ kips and some further cracks developed in the deck slab. The deck cracks spread about 5 ft on both sides of the interior support as shown in Figure 6.3(d). It should be noted that the girder remained in an uncracked condition.

6.2.4 Test 3 – Splice 2 Post-Cracking Performance

The main aim of Test 3 was to investigate the post-service load performance beyond the uncracked regime through to flexural failure. Test 3 returned to the same setup as Test 1, and loads were applied at 1 kip/s. The loads were paused at the limits shown in Table 6.3 to take photographs and to mark and measure new cracks as they evolved.

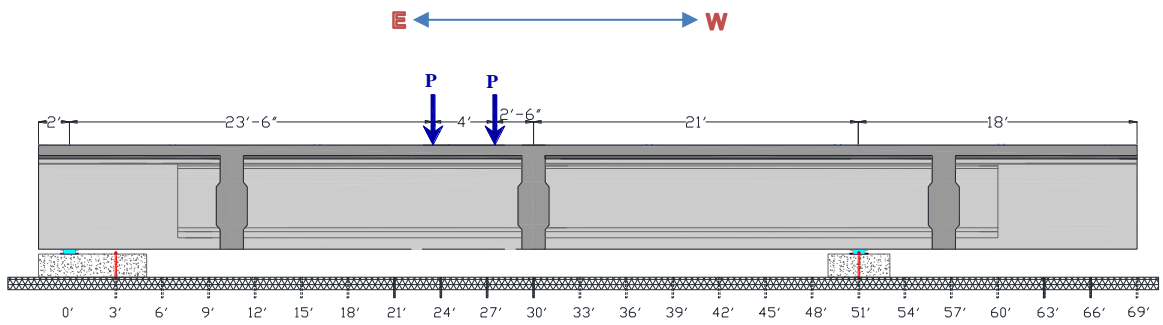
Table 6.3. Table of Events at Splice 2 for Test 3.

Case	Parameter	Target Value	Actuator Load, P (kips)
3a	At Cracking Moment	5145 kip-ft	$P = 225$
3b	At Yield Moment	6760 kip-ft	$P = 300$
3c	At Ultimate Positive Moment	8860 kip-ft	$P = 410$

Figure 6.4 shows the visual condition of Splice 2 at specific benchmarks. Cracks that were 0.002 in. wide first appeared in the bottom flange of Splice 2 at $P=225$ kips. These cracks propagated up from the flange into the web. When the loads had reached $P=270$ kips, a crack width of 0.004 in. was measured at the bottom flange. At $P=280$ kips, bearing cracks appeared right below the shear key.

As shown in Figure 6.4(d), when the loads reached 334 kips per actuator, the cracks in the bottom flange grew wider to 0.44 in. The main crack extended to the interface of Splice 2 and the adjacent girder, which led to a shear slip of 0.25 in. as shown in Figure 6.4(c). Due to a smaller moment capacity that existed at the CIP splice compared to the adjacent precast girder, most of the cracks appeared in the splice region. As shown in Figure 6.4(b), (c), and (d), a very large flexural crack appeared when the load exceeded $P=334$ kips. Nearby this large crack, additional flexural cracks and several diagonal shear cracks formed. Cracks concentrated mostly in the splice area.

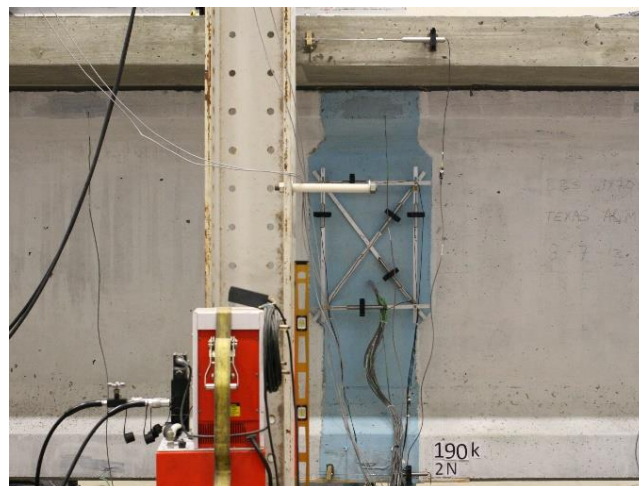
Figure 6.5 depicts the condition of the specimen during Test 3. When the load exceeded $P=400$ kips, a marked increase in crack width and height resulted in the neutral axis moving up toward the deck slab region. The resulting high stresses in the compression zone led to a sudden compression failure. The failure zone occurred close to Splice 2 in the deck, nearby the applied load point. The failure led to buckling of longitudinal reinforcement in the deck as shown in Figure 6.5(c) and (e). At this point, the measured shear slip between the splice and the adjacent girder was 0.7 in., as shown in Figure 6.5(d).



(a) Setup for Test 1 and Test 3

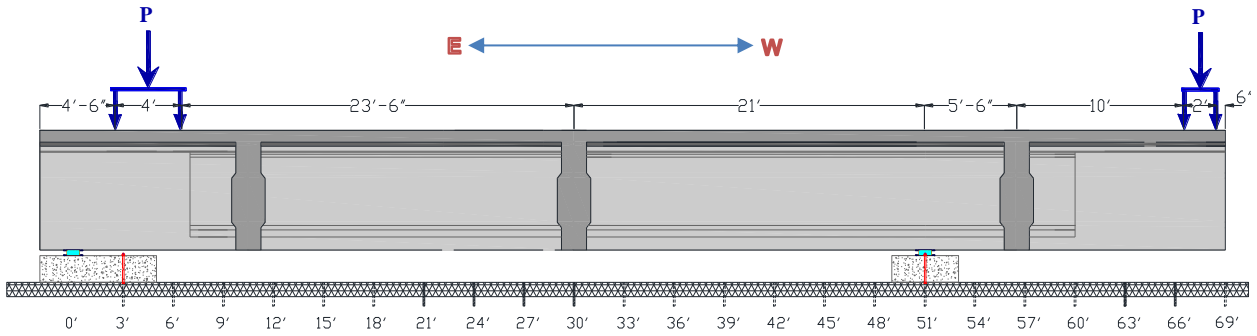


(b) Loading Setup



(c) At Service for Positive Moment ($P = 190$ kips)

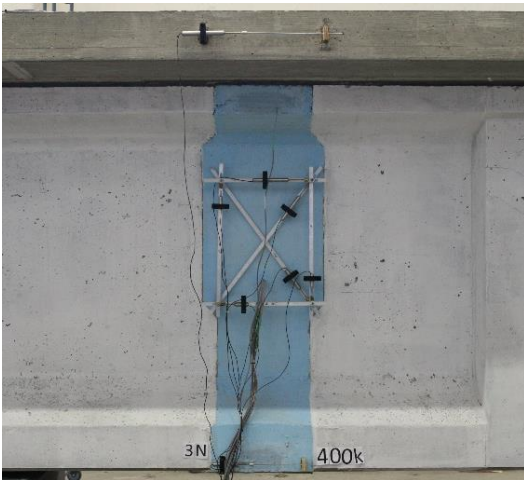
Figure 6.2. Specimen Setup and Visual Condition during Test 1.



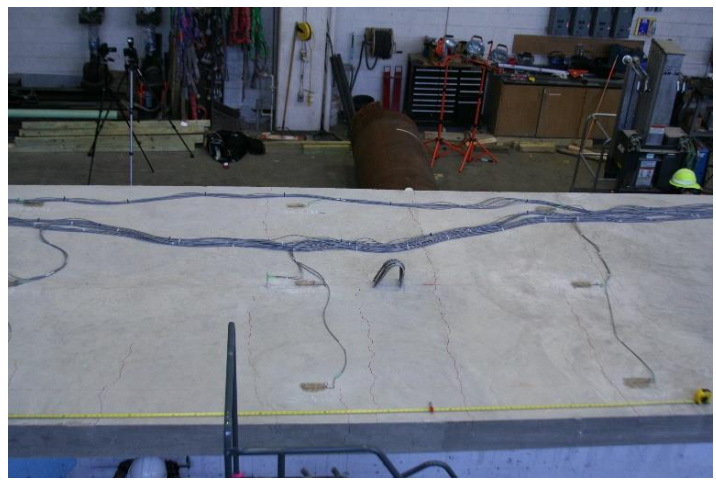
(a) Test Setup



(b) Actuator Setup

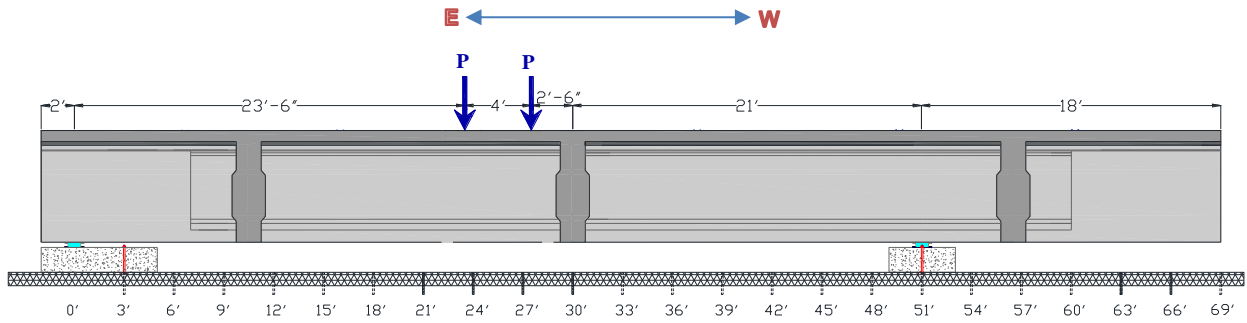


(c) After Cracking Moment
($P = 400$ kips)



(d) Cracks on Top of Deck ($P = 400$ kips)

Figure 6.3. Specimen Setup and Visual Condition during Test 2.



(a) Test Setup



(b) Splitting Crack at Interface of Splice 2
(Crack Width = 0.004 in.)



(c) Splice 2 - South View, Shear Slip after the
Crack Widened ($P = 334$ kips)

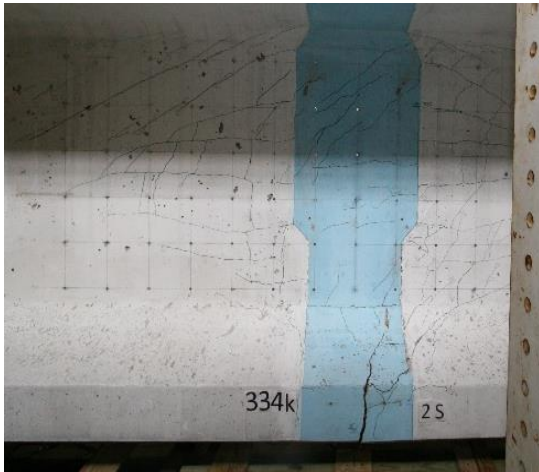


(d) Splice 2 - Shear Deformation due to
Interface Slip ($P = 400$ kips)



(e) Splice 2 - South View, Widened Crack at
Failure ($P = 400$ kips)

Figure 6.4. Test Setup and Visual Condition of Splice 2 during Test 3.



(a) Splice 2 - South View ($P = 334$ kips)



(b) Splice 2 - North View, Crack in the Center of Splice



(d) Splice 2 - Failure at $P = 400$ kips



(c) Compression Failure at $P = 400$ kips



(e) Buckling of Longitudinal Bars in Deck

Figure 6.5. Visual Condition of Specimen during Test 3.

6.2.5 Test 4 – Splice 3 Post-Cracking Performance

The main aim of Test 4 was to examine the nonlinear post-cracking negative moment performance of Splice 3 through to flexural failure. Due to previous damage that occurred at Splice 2 during Test 3, a tie-down system was provided as shown in the Test 4 setup in Figure 6.6(a). To measure the transferred load to the tie down bars, a load cell was placed between the deck and the tie-down beam across the top of the specimen.

Table 6.4 lists the pre-test computed events that were adopted as pause points during loading to investigate the general condition of the specimen and in particular Splice 3.

Table 6.4. Table of Events for Test 4.

Case	Parameter	Test Location	Target Value	Actuator Load, P (kips)
4a	At Decompression Moment	Interior Support	-4231 kip-ft	$P = 155$
4b	At Shear Cracking Load	Splice 3 (N)	460 kips	$P = 230$
4c	At Cracking Moment	Interior Support	-7008 kip-ft	$P = 240$
4d	At Ultimate Moment	Splice 3 (N)	-5150 kip-ft	$P = 320$
4e	At Cracking Moment	Splice 3 (N)	-7008 kip-ft	$P = 370$
4f	At Yield Moment	Interior Support	-14,774 kip-ft	$P = 500$
4g	At Maximum Loading	Interior Support	-16,177 kip-ft	$P = 600$

As in previous cases, loading continued at a rate of 1 kip/s for each of the two actuators. Loading was first paused at $P=155$ kips when the decompression moment was expected; no cracks were observed over the interior support.

At $P=240$ kips, the specimen returned to the cracking moment at the interior support and the previous cracks from Test 2 reopened once again. Crack widths were measured in the range of 0.002 to 0.004 in. By increasing the load up to $P=290$ kips, new cracks appeared in the deck that also ranged from 0.002 to 0.004 in. in width.

At $P=350$ kips, cracks of width 0.004 in. occurred in the top flange above the Splice 3. When loads increased to $P=360$ kips, diagonal shear cracks, 30° from the horizontal, emerged in the web of Splice 3. When reaching $P=400$ kips, the splitting cracks at the interface of Splice 3 and the adjacent precast girder grew to 0.022 in. At $P=435$ kips, based on gage monitoring,

transverse bars in Splice 3 yielded. A sudden horizontal compression crack appeared in the bottom flange of the girder, between the interior supports and Splice 3.

At $P=450$ kips, the horizontal crack extended and led to a sudden compression failure, as shown in Figure 6.6(e). Loading was stopped and cracks were measured over the deck and in Splice 3. Over the deck, cracks of width 0.002 to 0.006 in. spread at approximately 6 in. on average up to 90 in. from the point of loading. Beyond that location, cracks were spaced at 12 in. for an additional 12 ft.

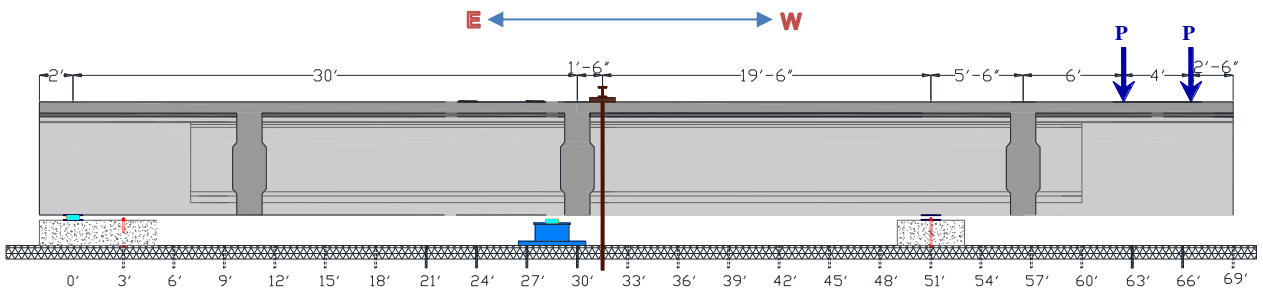
6.2.6 Test 5 – Splice 1

Test 5 investigated the performance of Splice 1 up to the lesser of the shear capacity of Splice 1 and the load capacity of the experimental system where $P=600$ kips per actuator. To avoid further damage to Splice 2 and to ensure that loading could attain higher limits, a temporary support beneath the beam soffit adjacent to Splice 2 was provided as shown in Figure 6.7. Having three supports made the structure indeterminate. Because the precise section properties of the damaged section were not available, the analysis of the indeterminate structure was not feasible. To provide a better understanding of the specimen behavior, the specimen was loaded in two stages:

- 1) Loading up to $P=200$ kips without the temporary support (determinate structure) and then unloading to zero.
- 2) Placing the temporary support and bearing pad with a small clearance of $5/8$ in. and reloading.

Before Stage 2 loading, the temporary support (the central blue support shown in Figure 6.7[a]) was placed at 28 ft from the abutment support and a bearing pad placed over it. The distance between the bearing pad and the soffit of the girder was adjusted to 0.625 in.

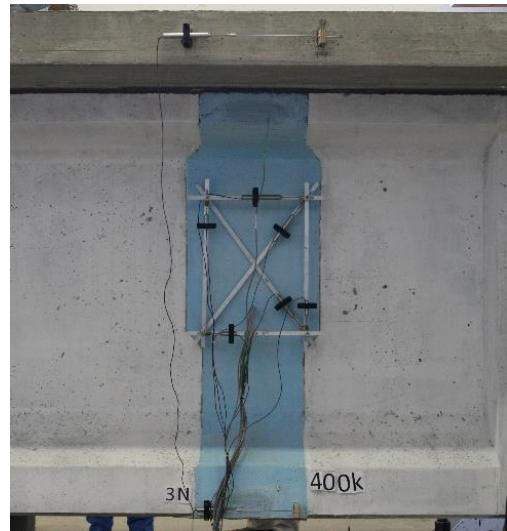
Table 6.5 presents the sequence of the events during Test 5. In this test, due to the short span of the girder, Splice 1 experienced a combination of high shear and relatively low moment. Loads were initially applied to the full span length of the specimen. At $P=215$ kips, the girder soffit met the bearing pad at the temporary support; at higher loads, the specimen became an indeterminate continuous beam. When reaching $P=200$ kips, cracks in Splice 2 started to re-open and loose concrete cover fell out of the splice connection.



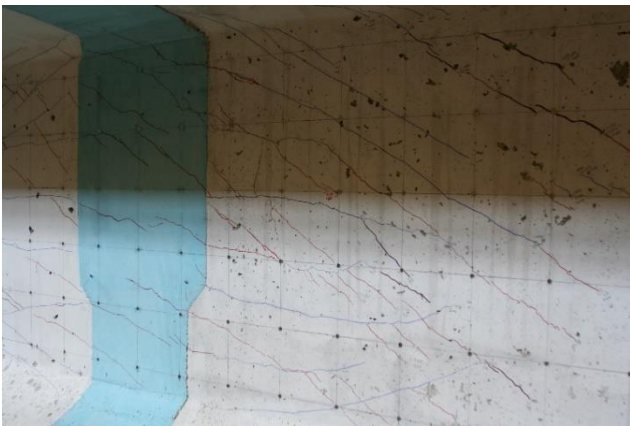
(a) Test Setup



(b) Tie Down and Load Cell Detail



(c) North View ($P = 400$ kips)



(d) South View ($P = 400$ kips)



(e) Compression Failure ($P = 450$ kips)

Figure 6.6. Specimen Setup and Visual Condition during Test 4.

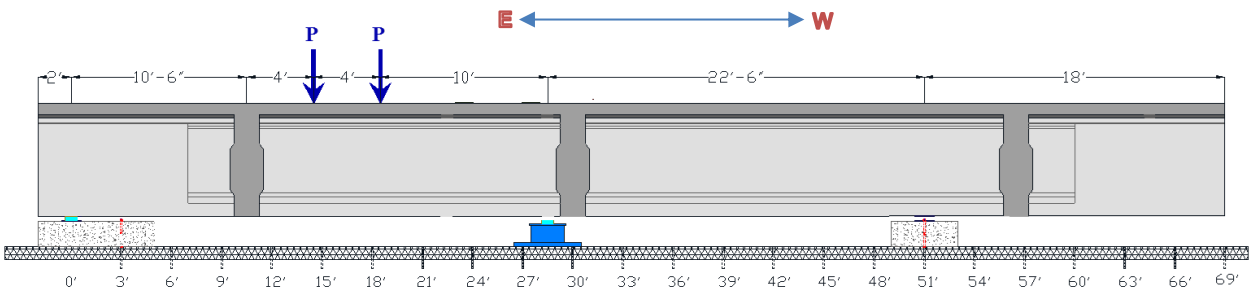
Table 6.5. Table of Events at Splice 1 for Test 5.

Case	Parameters	Target Value	Actuator Load, P (kips)
5a	At Service for Shear	125 kips	$P = 150$
5b	Decompression Moment	3650 kip-ft	$P = 290$
5c	At Service for Positive Moment	3990 kip-ft	$P = 325$
5d	At Ultimate Design Shear	450 kips	$P = 405$
5e	At Cracking Shear	460 kips	$P = 415$
5f	Cracking Moment	5160 kip-ft	$P = 465$
5g	Maximum Loading	6350 kip-ft	$P = 600$

- Prior to reaching the decompression load of $P=290$ kips, no new cracks were observed in Splice 1. At $P=400$ kips, diagonal cracks emerged in the web of Splice 1, aligned toward the loading point and the abutment support. The cracks extended and widened as the load increased to 405 kips (corresponding to the ultimate design shear V_u in the splice for the prototype bridge).
- At $P=430$ kips, the lower level of longitudinal reinforcement yielded and a sudden vertical crack appeared at the center of Splice 1 in the bottom flange. As the loading increased to $P=450$ kips, shear cracks emerged within the web of the girder adjacent to Splice 1 as shown in Figure 6.7(b). Cracks continued to grow and proliferate as shown in Figure 6.7(c) for $P=565$ kips where crack widths were measured in the range of 0.002 to 0.004 in.
- At $P=600$ kips, the actuators reached their maximum capacity and loading was held for specimen assessment. A significant vertical crack developed at the center of the splice as shown in Figure 6.7(d). This crack extended 20 in. up from the soffit and opened to 0.25 in.

When the actuators were unloaded, the specimen was thoroughly inspected and the condition was documented. Many of the flexural cracks that had opened to large widths during loading closed when the load was removed (see Figure 6.7[e]). To provide a visual understanding

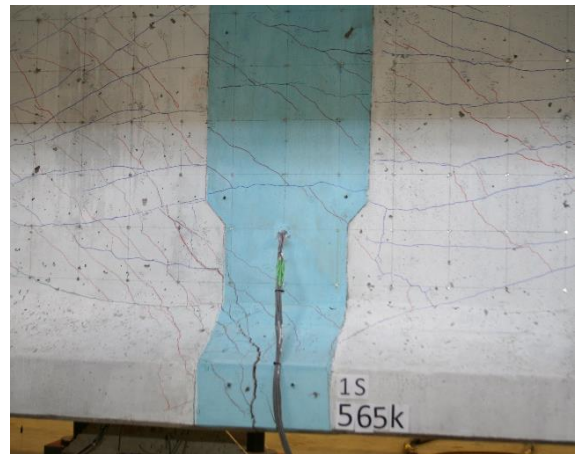
of the behavior of the specimen, the cracks were marked on the girder at specific loads, along with the crack width. Figure 6.8 shows the crack pattern for each of the three splices.



(a) Test Setup



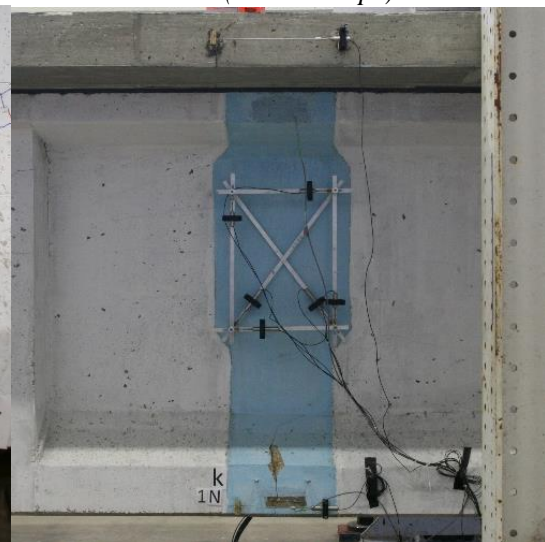
(a) Flexural Crack in Splice 1 ($P = 450$ kips)



(b) Growth of Flexural and Shear Cracks ($P = 565$ kips)

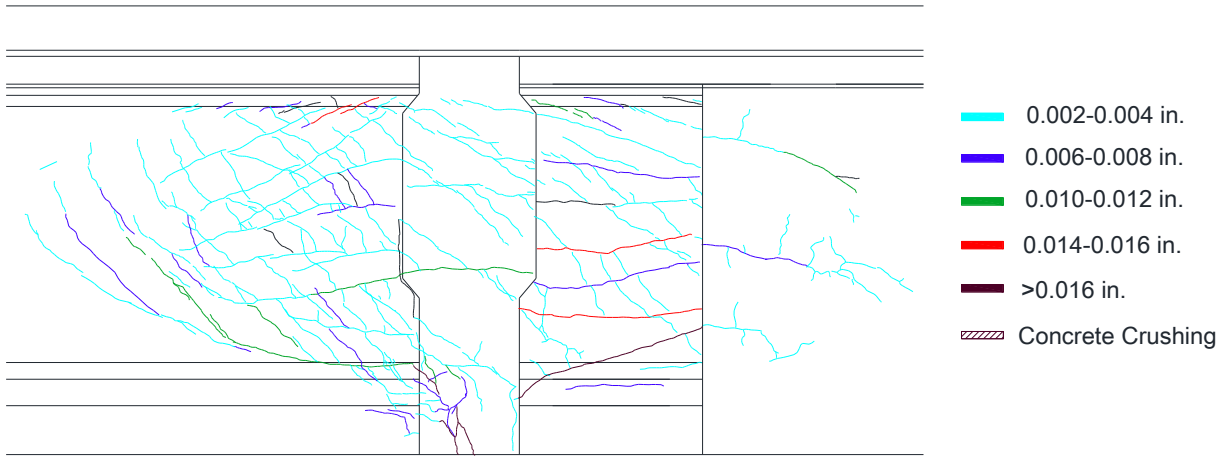


(c) At Maximum Load ($P = 600$ kips)

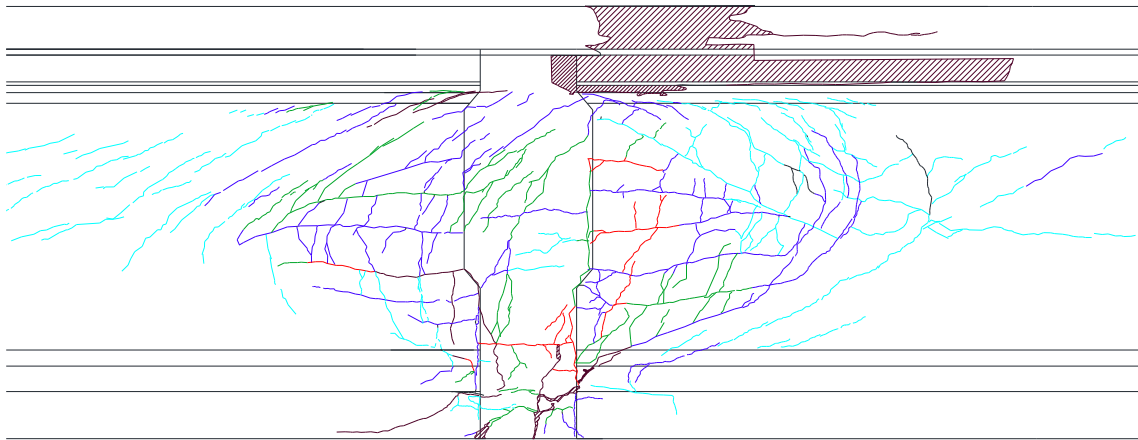


(d) Closed Cracks after Unloading

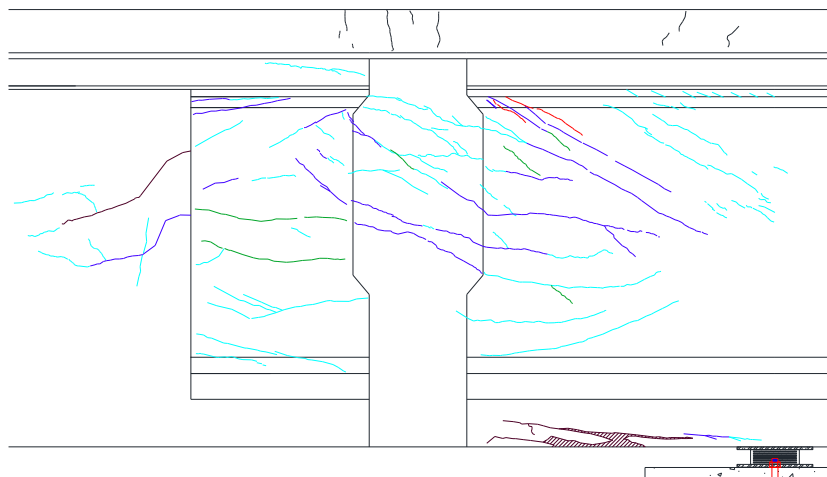
Figure 6.7. Specimen Setup and Visual Condition during Test 5.



(a) Splice 1



(b) Splice 2



(c) Splice 3

Figure 6.8. Crack Pattern.

6.3 DETAILED BEHAVIOR AND ANALYSIS

Data recorded during the post-tensioning process together with the data recorded during each of the five tests were used to evaluate the overall performance of the test specimen. Several graphs and tables are presented in this section to provide insight on splice zone performance under different combinations of positive and negative moments, along with varying levels of shear intensity. The overall performance of the specimen is evaluated with force-deformation analysis and beam longitudinal deformation profiles. Moment-curvature analysis, strain profile comparison, and force-strain analysis were used to study the performance of the splices in more detail.

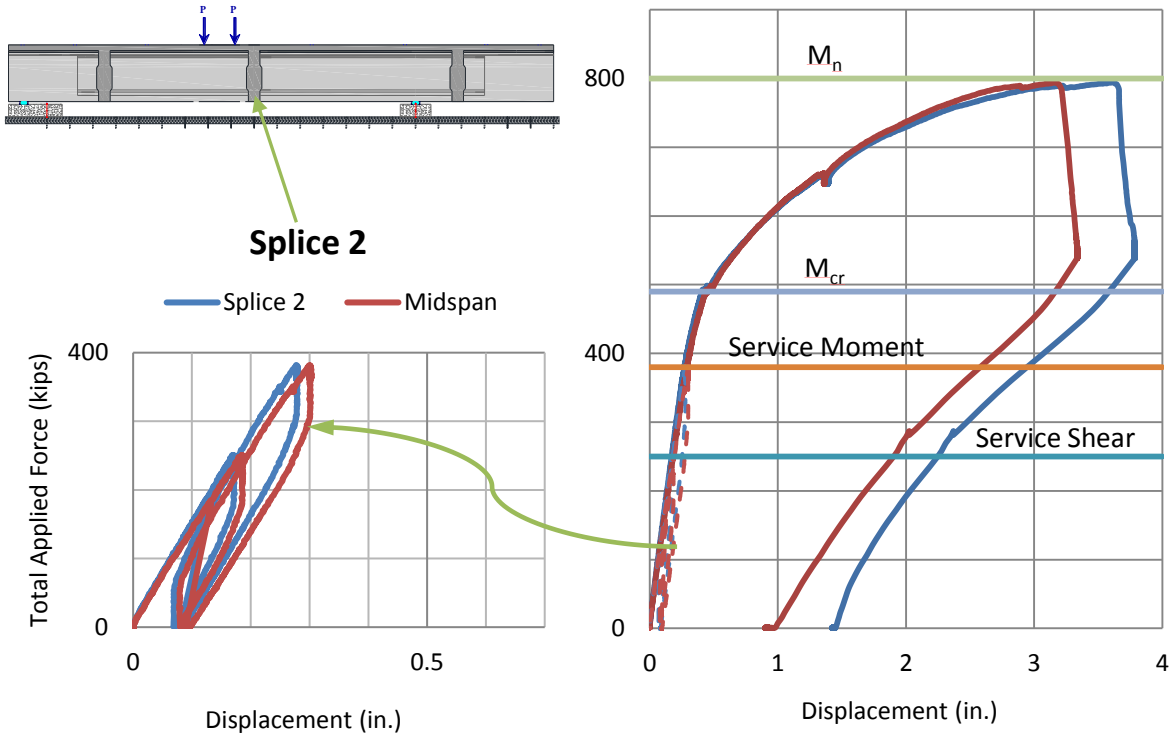
6.3.1 Force and Deformation Behavior and Analysis

Figure 6.9 shows the force-deformation diagrams for different stages of testing Splices 2 and 3. For Tests 1 and 3 on Splice 2, the total applied force from the two actuators is plotted against the displacements; whereas, for Tests 2 and 4, the vertical axis provides the total force applied to the overhang. Figure 6.9(a) and 6.9(c) present the service level performance.

The deformation generally varies linearly with loading up to the cracking moments. On reaching the cracking moment capacity, a momentary drop in force occurred as the first flexural cracks developed. Following cracking, cracked-elastic behavior occurred as the loading increased to about 85 percent of the ultimate moment. At this level, nonlinear behavior of the strands and longitudinal reinforcement initiated a more marked drop-off in stiffness.

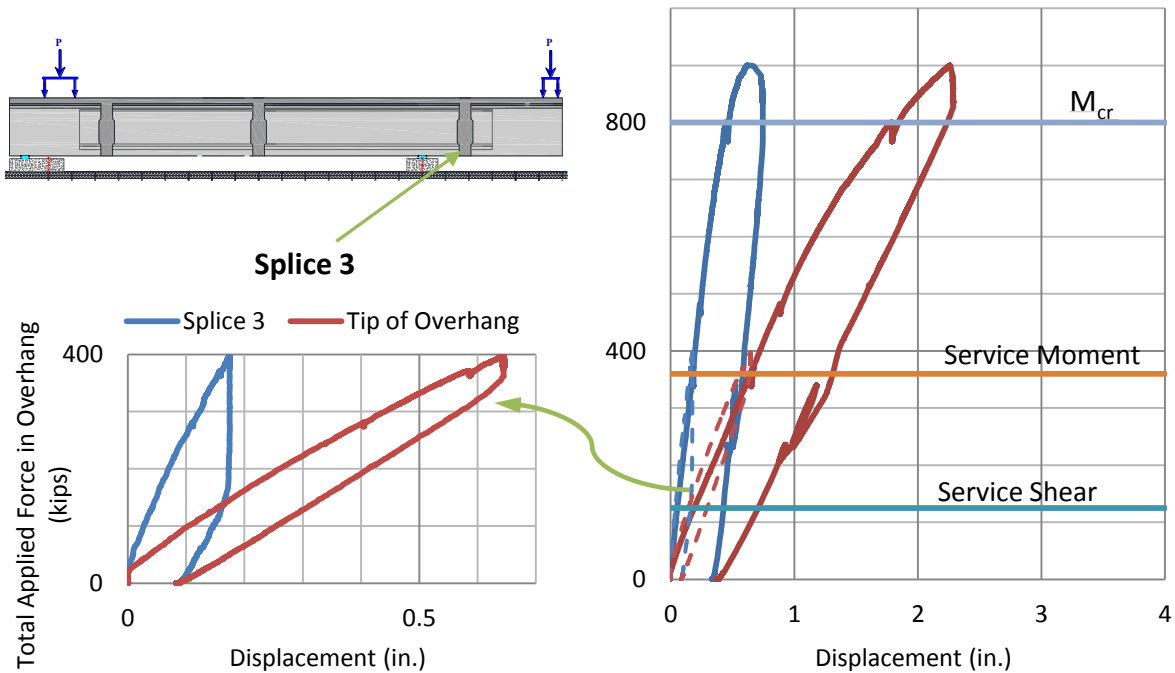
While the service load behavior appears to be somewhat nonlinear, this is attributable to the nonlinear behavior of the rubber bearing pads that were unscragged prior to loading. Thus hysteresis performance should not be interpreted as structural damage.

The splice was the weakest portion of the prestressed concrete beam due to discontinuity of the pretensioned prestress. Because the flexural capacity of the splice was about one-half of the adjacent girder, after the cracking moment was achieved, the damage concentrated in the splice region.



(a) Test 1: Service Load Performance

(b) Test 3: Ultimate Strength Performance



(c) Test 2: Service Load Performance

(d) Test 4: Ultimate Strength Performance

Figure 6.9. Force Deformation Diagram for Positive and Negative Moments.

6.3.2 Moment-Curvature

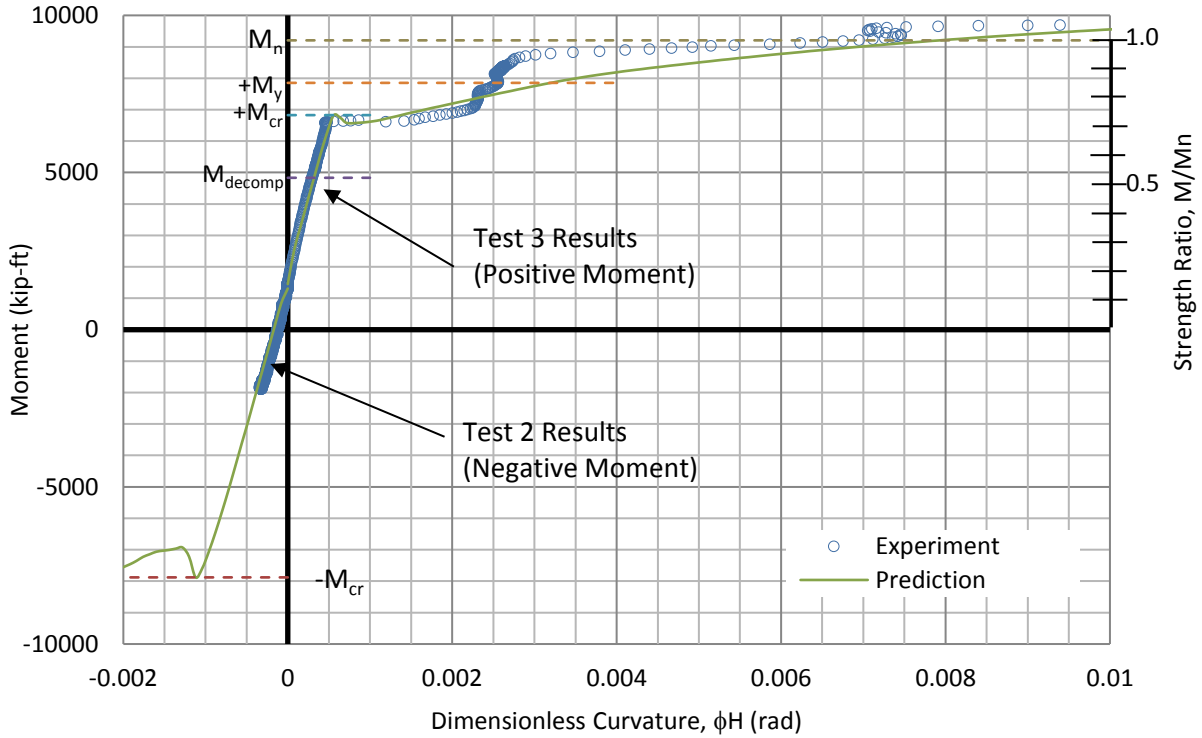
To predict the moment-curvature behavior at critical locations, a refined fiber element analysis was conducted. Material parameters were adopted from tests conducted on concrete samples on the date of testing and rebar tensile tests. Experimental data gathered from numerous gages in the splices and interior supports were used to infer the experimental behavior. Embedded concrete gages were considered as the best estimator of actual concrete strain during testing.

Both the numerical prediction and experimental data suggest that up to first cracking the moments varied linearly with curvature, therefore the cracked stiffness $EI_{uncracked}$ can be inferred. After the first flexural cracks appeared, the moment decreased slightly as the section stiffness decreased.

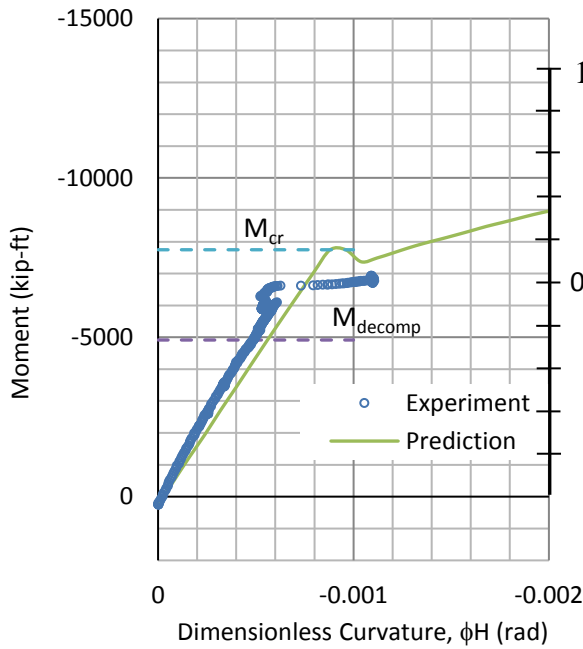
Figure 6.10 presents the moment-curvature diagram for the splices and interior support, for both positive and negative moment. Results from experiment are compared with the predicted behavior from numerical analysis. Results for Splice 2 show that even though the maximum moment capacity was predicted quite well for Test 3, the observed ductility was less than the prediction. As strains were measured at discrete points, it remains unknown whether those measured strains were at a crack or midway between cracks; such locations may provide upper and lower bounds of strain measurements, respectively.

Due to pretensioning, the moment capacity of the girder was somewhat greater than the splice. This greater girder flexural capacity is attributed to the presence of the pretensioned prestress primarily in the flanges of the girder; the pretensioned prestress was discontinuous through the splice somewhat weakening the splice zone.

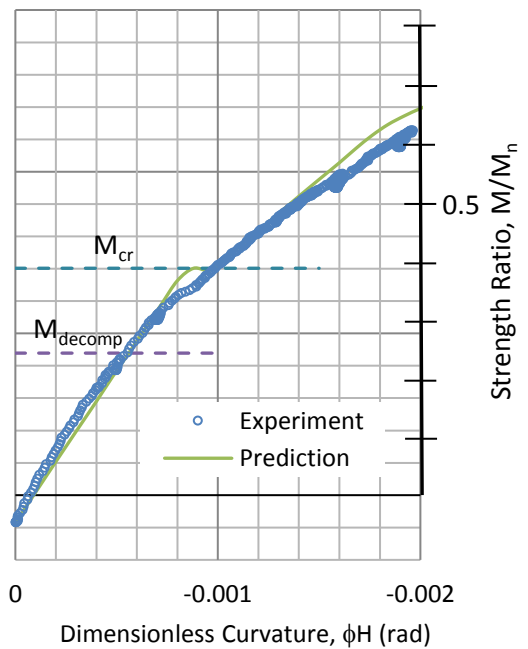
The overall section shape is more ductile when positive moments were applied due to the wide flange effect of the deck and the long internal lever arm. To provide better ductility under imposed negative moments, more compression mild steel is needed in the bottom flange.



(a) Splice 2 during Test 2 (Negative Moment) and Test 3 (Positive Moment)



(b) Splice 3 during Test 4



(c) Interior Support during Test 4

Figure 6.10. Moment-Curvature Diagrams for Splices and Interior Support.

6.3.3 Longitudinal Bar Strains

Figure 6.11 presents the behavior of the longitudinal reinforcing steel bars for the three splices at different test stages. Figure 5.24 presents the locations of the strain gages. Strain is plotted versus total applied load. Because the length of the affixed gages was 0.25 in. and the gages were covered with a heavy protective coating, researchers expected that the provided data are only representative of a small length of the bar. For the longitudinal bars, the gages were affixed 16 in. from the hook outside the development length to provide data representative of the maximum bar stresses, while staying in the splice region where maximum flexural demand on the bars was expected.

Strain behavior of the bars is linear and quite small at the beginning of loading, but after cracking and due to the reduction in moment of inertia, the bottom flange bars engage in providing equivalent tensile force, and from that point the deformation rate increased.

Figure 6.11(a) shows the strain variation in the longitudinal bars within Splice 2 during Test 3, where the positive moment was quite high. The gages indicate yielding of the longitudinal reinforcement in the bottom flange, as expected.

Figure 6.11(b) presents the strain in the longitudinal bars within Splice 3 during Test 4, where high negative moment and very high shear were applied. The maximum negative moment occurred at the interior support and the failure happened outside of the splice. Therefore, even though the top flange bars exhibit significant tensile strain, they did not yield.

Figure 6.11(c) depicts the strain variation in the longitudinal bars in Splice 1 during Test 5. A major crack suddenly appeared near the center of the bottom flange of Splice 1, which led to yielding in the bottom reinforcement. The top flange reinforcement gage indicated only a small compression strain.

6.3.4 Transverse Hoop Stirrups

Figure 6.12 presents the strain variation in the transverse reinforcing bars in each splices at different test stages. The gages were attached at mid-stirrup height, the location of the expected maximum transverse bar strain.

During Test 1, Splice 2 experienced a high positive moment and moderate shear. As shown in Figure 6.12(a), as the load increased the shear strain increased as expected, but the stirrups did not yield. It should be noted that a concentrated shear strain in terms of shear slip occurred at the

interface of Splice 2 and the adjacent girder, and a high interface displacement between Splice 1 and adjacent girder also occurred, which reduced the strain in the splice region.

Splice 3 underwent a moderate negative moment and a very high shear. After diagonal shear cracks emerged in the splice region, at least one stirrup in Splice 3 yielded, as shown in Figure 6.12(b).

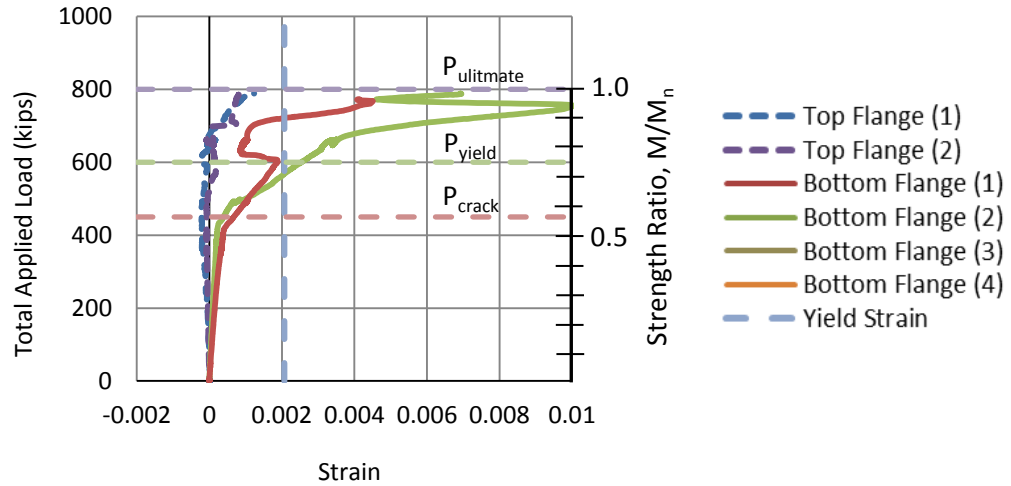
During Test 5, Splice 1 experienced low positive moment and high shear. Data from the gages exhibited very low strains (see Figure 6.12[c]), which is not expected based on the diagonal cracks observed in the splice region. The 0.25-in. long gages may have missed the location at which yielding occurs and therefore show lower strains.

6.3.5 Concrete Strains

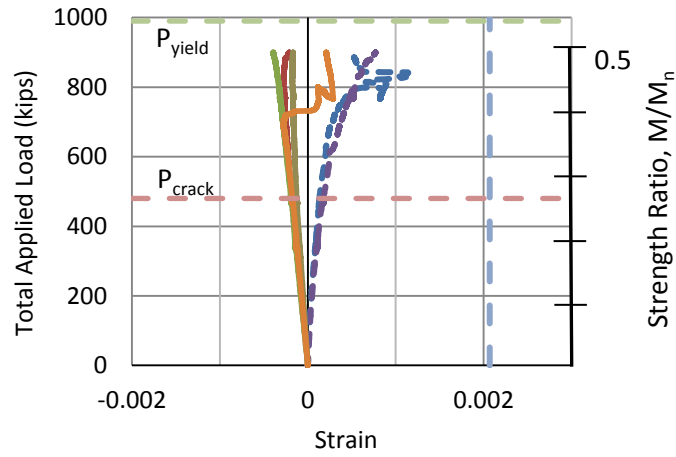
Figure 6.13 presents the concrete gage readings for Splices 2 and 3. Different types of instruments were used to measure the concrete strain, including surface gages, embedded gages, and LVDTs. Embedded concrete gages showed the most reliability, as they have a longer gage length as compared to the surface gages, and were placed internally in the member. Figure 6.13(b) shows the readings of the different installed instruments in Splice 2, with the embedded concrete gage being most sensitive in capturing higher strain values.

Figure 6.13(c) and 6.13(d) present the Splice 3 moment-curvature diagram and associated concrete gage readings during Test 4, respectively. During Test 4, the maximum negative moment occurred over the interior support and failure took place out of the splice region. Therefore, Splice 3 barely reached the cracking moment.

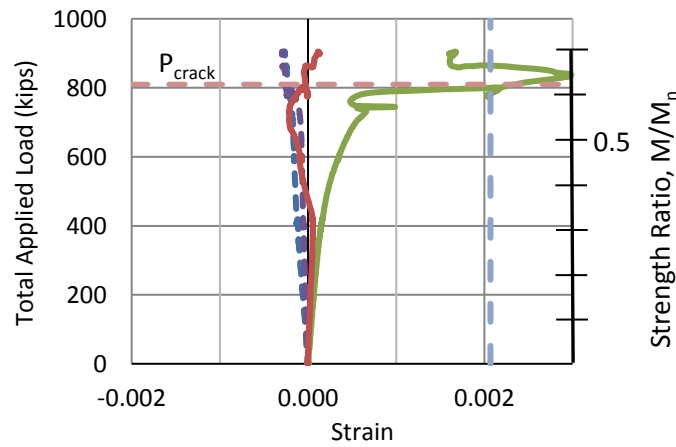
For the regions where the concrete was in compression, it was evident that different gage types provide comparable readings. On the other hand, in the presence of tensile cracks, the gages may either overestimate or underestimate the average strain in concrete, depending on the relative location with respect to those cracks.



(a) Test 3: Splice 2

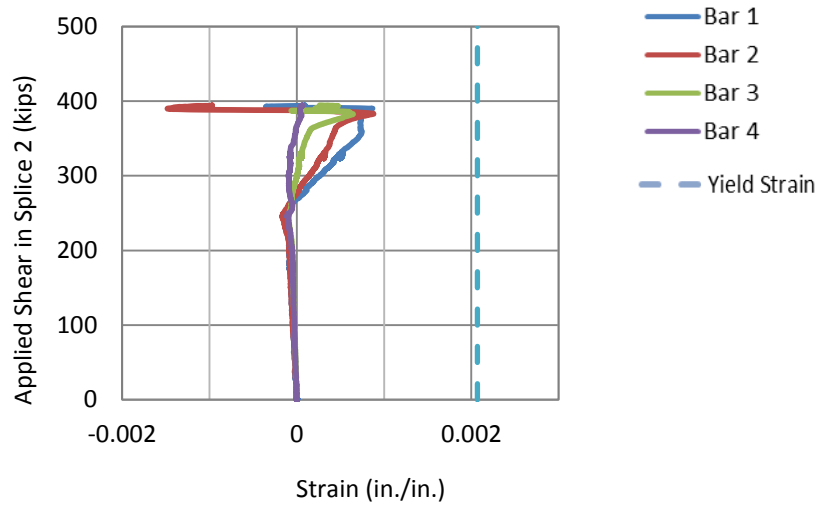


(b) Test 4: Splice 3

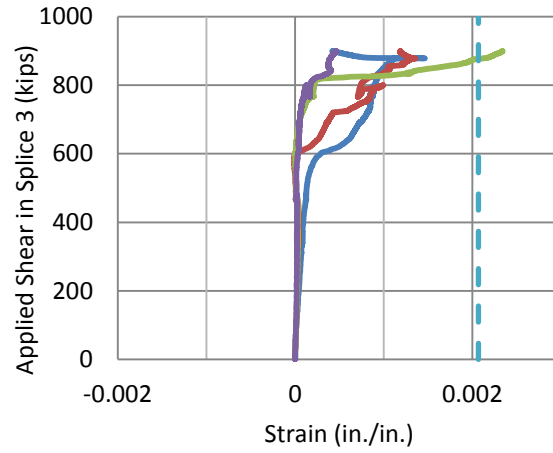


(c) Test 5: Splice 1

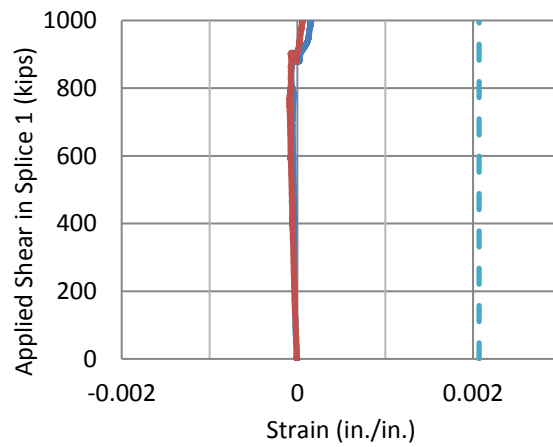
Figure 6.11. Longitudinal Reinforcement Behavior.



(a) Test 3: Splice 2

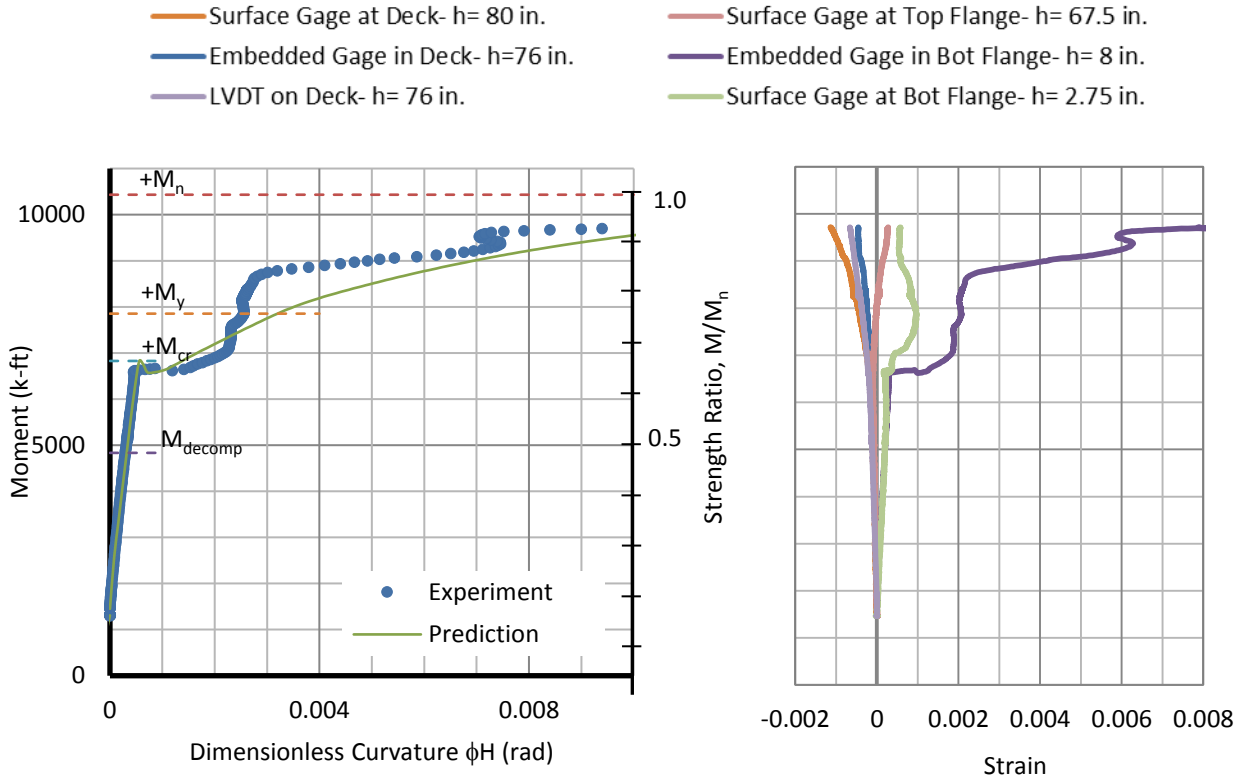


(b) Test 4: Splice 3



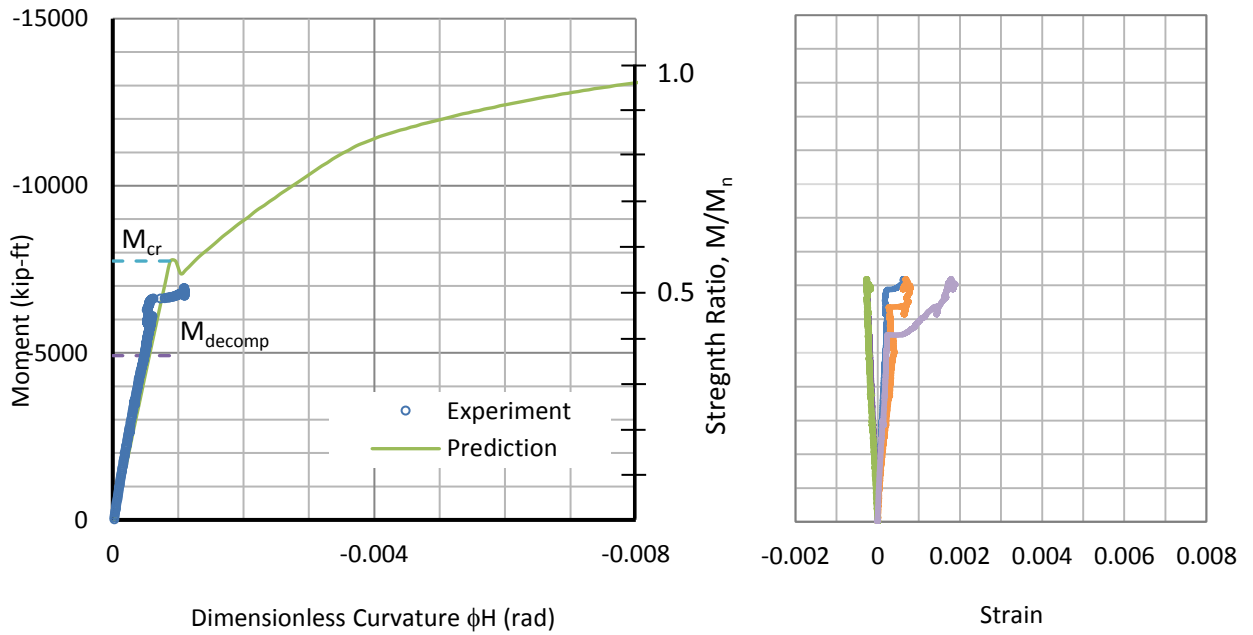
(c) Test 5: Splice 1

Figure 6.12. Transverse Bar Behavior.



(a) Moment-Curvature Diagram for Splice 2

(b) Collected Data from Gages in Splice 2



(c) Moment-Curvature Diagram for Splice 3

(d) Collected Data from Gages in Splice 3

Figure 6.13. Concrete Gage Readings and Associated Moment-Curvature Diagrams.

6.3.6 Strain Profiles

Figure 6.14 to Figure 6.19 present strain profiles for the splice regions during testing at key load steps. The upper row of the graphs presents strains profiles for *increments* of applied load. The first graph in the lower row shows the *initial* strain profile at the commencement of the relevant test and includes the effects of post-tensioning, creep, shrinkage, and the residual effects from the results of the previous tests. The first graphs on the lower row are then added to the incremental strains from above and the total result plotted beneath. Shown on all graphs are the computed linear strain profiles. Note that the upper graphs show the neutral axis for the uncracked section is 45 in. from the beam soffit.

Concrete gage readings may provide reliably crisp data after major cracks occur as the reading depends on the gage location between cracks. Moreover, if a crack passed nearby or through a gage's location, it may have ceased to function properly. It is for this reason the experimental results from the various different gages display scatter. In spite of this scatter, there is a remarkably satisfactory agreement between the linear profile predictions and the observed strains indicated by gages.

As shown in the figures, surface strain gages and embedded concrete gages have been used to plot the strain profiles. Because surface gages were attached to the side of the flanges, while embedded gages were within the central region of the section, the embedded gages appear to be more reliable, as they also provide more consistent agreement with the predictions.

The second row graphs show the total strain profile of the splices at different stages of loading. The total strain includes the post-tensioning effect, creep effect, and temporary support removal effect. Because there was no pretensioning in the splices and the deck, no prestress effects were considered in these profiles.

The prediction is based on moment-curvature analyses that used the plane sections hypothesis and nonlinear material stress-strain relations. The effect of shear deformation was not considered in the moment-curvature analysis. Creep effect prediction (based on experimental results and code values), support removal effect, and shrinkage effect were taken into consideration to predict the total strain profile in the second row of each figure.

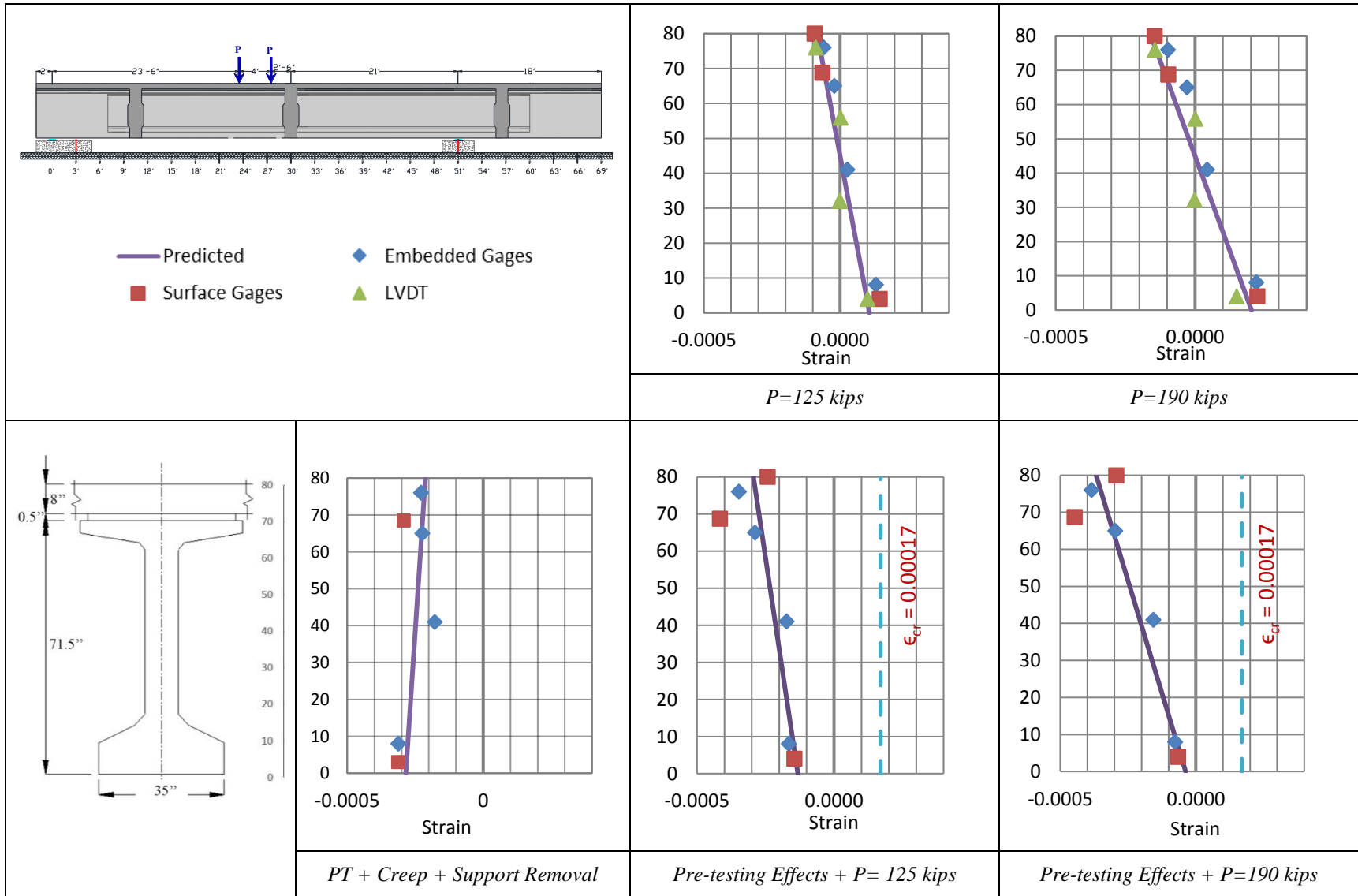


Figure 6.14. Bending and Total Strain Profile of Splice 2 during Test 1.

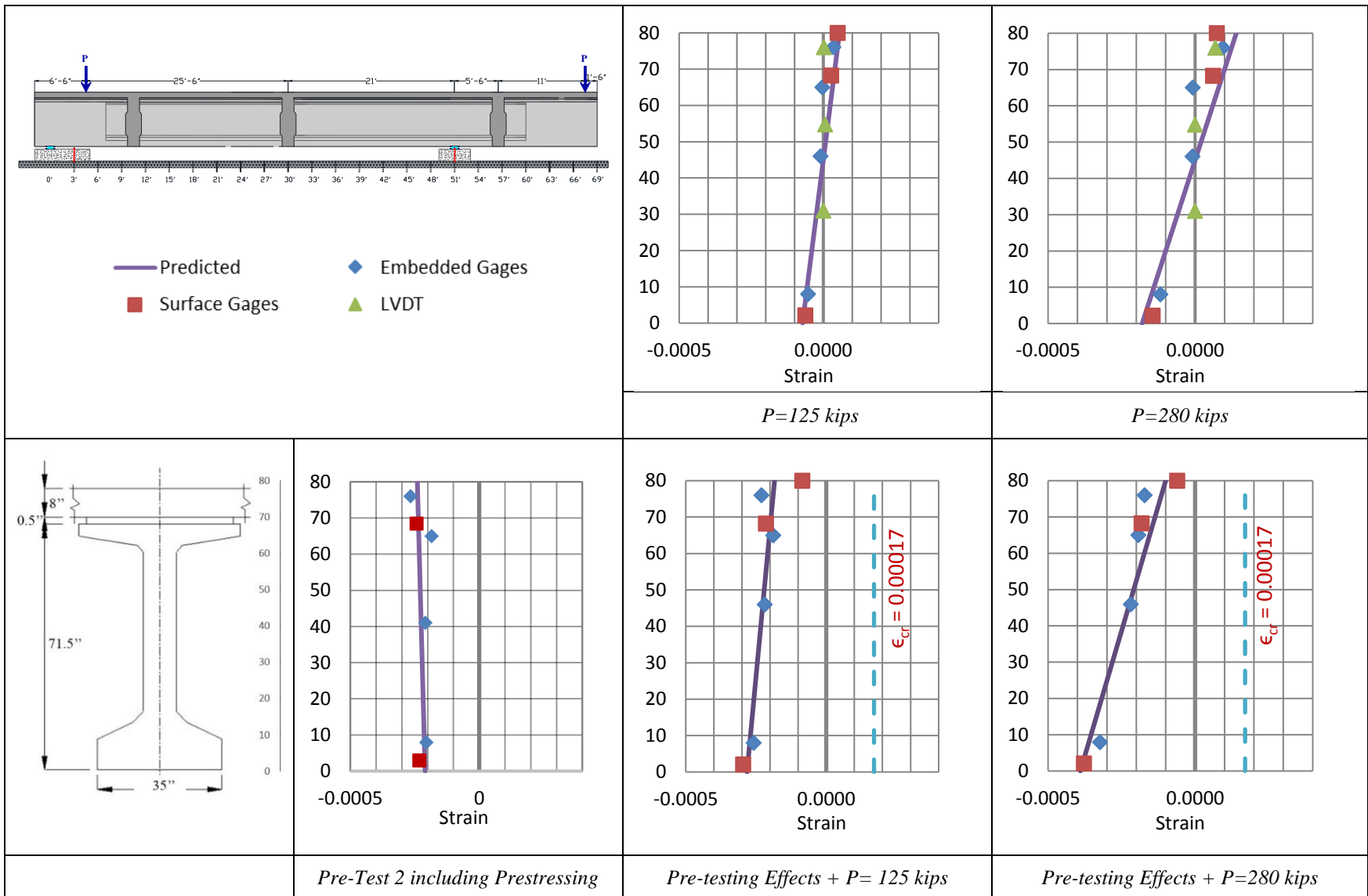


Figure 6.15. Bending and Total Strain Profile of Splice 3 during Test 2 – Part 1.

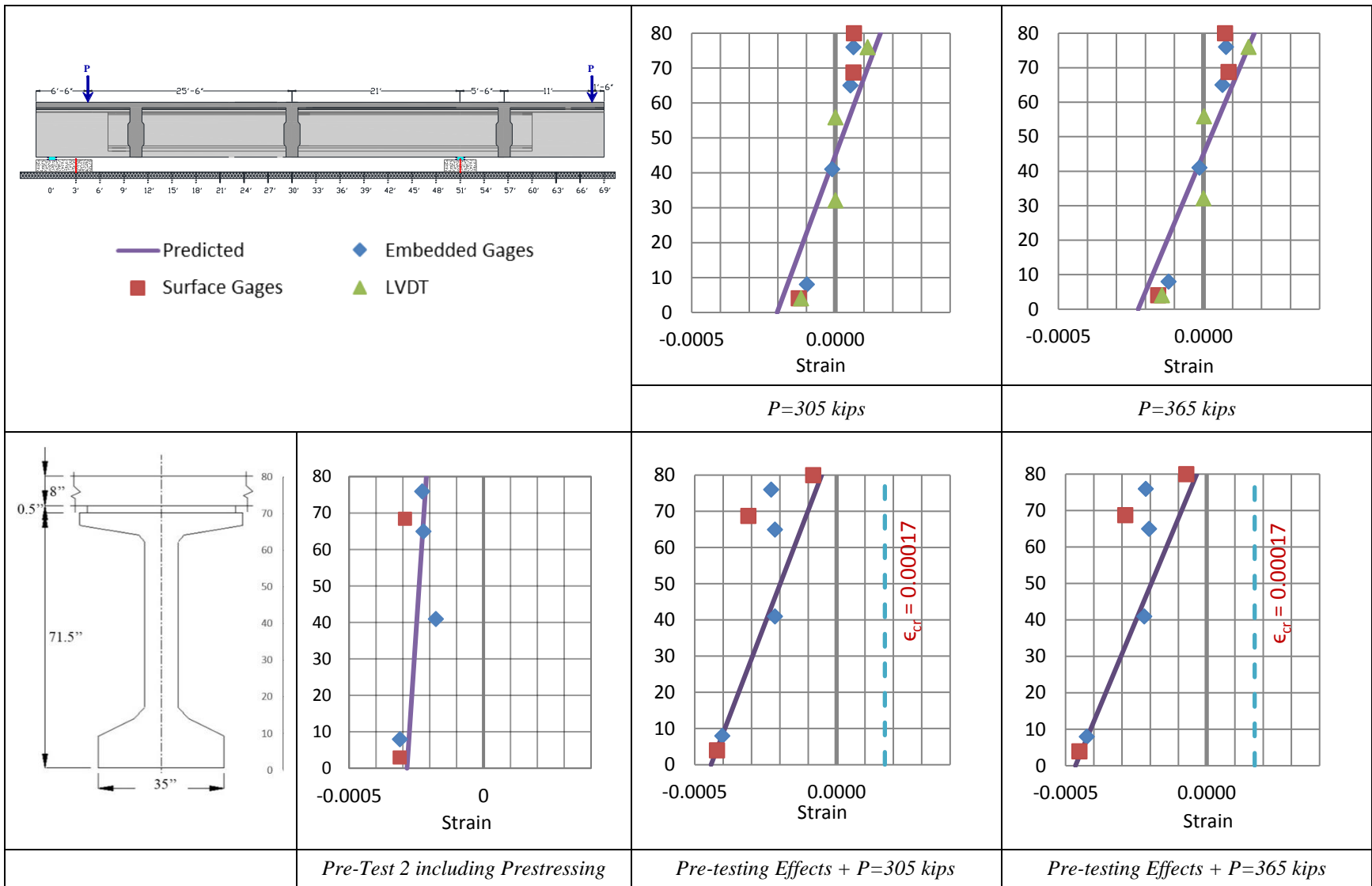


Figure 6.16. Bending and Total Strain Profile of Splice 2 during Test 2 – Part 2.

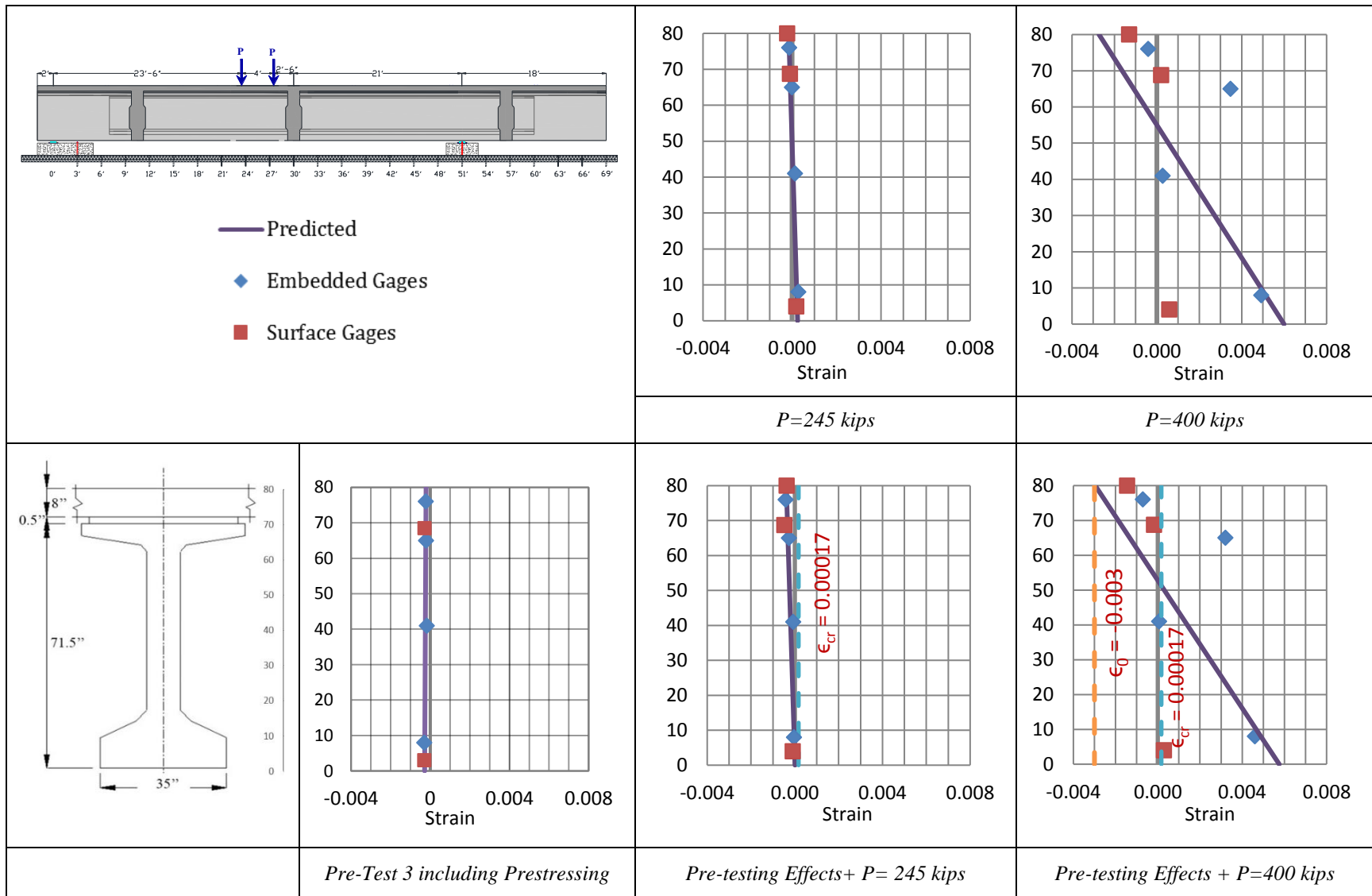


Figure 6.17. Bending and Total Strain Profile of Splice 2 during Test 3.

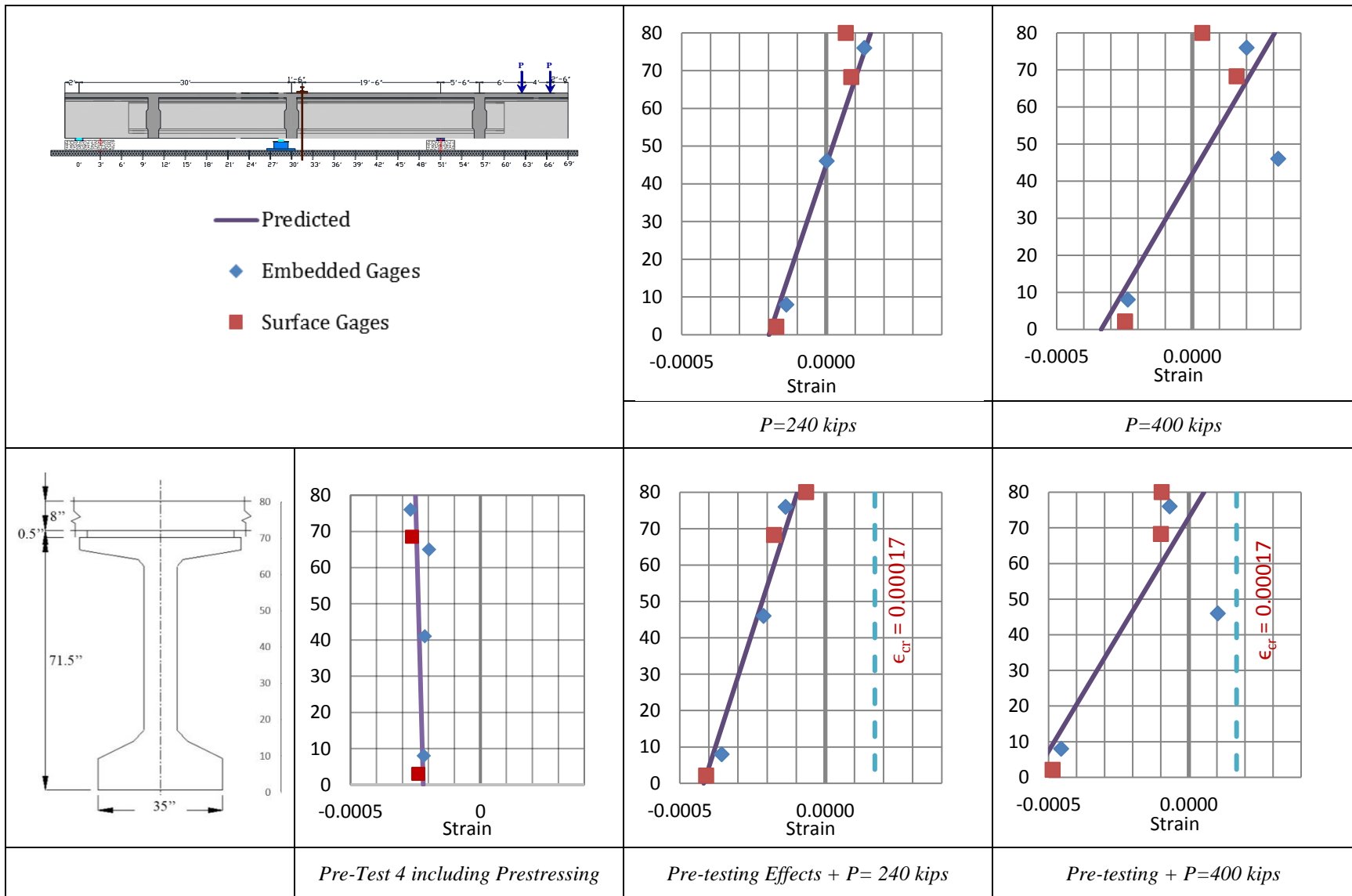


Figure 6.18. Bending and Total Strain of Splice 3 during Test 4.

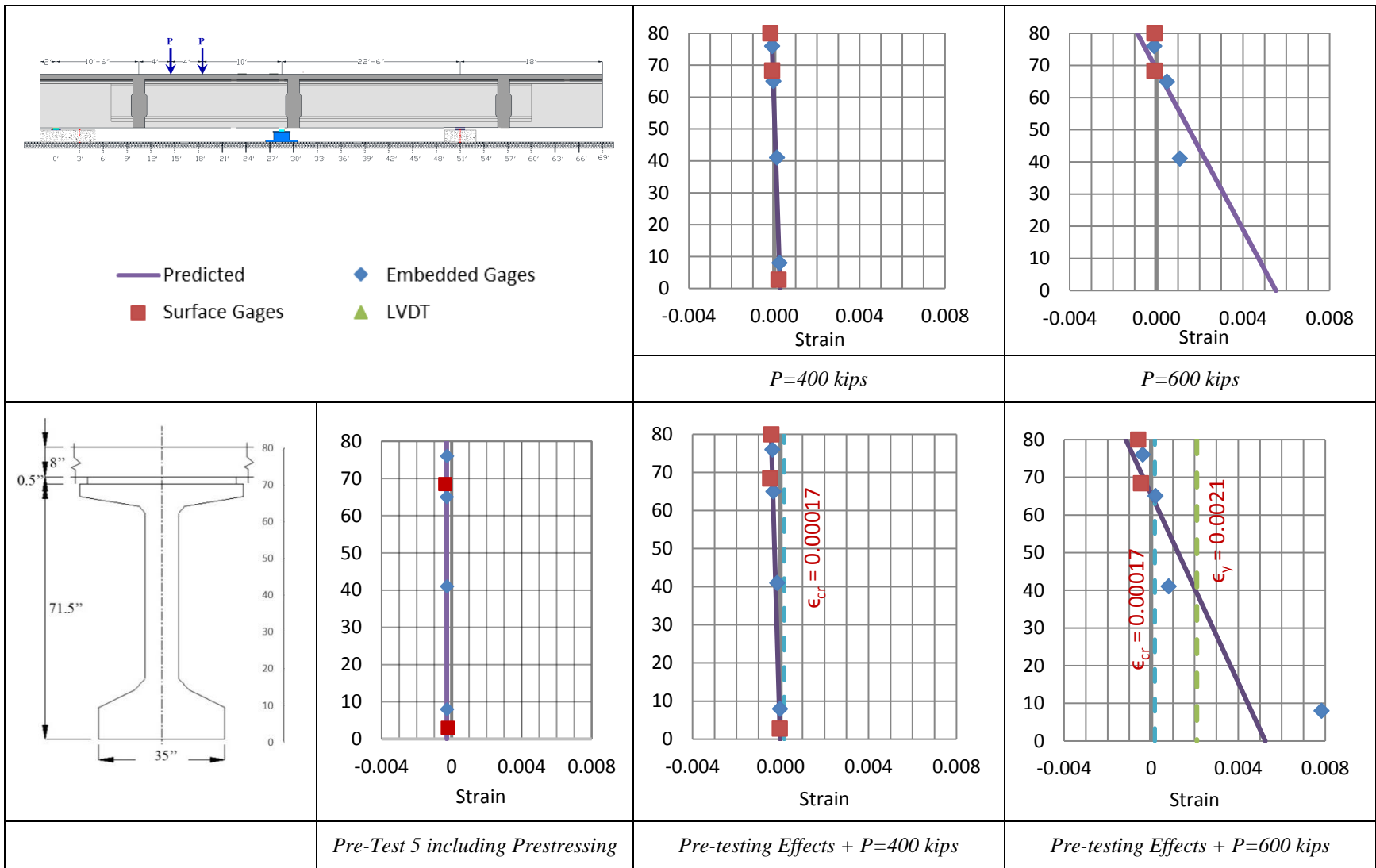


Figure 6.19. Bending and Total Strain Profile of Splice 1 during Test 5.

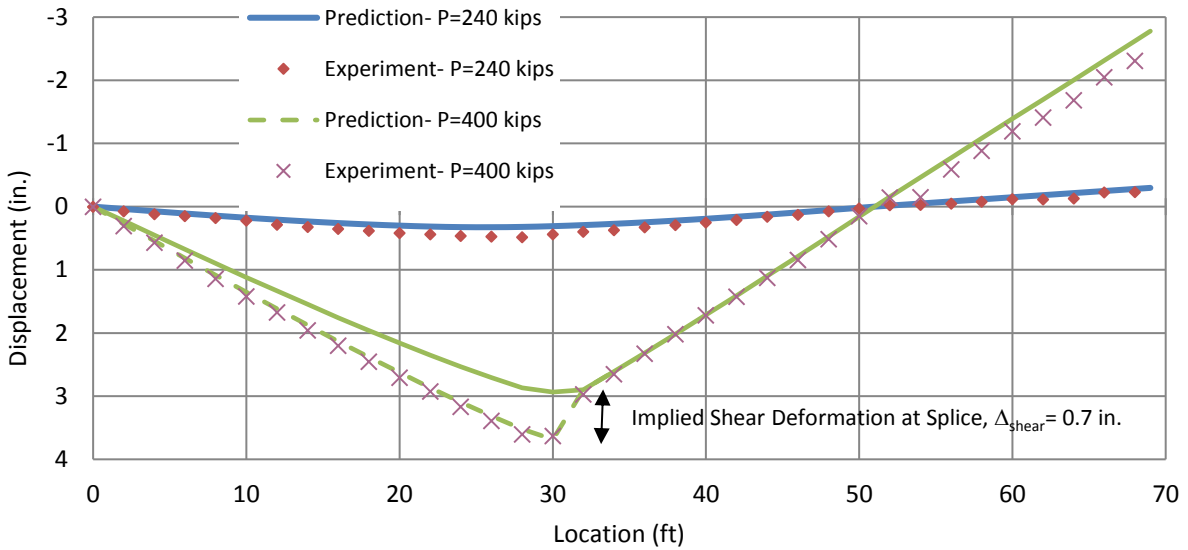
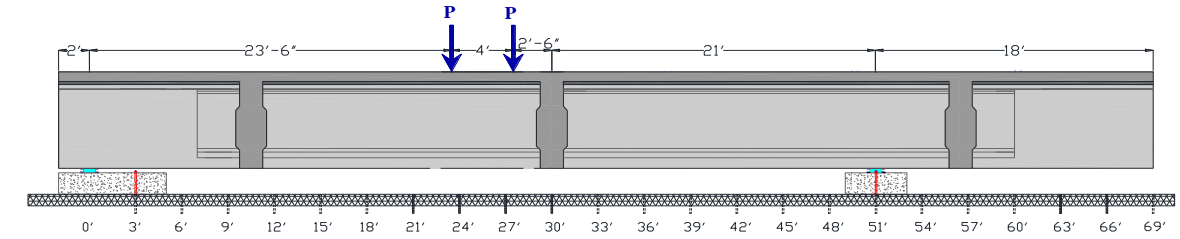
6.3.7 Longitudinal Beam Deflection Profile

Figure 6.20 shows the longitudinal beam deflection profile for Tests 3 and 4. A finite element model of the specimen was generated in SAP2000 that allowed for beam deformation prediction at different stages of loading. For Tests 1 and 2, uncracked section properties were adopted. For Test 3, up to cracking the specimen was treated as an uncracked section. After reaching cracking moment, the associated element in the model was defined as a cracked section with a reduced moment of inertia and reduced shear area. The reduction factor for the moment of inertia can be obtained from a moment-curvature analysis. The reduction factor is the ratio of the post-cracking slope to the initial slope of the moment-curvature diagram. The effect of plastic deformation beyond yield moment was calculated by assuming a plastic hinge with a 2 ft length in the splice region.

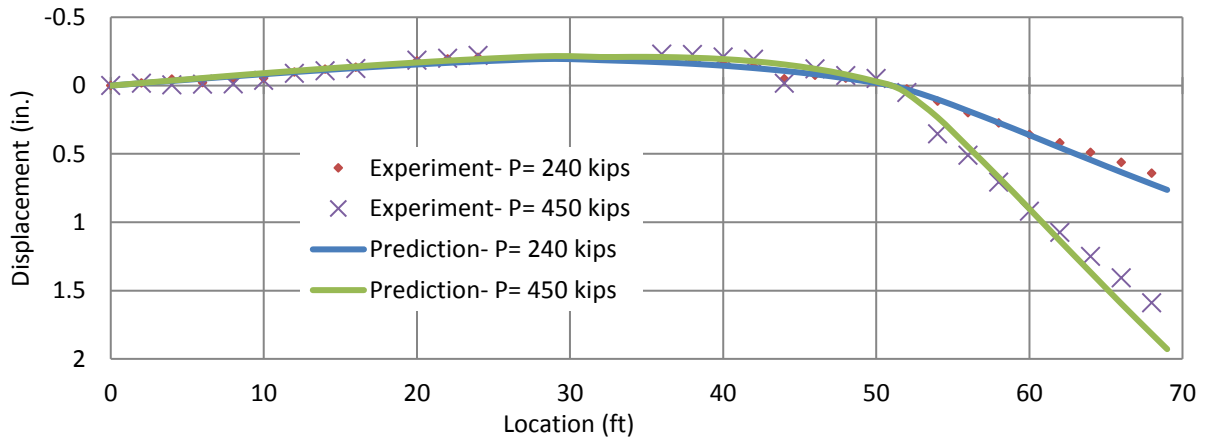
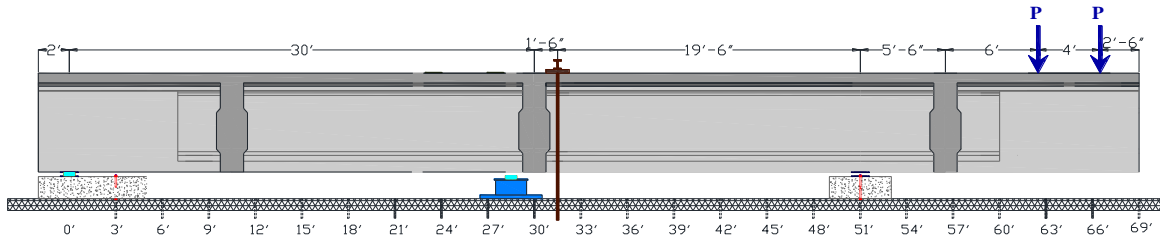
The deformation is predicted very well for Test 3, except for the overhang portion (beyond 51 ft). This difference is due to the fact that the string potentiometers have a lag in reading when they are being pulled. This phenomena leads to a difference between readings and prediction in Test 2 in the main span.

Numerical predictions match quite well on the north side of Splice 2 in Test 3, but as shown in Figure 6.4(d), there is a 0.7 in. difference at the splice interface that leads to a linear error in the left hand part. That difference comes from the slip of the girder at the interface of the splice connection, which propagates into the splice where the major crack has happened, as shown in Figure 6.20. The prediction was adjusted to take the interface slip into consideration.

For Test 4, a plastic hinge was considered over the support to account for the deformation beyond the yield moment. The rotation angle was calculated based on the curvature of the section and the length of the plastic hinge (which was considered to be 2 ft). Therefore, the final prediction is a combination of linear elastic bending and shear deflection (prior to cracking), non-linear elastic bending and shear deflection (from cracking moment to yield moment), and plastic deflection (beyond yield moment). The plastic deformation along with the uncracked and cracked deformation provides a reasonably close estimate of the actual deformation.



(a) Test 3: Cracking Moment ($P = 240$ kips) and Failure ($P = 400$ kips)



(b) Test 4: Cracking Moment ($P = 240$ kips) and Failure ($P = 450$ kips)

Figure 6.20. Longitudinal Beam Deformation.

6.4 DISCUSSION AND FINDINGS

Five different tests were carried out on the spliced girder specimen to provide a comprehensive understanding of the splice connection behavior under different combinations of positive and negative moment and shear. Based on the provided results and modeling predictions the findings are as follows:

- Pretensioning strands provide a significant contribution to the overall flexural capacity of the precast prestressed concrete sections. Because pretensioned prestress is not feasible within the splice region, these sections are somewhat weaker than the precast girder sections where the pretensioned prestress is fully developed. Therefore splices ideally need to be located in those locations where the overall (positive plus negative) moment demands are lower.
- Because of the existence of the deck, the splice sections are inherently ductile under positive bending. To add further flexural capacity and maintain the ductility capability, additional top and bottom reinforcement may be added through the splice connection.
- Splice and girder sections are inherently less ductile for negative moments. To provide appropriate ductility two options can be considered: either increasing the area of the bottom flange or embedding supplementary compression mild steel in the bottom flange.
- Small cracks tend to completely close after applied loads are removed; therefore post-tensioned concrete girder bridges can potentially provide improved durability.

7 SUMMARY, CONCLUSIONS, AND RECOMMENDATIONS

7.1 SUMMARY

Precast concrete girders have been commonly used in Texas as simply supported bridges spanning 50 to 150 ft. While very economic, this type of bridge cannot be used for span lengths beyond 150 ft because of limitations on length, weight, and height of the individual precast girders. However, if the girders are spliced within the span of the bridge, longer span lengths may be achieved. The objective of this project was to investigate the effectiveness of adopting in-span splicing, along with the load balancing effect of post-tensioning (PT) to expand the span length of concrete girder bridges up to 300 ft.

During Phase 1 of the project, the research team evaluated the current state-of-the-art and practice relevant to continuous precast, prestressed concrete girder bridges and recommended suitable continuity connection details for typical Texas bridge girders. Input from TxDOT engineers, precasters, and contractors was gathered to collect feedback on preliminary designs for continuous spliced precast, prestressed concrete bridge structures and splice details. The Phase 1 Research Report (Hueste et al. 2012) includes a review of the key techniques that have been used for spliced continuous precast concrete bridge girder systems; a discussion of a number of construction considerations; a summary of preliminary designs; a proposed general framework for categorizing connection splice types; a summary of input from precasters and contractors; and some potential connection details.

During Phase 2 of the project, the research team developed detailed design examples, conducted a parametric design study, and tested a full-scale modified Tx70 girder specimen containing three splice connections. In-span spliced bridge construction was adopted based on the Phase 1 results of various design cases with different span lengths, different cross sections, and different construction types. Based on a relatively aggressive design case and by considering limitations in the laboratory, a span configuration of 190-240-190 ft with four splices and five girder segments was considered as the prototype bridge for the experimental program. A full-size girder test specimen was extracted from the prototype bridge, with an overall length of 71 ft including three splices. The girder segments were precast and transported to the high bay laboratory. After casting the splices and the deck in the laboratory and instrumenting the specimen, PT was carried out, tendons were grouted, and loads were applied in five stages of testing. The

performance of the splices was monitored under positive and negative moment coupled with varying levels of shear intensity, for both service limit states and when the specimen was loaded to strength limit states and eventually failure (or maximum actuator loading). Hundreds of thousands of data points were recorded and analyzed to provide a thorough insight into the behavior of the entire girder specimen, particularly the splices, under different load combinations. Numerical modeling was carried out and evaluated based on the experimental results. Relevant articles of the AASHTO LRFD Specifications (2012) were reviewed and evaluated in light of the research findings. Based on the findings from Phases 1 and 2, recommendations regarding design, construction, and connection details for spliced continuous precast, prestressed concrete girder bridges are proposed. In addition, recommendations for future research are provided.

7.2 CONCLUSIONS

7.2.1 General

The use of in-span splices to make precast, prestressed concrete bridge girders continuous presents a viable alternative for increasing span lengths using standard precast girder sections. This system helps to bridge the gap between simply supported precast pretensioned concrete girder bridges and post-tensioned concrete segmental box or steel girder bridges. Different methods are available for the construction of spliced girder bridges, which are categorized into shored, unshored, and partially shored. The selection of the method of construction depends on the site conditions, availability of equipment, and the experience of the contractor. Spliced girder bridges present a competitive, economical, and high performance alternative to steel plate or segmental bridges for longer spans up to 300 ft. Experimental results show that the proposed splice detail will work appropriately for service and strength limit states, but additional provisions can be applied to enhance the performance of the bridge in post-elastic regions.

7.2.2 Design Cases and Parametric Study

Eight designs were explored for a parametric study that varied span lengths, cross sections, and types of construction. Based on the parametric study, the following conclusions were derived:

1. Load balancing is the key concept in the design of spliced precast concrete girder bridges.
2. A span length of 240 ft is possible by adopting shored construction using prismatic Tx70 girders (with 9 in. web), but not easily obtainable. A large numbers of tendons and mild steel is required in the pier region for ductility. A span length of 240 ft is also attainable by adopting partially shored construction using prismatic Tx70 girders for drop-in and end segments and a haunched on-pier segment.
3. A span length of 240 ft is possible using shored construction and prismatic Tx82 (9 in. or 10 in. web) girders. The compressive stresses at the different load stages are within limits but relatively small tensile stresses are observed in the pier region of the deck.
4. For transportation and handling purposes of the pier segments of the prismatic girder bridges in shored construction, temporary unbonded Dywidag threadbars of 1.25 in. diameter were included in the designs for shored construction. For partially shored construction on the other hand, for transportation and handling purposes of the haunched on-pier segments, pretensioning strands were provided in the bottom flange.
5. Tensile strain limits over the pier are a critical factor in setting the maximum span lengths of the girder segments. Mild steel reinforcement is added in the bottom flange of the on-pier girder segment as compression steel to improve ductility and the moment capacity of the girder section in the negative moment region.
6. For the considered shored construction designs, shoring towers are provided both in the end span and center span and are removed after pouring the deck and Stage II PT. The removal of shoring towers results in support removal moments that need to be considered in the design.
7. Based on design calculations, the newly cast splice can crack during the stage when the concrete deck is poured. Therefore, a partially prestressed splice is used, and mild steel is provided for serviceability and strength. Based on the computed stresses, the splice will be uncracked after Stage II PT is applied and at service conditions.
8. The stresses in the girders and the deck were checked at critical locations along the length of the bridge for the service limit states. The pier region of the beam experienced compressive stress levels that exceeded the allowable compressive stress at service conditions. This stress exceedance is addressed by providing supplemental mild steel reinforcement in the compression zone.

9. For the same span length, girder section, and method of construction, the advantages of using a Tx82 girder over a Tx70 girder include reduction in the total amount of prestressing steel, increased shear and moment capacities, and reduction in mild steel requirements for ductility in the pier region.
10. The thicker bottom flange for the haunched on-pier segment allows for higher moment and shear capacities at ultimate.
11. In partially shored construction, the back-span shoring towers are removed after Stage I PT and before casting the deck. This prevents transferring any residual stresses due to removal of the shoring towers to the deck.
12. The design for unshored construction can be carried out similarly to partially shored design. A temporary connection (tie downs) can be provided at the pier instead of providing back-span shoring towers. The tie downs would be removed after Stage I PT and before pouring the deck. However, wider piers are required for stability and overturning, and the details for the connection are more complicated.

7.2.3 Fabrication and Construction

Based on observations during fabrication and construction of the spliced girder specimen, as well as the design and analysis tasks, the following conclusions are provided regarding fabrication and construction:

1. Construction sequence can significantly affect the stresses during construction and therefore prestressing layout and sequence. An optimum construction sequence should be developed by the designer. The contractor must follow the same sequence and any possible change in construction sequence and schedule should be coordinated with the designer.
2. Continuous spliced precast girder construction usually requires very deep sections (70 in. deep or higher). Flowability of concrete must be assured to make sure that concrete fills the entire section, especially in congested areas such as the anchorage zones.
3. Narrow webs and existence of ducts in the web provides regions prone to cracking. Special attention should be paid to this issue during fabrication, release, and transportation of the precast segments.
4. Thicken ends for anchorage of the PT tendons are prone to thermal cracks due to the large volume of concrete in these regions. Casting the segments should be done in appropriate

environmental conditions, and special consideration must be taken into account for very high or very low temperatures.

5. Two methods are typical for construction of spliced concrete girder bridges: shored and partially shored (hybrid); each provides some advantages over the other. Based on contractors' input, partially shored construction is preferable over shored construction because it reduces the total cost of construction by cutting back the expense of temporary supports. However, this method may require haunched segments over the piers, which increases the girder fabrication cost.

7.2.4 Performance of the Superstructure and Splices

A partially prestressed splice with mild steel reinforcement and continuity PT running through the connection was assessed in this research. Based on the experimental program for the full-scale girder specimen with three splices and the conducted numerical analyses, the following conclusions are provided:

1. The spliced girder specimen performed well for the service limit states, both in positive and negative moment and shear. No cracks were observed while loads were maintained at service limit states.
2. The spliced girder specimen maintained its integrity and stability up to loads corresponding to ultimate limit states (or up to the maximum load per actuator). Both flexural and shear cracks emerged in the flanges and the web, and propagated as the applied loads increased, but failure did not occur in the splices prior to reaching the target strength corresponding to ultimate conditions. The positive moment in Splice 2 reached the factored design positive moment M_u for the splice in the prototype bridge. For Splice 3 in the overhang, the negative moment reached the factored design negative moment M_u before failure occurred at the interior support. Splice 1 near the end support was subjected to a combination of high shear and low moment such that the applied shear exceeded the factored design shear V_u for the splice in the prototype bridge, followed by additional loading up to the maximum actuator load.
3. Because the splices lack the effect of pretensioning and Stage 1 PT, their moment capacity is significantly lower than that of the adjacent precast girder segments. Therefore, most of the cracks initiated propagated in the splice regions. Therefore splice connections ideally need to

be placed in those locations where the overall (positive plus negative) moment demands are lower, namely points of contraflexure for the uniform dead load.

4. As most of the cracks concentrate in the splice region, flexural and shear stiffness of these sections are significantly lower than adjacent uncracked sections. Experimental and numerical results suggest that shear deformation under ultimate loads cannot be neglected in these regions and should be considered in total deformation calculations.
5. Moment curvature analysis suggests that the splices have generally lower flexural capacity but higher ductility compared to the precast girder segments that contain pretensioning. The higher ductility in the splices can be attributed to a higher reserve capacity for the concrete in compression. Because the pretensioning strands are terminated in the splice regions, lower compressive stresses are initially generated in these sections, leading to a higher ductility of those sections.
6. The tested splice and girder sections are inherently less ductile for negative moments. To provide appropriate ductility two options can be considered: either increasing the area of the bottom flange, or embedding supplementary compression mild steel in the bottom flange.
7. The tested splice sections have moderate ductility under positive bending. This higher ductility compared to negative moment is attributed to the effectiveness of deck concrete and reinforcement in providing supplementary compression capacity as compared to negative moment. To add additional flexural capacity and maintain the ductility capability in positive bending, additional top and bottom reinforcement may be added through the splice connection.
8. Anchorage zones were designed based on strut and tie analysis. The anchorage zones exhibited acceptable performance during application of PT and during load testing of the specimen as the measured strains remained well below the strain corresponding to cracking
9. The non-contact splices provided with minimal mild reinforcement provided sufficient crack control under service-level loads. However, when they began to yield and the major crack in the splice grew, their load path was not sufficient and they did not provide a significant contribution at ultimate conditions.
10. The mild steel could be extended and spliced mechanically or by welding through the splice. The optimum amount of mild steel would be a tradeoff between the provided capacity and avoiding congestion in the splice region.

11. Small to moderate cracks were observed to close completely after the loads were removed due to the presence of the continuous PT.
12. Interface shear is an important aspect of splice connection. The tested specimen did not have any special preparation at the girder to splice interface. Based on the AASHTO LRFD Specifications (AASHTO 2012), intentionally roughening the surface of the adjacent girders at the connection can greatly improve the shear transfer capacity of the connection. For the tested specimen, the use of shear keys was found to enhance the interface shear capacity of the splices.

7.3 RECOMMENDATIONS FOR DESIGN AND IMPLEMENTATION

Important details need to be considered in the design of spliced precast concrete girder bridges. Through the various stages of research, additional obstacles and challenges were discovered, which led to a more thorough design. The following findings and recommendations focus on feasibility, construction, design, cross-section selection, and splice performance and detailing. This section highlights and discusses several important articles of the AASHTO LRFD Specifications (2012) relevant to spliced precast girder bridges. However, it is not intended to be an exhaustive review of the relevant specifications for this bridge type, which are detailed by AASHTO (2012).

7.3.1 Feasibility

With respect to feasibility of spliced precast concrete girder bridges, the following observations and recommendations are provided.

1. In-span spliced girder technology allows the span length of precast concrete girder bridges to be extended beyond typical span-to-depth ratios without exceeding the transportable girder segment length limit of about 140 ft.
2. While the Tx70 girder can be used for spliced bridges, modifications were needed including an increased top flange thickness and increased web thickness. Using a Tx82 girder reduces the prestressing and reinforcement requirements relative to a Tx70 girder. In addition, TxDOT is currently implementing deeper Texas I-shaped precast girders including constant depth STx sections and haunched HSTx sections.

3. The moment capacity within the splice is considerably lower than for the adjacent girder segments. It is highly recommended to provide splices in low moment regions, namely points of contraflexure for the dead load. Therefore, it is suggested to use up to two splices in interior spans and one splice in the end spans. Assuming two splices per span and considering the length limit on individual girders, the maximum span length is limited to twice the maximum length for the individual girder segments.

7.3.2 Construction

With respect to construction considerations for spliced precast concrete girder bridges, the following observations and recommendations are provided.

1. The construction method and sequence is an important consideration in the design. It is essential to check the stresses at critical locations for all construction loads. The sequence of construction can vastly impact the construction stresses and should be selected to minimize the construction loads. It is advisable for the engineer to consult with the contractor regarding the feasibility of the proposed sequence.
2. The design includes stress checks for various stages of construction. The sequence of construction will lead to variations in the critical construction loads. It is essential to follow the sequence that is provided by designer and to check how any changes in the construction will impact the design.
3. Two primary methods may be considered for construction of spliced concrete girder bridges: shored and partially shored (hybrid). Based on input from contractors, partially shored construction is preferable over shored construction because it can lower the initial cost of construction. On the other hand, this method usually requires haunched segments over the pier to avoid compression failure in the girder, which leads to increased fabrication cost.
4. It is recommended that part of the post-tensioning be applied after casting the deck and when it has reached its design strength. This will greatly enhance the durability of the structure and significantly decreases the corrosion in the deck by limiting the cracks in negative moment regions. Based on AASHTO (2012) Commentary Article C5.14.1.3.4, full deck replacement will be problematic in this case, as it will impose an overstress on the girder that may lead to failure. To avoid full deck replacement, a sacrificial concrete layer that is isolated from the

deck by a waterproof layer is suggested. More options for avoiding full deck replacement are proposed by Castrodale and White (2004).

7.3.3 Design

With respect to design of spliced precast concrete girder bridges, the following observations and recommendations are provided.

1. It is desirable to balance the dead load throughout construction, as much as practical, to ensure that the segments are aligned through the splice connections; after casting the deck and applying all PT, the bridge has negligible deflection and is under a constant state of uniaxial compressive prestress.
2. Sequencing of the precast, prestressed concrete girder fabrication, CIP concrete on site, and PT operations are also important factors in the design. Stresses should be checked at each stage of construction.
3. Pretensioning strands have the primary contribution to the bending capacity of the I-shaped Tx prestressed girder sections because they are located in the flanges. Because no pretensioning strand is provided in the splice area, these sections are significantly weaker than the girder sections where the pretensioning is fully transferred and developed. Therefore splices should be located in the regions with the lowest moment demand, namely the points of contraflexure for the dead load.
4. Considering the significant contribution of pretensioning to the flexural capacity, it would be beneficial to extend the pretensioning strands into the splices. To provide connectivity and a well-developed load path, they need to be coupled in the middle of the splice. This has a strong potential to enhance the flexural capacity of the splice, but will cause some construction problems and additional congestion for concrete placement.
5. Because of the existence of the deck, splice sections can be very ductile in positive bending. But to take full advantage of the potential ductility, more mild steel should be placed in the bottom flange and the deck.
6. The girder section considered has low ductility under negative moments. Increasing the area of the bottom flange or implementing compression mild steel in the bottom flange will provide higher ductility. Alternately, haunched sections can be provided over the piers.

7. Article 5.5.4.2.1 (AASHTO 2012) provides values for the resistance factor ϕ for ultimate (strength-based) design conditions for different limit states. As Figure C5.5.4.2.1-1 suggests, the resistance factor for prestressed concrete sections in bending varies between 0.75 to 1.0 and is a function of the net tensile strain ϵ_t in the extreme tension steel at nominal conditions. The concept of compression-controlled and tension-controlled sections is elaborated in Article 5.7.2.1 (AASHTO 2012). Following the same approach as Article 5.5.4.2.1, the definition is solely based on the net strain in the extreme tension steel. There is no specification on type of the steel and the criterion applies to both prestressing steel and mild steel. The results of the experimental study for this project suggests that if the mild steel contributes only minimally to the flexural strength, the strain in the mild steel cannot be a reliable criterion for ductility. Therefore, it is suggested that it would be more appropriate to use the net tensile strain at the level of the cgs of the tension steel or at the level of the PT tendon closest to the tension fiber for determination of the resistance factor for flexure. This is suggested as an area for future research.
8. Table 5.5.4.2.2-1 (AASHTO 2012) defines the resistance factors for flexure and shear for joints in segmental construction. It does not specify the type of joint, but the resistance factors vary based on the use of normal weight concrete versus sand-lightweight concrete and fully bonded tendons versus unbonded or partially bonded tendons. For example, the flexural resistance factor for joints with normal weight concrete and fully bonded tendons is 0.95. This value could also be considered for the splice region for spliced precast girders using fully bonded tendons and normal weight concrete. Because splices between precast girders lack pretensioning effects and mild steel contributes to bending resistance more than in the precast girder segments, the performance of the splice is expected to be more ductile than precast girders. Therefore, it is suggested that the resistance factor for splices be the same as in the precast girder section, following Article 5.5.4.2.1 and Figure C5.5.4.2.1-1 (AASHTO 2012).
9. Article 5.7.3.1.1 (AASHTO 2012) provides expressions for calculating the stress in prestressing steel f_{ps} at nominal flexural resistance by first calculating the corresponding depth of the neutral axis. In the provided expressions (Eq. 5.7.3.1.1-1 and 5.7.3.1.1-3), the entire prestressing steel area is assumed to be taken at one level. If pretensioning and PT is used, this formula can result in non-conservative results, as the strain in the PT strands may be significantly less than for the pretensioning steel if the PT ducts are near the mid-height of the

section. It is recommended that a detailed strain compatibility analysis be used to provide a more accurate estimate of the flexural strength of the girder section at critical locations.

10. Article 5.7.3.5 (AASHTO 2012) allows moment redistribution for negative moments if the net tensile strain in the extreme tension steel ε_t is equal to or greater than 0.0075. Test results suggest that if an adequate area of mild steel reinforcement is not provided, the behavior of the girder in negative moment will not be sufficiently ductile to allow for moment redistribution. If the ductility of the sections is enhanced, by implementing more mild steel in the compression zone, spliced prestressed precast concrete girder bridges will have another advantage over simply supported bridges.
11. Short- and long-term prestress losses should be considered for different ages of the bridge.
12. Considering the continuous structure, primary and secondary effect of temperature variation should be considered.
13. AASHTO provides different methods for considering the creep effect, which are conservative. More accurate analysis can be provided using commercial software that includes time-step methods.

7.3.4 Cross-Section Selection

With respect to cross-section selection for spliced precast concrete girder bridges, the following observations and recommendations are provided.

1. It is recommended to use a haunched section for on-pier segment in a partially shored construction. Negative moment will be critical over the pier and deeper section along with more mild steel is required to provide sufficient capacity.
2. Based on precasters' input and hauling limitations, the desirable maximum length of individual segments is 140 ft.
3. Maximum weight of the individual girders are advised to be limited to 200 kips. Some contractors suggest that by using modern craned, heavier segments can also be erected.
4. To avoid possible complication during hauling, the precasters suggested that the height of the girder segments be limited to 10 ft.
5. To minimize initial cost of the projects, using standard shapes and other precasting elements are critical.

6. Two different approaches can be adopted for increasing the section depth over the support: increasing the depth of the web while maintaining a constant flange thickness, or increasing the thickness of the bottom flange while maintaining a constant web depth. The second method will add to the dead weight of the structure, but precasters have indicated that it is preferred over the first method, as it is more feasible to fabricate.
7. Even though use of standard shape is preferred over haunched segments, for partially shored method of construction, prismatic shapes will have difficulties with accommodating the required pre-tensioning strands and compression mild steel.
8. Contractors have expressed concerns about lateral stability of the haunched section during erection. This concern is mostly mentioned when increased web depth is used to increase the depth of the section. AASHTO Article 4.6.5 (AASHTO 2012) notes requirements for investigation of stability of continuous beam bridges. Because longer aspect ratios are used for spliced precast girders, as compared to simply supported bridges, the overall stability of the spliced girders should be checked, particularly during the construction process.

7.3.5 Splice Performance and Detailing

With respect to splice performance and detailing for spliced precast concrete girder bridges, the following observations and recommendations are provided.

1. Splice Performance

- The tested splice connection detail was selected to represent more critical design parameters. The splice connections in the test specimen performed well under service loads with no observed cracking.
- The splice connections in the test specimen exhibited acceptable performance with respect to strength up to ultimate with some concentrated cracking due to the lack of pretensioning through the splice connections. Therefore, splices ideally need to be located in regions where the overall (positive and negative) moment demands are lower.
- Due to the effect of PT, small cracks in the specimen closed after removal of loads. This beneficial effect may lead to better durability and lower maintenance costs in bridge structures.

- Although the spliced connections performed very well at service limits and provided sufficient capacity for ultimate strength limits, some modifications can improve their performance for extreme events.

2. *Mild Steel*

- The non-contact splices used for the mild reinforcement extending into the connection were effective under service level loads. However, they are loaded up to ultimate, the bars yield, and the crack in the splice widened significantly.
- The mild steel can be extended and spliced, mechanically or by welding. The optimum amount of mild steel would be a tradeoff between the provided capacity and the congestion in the splice region.

3. *Splice Length*

- Due to the lack of pretensioning and Stage I PT in the splice region, the splice is a weak link in the bridge. Therefore it is desirable to minimize the length of splices. On the other hand, enough space is required to accommodate the duct connection in the splice region. Depending on the stiffness and the size of the ducts that are being used, a distance of 18 in. to 24 in. is the optimum length for the splice. Some researchers have suggested that the length of the splice can be extended even more to provide better development for rebar.

4. *Shear at Interface of Splice and Girder*

- The use of shear keys was effective in enhancing the interface shear capacity of the splices. Bearing cracks were observed immediately below the shear key. The cracks suggest that a portion of the shear was transferred in bearing through the shear keys.
- Interface shear is an important aspect of splice connection. Based on the AASHTO LRFD Specifications (2012), intentionally roughening the surface at the interface of the girder and connection can greatly improve the shear transfer capacity.
- Locally increasing the web width at the splice is also expected to improve the spliced connection behavior.

5. *Ductility*

- Because of the existence of the deck, the splice connections showed moderate deformability under positive bending. To increase flexural capacity, and maintain the ductility capability, additional top and bottom reinforcement may be added through the

splice connection. In addition, lowering the PT steel centroid through the splice is also expected to improve the splice connection behavior.

- The splice and girder sections are inherently less ductile for negative moments. To provide appropriate ductility under negative bending, two options may be considered: increasing the area of the bottom flange or embedding supplementary compression mild steel in the bottom flange.

7.4 RECOMMENDATIONS FOR FUTURE RESEARCH

Recommendations to extend the results of this research include the following:

1. For the experimental study, in-span splices with a partially prestressed detail, including minimal non-contact mild steel, were adopted and tested. Additional experimental data are needed to investigate the performance of other types of splice details (such as bent strands and spliced strands).
2. In shored construction, splices are prone to cracking in negative bending over the temporary supports before the PT has been applied. Supplementary mild steel was provided to control the cracking in the splices. As another alternative, the effectiveness of local external PT at the splices (stitch splicing) can be evaluated through an analytical and experimental study.
3. If the bridge deck needs to be completely removed and replaced, PT that is resisted by the deck may overstress the girder sections. In order to overcome potential issues, a portion of the PT could be applied using external tendons. This portion can be released during deck replacement and then re-stressed after the deck is at sufficient strength. Numerical studies and experimental investigation could assess the effectiveness of this construction method.
4. Interface slip occurred in the splice region where the interface crack extended and led to failure. This displacement cannot be captured by Euler or even Timoshenko beam theory. Additional analysis should be conducted to investigate the shear deformation of the structure after cracking especially in disturbed regions.
5. Article 5.5.4.2.1 (AASHTO 2012) provides values for the resistance factor ϕ for ultimate (strength-based) design conditions for different limit states. Further investigation to assess and provide specific guidance for resistance factors for use with concrete girders having both prestressing steel and mild steel reinforcement is encouraged.

REFERENCES

- AASHTO (2003). *AASHTO LRFD Bridge Design Specifications*. 4th Edition, American Association of State Highway and Transportation Officials (AASHTO), Customary U.S. Units, Washington, D.C.
- AASHTO (2012). *AASHTO LRFD Bridge Design Specifications*. 4th Edition, American Association of State Highway and Transportation Officials (AASHTO), Customary U.S. Units, Washington, D.C.
- Abdel-Karim, A. and M.K. Tadros (1995). "State-of-the-Art of Precast/Prestressed Concrete Spliced I-Girder Bridges." *Precast/Prestressed Concrete Institute*, Chicago, IL, 143 pages.
- Alawneh, M. (2013). "Curved Precast Prestressed Concrete Girder Bridges." *Ph.D. Dissertation*, University of Nebraska, Lincoln, Nebraska, 359 pages.
- ASTM (2013). "C109, Standard Test Method for Compressive Strength of Hydraulic Cement Mortars (Using 2-in. or [50-mm] Cube Specimens)." *Annual Book of ASTM Standards*. American Society for Testing and Materials (ASTM), West Conshohocken, PA.
- ASTM C172 (2003). "Standard Practice for Sampling Freshly Mixed Concrete." *Annual Book of ASTM Standards*. American Society for Testing and Materials (ASTM), West Conshohocken, PA.
- ASTM C31 (2003). "Standard Practice for Making and Curing Concrete Test Specimens in the Field." *Annual Book of ASTM Standards*. American Society for Testing and Materials (ASTM), West Conshohocken, PA.
- ASTM C39 (2004). "Standard Test Method for Compressive Strength of Cylindrical Concrete Specimens." *Annual Book of ASTM Standards*. American Society for Testing and Materials (ASTM), West Conshohocken, PA.
- ASTM A370 (2008). "Standard Test Methods and Definitions for Mechanical Testing of Steel Products." *Annual Book of ASTM Standards*. American Society for Testing and Materials (ASTM), West Conshohocken, PA.
- ASTM C469 (2010). "Standard Test Method for Static Modulus of Elasticity and Poisson's Ratio of Concrete in Compression." *Annual Book of ASTM Standards*. American Society for Testing and Materials (ASTM), West Conshohocken, PA.

- ASTM C496 (2011). “Standard Test Method for Splitting Tensile Strength of Cylindrical Concrete Specimens.” *Annual Book of ASTM Standards*. American Society for Testing and Materials (ASTM), West Conshohocken, PA.
- ASTM C512 (2010). “Standard Test Method for Creep of Concrete in Compression.” *Annual Book of ASTM Standards*. American Society for Testing and Materials (ASTM), West Conshohocken, PA.
- ASTM C596 (2009). “Standard Test Method for Drying Shrinkage of Mortar Containing Hydraulic Cement.” *Annual Book of ASTM Standards*. American Society for Testing and Materials (ASTM), West Conshohocken, PA.
- ASTM C78 (2010). “Standard Test Method for Flexural Strength of Concrete (using Simple Beam with Third-Point Loading).” *Annual Book of ASTM Standards*. American Society for Testing and Materials (ASTM), West Conshohocken, PA.
- Bentley Systems (2013). LEAP CONSPLICE, Bentley Systems, Inc., Exton, PA.
- Bishop, E.D. (1962). “Continuity Connection for Precast Prestressed Concrete Bridges.” *ACI Journal*, V. 59, No. 4, American Concrete Institute, Detroit, MI, pp. 585–600.
- Castrodale, R.W. and C.D. White (2004). “Extending Span Ranges of Precast Prestressed Concrete Girders.” Transportation Research Board, National Cooperative Highway Research Program, *Report No. 517*, 603 pages.
- Caroland, W.B., D. Depp, H. Janssen, and L. Spaans (1992). “Spliced Segmental Prestressed Concrete I-Beams for Shelby Creek Bridge.” *PCI Journal*, V. 37, No. 5, pp. 22–33.
- Dimmerling, A., R.A. Miller, R. Castrodale, A. Mirmiran, M. Hastak, and T.M. Baseheart (2005). “Connections Between Simply Supported Concrete Beams Made Continuous: Results of National Cooperative Highway Research Program Project 12-53.” *Transportation Research Record: Journal of the Transportation Research Board*, Washington, D.C., pp. 126–133.
- EN, BS. (1996). “447: Grout for Prestressing Tendons- Basic Requirements.” *European Committee for Standardization*.
- Endicott, W.A. (1996). “Precast Super Bulb Tees Create Innovative Bridge.” *Ascent Winter*, PCI, pp. 30–32.

- Endicott, W.A. (2005). “A Fast Learning Curve: Colorado Flyover Provides Strong Example of the Concept of Curved U-Girders for Use in a Variety of Bridge Projects.” *Ascent Winter, PCI*, pp. 36–49.
- Fitzgerald, J.B. and T.W. Stelmack (1996). “Spliced Bulb-Tee Girders Bring Strength and Grace to Pueblo’s Main Street Viaduct.” *PCI Journal*, V. 41, No. 6, pp. 40–54.
- Hueste, M.D, J.B. Mander, and A.S. Parkar (2012). “Continuous Prestressed Concrete Girder Bridges Volume 1: Literature Review and Preliminary Designs.” Texas Department of Transportation, *Report No. 0-6651-1*, 176 pages.
- Janssen, H.H. and L. Spaans (1994). “Record Span Spliced Bulb-Tee Girders Used in Highland View Bridge.” *PCI Journal*, Vol. 39, No. 1, pp. 12–19.
- Kaar, P.H., L.B. Kriz, and E. Hognestad (1960). “Precast-Prestressed Concrete Bridges, 1. Pilot Tests of Continuous Girders.” *Journal of PCA Research and Development Laboratories*, V. 2, No. 2, pp. 21–37.
- Karthik, M. M., J. B. Mander (2011). “Stress-Block Parameters for Unconfined and Confined Concrete Based on a Unified Stress-Strain Model.” *ASCE Journal of Structural Engineering*, V. 137, No. 2.
- Koch, S. (2008). “Prestressed PCBT Girders Made Continuous and Composite with a Cast-in-Place Deck and Diaphragm.” *Master of Science Thesis*, Virginia Polytechnic Institute and State University, Blacksburg, Virginia, 140 pages.
- Koch, S., and Roberts-Wollmann, C.L. (2008). Design Recommendations for the Optimized Continuity Diaphragm for PCBT Girders. FHWA/VRTC 06-CR1, Virginia Transportation Research Council, 70 pages.
- Lounis, Z., M.S. Mirza, and M.Z. Cohn (1997). “Segmental and Conventional Precast Prestressed Concrete I-Bridge Girders.” *ASCE Journal of Bridge Engineering*, V. 2, No. 3, pp.73–82.
- MATLAB (2014), The MathWorks, Inc., Natick, Massachusetts, United States.
- Mattock, A.H. and P.H. Kaar (1960). “Precast-prestressed Concrete Bridges III: Further Tests of Continuous Girders.” *Journal of PCA Research and Development Laboratories*, V. 2, No. 3, pp. 51–78.
- Menegotto, M., and P. E. Pinto (1973). “Method of Analysis for Cyclically Loaded RC Frames Including Changes in Geometry and Non-elastic Behaviour of Elements under Combined

- Normal Force and Bending.” *IABSE Congress Reports of the Working Commission*, V. 13.
- Miller, R.A., R.W. Castrodale, A. Mirmiran, and M. Hastak (2004). “Connection of Simple Span Precast Concrete Girders for Continuity.” *Report 519*, National Cooperative Highway Research Program, 203 pages.
- Mirmiran, A., S. Kulkarni, R. Miller, M. Hastak, B. Shahrooz, and R. Castrodale (2001). “Positive Moment Cracking in the Diaphragms of Simple-Span Prestressed Girders Made Continuous.” *SP 204 Design and Construction Practices to Mitigate Cracking*, E. Nawy, Ed., American Concrete Institute, Detroit, MI, pp.117–134.
- Moore, A., C. Williams, D. Al-Tarafany, J. Felan, J. Massey, T. Nguyen, K. Schmidt, D. Wald, O. Bayrak, J. Jirsa, W. Ghannoum (2015). “Shear Behavior of Spliced Post-Tensioned Girders.” *Rep. No. 0-6652-1*. Center for Transportation Research, University of Texas at Austin.
- Newhouse, C.D., C.L. Roberts-Wollmann, and T.E. Cousins (2005). “Development of an Optimized Continuity Diaphragm for New PCBT Girders.” *FHWA/VRTC 06-CR3*, Virginia Transportation Research Council, 77 pages.
- Nikzad, K.A., T. Trochalakis, S.J. Seguirant, and B. Khaleghi (2006). “Design and Construction of the Old 99 Bridge – An HPC Spliced Girder Structure.” *PCI Journal*, V. 23, No. 18, pp. 98–109.
- Priestley, M.J.N. (1976). “Ambient Thermal Stresses in Circular Prestressed Concrete Tanks.” *ACI Journal Proceedings*, American Concrete Institute, V. 73, No. 10.
- Prouty, J.M. (2014). “Sustainable and Durable Infrastructure with Advanced Construction Materials.” *Master of Science Thesis*, Texas A&M University, 134 pages.
- PTI (2000). *Anchorage Zone Design: Preprint of Chapter VIII, Post-tensioning Manual*. Post-Tensioning Institute.
- Ronald, H.D. (2001). “Design and Construction Considerations for Continuous Post-tensioned Bulb Tee Girder Bridges.” *PCI Journal*, V. 46, No. 3, pp. 44–66.
- Sarremejane, T. (2014). “Analysis of Short and Long Term Deformations in a Continuous Precast Prestressed Concrete Girder.” *Master of Science Thesis*, Texas A&M University, College Station, 114 pages.

- Segel, E. and D. Sanders (2014), "Mitigating Web Cracking in Post-tension Applications," *REU Report*, University of Nevada, Reno, August.
- Sun, C. (2004), "High Performance Concrete Bridge Stringer System." *Ph.D. Dissertation*, The University of Nebraska- Lincoln, 228 pages.
- Tadros, M.K. and C. Sun (2003). "Implementation of the Superstructure/Substructure Joint Details." University of Nebraska, Omaha, Department of Civil Engineering, *Nebraska Department of Roads Research Report*, Project No. SPR-PL-1(038), 514 pages.
- Tadros, M.K. (2007). "Design Aids for Threaded Rod Precast Prestressed Girder Continuity System." *Nebraska Department of Roads Research Report*, 103 pages.
- Tex-407-A (2008). "Sampling Freshly Mixed Concrete." *Standard Specifications for Construction and Maintenance of Highways, Streets, and Bridges*. Texas Department of Transportation, Austin.
- Tex-447-A (2008). "Making and Curing Concrete Test Specimens." *Standard Specifications for Construction and Maintenance of Highways, Streets, and Bridges*. Texas Department of Transportation, Austin, TX.
- TxDOT (2013). *Texas Department of Transportation Bridge Design Manual - LRFD*. Revised March 2013. Texas Department of Transportation. Austin, TX. <<http://onlinemanuals.txdot.gov/txdotmanuals/lrf/lrf.pdf>>
- TxDOT (2015). *Texas Department of Transportation Prestressed Concrete I-Girder Details*. Texas Department of Transportation. Austin, TX. <<http://ftp.dot.state.tx.us/pub/txdot-info/cmd/cserve/standard/bridge/igdstds1.pdf>>
- Urmson, C.R., & J.B. Mander (2011). "Local Buckling Analysis of Longitudinal Reinforcing Bars." *Journal of Structural Engineering*, 138(1), pp. 62-71.
- Webber (2014). WRQ SH 183A SYLVAN AVENUE BRIDGES. <<http://wwwebber.com/wrq-sh-183a-sylvan-avenue-bridges/>>.
- Williams C., A. Moore, D. Al-Tarafany, J. Massey, O. Bayrak, J. Jirsa, W. Ghannoum (2015). "Behavior of the Splice Regions of Spliced I-Girder Bridges." *FHWA/TX-15/0-6652-2*. Center for Transportation Research, University of Texas at Austin, 266 pages.

APPENDIX A.
MATERIAL PROPERTIES:
CONCRETE, MILD STEEL, AND PRESTRESSING STRAND

A.1 CONCRETE

The concrete mixtures used in the girder specimen fabrication were characterized by measuring both fresh and hardened properties. A summary of the mixture proportions and test results are provided below. Additional details were documented by Prouty (2014).

A.1.1 Mixture Proportions

A.1.1.1 Girder Segments

The SCC used for the girder segments was designed by the precast plant to meet the project specified concrete compressive strength requirements of 6 ksi at release and 8.5 ksi at service. The mixture proportions for the precast girder SCC are provided in Table A.1.

Table A.1. Girder SCC Mixture Proportions Summary.

Materials		Type	Supplier	Quantity
Cement (lb/yd ³)		III	Alamo Cement	564
Fly Ash (lb/yd ³)		Class F	-	188
Water (lb/yd ³)		-	-	266
Aggregate, lb/yd ³	Coarse (MNAS 3/4 in.)	Limestone	Vulcan (1604 plant)	1499
	Fine	Manufactured Sand	Vulcan (1604 plant)	1359
Admixtures (oz/yd ³)		HRWR	Sika 4100	29.9
		Retarder	Sika	9.0

A.1.1.2 Connections

The CIP concrete for the splice connections was designed to satisfy slump, strength, and practical fabrication requirements. The concrete required a high slump in order to flow through the reinforcement between the girder segments. The connections also needed to reach at least the 8.5 ksi compressive strength at service that was specified for the girder segments. Conventional

concrete (CC) mixture proportions used in a study performed by Trejo et al. (2008) were adapted and tested to find an acceptable connection concrete mix. After several trial batches were tested, the CC mixture proportions were chosen for the connections as shown in Table A.2. The connections were cast using one 4 cubic yard batch.

Table A.2. Splice Concrete Mixture Proportions.

Material		Type	Quantity
Cement (lb/yd ³)		III	700
Water (lb/yd ³)		-	200
w/c ratio		-	0.29
Aggregate (lb/yd ³)	Coarse (MNAS ¾ in.)	River Gravel	1935
	Fine	Mfd. Sand	1232
HRWRA/Superplasticizer (oz/yd ³)		PS 1466	91

A.1.1.3 Deck

After the splice concrete gained sufficient strength, the mild steel and concrete for the deck were placed one week later. A TxDOT Class S concrete with specified 28-day strength of 4 ksi was used for the deck concrete.

A.1.2 Fresh Concrete Properties

A.1.2.1 General

Fresh property tests such as slump, slump flow, and unit weight; and sample fabrication for testing hardened material properties, were conducted on the day of casting the precast girder segments, splice connections, and CIP deck concrete. Representative samples of the concrete mixtures were taken and tested per standard testing procedures (ASTM C172 2010, Tx-407-A 2008). Summaries of the applicable ASTM and TxDOT standards for fresh properties are provided in Table A.3.

Table A.3. Overview of Fresh Property Tests for Concrete.

Property	ASTM Standard	TxDOT Standard
Slump	C143 (2012)	Tex-415-A (2008)
Slump Flow	C1611 (2009)	-
Unit Weight	C138 (2013)	Tex-417-A (2008)
Temperature	C1064 (2012)	Tex-422-A (2008)
Air Content	C231 (2010)	Tex-416-A (2008)

A.1.2.2 Girder Segments

Fresh properties of the SCC for the precast girder segments and ambient conditions on the day of casting are summarized in Table A.4.

Table A.4. Summary of Girder Concrete Fresh Properties.

Batch	Slump Flow (in.)	Unit Weight (kcf)	Air Content (%)	Concrete Temperature (°F)	Ambient Temperature (°F)	RH (%)
B1	26.5	-	8	96	107.4	24.4
B3	26.0	0.146				
B5	22.0	0.144				

A.1.2.3 Connections

The connection mixture was adjusted for aggregate moisture correction factors. The aggregates and approximately one-third of the water were transported in a mixing truck from a local quarry to the TAMU High Bay Structural and Material Testing Laboratory (HBSMTL). The Type III cement, superplasticizer admixture, and remaining water were added at the laboratory.

The Type III cement powder was measured by weight into a one cubic yard hopper. The cement was added to the mix by backing the mix truck into the TAMU HBSMTL and using the laboratory crane to lift the hopper above the truck and deposit the cement. Water was added to the truck monitored by the truck volume meter by gallons. The amount of cement required was more than one cubic yard, so the process was repeated as efficiently as possible in order to maintain

even distribution and avoid clumping of the cement between hopper loads while mixing. One-third of the remaining water was added in between hopper loads to help with the mixing. The superplasticizer was mixed with water separately in nine 5-gallon buckets and then added manually to the truck between loading the cement. Figure A.1(a) depicts adding pre-measured barrels of cement powder to fill the hopper. Figure A.1(b) illustrates the first hopper of cement powder being added to the concrete mix truck. Figure A.1(c) displays the addition of the superplasticizer water being added to the mixture after the first hopper of cement was added. The concrete was mixed in the truck continually throughout the process for a total of 28 minutes.



(a) Measuring cement into hopper



(b) Adding cement to truck



(c) Adding admixture-water mix to truck

Figure A.1. Adding Materials to Concrete Mixture.

A sample of the fresh concrete was taken and the slump was measured to be 10 in. The concrete was observed to not be mixed adequately so the concrete was mixed for three to five more minutes and the slump measured again. The initial slump was found to be 9.75 in., and by observation the mix was acceptable to begin the process of pouring the connections. The slump was monitored throughout the pour at certain time intervals and recorded in Table A.5. The measured unit weight was 0.151 kcf.

Table A.5. Slump of Connection Concrete.

Time	Slump (in.)	Notes
3:50 pm	9.75	Begin casting, sampled from truck
4:03 pm	9.50	Sampled from truck
4:17 pm	9.25	Sampled from truck
4:38 pm	9.25	End of casting, sampled from hopper

Fresh concrete for the test samples were taken directly from the truck into wheelbarrows as needed throughout the pour. All connection concrete samples were cured and stored with the same specifications as the girder samples. However, due to unforeseen maintenance issues with the curing room sprayers the connection samples were not kept at a constant high humidity and some moisture was lost. The temperature and RH of the room were monitored. The temperature stayed constant ± 73 °F and the research team periodically wet the samples.

A.1.2.4 Deck

Fresh properties for the conventional CIP deck concrete were monitored and are summarized in Table A.6.

Table A.6. Summary of Deck Concrete Fresh Properties.

Batch	Slump (in.)	Unit Weight (kcf)	Air Content (%)	Concrete Temperature (°F)	Ambient Temperature (°F)	RH (%)
B1	4.5	0.144	5.0	68	70	48
B2	3.0	0.147	5.2	67		

The deck samples faced similar issues as the connection samples in terms of curing of samples and moisture loss. The same process was used to monitor and wet the samples.

A.1.3 Hardened Concrete Properties

A.1.3.1 General

Hardened mechanical property tests, such as compressive strength, modulus of rupture (MOR), splitting tensile strength (STS), and modulus of elasticity (MOE) are measured based on different test sample ages per standard test methods (ASTM C39, C78, C496, and C469, respectively). Shrinkage testing (ASTM C596) and creep testing (ASTM C512) were also conducted to provide

information on the general long-term behavior of the concrete. Summaries of the applicable ASTM and TxDOT standards for hardened properties are provided in Table A.7. All laboratory concrete samples were made and cured in accordance with ASTM and TxDOT testing procedures (ASTM C31 2003 and Tex-447-A 2008).

Table A.7. Overview of Hardened Property Tests for Concrete.

Property	ASTM Standard	TxDOT Standard	Recommended Test Age
Compression Strength	C39 (2012)	Tex-418-A (2008)	1, 3, 28, 90 days
Modulus of Elasticity	C469 (2010)	-	As desired
Splitting Tensile Strength	C496 (2011)	Tex-421-A (2008)	28 days
Modulus of Rupture	C78 (2010)	Tex-448-A (2008)	As desired
Shrinkage	C596 (2009)	-	1, 2, 3, 4 weeks
Creep	C512 (2010)	-	-

Table A.8 summarizes the test matrix and the test ages of standard mechanical property tests conducted for the precast girder concrete by batch. Three samples were made for each test age. MOE and STS samples were made for Batches 2, 4, and 6. Batches 4 and 6 were chosen to be representative for MOR samples. However, on the day of casting, limited concrete was available for sampling from Batch 4, so only three MOR beam samples were made for Batch 4 instead of the originally planned nine samples.

Table A.8. Test Matrix for Spliced Girder Segment Concrete by Batch.

Age	f'_c	MOE	MOR	STS
3 days	B2, B4, B6	-	-	-
7 days	B1 - B8	B2, B4, B6	B6	B2, B4, B6
28 days	B1 - B8	B2, B4, B6	B4, B6	B2, B4, B6
56 days	B2, B4, B6	B2, B4, B6	B6	B2, B4, B6
91 days	B2, B4, B6	-	-	-
Test Day (222 days)	B2, B4, B6	-	-	-

All cylinder and beam test samples for the SCC girder segments were covered and left to cure overnight next to the full-scale specimen. The following day the samples were transported back to the TAMU laboratory facilities. The samples were then de-molded and moved to the appropriate curing room environments.

A.1.3.2 Compressive Strength

Compressive strength samples were fabricated and tested for the girder, connection, and deck concrete. All batches have been graphed and the overall f'_c of the spliced girder is illustrated in Figure A.2. The relationships of strength gain are broken down further in the following sections.

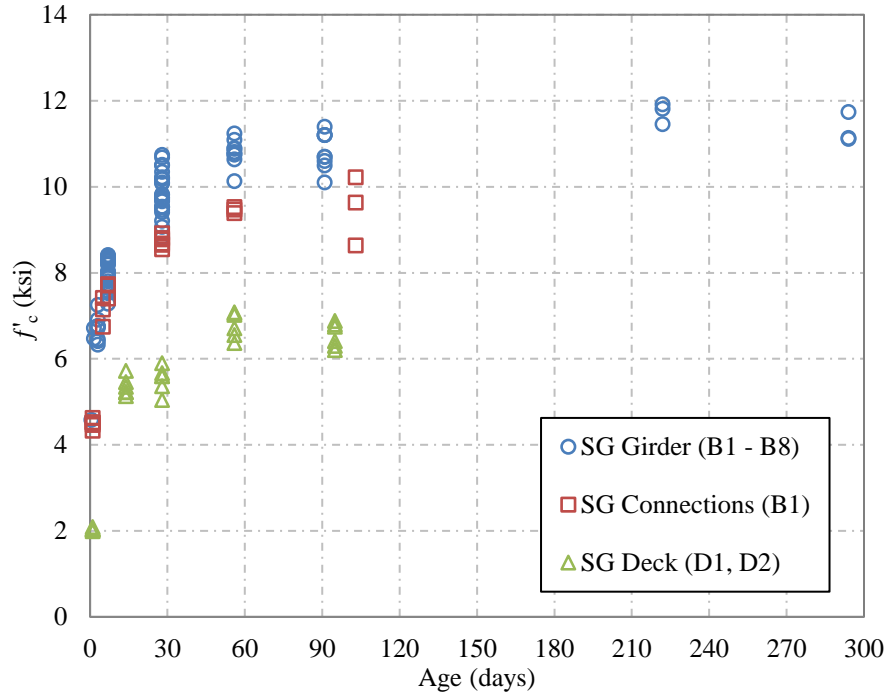
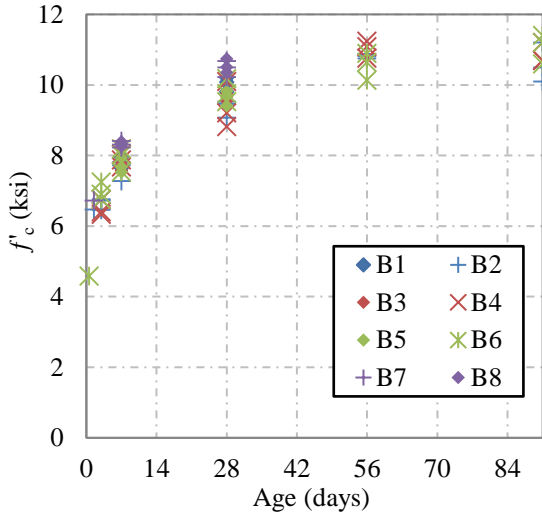


Figure A.2. Spliced Girder Concrete Compressive Strength Data.

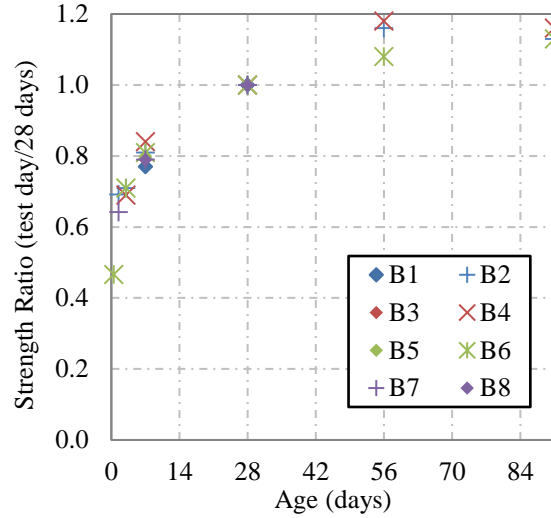
A.1.3.2.1 Girder Segments

Compressive strength samples were made for all eight girder batches. Compression strength tests were performed at 13 hours and at release (37 hours) by the precaster. Day of testing samples were tested two days prior to the first full-scale specimen test for the purpose of refining design calculations and predictions of the loads corresponding to different failure modes.

The development of compressive strength from 1 day to 91 days and the ratio of compressive strength at each test age compared to the average 28-day strength of the corresponding batch can be seen in Figure A.3. The high early strength achieved at 3 days is approximately 70 percent of the 28-day strength of each batch.



(a) f'_c versus time



(b) Compressive strength ratio

Figure A.3. Girder Concrete Compressive Strength Experimental Data.

The average compressive strength gain for each batch can be seen in Figure A.4. The average 3-day compressive strength for girder Batches 2, 4, and 6 was almost 7 ksi. The target concrete compressive strength at service of 8.5 ksi was exceeded for all batches by up to 2 ksi. The 7-day, 28-day, and 56-day compressive strengths for Batch 2, 4, and 6 are reported in Table A.9. The average compressive strength of the girder concrete reached by 91 days was 10.8 ksi.

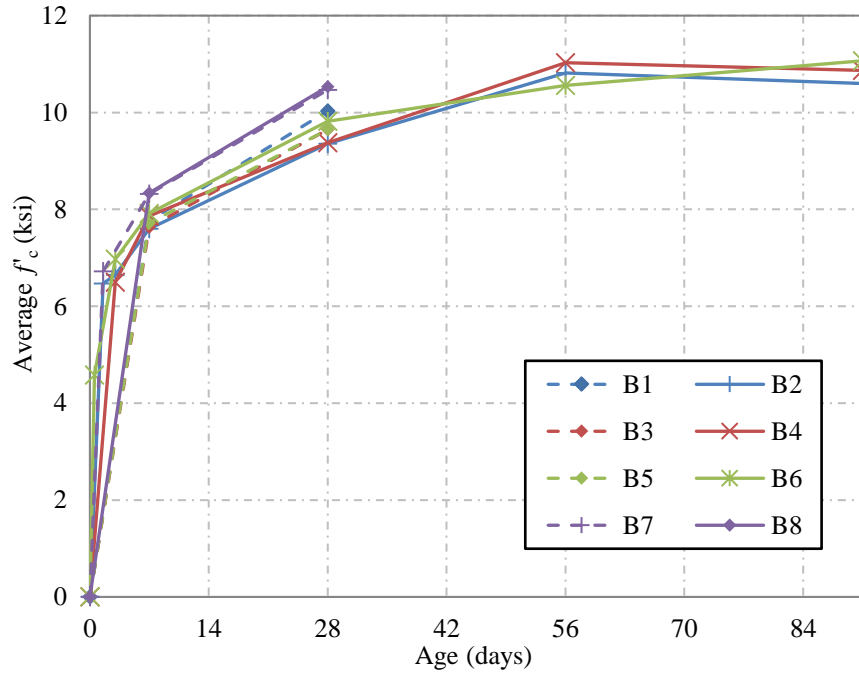


Figure A.4. Girder Concrete Average Compressive Strength Experimental Data.

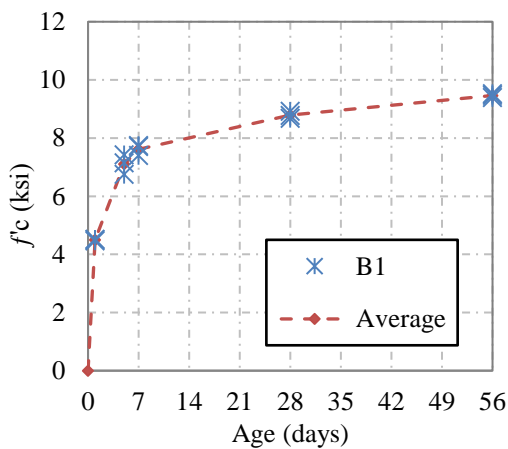
Table A.9. Girder Concrete Average Measured Compressive Strength (ksi).

Age	B1	B2	B3	B4	B5	B6	B7	B8
13 hours	-	-	-	-	-	4.58	-	-
At Release (37 hours)	-	6.47	-	-	-	-	6.72	-
3 days	-	6.65	-	6.50	-	6.97	-	-
7 days	7.77	7.60	7.63	7.87	7.72	7.91	8.32	8.34
28 days	10.0	9.35	9.65	9.38	9.65	9.82	10.5	10.5
56 days	-	10.8	-	11.0	-	10.6	-	-
91 days	-	10.6	-	10.9	-	11.1	-	-
Day of Test (222 days)	-	11.7	-	-	-	-	-	-
After Testing (294 days)	-	-	-	11.4	-	11.1	-	-

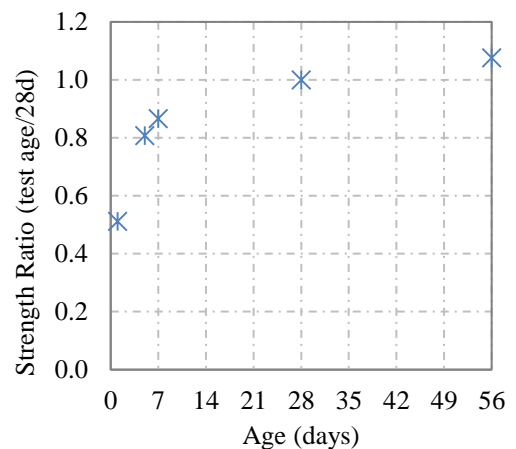
A.1.3.2.2 Connections

Compressive strength development of the splice connection concrete from 1 day to 56 days is shown in Figure A.5. All specimens were fabricated from the same batch. On the day of testing for the spliced girder, the compressive strength of the connection concrete samples (test age of 103 days) was 9.5 ksi.

The benefit of the use of Type III cement for high early strength can be seen in Figure A.5. Within three days the compressive strength was already 50 percent of the 28-day strength. The strength increase was rapid; the 7-day compressive strength was 87 percent of the 28-day strength. While Type III cement was selected for the connection concrete for the laboratory specimen, it is noted that typical field applications generally call for Type I/II cement, which provides a longer period of workability. Table A.10 provides the average compressive strength results at each age.



(a) f'_c versus time



(b) Compressive strength ratio

Figure A.5. Connection Concrete Compressive Strength Experimental Data.

Table A.10. Connection Concrete Average Measured Compressive Strength.

Age	f'_c (ksi)
1 day	4.50
5 days	7.11
7 days	7.62
28 days	8.79
56 days	9.46
Day of Test (103 days)	9.50

A.1.3.2.3 Deck

The development of compressive strength of the deck concrete from 1 day to 56 days and the ratio of compressive strength at each test age compared to the average 28-day strength of the corresponding batch can be seen in Figure A.6.

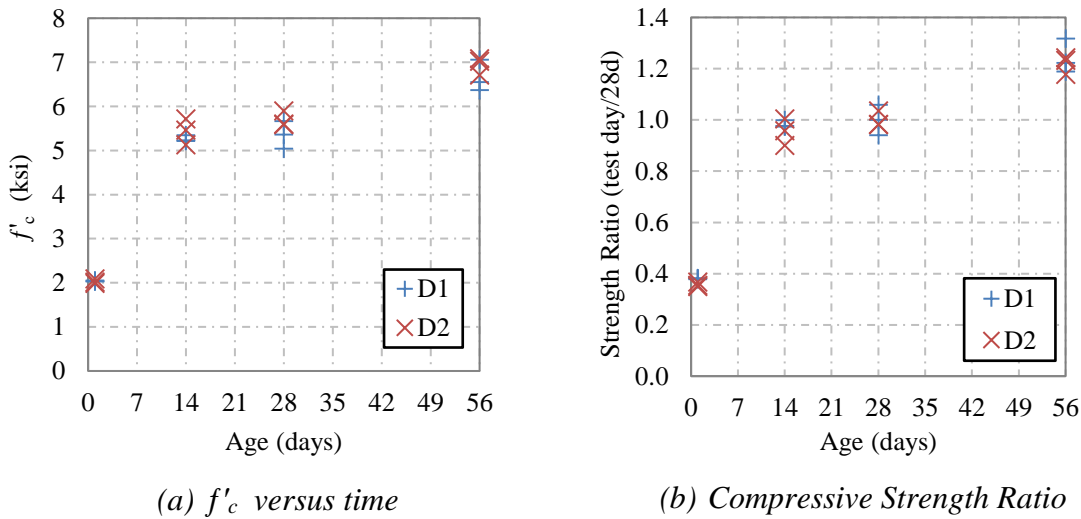


Figure A.6. Deck Concrete Compressive Strength Experimental Data.

On the day of testing for the spliced girder, the compressive strength of the deck concrete (test age of 95 days) was an average of 6.56 ksi. The 1-day compressive strength of the deck concrete was 40 percent of the 28-day strength; and by 14 days the deck concrete achieved at least

90 percent of the 28-day compressive strength. Table A.11 reports the average compressive strength results for the deck batches.

Table A.11. Deck Concrete Average Measured Compressive Strength.

Age	B1 (ksi)	B2 (ksi)
1 day	2.04	2.03
14 days	5.27	5.44
28 days	5.36	5.70
56 days	6.66	6.94
Day of Test (95 days)	6.81	6.30

A.1.3.3 Modulus of Elasticity

MOE samples were fabricated and tested for the girder, connection, and deck concrete. All batches are graphed and the overall MOE of the spliced girder is illustrated in Figure A.7.

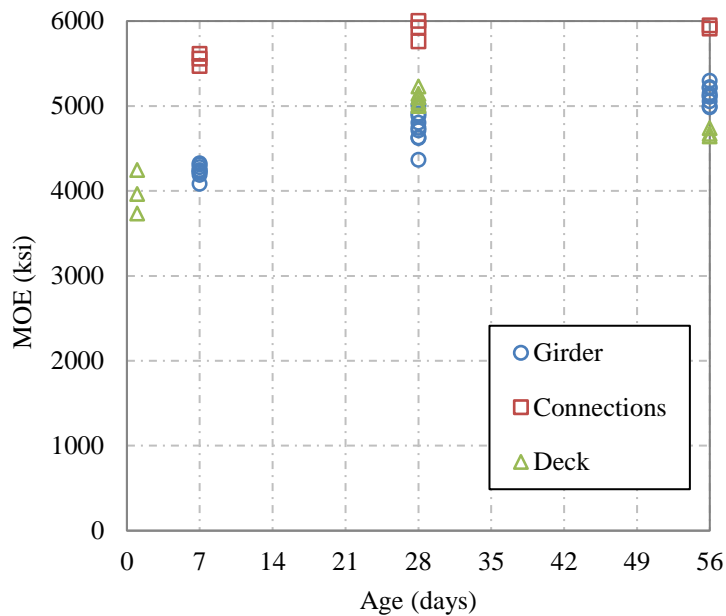


Figure A.7. Spliced Girder MOE Experimental Data.

A.1.3.3.1 Girder Segments

MOE samples were made for the precast girder Batches 2, 4, and 6. Batch 4 samples yielded more consistent results at each age than the other two batches. Figure A.8 shows the MOE development of the samples over time and compares the MOE to the average compressive strength at each age.

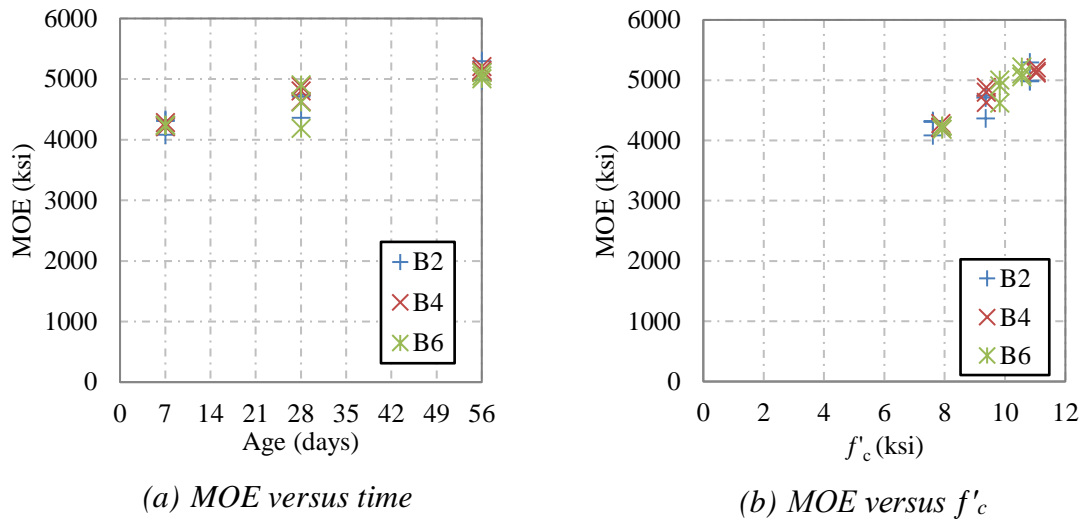


Figure A.8. Girder Concrete MOE Experimental Data.

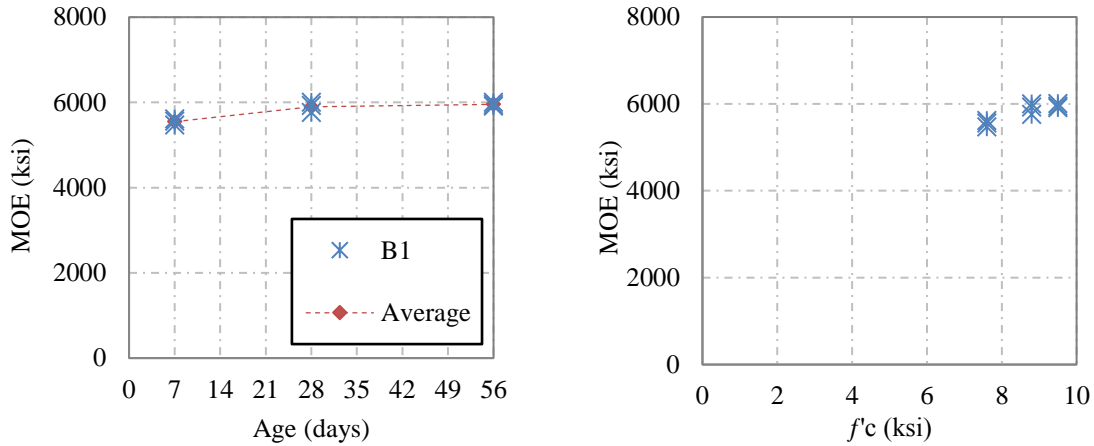
The experimental data shows that by seven days, the MOE was over 4000 ksi and only increased by 1000 ksi between 7 and 56 days. The average experimental MOE values for each batch and age tested are reported in Table A.12.

Table A.12. Girder Concrete Average Measured MOE (ksi) by Batch.

Age	B2	B4	B6
7 days	4239	4240	4224
28 days	4607	4772	4845
56 days	5091	5158	5128

A.1.3.3.2 Connections

The development of MOE from 7 days to 56 days can be seen in Figure A.9. The connection CC 28-day MOE was over 1000 ksi higher than the girder SCC MOE values. All specimens are from the same batch.



(a) MOE versus time

(b) MOE versus f'_c

Figure A.9. Connection Concrete MOE Experimental Data.

The experimental data shows that by seven days, the MOE was over 5500 ksi and increased by less than 500 ksi between 7 and 56 days. The average experimental MOE values for each age tested are reported in Table A.13.

Table A.13. Connection Concrete Average Measured MOE.

Age	MOE (ksi)
7 days	5548
28 days	5895
56 days	5954

A.1.3.3.3 Deck

The development of MOE from 7 days to 56 days can be seen in Figure A.10. The average experimental MOE values for each age tested are reported in Table A.14.

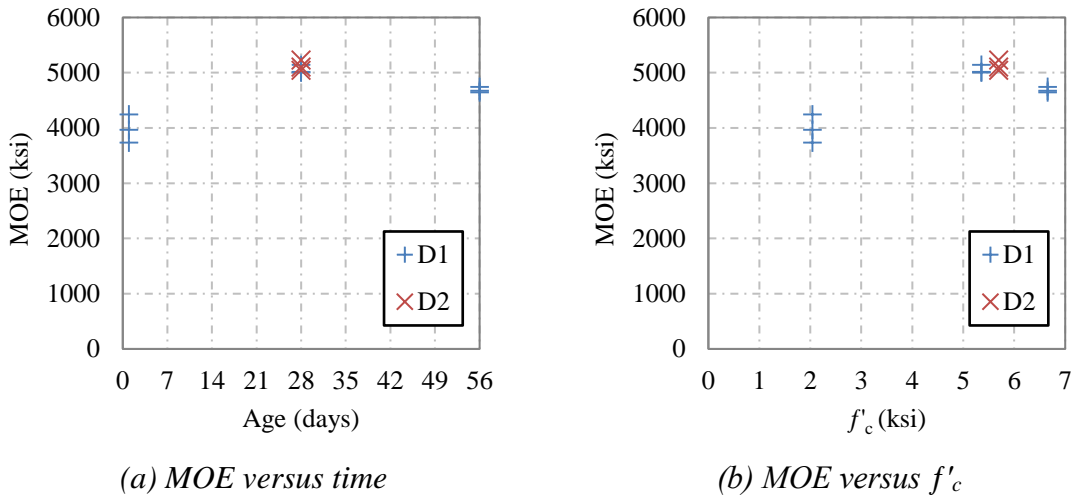


Figure A.10. Deck Concrete MOE Experimental Data.

The experimental data show the initial MOE at one day was almost 4000 ksi and increased by over 1000 ksi at 28 days. The MOE decreased by 500 ksi between 28 and 56 days. This trend was observed by averaging three samples at each age. Note that each experimental value was within the acceptable coefficient of variation.

Table A.14. Deck Concrete Average Measured MOE (ksi) by Batch.

Age	B1	B2
1 day	3981	-
28 days	5052	5125
56 days	4684	-

A.1.3.4 Splitting Tensile Strength

The STS data for the girder, connection, and deck concrete were graphed, and the overall trend is illustrated in Figure A.11.

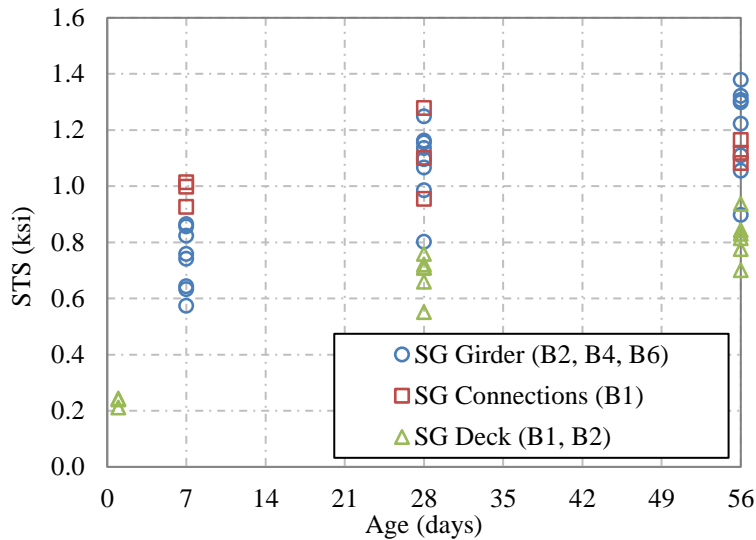


Figure A.11. Spliced Girder STS Experimental Data.

A.1.3.4.1 Girder Segments

STS samples were tested for precast girder Batches 2, 4, and 6. Figure A.12 shows the development of STS over time as well as the development of STS versus the average compressive strength at each age.

Although Batch 6 had a lower average STS at seven days, it had the highest average STS at 28 and 56 days. Batch 2 consistently had the minimum individual STS value at each test age. The average experimental STS values for each batch and age tested are reported in Table A.15.

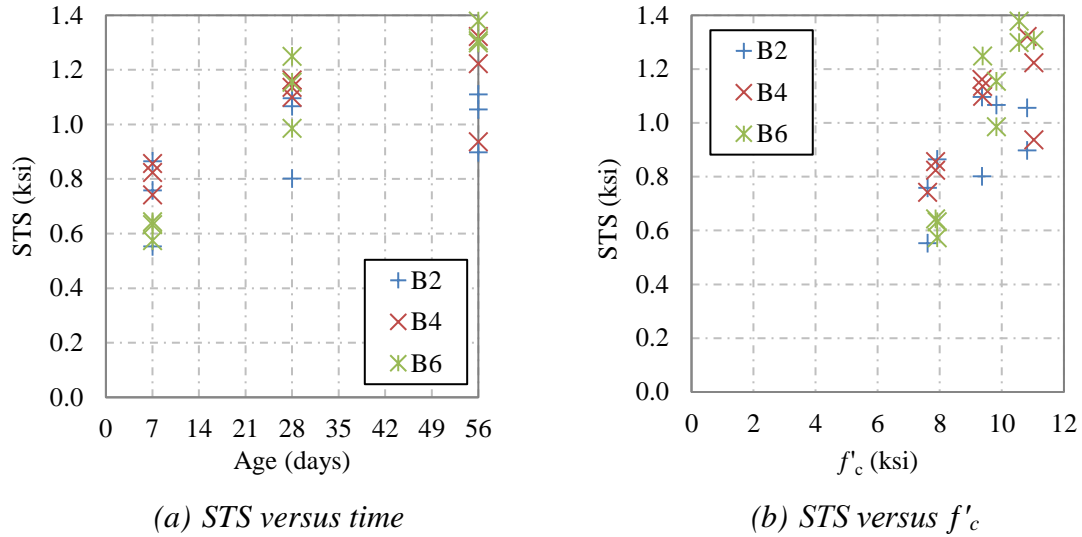


Figure A.12. Girder Concrete STS Experimental Data.

Table A.15. Girder Concrete Average STS (ksi) by Batch.

Age	B2	B4	B6
7 days	0.726	0.807	0.617
28 days	0.988	1.13	1.13
56 days	1.02	1.16	1.33

A.1.3.4.2 Connections

The development of STS for the connection concrete from 7 days to 56 days can be seen in Figure A.13. The average experimental STS values for each age tested are reported in Table A.16.

The STS for the connection concrete on the day of testing the spliced girder specimen (test age of 103 days) was 0.999 ksi. All specimens were from the same batch. By seven days the connection concrete STS reached 0.979 ksi and increased to 1.12 ksi by 56 days. However, the measured STS of the connection concrete on the day of the girder test was about 10 percent lower than the average at 56 days. As discussed by Ozyildirim and Carino (2006), the STS when compared to compressive strength does not remain constant but decreases as compressive strength increases.

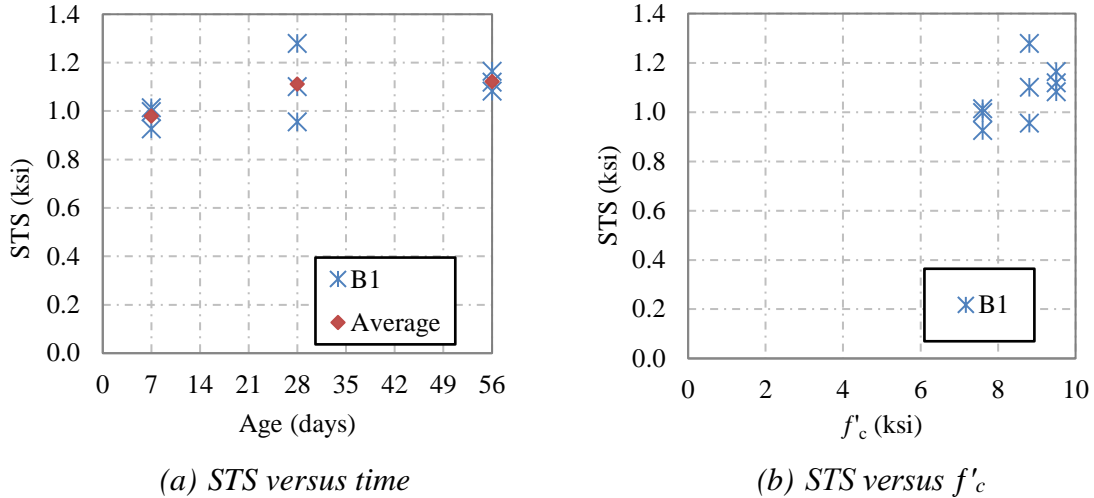


Figure A.13. Connection Concrete STS Data.

Table A.16. Connection Concrete Average Measured STS.

Age	STS (ksi)
7 days	0.979
28 days	1.11
56 days	1.12
Day of Test (103 days)	0.999

A.1.3.4.3 Deck

The development of STS for the deck concrete up to 56 days can be seen in Figure A.14. The average experimental STS values for each age tested are reported in Table A.17. The experimental data depicts the initial STS of the deck concrete at one day was slightly over 0.2 ksi and increased by about 0.45 ksi at 28 days. The STS increased by 0.13 ksi between 28 and 56 days.

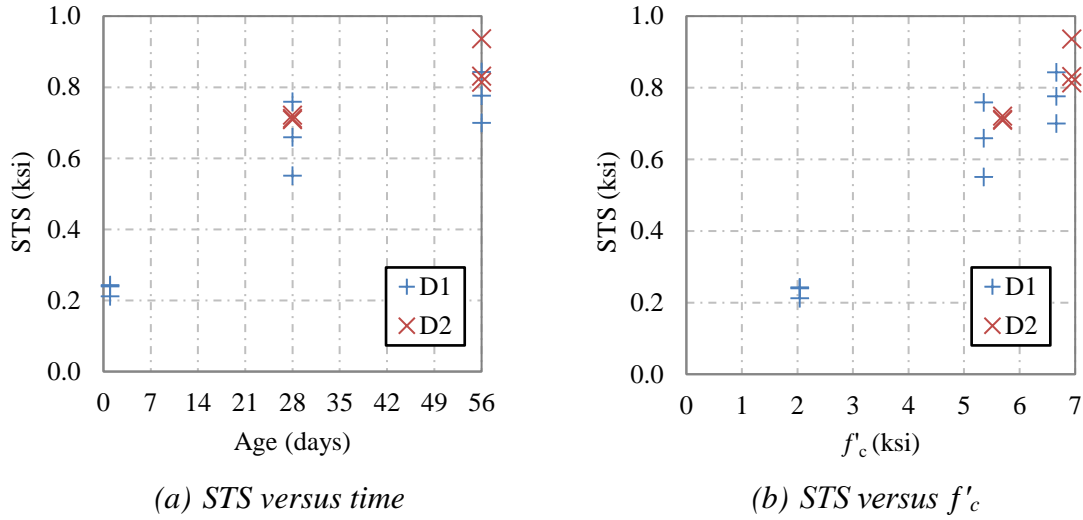


Figure A.14. Deck Concrete STS Experimental Data.

Table A.17. Deck Concrete Average Measured STS (ksi) by Batch.

Age	B1	B2
1 day	0.232	-
28 days	0.656	0.714
56 days	0.773	0.860

A.1.3.5 Modulus of Rupture

MOR samples were fabricated and tested for the girder, connection, and deck concrete. All batches have been graphed and the overall MOE of the spliced girder is illustrated in Figure A.15.

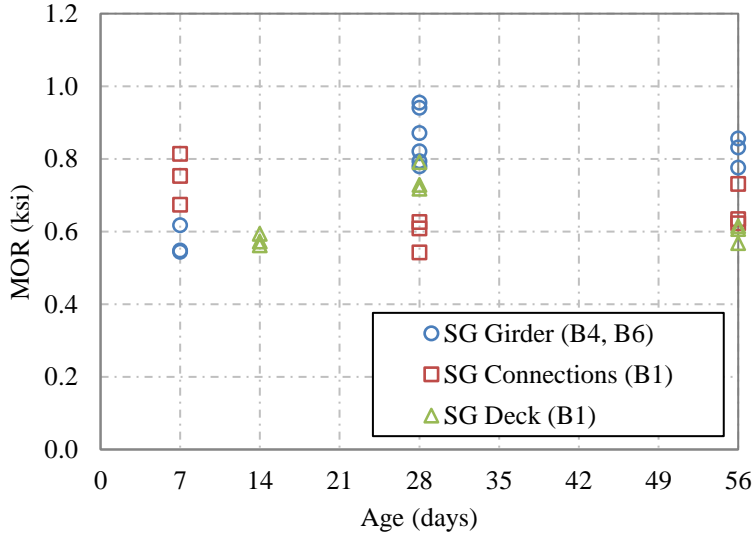


Figure A.15. Spliced Girder MOR Experimental Data.

A.1.3.5.1 Girder Segments

MOR samples were made for Batch 4 at 28 days and Batch 6 at 7, 28, and 56 days. Figure A.16 shows the development of MOR over time as well as the development of MOR versus the average compressive strength at each age. The MOR for Batch 6 increased by 75 percent from 7 to 28 days but the measured MOR was lower at 56 days. The average experimental MOR values for each batch and age tested are reported in Table A.18.

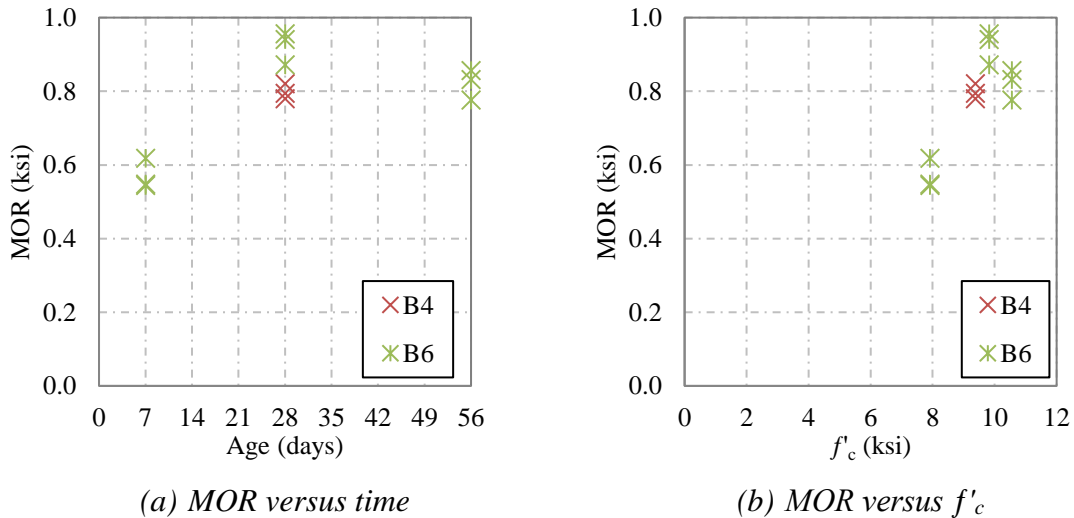


Figure A.16. Girder Concrete MOR Data.

Table A.18. Girder Concrete Average MOR (ksi) by Batch.

Age	B4	B6
7 days	-	0.570
28 days	0.798	0.923
56 days	-	0.821

A.1.3.5.2 Connections

The development of MOR for the connection concrete from 7 days to 56 days can be seen in Figure A.17. The average experimental MOR values for each age tested are reported in Table A.19. All specimens are from the same batch.

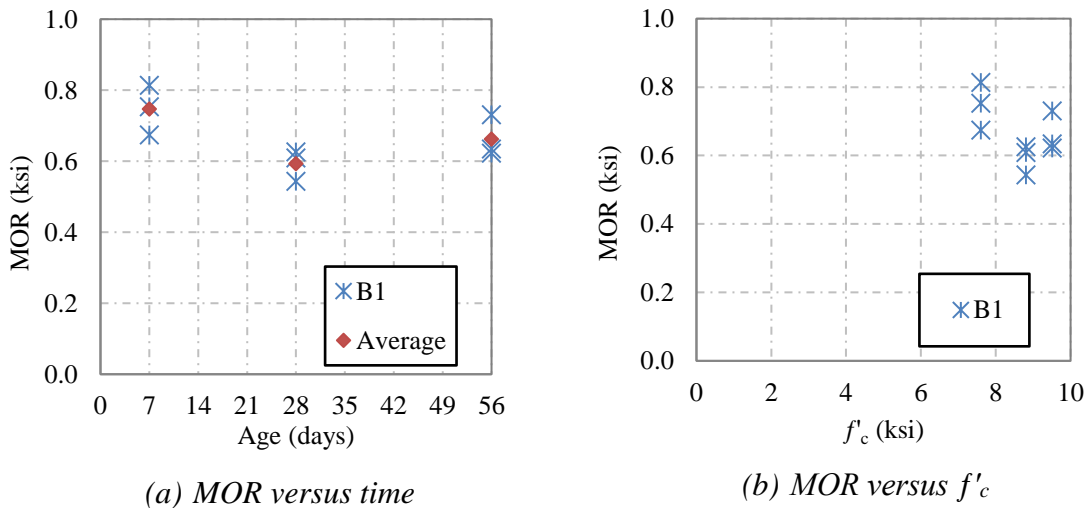


Figure A.17. Connection Concrete MOR Data.

Table A.19. Connection Concrete Average Measured MOR.

Age	MOR (ksi)
7 days	0.747
28 days	0.593
56 days	0.662

A.1.3.5.3 Deck

The development of MOR for Batch 1 of the deck concrete from 7 days to 56 days is shown in Figure A.18. The average experimental MOR values for each age tested are reported in Table A.20.

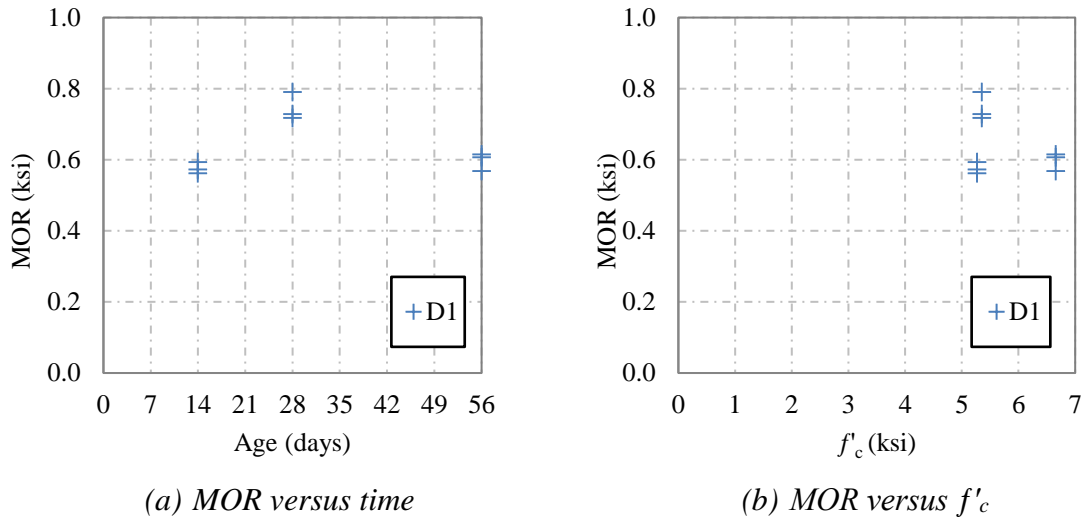


Figure A.18. Deck Concrete MOR Experimental Data.

Table A.20. Deck Concrete Average Measured MOR.

Age	MOR (ksi)
14 days	0.576
28 days	0.746
56 days	0.597

A.1.3.6 Shrinkage

Four prisms for shrinkage testing were cast for each of girder Batches 2, 4, and 6. However, only three prisms were tested for Batch 6. The shrinkage results are plotted in Figure A.19. Shrinkage readings are reported as positive values. Negative values indicate initial expansion of the concrete at early ages. The maximum magnitude of shrinkage strain was about 0.0003 at 280 days.

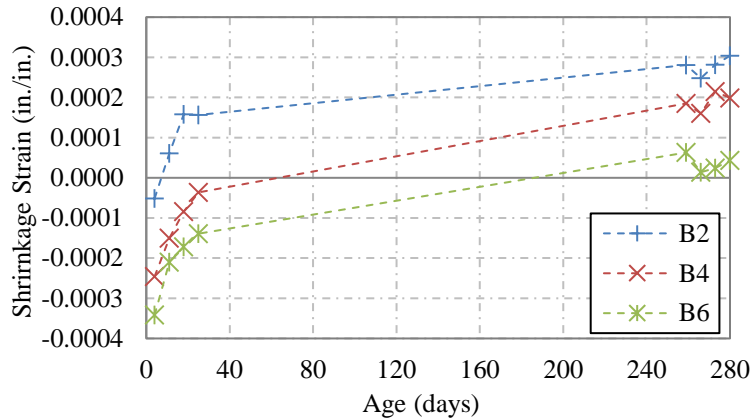


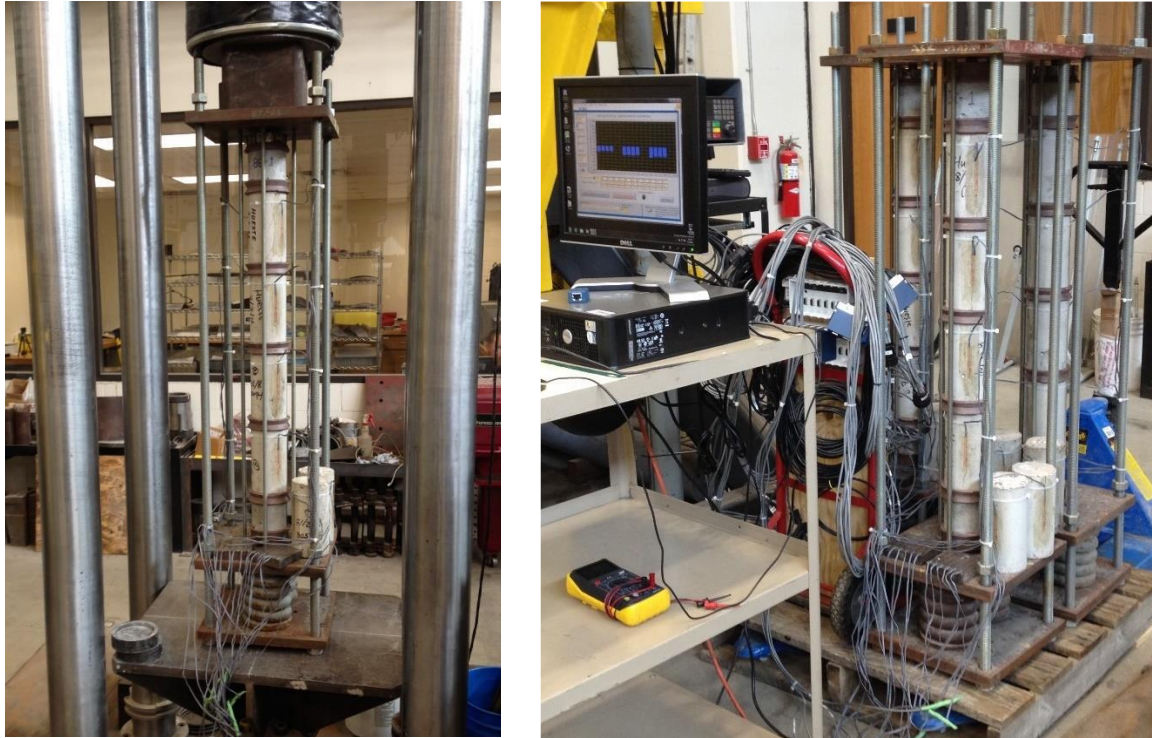
Figure A.19. Spliced Girder Shrinkage Data.

A.1.3.7 Creep

Cylinders from Batches 2, 4 and 6 (taken on August 7, 2013) from the precast girder concrete were used to perform the creep testing. Three creep frames were used. Each frame was composed of three steel plates, four rods, and two springs as shown in Figure A.20. The springs were located at the base of the frame between the two bottom steel plates. Four concrete cylinders were stacked between two half concrete cylinders (top and bottom) and all the cylinders were compressed between two steel plates. Each frame required seven cylinders, five which were loaded in compression in the creep frame (four plus two halves) and two that were outside of the frame and used as a reference for shrinkage. Each cylinder (except the half cylinders) was gaged longitudinally on opposite sides. Cylinders compressed in the frame were sulfur capped to ensure that the proper alignment between them was maintained. In addition, two steel plates were gaged (six gages per plate) to compensate for temperature strains. To summarize, each creep frame requires seven cylinders, two steel plates (for temperature effects) and 24 strain gages total.

Table A.21 presents the target and actual forces applied to each creep frame. Each frame was loaded to varying levels of force as a function of the compressive strength f'_c at the time of loading, as shown in Table A.21. This was done to provide a general understanding of the relative creep effects under the varying levels of sustained compression provided by the pretensioning alone, post-tensioning alone, and combined pretensioning and post-tensioning experienced by the precast girder segments during the specimen construction. Measured strain data for the creep samples were recorded from the time the samples were loaded. Data were recorded at one-second intervals during load application to capture the effect of elastic shortening on the concrete cylinders

in the frames. After loading, the frequency of data recording was decreased to 20 minutes to measure the effect of creep over time.



(a) Loading the Creep Frame (b) Creep Frames Loaded and Recording Data

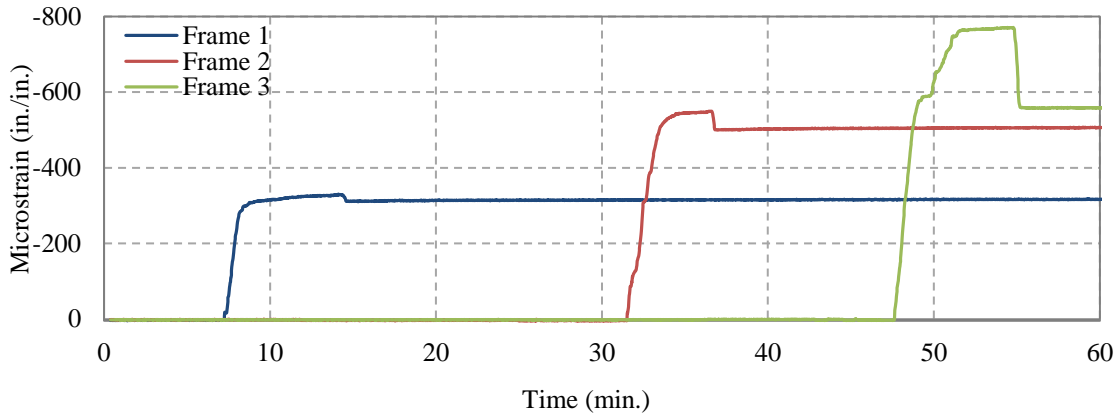
Figure A.20. Loading of the Creep Frames

Table A.21. Force Applied to the Creep Frames

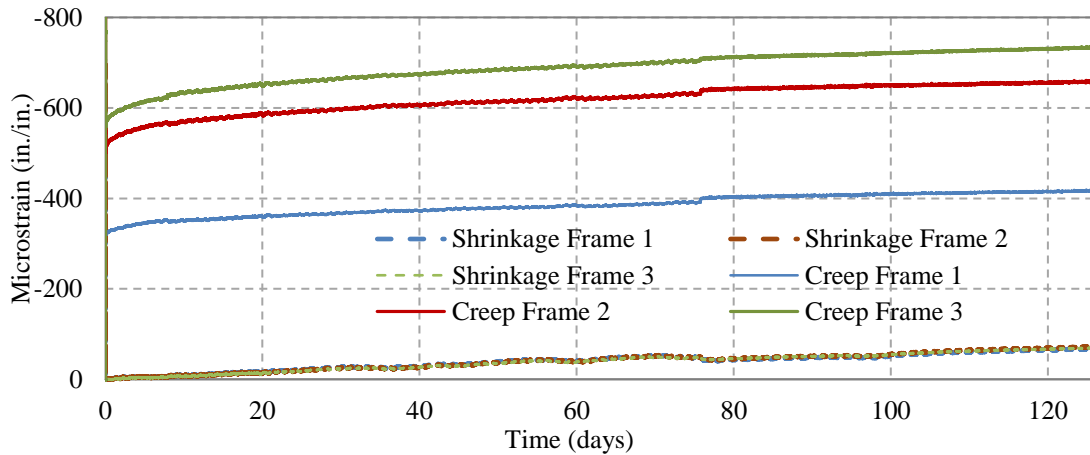
Loading	Desired Force (kips)	Applied Force (kips)
Frame 1	$0.15 f'_c = 21.5$	21.5
Frame 2	$0.25 f'_c = 35.9$	34.6
Frame 3	$0.35 f'_c = 50.3$	38.2

Figure A.21 presents the evolution of compressive strain as a function of time, where the negative values represent compression. The first graph shows the compressive strain during loading and the second graph shows the data obtained over 126 days. The effect of creep is clear as the compressive creep strain increases over time. The shrinkage measurements for the unloaded control cylinders are shown as well. The three frames show the same rate of shrinkage. This effect

has been subtracted from the actual data in order to show the effect of creep only for the data provided in the graph. Note that the slight jump in the data around day 75 can be attributed to the creep frames being physically moved to another room in the lab.



(a) Data during the loading of the frames.



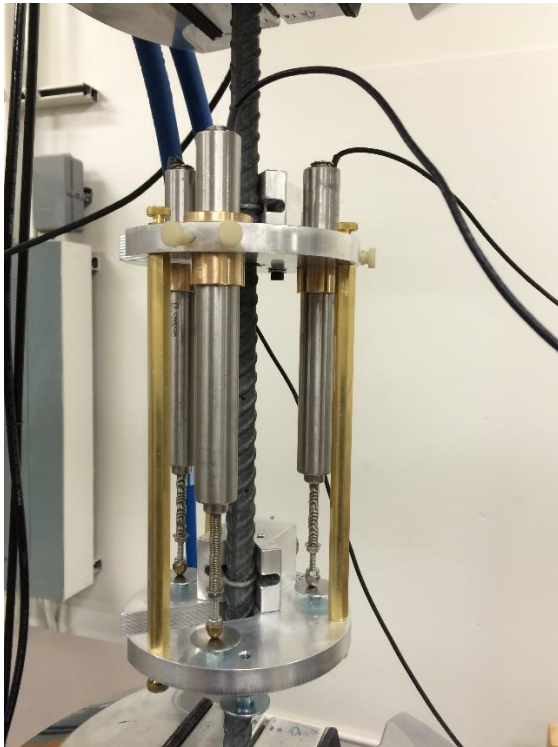
(b) Data from the creep frames over 126 days.

Figure A.21. Data from the Creep Frames.

A.2 MILD STEEL

Stress-strain tests were carried out on #5 and #6 bars based on the ASTM A370-A8 standard. Tests were conducted on five #5 and five #6 bars. The grip-to-grip distance of the device was 16 in. An extensometer consisting of three LVDTs was used to measure the elongation, and the average of the three readings is report. The gage length was set to 8 in. as recommended in Article A9.3.1 of

the ASTM A370. A MTS hydraulic jack with displacement control was used to load the specimen. Figure A.22 shows the test setup and a typical failure of a reinforcing bar.



(a) Test Setup



(b) Failure within the Gage Area

Figure A.22. Mild Steel Stress-Strain Test.

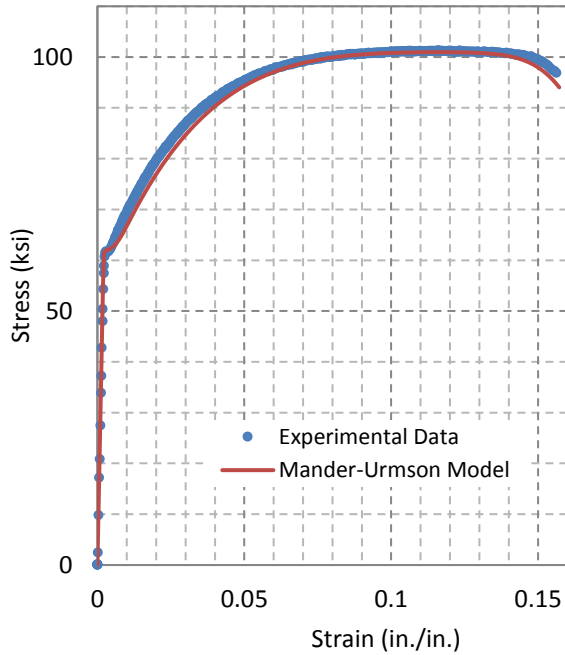
Table A.22 and Table A.23 present the results of the stress-strain tests on the #5 and #6 bars, respectively. Figure A.23 depicts typical stress-strain curves for the #5 and #6 mild steel bars based on experimental results and compares it with the Urmson-Mander (2012) model that was used in the numerical modeling.

Table A.22. Mechanical Properties of #5 Bars.

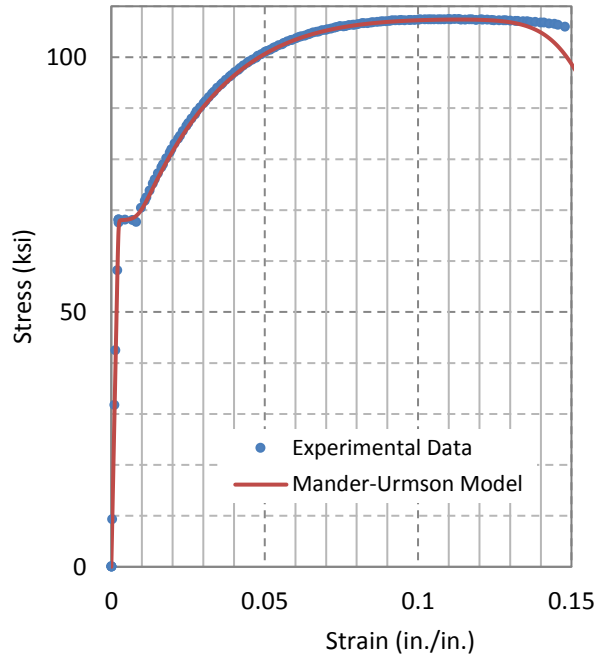
Test #	Loading Rate, in./sec.	Yield Stress (f_y), ksi	Young's Modulus (E), ksi	Ultimate Stress (f_{su}), ksi	Ultimate Strain (ϵ_{su}), in./in.
1	0.0167	65.1	29,868	101.6	0.133
2	0.0084	63.5	27,578	105.8	0.122
3	0.0020	60.5	28,900	99.1	0.182
4	0.0050	61.7	27,753	101.3	0.157
5	0.0050	62.3	27,273	102.0	0.168
Average	-	62.6	28,275	102.0	0.152

Table A.23. Mechanical Properties of #6 Bars.

Test #	Loading Rate, in./sec.	Yield Stress (f_y), ksi	Young's Modulus (E), ksi	Ultimate Stress (f_{su}), ksi	Ultimate Strain (ϵ_{su}), in./in.
1	0.0167	68.1	29,109	107.5	0.156
2	0.0084	68.0	29,096	107.5	0.155
3	0.0050	67.5	30,299	107.3	0.153
4	0.0050	67.9	29,587	107.3	0.168
5	0.0084	68.2	28,599	107.6	0.168
Average	-	67.9	29338	107.4	0.160



(a) #5 Rebar



(b) #6 Rebar

Figure A.23. Stress-Strain Curve for Mild Steel.

A.3 PRESTRESSING STRAND

Tensile strength test was carried out on five 0.6 in. diameter prestressing strands. An MTS hydraulic jack was used to pull the specimens. The grip-to-grip distance was 16 in., as specified by ASTM A370-A8. An extensometer with three LVDTs having a gage length of 8 in. was used to measure the strain. Because the wires started untwisting after reaching their yield strength, the gage was removed after yielding occurred. Figure A.24 presents the test setup and failure of the specimen. Table A.24 summarizes the loading rates for each test and mechanical properties of the strands. Stresses were determined using the nominal area.



(a) Test Setup

(b) Untwisting after Yielding

(c) Failure at Grip

Figure A.24. Prestressing Strand Tensile Test.

Table A.24. Mechanical Properties of Prestressing Strands.

Test #	Loading Rate, in./sec	Yield Stress (f_y), ksi	Young's Modulus (E), ksi	Ultimate Strength, ksi
1	0.0167	213	27,936	272.6
2	0.0167	211	28,635	271.9
3	0.0084	207	28,581	271.8
4	0.0084	203	28,538	273.3
5	0.0050	201	28476	272.7

APPENDIX B.
DETAILED DRAWINGS OF CONTINUOUS PRECAST PRESTRESSED
CONCRETE BRIDGE GIRDER SPECIMEN

CONTINUOUS PRECAST PRESTRESSED CONCRETE GIRDER BRIDGE SPECIMEN CONSTRUCTION AT TEXAS A&M UNIVERSITY

TXDOT PROJECT NO. 0-6651

TEXAS A&M TRANSPORTATION INSTITUTE
TEXAS A&M UNIVERSITY
COLLEGE STATION, TEXAS

TEXAS A&M TRANSPORTATION INSTITUTE
TEXAS A&M UNIVERSITY

CONTINUOUS PRESTRESSED CONCRETE
GIRDER BRIDGES

COVER SHEET (R1)

TXDOT PROJECT NO.	DRAWING NO.	DATE
0-6651	S6651-0	03/07/2014

GENERAL NOTES

GOVERNING CRITERIA

1. AASHTO LRFD BRIDGE DESIGN SPECIFICATIONS (2012).
2. TXDOT BRIDGE DESIGN MANUAL – LRFD (2011).
3. TXDOT STANDARD SPECIFICATIONS FOR CONSTRUCTION AND MAINTENANCE OF HIGHWAYS, STREETS AND BRIDGES (2004). THESE SPECIFICATIONS CAN BE FOUND AT <ftp://ftp.dot.state.tx.us/pub/txdot-info/des/specs/specbook.pdf>
 - PRECAST PRESTRESSED CONCRETE STRUCTURAL MEMBERS SHALL BE IN ACCORDANCE WITH ITEM 425.
 - CONCRETE SHALL BE IN ACCORDANCE WITH ITEM 421.
 - PRESTRESSING SHALL BE IN ACCORDANCE WITH ITEM 426.
 - REINFORCING STEEL SHALL BE IN ACCORDANCE WITH ITEM 440.

MATERIALS

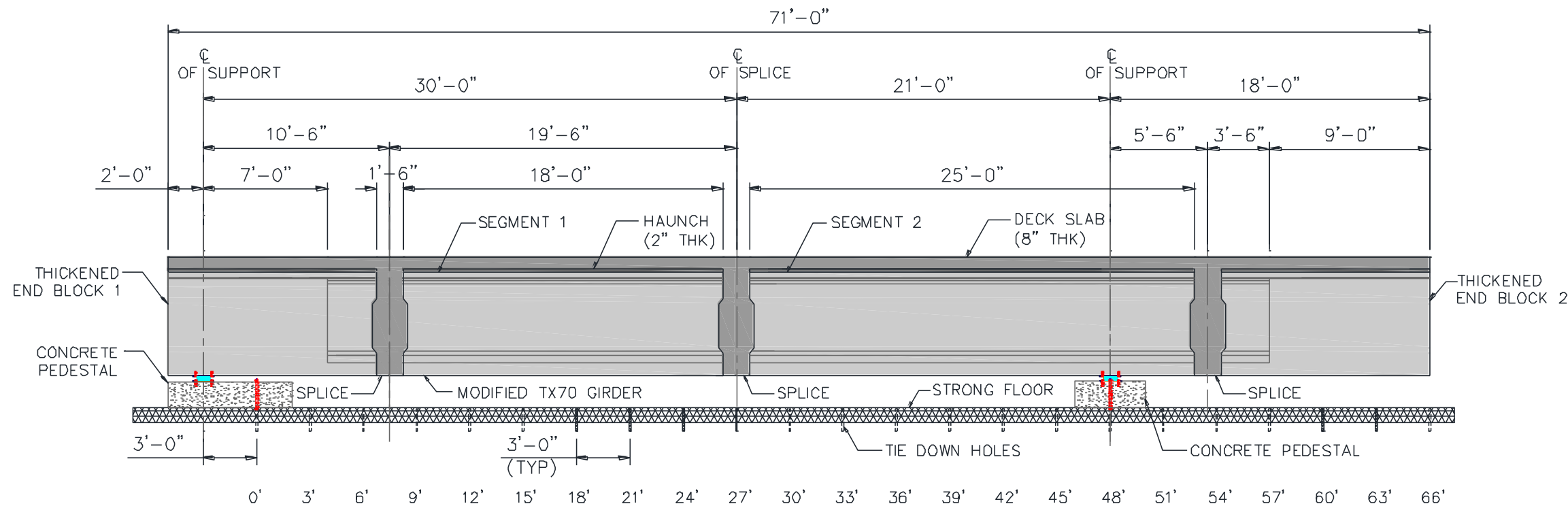
1. ALL CONCRETE SHALL BE TXDOT CLASS H CONCRETE WITH MINIMUM RELEASE STRENGTH $f'_{ci} = 6.5$ ksi AND MINIMUM SERVICE STRENGTH $f'_c = 8.5$ ksi (SEE TXDOT STANDARD SPECIFICATION ITEM 421). THE CONCRETE SHALL BE A SELF-CONSOLIDATING CONCRETE MIX THAT HAS RECEIVED TXDOT APPROVAL FOR PRECAST CONCRETE BRIDGE GIRDERS. ANY EXCEPTION TO THE USE OF SELF-CONSOLIDATING CONCRETE MUST BE APPROVED BY THE RESEARCH TEAM.
2. PRESTRESSING STEEL SHALL BE 0.6 in. DIAMETER 7-WIRE LOW RELAXATION GRADE 270 STRANDS. STRAND PARAMETERS SHALL BE AS SPECIFIED IN THE PROJECT SCOPE DOCUMENT.
3. POST-TENSIONING STEEL WILL BE 3 TENDON DUCTS WITH 19-0.6 in. DIAMETER 7-WIRE LOW RELAXATION GRADE 270 STRANDS IN EACH. EACH DUCT SHALL BE OF DIAMETER $3\frac{5}{8}$ in. POST-TENSIONING DUCTS SHALL BE SEMI-RIGID SPIRALLY CRIMPED, CORRUGATED DUCTS OF GALVANIZED, COLD ROLLED STEEL CONFORMING TO ASTM A653. CORRUGATIONS MUST HAVE A MINIMUM AMPLITUDE OF 0.094 in.
4. POST-TENSIONING CONTRACTOR WILL BE RESPONSIBLE FOR INSTALLING, STRESSING AND GROUTING THE TENDONS IN THE LABORATORY ACCORDING TO TXDOT STANDARD SPECIFICATIONS. THE RESEARCH TEAM WILL PROVIDE A LIST OF APPROVED PRE-PACKAGED, NON-SHRINK GROUTS.
5. ALL REINFORCING STEEL SHALL BE ASTM A615 GRADE 60.

GIRDER SEGMENTS

1. MODIFIED TX70 GIRDER SECTION SHALL BE USED. FOR DETAILS SEE DRAWING S6651-7.
2. ALL DIMENSIONS SHALL BE CONSIDERED IN-PLACE DIMENSIONS.
3. EXTERIOR TOP SURFACES OF ALL GIRDER SEGMENTS SHALL BE CLEAN AND INTENTIONALLY ROUGHENED TO AN AMPLITUDE OF 0.25 in.
4. A FEW PRESTRESSING STRANDS SHALL BE EXTENDED TO THE CENTERLINE OF SPLICE. FOR DETAILS SEE DRAWINGS S6651-3 TO S6651-7.
5. ALL POST-TENSIONING STEEL DUCTS SHALL BE KEPT FLUSH WITH THE ENDS OF GIRDER SEGMENTS. FOR DETAILS SEE DRAWINGS S6651-3 TO S6651-7. PRECASTER SHALL BE RESPONSIBLE FOR PROVIDING CONNECTIONS OF COUPLERS AND TRANSITION FITTINGS FOR THE DUCTS AT THE SPLICE LOCATIONS.
6. IN HANDLING, GIRDERS MUST BE MAINTAINED IN AN UPRIGHT POSITION AT ALL TIMES AND MUST BE LIFTED AT THE LIFTING POINTS SPECIFIED IN THE PROJECT SCOPE DOCUMENT.
7. THE PRECASTER IS RESPONSIBLE FOR GIRDER STABILITY AT THE CASTING YARD AND DURING TRANSPORTATION. CRACKED GIRDERS WILL NOT BE ACCEPTED WITHOUT APPROVAL OF TAMU/TTI PERSONNEL.

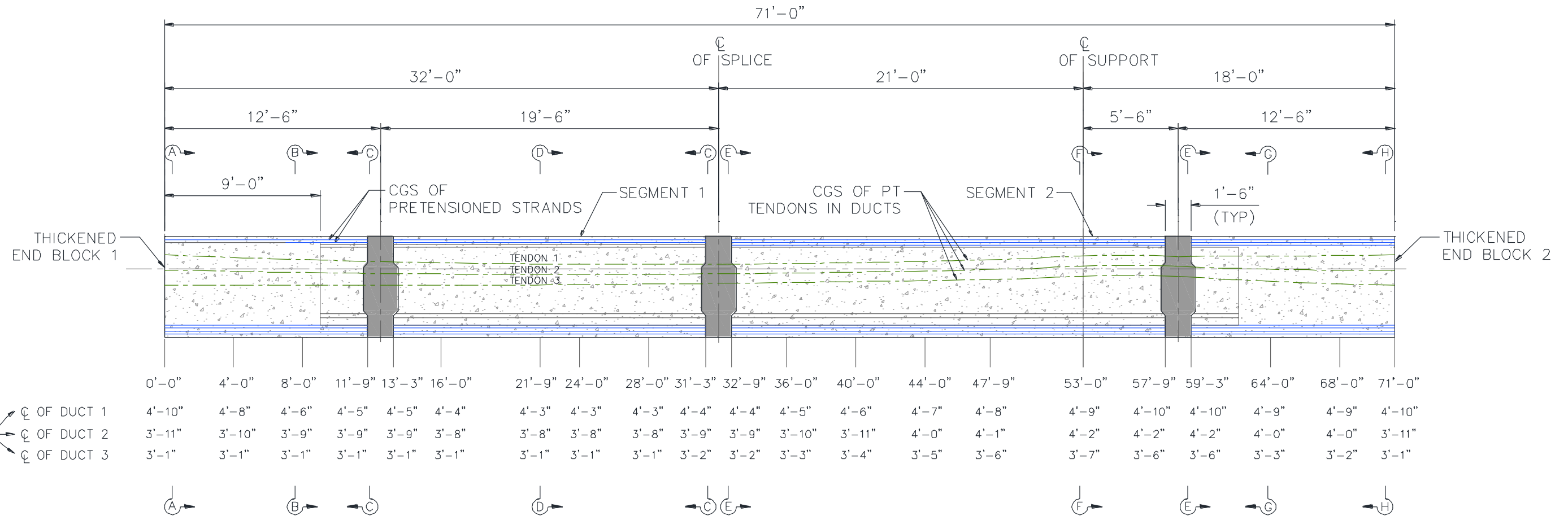
LIST OF DRAWINGS

1. GENERAL NOTES AND SPECIMEN DETAIL.....S6651-1
2. POST-TENSIONING TENDON PROFILE.....S6651-2
3. THICKENED END BLOCK 1 DETAILS.....S6651-3
4. THICKENED END BLOCK 2 DETAILS.....S6651-4
5. SEGMENT 1 DETAILS.....S6651-5
6. SEGMENT 2 DETAILS.....S6651-6
7. MODIFIED TX70 GIRDER AND SPLICE DETAILS.....S6651-7
8. BAR BENDING DETAILS.....S6651-8



SPECIMEN DETAIL

TEXAS A&M TRANSPORTATION INSTITUTE TEXAS A&M UNIVERSITY		
CONTINUOUS PRESTRESSED CONCRETE GIRDER BRIDGES		
GENERAL NOTES AND SPECIMEN DETAIL (R1)		
TXDOT PROJECT NO.	DRAWING NO.	DATE
0-6651	S6651-1	03/07/2014



POST-TENSIONING TENDON PROFILE

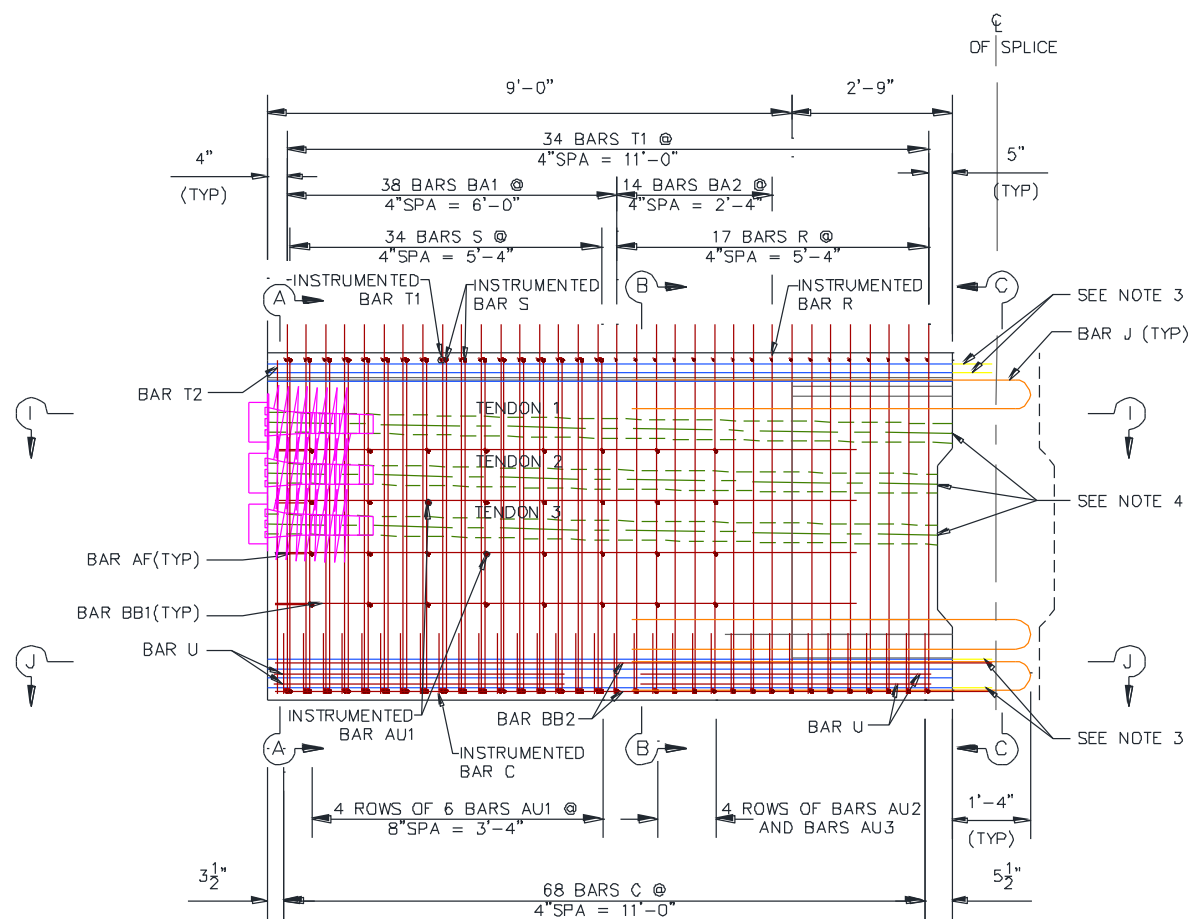
NOTES:

1. MODIFIED TX70 GIRDER SECTION SHALL BE USED. FOR DETAILS SEE DRAWING S6651-7.
2. HORIZONTAL DIMENSIONS ARE MEASURED ALONG CENTER LINE OF GIRDER.
3. A FEW PRESTRESSING STRANDS SHALL BE EXTENDED TO THE CENTERLINE OF SPLICE. FOR DETAILS SEE DRAWINGS S6651-3 TO S6651-7.
4. ALL POST-TENSIONING STEEL DUCTS SHALL BE KEPT FLUSH WITH THE ENDS OF GIRDER SEGMENTS. FOR DETAILS SEE DRAWINGS S6651-3 TO S6651-7. PRECASTER SHALL BE RESPONSIBLE FOR PROVIDING CONNECTIONS OF COUPLERS AND TRANSITION FITTINGS FOR THE DUCTS AT THE SPLICE LOCATIONS.
5. DIMENSIONS TO CENTER LINE OF DUCTS GIVEN FROM THE GIRDER SOFFIT.
6. POST-TENSIONING CONTRACTOR WILL BE RESPONSIBLE FOR INSTALLING, STRESSING AND GROUTING THE TENDONS IN THE LABORATORY ACCORDING TO TXDOT STANDARD SPECIFICATIONS. THE RESEARCH TEAM WILL PROVIDE A LIST OF APPROVED PRE-PACKAGED, NON-SHRINK GROUTS.
7. THE DUCTS SHALL BE TIED TO THE REINFORCING BARS AT MAXIMUM INTERVAL OF 2 ft TO PREVENT DISPLACEMENT OF THE DUCTS DURING CONCRETE CASTING.
8. DUCTS SHALL HAVE GROUTING VENTS AT EACH HIGH AND LOW POINT ALONG THE TENDON PROFILE.
9. AFTER INSTALLATION, THE ENDS OF THE DUCTS SHALL BE SEALED AT ALL TIMES TO PREVENT ENTRY OF WATER AND DEBRIS.
10. THE PRECASTER SHALL NOT SET THE GIRDER SIDE FORMS IN PLACE UNTIL THE TAMU/TTI PERSONNEL HAS INSPECTED AND APPROVED THE DUCT PROFILE AND REINFORCING CAGE.
11. BEFORE THE GIRDERS ARE TRANSPORTED FROM THE PRECASTING PLANT, THE PRECASTER SHALL DEMONSTRATE THAT THE DUCTS ARE NOT BLOCKED.

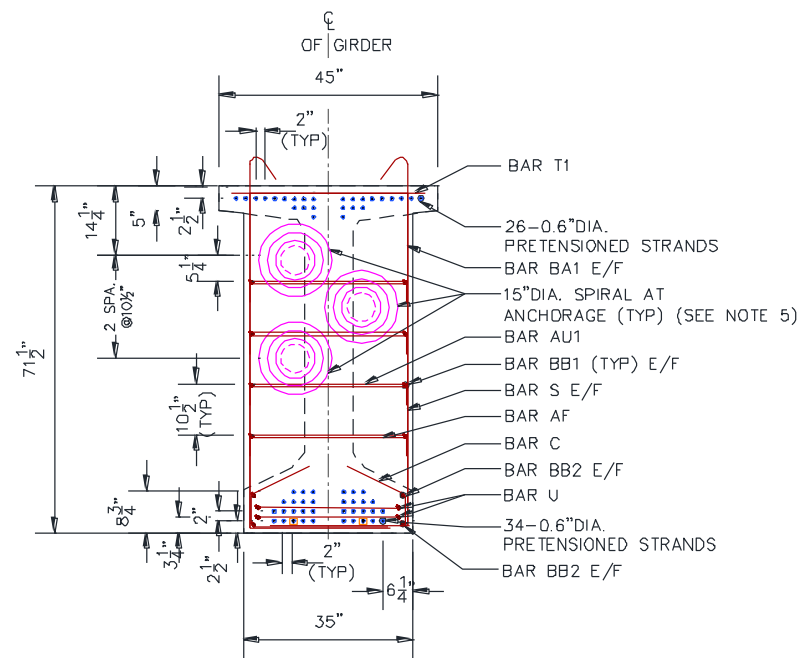
SECTION INFORMATION:

FOR SECTIONS A-A, B-B, SEE DRAWING S6651-3.
 FOR SECTIONS G-G, H-H, SEE DRAWING S6651-4.
 FOR SECTION D-D, SEE DRAWING S6651-5.
 FOR SECTION F-F, SEE DRAWING S6651-6.
 FOR SECTIONS C-C, E-E, AND SPLICE DETAILS, SEE DRAWING S6651-7.

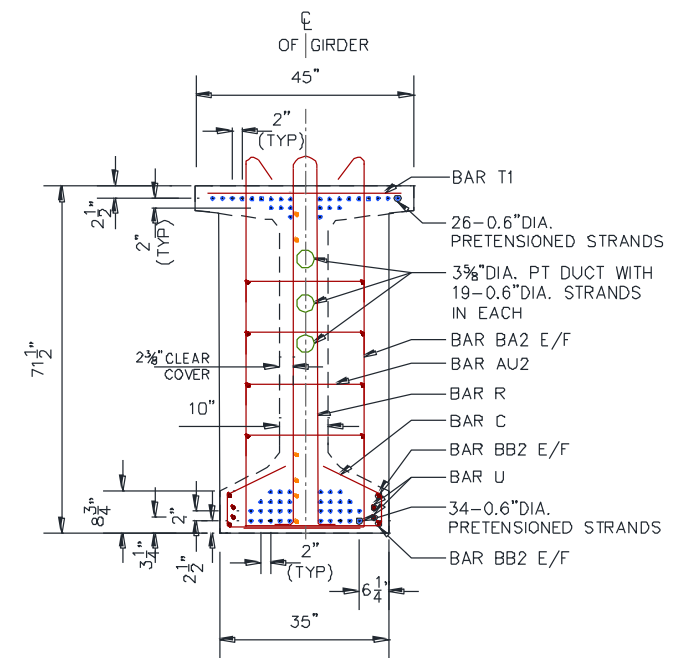
TEXAS A&M TRANSPORTATION INSTITUTE TEXAS A&M UNIVERSITY		
CONTINUOUS PRESTRESSED CONCRETE GIRDER BRIDGES		
POST-TENSIONING TENDON PROFILE (R1)		
TXDOT PROJECT NO.	DRAWING NO.	DATE
0-6651	S6651-2	03/07/2014



THICKENED END BLOCK 1 DETAIL



SECTION A-A



SECTION B-B

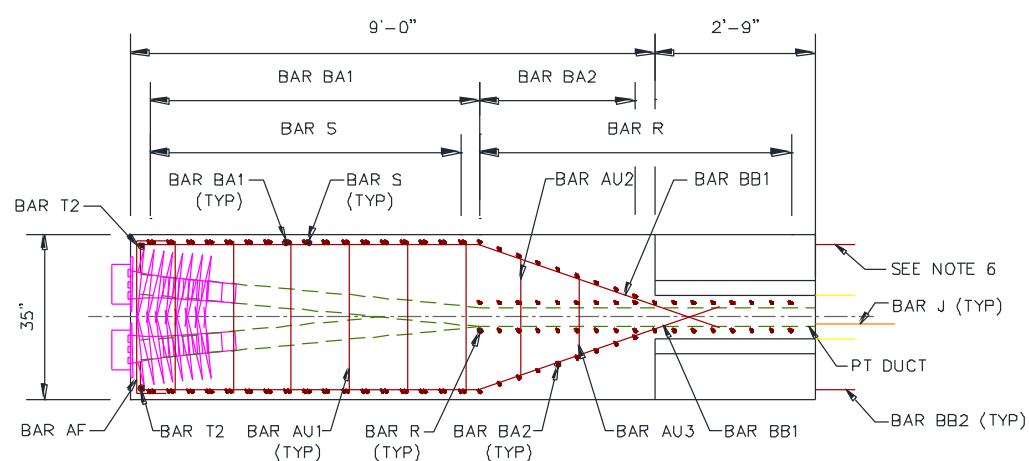
⊕ STRANDS DEBONDED 6'-0" FROM THE ANCHORAGE END OF THICKENED END BLOCK 1 (2 TOTAL)

NOTES:

1. MODIFIED TX70 GIRDER SECTION SHALL BE USED. FOR DETAILS SEE DRAWING S6651-7.
2. A TOTAL OF TWO PRESTRESSING STRANDS IN THE BOTTOM FLANGE OF THICKENED END BLOCK 1 SHALL BE DEBONDED 6 ft FROM THE ANCHORAGE END (SHOWN IN SECTION A-A).
3. A TOTAL OF TEN PRESTRESSING STRANDS SHALL BE EXTENDED TO THE CENTERLINE OF SPLICE (SHOWN IN YELLOW IN SECTION C-C).
4. ALL POST-TENSIONING STEEL DUCTS SHALL BE KEPT FLUSH WITH THE ENDS OF GIRDER SEGMENTS. PRECASTER SHALL BE RESPONSIBLE FOR PROVIDING CONNECTIONS OF COUPLERS AND TRANSITION FITTINGS FOR THE DUCTS AT THE SPLICE LOCATIONS.
5. POST-TENSIONING CONTRACTOR WILL BE RESPONSIBLE FOR DESIGN AND TESTING OF TENDON ANCHORAGE COMPONENTS. INCLUDED IN THIS RESPONSIBILITY IS THE PROPER PERFORMANCE OF THE BEARING PLATE AND LOCAL ZONE CONFINEMENT REINFORCEMENT.
6. BAR BB2 SHALL BE EXTENDED BEYOND THE FACE OF THE GIRDER SEGMENT INTO THE SPLICE.
7. FOR BAR BENDING DETAILS AND QUANTITIES, SEE DRAWING S6651-8.
8. 1 1/2 in. CLEAR COVER UNLESS NOTED OTHERWISE.

SECTION INFORMATION:

FOR SECTION C-C, AND SPLICE DETAILS SEE DRAWING S6651-7.
FOR SECTION J-J, SEE DRAWING S6651-4.



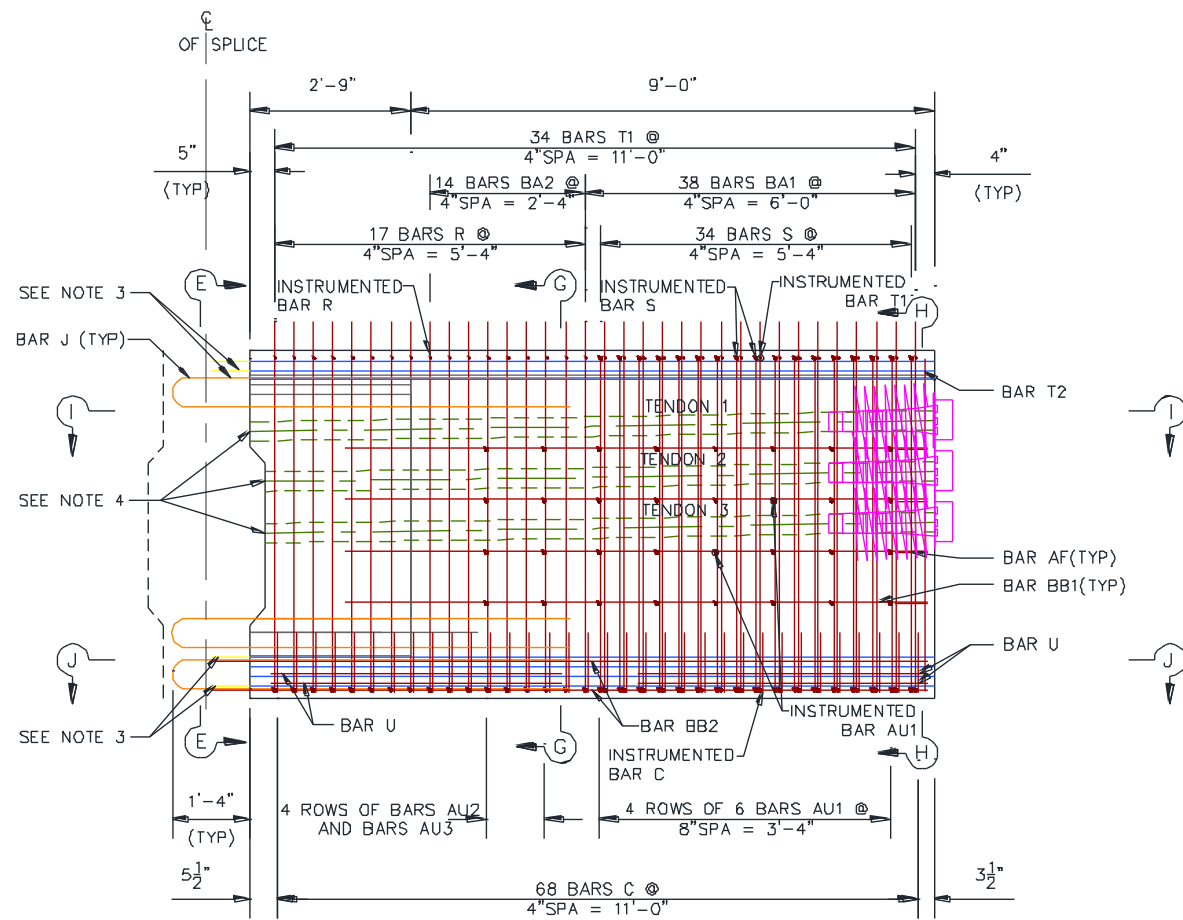
SECTION I-I

TEXAS A&M TRANSPORTATION INSTITUTE
TEXAS A&M UNIVERSITY

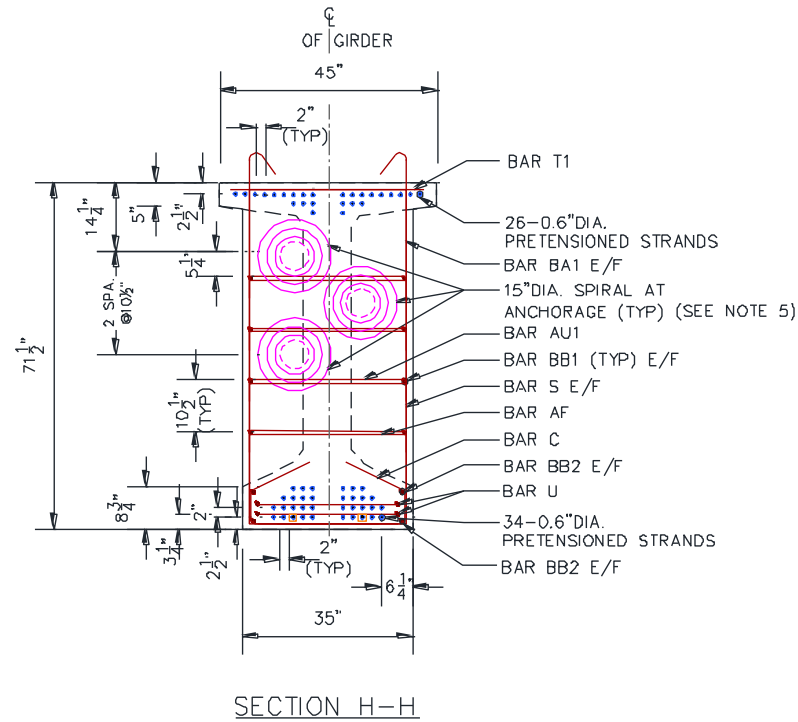
CONTINUOUS PRESTRESSED CONCRETE
GIRDER BRIDGES

THICKENED END BLOCK 1
DETAILS (R1)

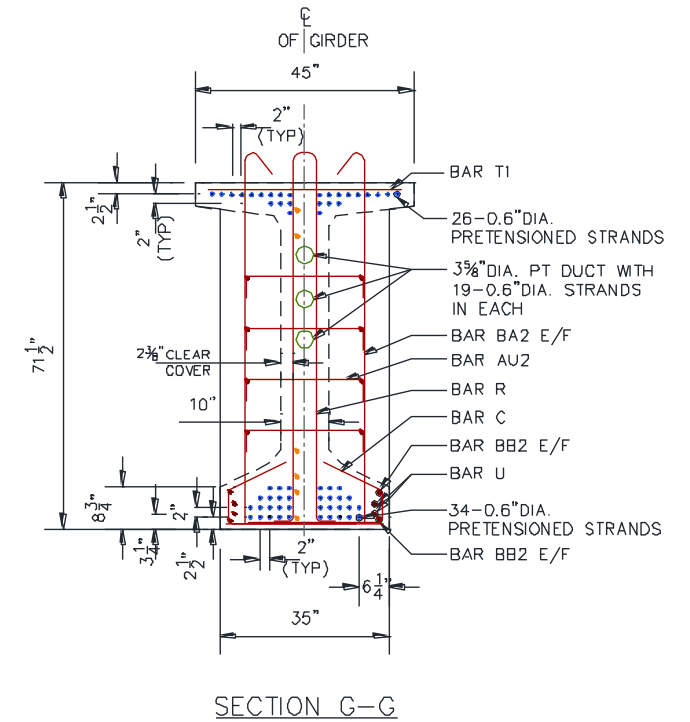
TxDOT PROJECT NO.	DRAWING NO.	DATE
0-6651	S6651-3	03/07/2014



THICKENED END BLOCK 2 DETAIL



SECTION H-H



SECTION G-G

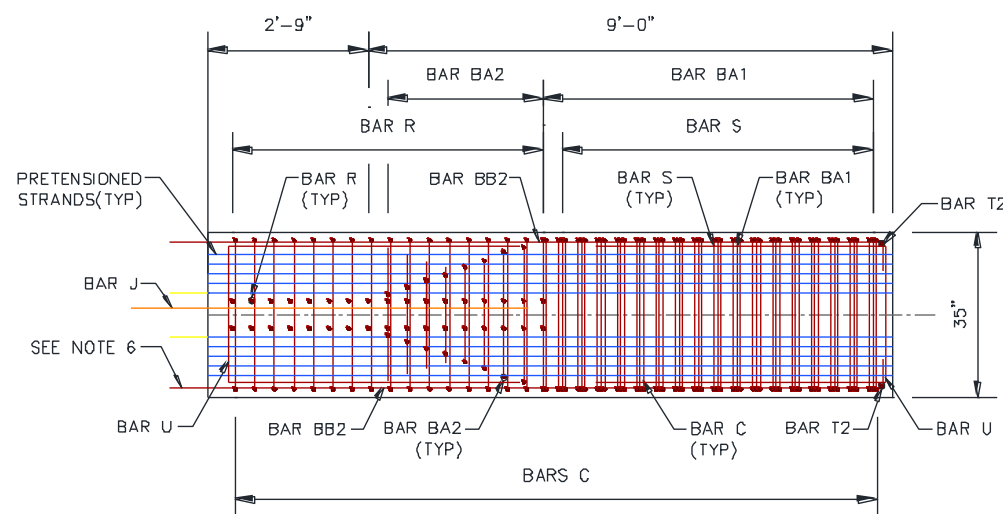
STRANDS DEBONDED 6'-0" FROM THE ANCHORAGE END OF THICKENED END BLOCK 2 (2 TOTAL)

NOTES:

1. MODIFIED TX70 GIRDER SECTION SHALL BE USED. FOR DETAILS SEE DRAWING S6651-7.
2. A TOTAL OF TWO PRESTRESSING STRANDS IN THE BOTTOM FLANGE OF THICKENED END BLOCK 2 SHALL BE DEBONDED 6 ft FROM THE ANCHORAGE END (SHOWN IN SECTION H-H).
3. A TOTAL OF TEN PRESTRESSING STRANDS SHALL BE EXTENDED TO THE CENTERLINE OF SPLICE (SHOWN IN YELLOW IN SECTION E-E).
4. ALL POST-TENSIONING STEEL DUCTS SHALL BE KEPT FLUSH WITH THE ENDS OF GIRDER SEGMENTS. PRECASTER SHALL BE RESPONSIBLE FOR PROVIDING CONNECTIONS OF COUPLERS AND TRANSITION FITTINGS FOR THE DUCTS AT THE SPLICE LOCATIONS.
5. POST-TENSIONING CONTRACTOR WILL BE RESPONSIBLE FOR DESIGN AND TESTING OF TENDON ANCHORAGE COMPONENTS. INCLUDED IN THIS RESPONSIBILITY IS THE PROPER PERFORMANCE OF THE BEARING PLATE AND LOCAL ZONE CONFINEMENT REINFORCEMENT.
6. BAR BB2 SHALL BE EXTENDED BEYOND THE FACE OF THE GIRDER SEGMENT INTO THE SPLICE.
7. FOR BAR BENDING DETAILS AND QUANTITIES, SEE DRAWING S6651-8.
8. 1 1/2 in. CLEAR COVER UNLESS NOTED OTHERWISE.

SECTION INFORMATION:

FOR SECTION E-E, AND SPLICE DETAILS SEE DRAWING S6651-7.
FOR SECTION I-I, SEE DRAWING S6651-3.



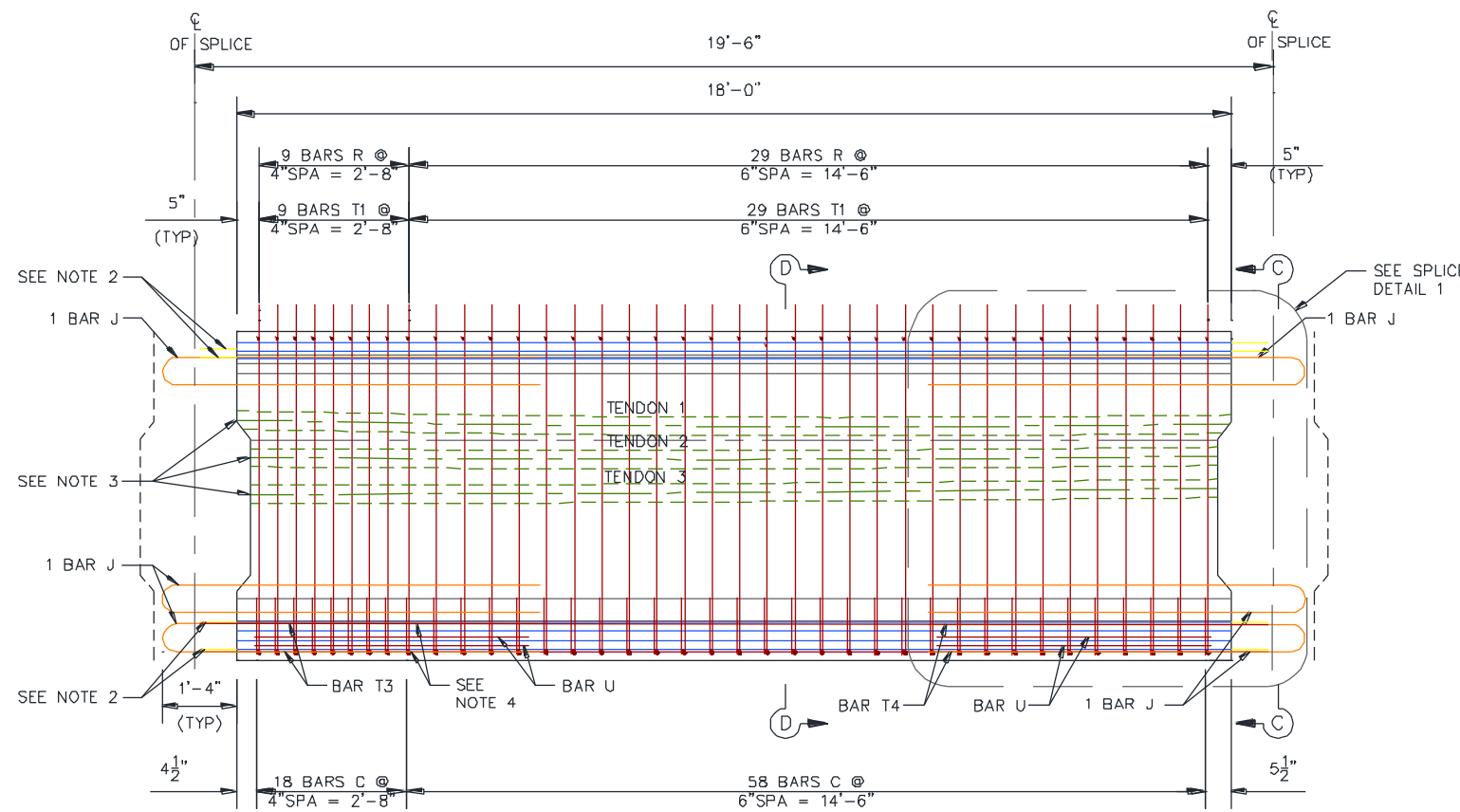
SECTION J-J

TEXAS A&M TRANSPORTATION INSTITUTE
TEXAS A&M UNIVERSITY

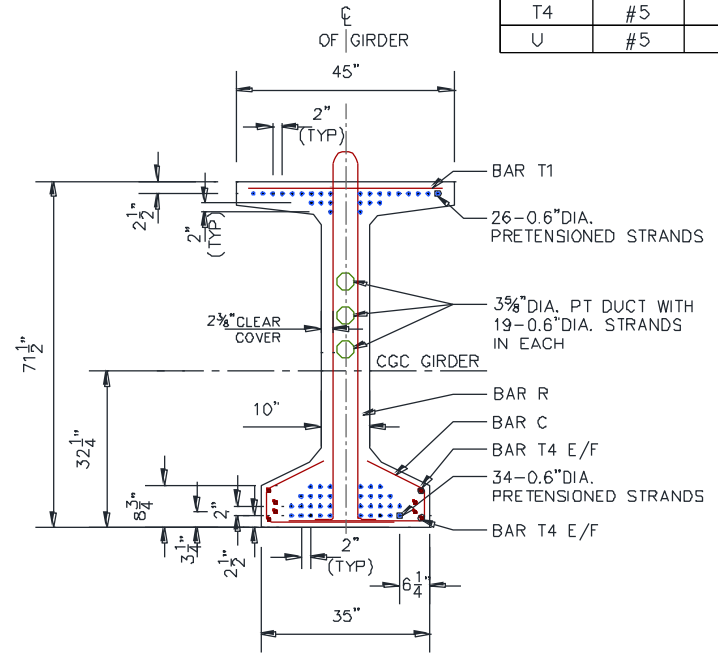
CONTINUOUS PRESTRESSED CONCRETE
GIRDER BRIDGES

THICKENED END BLOCK 2
DETAILS (R1)

TxDOT PROJECT NO.	DRAWING NO.	DATE
0-6651	S6651-4	03/07/2014



SEGMENT 1 DETAIL



SECTION D-D

BILL OF REINFORCING STEEL						
SEGMENT 1 (7)						
BAR	SIZE	TOTAL NO. OF BARS	NO. OF BARS INSTRUMENTED (8)	NO. OF BARS TO FABRICATE	LENGTH	WEIGHT (lb)
C	#4	76	-	76	4'-0"	207
J	#6	6	6	-	14'-2"	128
R	#5	38	-	38	13'-10"	553
T1	#3	38	-	38	3'-5"	49
T3	#5	4	-	4	7'-8"	32
T4	#5	4	-	4	15'-8"	66
U	#5	4	-	4	12'-5"	52

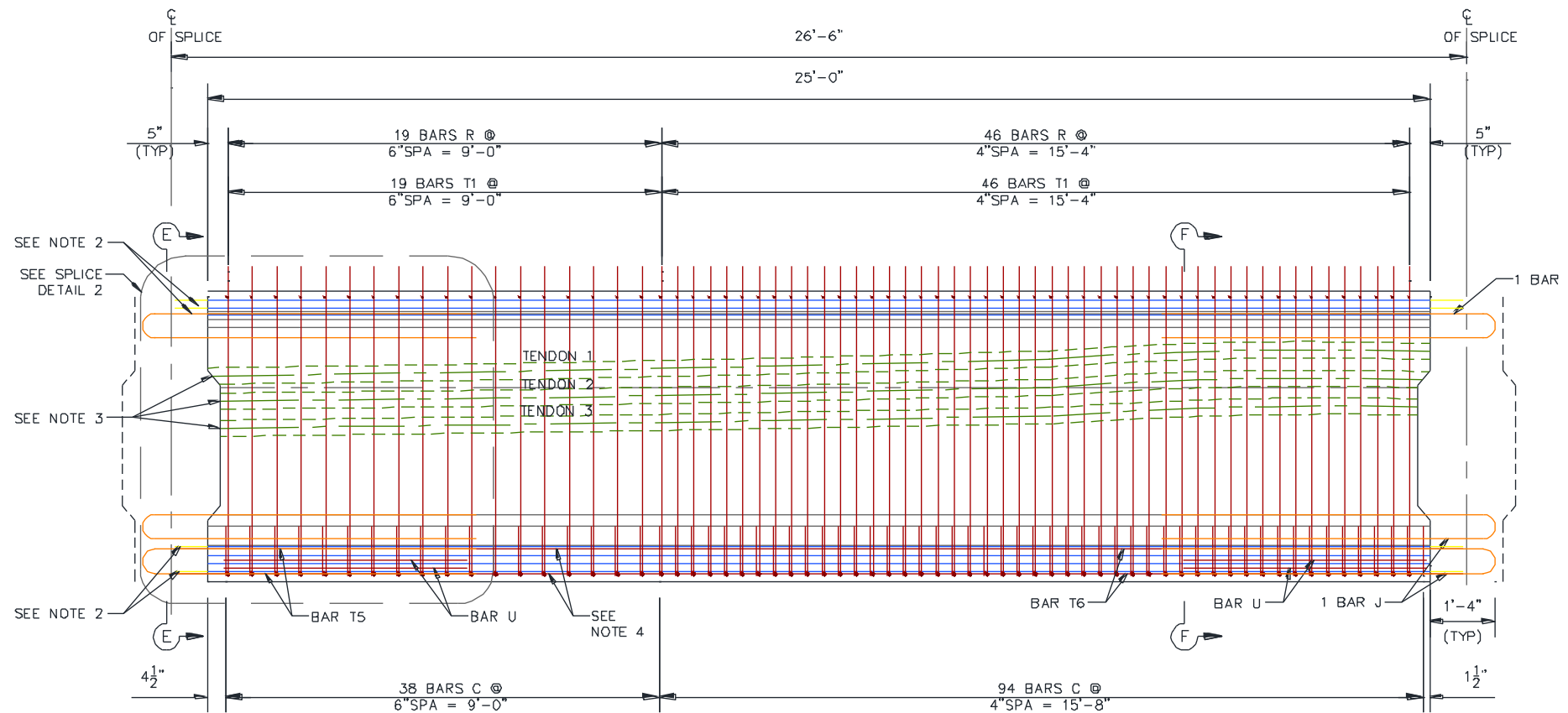
NOTES:

1. MODIFIED TX70 GIRDER SECTION SHALL BE USED. FOR DETAILS SEE DRAWING S6651-7.
2. A TOTAL OF TEN PRESTRESSING STRANDS SHALL BE EXTENDED TO THE CENTERLINE OF SPLICE (SHOWN IN YELLOW IN SECTION C-C).
3. ALL POST-TENSIONING STEEL DUCTS SHALL BE KEPT FLUSH WITH THE ENDS OF GIRDER SEGMENTS. PRECASTER SHALL BE RESPONSIBLE FOR PROVIDING CONNECTIONS OF COUPLERS AND TRANSITION FITTINGS FOR THE DUCTS AT THE SPLICE LOCATIONS.
4. BARS T3 AND T4 SHALL BE EXTENDED BEYOND THE FACE OF THE GIRDER INTO THE SPLICE. BARS T3 AND T4 ARE LAP-SPLICED FOR A LENGTH OF 4 FT.
5. FOR BAR BENDING DETAILS, SEE DRAWING S6651-8.
6. 1 1/2 in. CLEAR COVER UNLESS NOTED OTHERWISE.
7. REBAR QUANTITIES SHOWN FOR ONE SEGMENT ONLY.
8. INSTRUMENTED BARS SHALL BE PROVIDED BY THE RESEARCH TEAM.

SECTION INFORMATION:

FOR SECTION C-C, AND SPLICE DETAIL 1 SEE DRAWING S6651-7.

TEXAS A&M TRANSPORTATION INSTITUTE TEXAS A&M UNIVERSITY		
CONTINUOUS PRESTRESSED CONCRETE GIRDER BRIDGES		
SEGMENT 1 DETAILS (R1)		
TxDOT PROJECT NO.	DRAWING NO.	DATE
0-6651	S6651-5	03/07/2014



SEGMENT 2 DETAIL

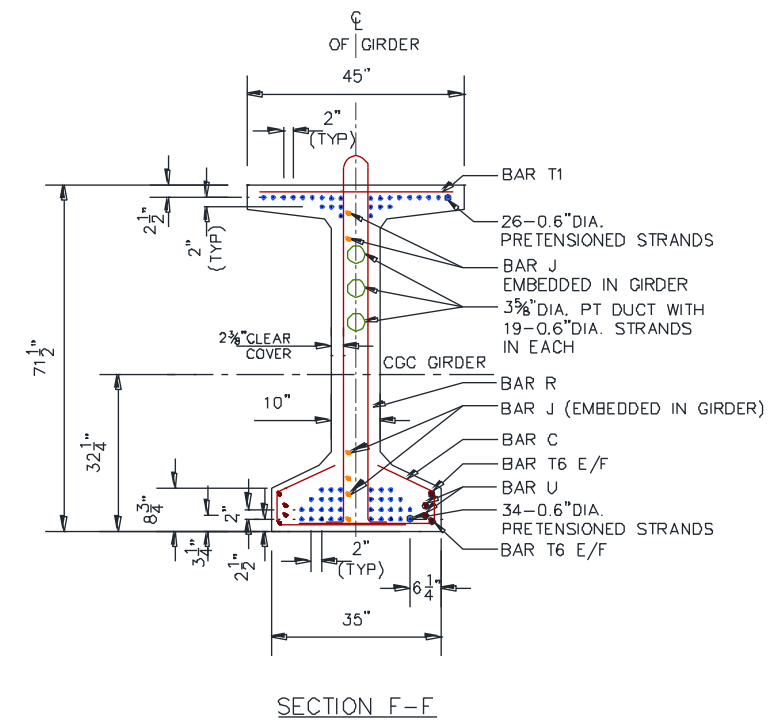
NOTES:

1. MODIFIED TX70 GIRDER SECTION SHALL BE USED. FOR DETAILS SEE DRAWING S6651-7.
2. A TOTAL OF TEN PRESTRESSING STRANDS SHALL BE EXTENDED TO THE CENTERLINE OF SPLICE (SHOWN IN YELLOW IN SECTION E-E).
3. ALL POST-TENSIONING STEEL DUCTS SHALL BE KEPT FLUSH WITH THE ENDS OF GIRDER SEGMENTS. PRECASTER SHALL BE RESPONSIBLE FOR PROVIDING CONNECTIONS OF COUPLERS AND TRANSITION FITTINGS FOR THE DUCTS AT THE SPLICE LOCATIONS.
4. BARS T5 AND T6 SHALL BE EXTENDED BEYOND THE FACE OF THE GIRDER INTO THE SPLICE. BARS T5 AND T6 ARE LAP-SPLICED FOR A LENGTH OF 4 FT.
5. FOR BAR BENDING DETAILS, SEE DRAWING S6651-8.
6. 1/2 in. CLEAR COVER UNLESS NOTED OTHERWISE.
7. REBAR QUANTITIES SHOWN FOR ONE SEGMENT ONLY.
8. INSTRUMENTED BARS SHALL BE PROVIDED BY THE RESEARCH TEAM.

SECTION INFORMATION:

FOR SECTION E-E, AND SPLICE DETAIL 2 SEE DRAWING S6651-7.

BILL OF REINFORCING STEEL						
SEGMENT 2 (7)						
BAR	SIZE	TOTAL NO. OF BARS	NO. OF BARS INSTRUMENTED (8)	NO. OF BARS TO FABRICATE	LENGTH	WEIGHT (lb)
C	#4	132	-	132	4'-0"	359
J	#6	6	6	-	14'-2"	128
R	#5	65	-	65	13'-10"	946
T1	#3	65	-	65	3'-5"	83
T5	#5	4	-	4	12'-8"	53
T6	#5	4	-	4	17'-8"	75
U	#5	4	-	4	12'-5"	52

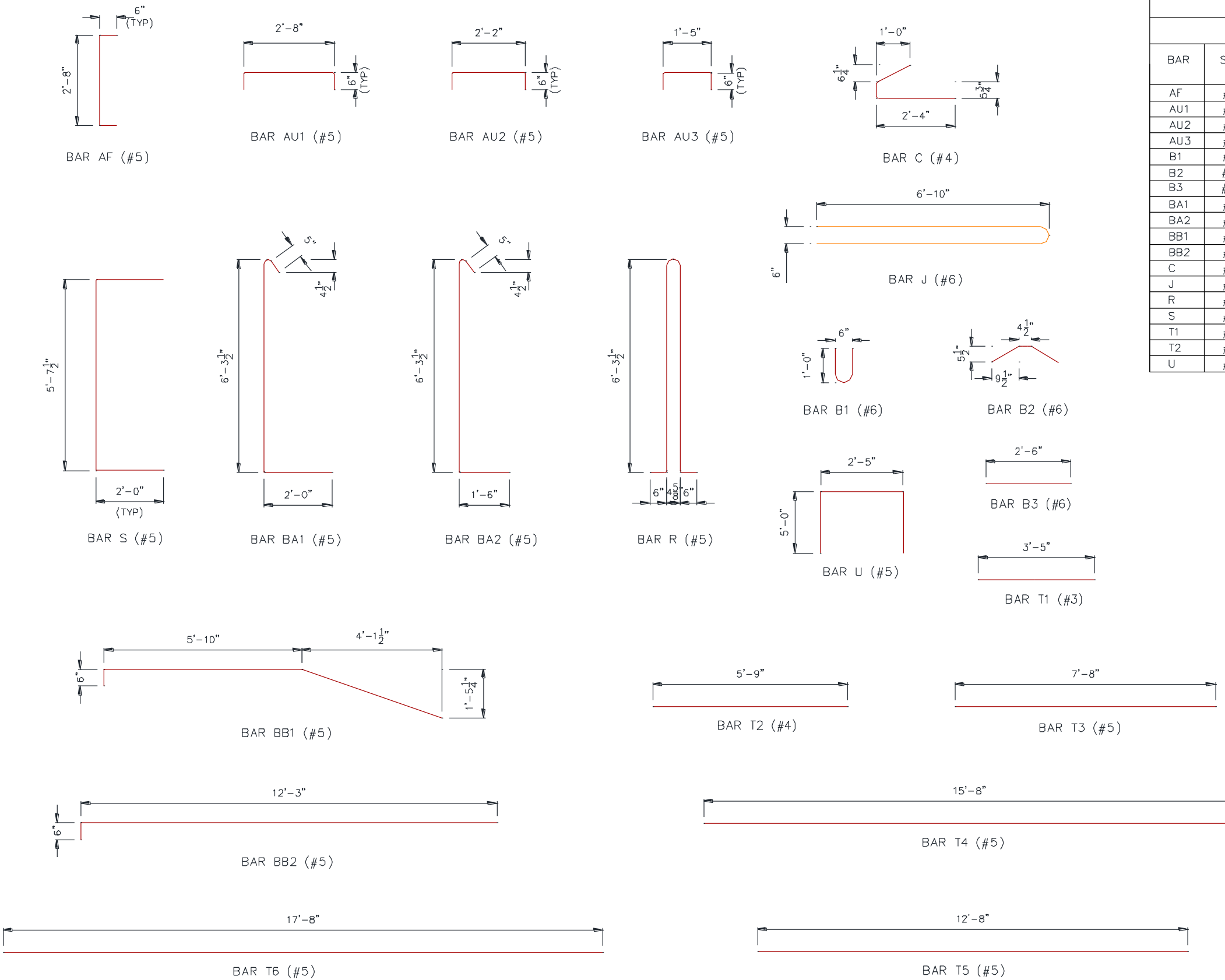


TEXAS A&M TRANSPORTATION INSTITUTE
TEXAS A&M UNIVERSITY

CONTINUOUS PRESTRESSED CONCRETE
GIRDER BRIDGES

SEGMENT 2 DETAILS (R1)

TxDOT PROJECT NO.	DRAWING NO.	DATE
0-6651	S6651-6	03/07/2014



BILL OF REINFORCING STEEL						
THICKENED END BLOCK (3) (4)						
BAR	SIZE	TOTAL NO. OF BARS	NO. OF BARS INSTRUMENTED (6)	NO. OF BARS TO FABRICATE	LENGTH	WEIGHT (lb)
AF	#5	4	-	4	3'-9"	16
AU1	#5	24	2	22	3'-9"	95
AU2	#5	4	-	4	3'-3"	14
AU3	#5	4	-	4	2'-6"	11
B1	#6	12	-	12	2'-6"	45
B2	#6	12	-	12	2'-3"	41
B3	#6	12	-	12	2'-6"	45
BA1	#5	38	-	38	8'-10"	354
BA2	#5	14	-	14	8'-4"	123
BB1	#5	8	-	8	10'-8"	90
BB2	#5	4	-	4	12'-9"	54
C	#4	68	1	67	4'-0"	185
J	#6	3	3	-	14'-2"	64
R	#5	17	1	16	13'-10"	247
S	#5	34	2	32	9'-7"	344
T1	#3	34	1	33	3'-5"	43
T2	#4	2	-	2	5'-9"	8
U	#5	4	-	4	12'-5"	52

NOTES:

1. ALL REINFORCING STEEL SHALL BE ASTM A615 GRADE 60.
2. ALL BAR DIMENSIONS ARE TO CENTER LINE OF BAR.
3. QUANTITIES SHOWN FOR ONE THICKENED END BLOCK SEGMENT ONLY.
4. BAR DETAILS AND QUANTITIES ARE TYPICAL FOR BOTH THICKENED END BLOCK SEGMENTS 1 AND 2.
5. ALL STANDARD HOOKS AND BENDS SHALL MEET THE REQUIREMENTS OF AASHTO LRFD BRIDGE DESIGN SPECIFICATIONS (2012).
6. INSTRUMENTED BARS SHALL BE PROVIDED BY THE RESEARCH TEAM, SEE DRAWINGS S6651-3 AND S6651-4.

TEXAS A&M TRANSPORTATION INSTITUTE
TEXAS A&M UNIVERSITY

CONTINUOUS PRESTRESSED CONCRETE
GIRDER BRIDGES

BAR BENDING DETAILS (R1)

TxDOT PROJECT NO.	DRAWING NO.	DATE
0-6651	S6651-8	03/07/2014